Benzoxaboroles and Boronic Acids for Sensing Applications

Lampard, Emma

Award date:
2018

Awarding institution:
University of Bath

Benzoxaboroles and Boronic Acids for Sensing Applications

Emma Victoria Lampard

A thesis submitted for the degree of Doctor of Philosophy

University of Bath

Department of Chemistry

September 2017

Signature ……. Date ...…..…….

Acknowledgements

First and foremost I would like to thank my supervisors, Professor Tony James, Professor Steven Bull and Dr Darrell Patterson (deceased) for their guidance and support throughout my PhD. Particular thanks go to Steve and Tony for encouraging me to pursue a PhD and for giving me the opportunity to work within their research groups; it really has been an invaluable experience. I truly appreciate all of their help and guidance over the past few years and their continual enthusiasm and patience.

I would also like to thank those who provided expert analytical support. Specifically, John Lowe for all of his NMR assistance and for always taking the time to help with any queries. Thanks also go to Stephen Flower for helping with the UV-Vis spectrometer and constantly listening to my never-ending stream of questions.

I have supervised a number of undergraduate and master's students throughout my PhD, some of whom have directly contributed towards my research progress. Therefore, I would like to thank Kat Filer, Manunya Tepakidareekul and Thitima Sombuttan for all of their hard work.

A big thank you also goes to all of the James and Bull group members, both past and present, who have not only taught me so much but have also been great fun to work with. To Dr David Tickell, Dr Richard Blackburn, Dr Ruth Lawrence, Dr Caroline Jones, Dr Robert Chapman, Bill Cunningham, Adam Sedgwick, Liam Stephens, Jordan Gardiner, Josh Tibbetts, Maria Odyniec and Maria Weber thanks for making the lab such a great place to work.

To Mum, Dad, Kelly and Charlie, thank you for the love, encouragement and support that has helped me through this research. Thanks also go to Dave for his help, support, patience and reassurance, and for cheering me up when I've had a bad day in the lab.

Finally, I acknowledge the Engineering and Physical Sciences Research Council and the Centre for Sustainable Chemical Technologies who funded my research.

Abstract

All the work in this thesis is based on the boronic acid functionality, and its applications in different sensing systems.

Chapter 1 introduces the concept of sensors. Different types of sensing mechanisms are introduced, and the applications of some chemical sensors are discussed. Boronic acids and esters have been widely employed in self-assembly and supramolecular chemistry, and the reversible binding of diols with boronic acids to form boronic esters has been exploited in the development of new chemical sensors for carbohydrates, including glucose. Boronic acid-containing molecules have found uses in a wide range of important sensing applications, including optical and electrochemical sensors for an array of biologically relevant materials. Benzoxaboroles, a distinct type of boronic acid with enhanced sugar binding properties, are also introduced.

Chapter 2 describes the synthesis of a benzoxaborole-functionalised acrylamide monomer for applications in membrane separations. The high affinity of benzoxaboroles for the diol functionality has led to the utilisation of this functional group in many areas of materials chemistry. A new route to the benzoxaborole-functionalised monomer has been developed from readily available precursors. The new route is suitable for larger scale synthesis, giving the desired product in higher yields compared to previously published syntheses.

Chapter 3 describes the use of a dye displacement assay for the detection of monosaccharides. A series of blank, benzoxaborole-functionalised and phenylboronic acid pinacol ester-functionalised hydrogels were prepared and their relative saccharide binding affinities were determined. The benzoxaborole-functionalised hydrogels showed enhanced binding affinity for all the reducing monosaccharide sugars studied. The enhanced binding to D-glucose is of particular importance, due its implications in type 2 diabetes, driving the need for new methods of detection for this particular sugar. The binding affinity of the hydrogels for non-reducing sugars is also investigated.

Chapter 4 describes the synthesis and fluorescence properties of probes for the detection of hydrogen peroxide. Hydrogen peroxide is a member of a class of compounds called reactive oxygen species. Reactive oxygen species are important mediators in the pathological processes of many diseases including cerebral and cardiovascular diseases,

inflammatory diseases, neurodegenerative diseases, diabetes and cancer. Because of the broad physiological and pathological consequences of these species, the development of new and better methods for their detection are required. A series of boronic acid pinacol ester probes were synthesised and analysed for their ability to detect hydrogen peroxide. The structure of the probes was altered using different substituents on the aromatic ring, and a novel oxazole probe was also synthesised.

Abbreviations

α	Alpha
A	Absorbance
Å	Angstrom
Ac	Acetyl
AcOH	Acetic acid
app.	Apparent
aq.	Aqueous
Ar	Aryl
ARS	Alizarin Red S
β	Beta
br.	Broad
BOB	Benzoxaborole
Bn	Benzyl
Bu	Butyl
$B_2(pin)_2$	Bis(pinacolato)diboron
$CDCl_3$	Chloroform, deuterated
cm	Centimetre
cm^{-1}	Wavenumbers
conc.	Concentrated
c	Concentration
dm	Decimetre
°	Degree
°C	Degrees Celsius
δ	Delta, Chemical shift
d	Deuterated
DCM	Dichloromethane
DIPEA	*N*,*N*-diisopropylethylamine
DMF	*N*,*N*-dimethylformamide
DMSO	Dimethyl sulfoxide
d	Doublet
dd	Doublet of doublets

ddd	Doublet of doublet of doublets
dppf	1,1'-Bis(diphenylphosphino)ferrocene
dt	Doublet of triplets
E	Trans
ε	Molar absorption coefficient
ESI	Electrospray ionisation
equiv.	Equivalents
Et	Ethyl
Et_2O	Diethyl ether
EtOH	Ethanol
EtOAc	Ethyl acetate
FRET	Förster Resonance Energy Transfer
FTIR	Fourier transform infrared
g	Gram
h	Hour
H_2	Hydrogen
HBTU	*N*,*N*,*N*',*N*'-Tetramethyl-O-(1H-benzotriazol-1-yl)uronium hexafluorophosphate
HCl	Hydrochloric acid
$HO^{\cdot}$	Hydroxyl radical
HOCl	Hypochlorous acid
HOMO	Highest Occupied Molecular Orbital
H_2O_2	Hydrogen Peroxide
HNO_3	Nitric acid
H_2SO_4	Sulfuric acid
Hz	Hertz
I	Fluorescence intensity
ICT	Internal Charge Transfer
IFN-γ	Interferon gamma
I/I_0	Relative fluorescence intensity
IR	Infrared
J	Coupling constant
KCl	Potassium chloride

KH_2PO_4	Potassium phosphate monobasic
LE	Locally excited
LiOH	Lithium hydroxide
lit.	Literature
LPS	Lipopolysaccharide
LUMO	Lowest Unoccupied Molecular Orbital
m/z	Mass-to-charge ratio
mp	Melting point
MHz	Megahertz
m	*meta*
MeCN	Acetonitrile
MeO	Methoxy
MeOH	Methanol
Me	Methyl
$MgSO_4$	Magnesium sulfate
m	multiplet
mg	Milligram
mL	Millilitre
mm	Millimetre
mmol	Millimole
min	Minute
M	Molar
mM	Millimolar
MS	Mass spectrometry
mol%	Mole percentage
$NaBH_4$	Sodium borohydride
$NaHCO_3$	Sodium hydrogen carbonate
Na_2HPO_4	Sodium phosphate dibasic
nm	Nanometre
nM	Nanomolar
NaOH	Sodium hydroxide
NH_4Cl	Ammonium chloride
NMR	Nuclear Magnetic Resonance

o	*ortho*
$O_2^{\cdot -}$	Superoxide anion radical
$^1O_2$	Singlet oxygen
$ONOO^-$	Peroxynitrite
p	*para*
PBA	Phenylboronic acid
PBS	Phosphate Buffered Saline
Pd/C	Palladium on carbon
PET	Photoinduced Electron Transfer
ppm	Parts per million
$POCl_3$	Phosphorus(V) oxychloride
Petrol	Petroleum ether
Ph	Phenyl
Pr	Propyl
q	Quartet
rt	Room temperature
ROS	Reactive oxygen species
RNS	Reactive nitrogen species
s	Singlet
TLC	Thin layer chromatography
THF	Tetrahydrofuran
t	Triplet
tert or ^{t}	Tertiary
td	Triplet of doublets
TMEDA	*N*,*N*,*N*′,*N*′-tetramethylethylenediamine
μL	Microlitre
UV	Ultraviolet
UV-Vis	Ultraviolet-Visible spectroscopy
λ	Wavelength
$\tilde{\nu}\bar{\upsilon}\nu$	Wavenumber
v/v	Volume/volume
w/v	Weight/volume
w/w	Weight/weight

List of Novel Compounds

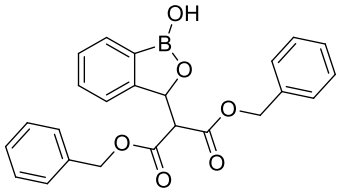

dibenzyl 2-(1-hydroxy-1,3-dihydrobenzo[*c*][1,2]oxaborol-3-yl)malonate – **24**

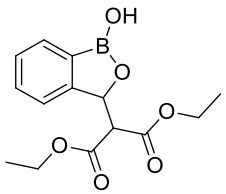

diethyl 2-(1-hydroxy-1,3-dihydrobenzo[*c*][1,2]oxaborol-3-yl)malonate - **26**

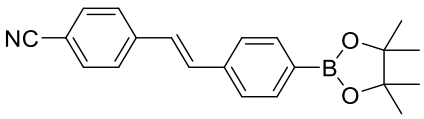

(*E*)-4-(4-(4,4,5,5-tetramethyl-1,3,2-dioxaborolan-2-yl)styryl)benzonitrile – **71**

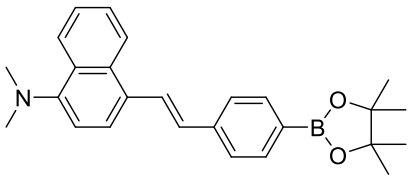

(*E*)-*N*,*N*-dimethyl-4-(4-(4,4,5,5-tetramethyl-1,3,2-dioxaborolan-2-yl)styryl)naphthalen-1-amine – **76**

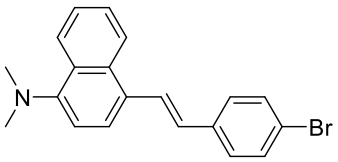

(*E*)-4-(4-bromostyryl)-*N*,*N*-dimethylnaphthalen-1-amine – **83**

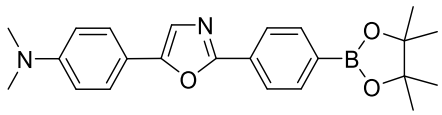

N,*N*-dimethyl-4-(2-(4-(4,4,5,5-tetramethyl-1,3,2-dioxaborolan-2-yl)phenyl)oxazol-5-yl)aniline - **77**

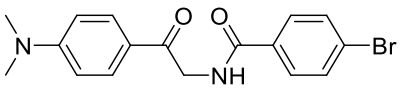

4-bromo-*N*-(2-(4-(dimethylamino)phenyl)-2-oxoethyl)benzamide – **79**

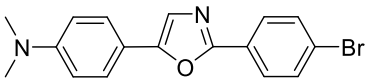

4-(2-(4-bromophenyl)oxazol-5-yl)-*N*,*N*-dimethylaniline – **80**

Contents

1 Introduction

1.1 General Introduction

Identification of chemical and biological substances is a very important task and the need to quickly and accurately determine a substance is at the heart of chemical, medical and environmental issues. Chemosensors (chemical sensors) can be made to specifically detect and report the presence of target analytes even when the target is in a complex solution. Boronic acid-containing molecules have found uses in a wide range of important sensing applications, including optical and electrochemical sensors for an array of biologically relevant materials. Many boron-based sensors have been developed for the detection of saccharides, leading to applications as glucose sensors for monitoring blood glucose levels in patients with type 2 diabetes, as well as for the detection of oligosaccharide disease biomarkers. The strong interactions that occur between boron and anions has also led to the development of a variety of different boron-based anion sensors. The research conducted in this field is driven by the need to monitor compounds of industrial, environmental and biological significance.

1.2 Introduction to Sensors and Molecular Recognition

The process of molecular recognition describes the selective interaction of two substances, typically denoted as the host and the guest.[1] Importantly, recognition is not just defined as a binding event, but requires selectivity between the host and the guest. From a practical perspective, the concept of molecular recognition requires specific interactions between two or more molecules *via* non-covalent bonding interactions such as hydrogen bonding, van der Waals forces, hydrophobic forces, π-π interactions, metal coordination and electrostatic effects.[2] However, as the area has developed, molecular recognition and sensing systems have expanded to include covalent bonds and reaction-based systems.

Biological systems have evolved with extremely selective binding sites, leading to binding of guest molecules with near perfect selectivity. In an attempt to reproduce the selectivity shown by biological receptors, chemists must design suitable and compatible structural features into synthetic host molecules.[3] This selectivity arises from the pairing

of host and guest compounds with carefully matched electronic, geometric and polar elements. For synthetic receptors, it is therefore possible to design receptors for any chosen analyte through careful structural design and choice of functional groups.

Following the definition given by IUPAC, a chemical sensor is a device that transforms chemical information into an analytically useful signal. The chemical information may originate from a chemical reaction or from a physical property of the system.[4] To be classified as a sensor, the system must incorporate a mechanism that can report the binding event to the macroscopic world (Scheme 1).

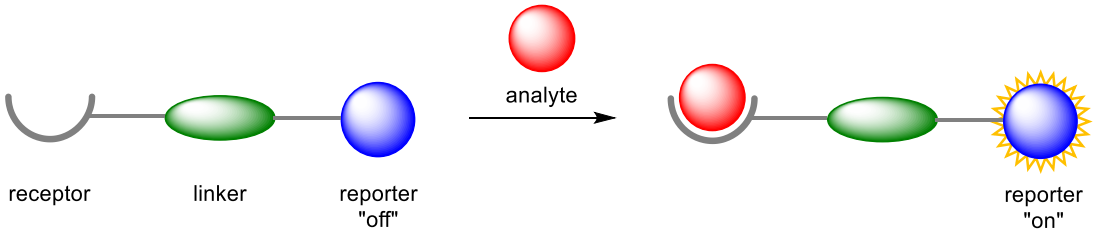

Scheme 1. A basic sensor design, showing 'off-on' characteristics.

Chemical sensors can broadly be classified as either biosensors, or synthetic sensors (chemosensors).[5] Biosensors utilise existing biological elements for recognition. Many physiologically important analytes already have corresponding biological receptors which display high selectivity. If these receptors can be connected to a signal transducer then a biosensor can be developed. Synthetic sensors incorporate a synthetically prepared element for recognition. Whilst some synthetic receptors have been designed to mimic active sites in naturally occurring biological molecules, synthetic receptors can be, and often are, designed entirely from first principles.

There are several techniques available for reporting molecular recognition events.[3] NMR spectroscopic techniques can provide useful information, although they only operate within a limited concentration window, with sensitivity limited to millimolar concentrations. Circular dichroism (CD) spectroscopy can be used to monitor optical rotation in systems that respond structurally to binding. Chemosensors that incorporate a redox active component allow electrochemical signals to be measured, often with excellent selectivity. However, perhaps the most important techniques are optical systems, utilising UV-Vis, fluorescence and phosphorescence properties. Colour changes detectable by the naked eye can allow immediate confirmation of the presence of a target analyte, along with UV-Vis spectroscopy to quantitatively determine the

concentration of a species. Fluorescence possesses many advantages, which has seen this technique become the most widely used in sensor research. Fluorescence can be used for *in vivo* analyte monitoring and is an extremely sensitive technique, with the ability to detect even single molecules in solution.[3] Phosphorescence as an optical signal is less common, but has seen some use, for example in pressure-sensitive paint for aviation research.[6]

The development of strategies for the selective binding of target molecules by rationally designed synthetic receptors remains a sought-after goal. The research conducted in this field is driven by the need to monitor compounds of industrial, environmental and biological significance.

1.2.1 Classification of Sensors

Chemical sensors are often classified according to the operating principle of the transducer.

1.2.1.1 Optical Sensors

Optical sensors report changes of optical phenomena, resulting from the interaction of the analyte with the receptor. Optical transduction can be based on light emission or light absorption by the sensing element. Such processes are associated with transitions between energy levels of certain species included in the sensing element. This group may be further subdivided according to the type of optical properties which have been incorporated into the chemical sensor.[4] Absorbance-based sensors measure the absorbance in a transparent medium, caused by the absorptivity of the analyte itself or by a reaction with a suitable indicator. Reflectance sensors measure reflectance in non-transparent media, usually using an immobilized indicator. Luminescence sensors are based on the measurement of the intensity of light emitted by a chemical reaction in the receptor system. Fluorescent sensors commonly measure the fluorescence emission, but some sensors are based on the selective quenching of fluorescence. Refractive sensors measure changes in refractive index of a solution that are caused by the presence of an analyte. This can also include a surface plasmon resonance effect. Optothermal sensors are based on a measurement of the thermal effect caused by light absorption. Light scattering sensors are based on effects caused by particles of definite size present in the sample.

1.2.1.2 Electrochemical Sensors

Electrochemical sensors transform the effect of the electrochemical interaction of the analyte with an electrode into a useful signal.[4] Sensors for aqueous solution samples can be based on electrochemical transduction methods. Electrochemistry deals with ion transport, ion distribution and electron-transfer reactions at the solution interface with an electrode. Besides electrolyte solutions, electrochemistry also addresses charge-transfer processes in systems involving ionic solids, which are also of relevance to certain types of chemical sensor.[7] Determination of ions can be achieved by means of sensors based on potentiometric transduction. The sensing element in potentiometric ion sensors is a membrane with ion-selective molecular receptors or receptor sites in a solid material. This membrane is placed between two solutions, one of them being the sample and the other one a solution containing the analyte ion at a constant concentration. Ion exchange at each side of the membrane leads to the development of a potential difference between the two sides of the membrane. This potential difference can be measured and related to the concentration of the analyte ion in the sample. Measurement of electric current forms another class of transduction method in electrochemical sensors, commonly known as amperometric sensors.

1.2.1.3 Mass Sensitive Sensors

Mass sensitive devices transform the mass change at a specially modified surface into a change of a property of the support material.[4] The mass change is caused by accumulation of the analyte and can be monitored by means of a mass transducer based on a vibrating piezoelectric crystal, known as the quartz crystal microbalance. The response signal of this transducer is the vibration frequency, which depends on the overall mass of the device.[7]

1.2.1.4 Other Types of Sensors

Other types of sensors can include magnetic devices based on the change of paramagnetic properties of a gas being analysed that are used in certain types of oxygen monitors.[4] Thermometric devices are based on the measurement of the heat effects of a specific chemical reaction or adsorption which involve the analyte. The heat effects may be measured in various ways, for example in catalytic sensors the heat of a combustion reaction or an enzymatic reaction is measured by use of a thermistor. Other physical

properties, for example X- or β-radiation may form the basis for a chemical sensor for determination of the chemical composition.

Sensors may also be classified according to the application to detect or determine a given analyte. Examples are sensors for pH or metal ions, or for determining concentration levels of oxygen or other gases. Another basis for the classification of chemical sensors may be according to the mode of application, for example sensors intended for use *in vivo*, or sensors for monitoring of industrial processes.

1.2.2 Applications of Sensors

In general, chemical sensors have been developed to provide alternatives to standard analytical methods based on chromatography, spectrometry, biochemical or microbiological techniques.[7] A chemical sensor can provide an inexpensive solution to a particular analytical problem without the need for expensive, multifunctional analytical equipment. In addition, chemical sensors are suitable for field chemical analysis in environmental investigations and are useful in point-of-care medicinal applications. Of great interest is the application of chemical sensors to the *in vivo* determination and monitoring of chemical species of physiological relevance. The use of sensors is faster than conventional chemical, biochemical or microbiological assays.[7] Therefore, it is not surprising that chemical sensors have found a broad range of applications in various areas.

1.2.2.1 Chemical Sensors for Environmental Applications

Environmental applications of chemical sensors focus mainly on assessing water quality and levels of air pollution.[8] Air pollution by industrial activities and automotive traffic is caused by toxic gases (sulfur, nitrogen and carbon oxides, hydrogen cyanide, *etc*.) and other toxic vapours. Of particular relevance is the control of industrial environmental pollution caused by hazardous gases and vapours, such as those which are toxic, flammable or explosive. Water pollution directly affects aquatic organisms and, more generally, any organisms that need water for survival. The main water pollutants monitored by chemical sensors are toxic ions (e.g., mercury, lead, cadmium and cyanide ions) and ions originating from agricultural activities. The use of fertilisers can lead to contamination of water sources by nitrate and phosphate ions that can disrupt aquatic ecological systems.[9] Agriculture is also a source of water pollution by toxic

pesticide residues. In addition to the general environmental impact, water quality is also a crucial issue in the supply of drinking water.

1.2.2.2 Chemical Sensors for Healthcare Applications

One of the main areas for the application of chemical sensors is healthcare, in which chemical sensors are utilised for *in vitro* or *in vivo* determination of chemical species of physiological relevance.[10] The functioning of *in vivo* sensors depends to a large extent on their biocompatibility. Glucose determination in blood is very important in diabetic health care and sensors for the self-monitoring of blood glucose are widely available.[11] Intensive research efforts are now devoted to the development and improvement of *in vivo* glucose sensors, where integrated glucose sensors and insulin delivery systems can automatically maintain the insulin level in blood within normal limits. Detection of pathogenic bacteria and viruses is another application of chemical sensors in clinical investigations. Pathogens can be detected by either immunological sensors or by nucleic acid-based sensors.[12] Normal biological processes, pathogenic processes, or pharmacologic responses to a therapeutic intervention can be assessed by means of biomarkers that are substances used as indicators of pathological states. Chemical sensors for biomarkers have been developed for the diagnosis of various forms of cancer, cardiovascular diseases and hormone-related health problems.[13]

1.2.2.3 Chemical Sensors for the Food Industry, Agriculture and Biotechnology

Various chemical sensors have been developed in order to assess the quality of food products, and also for monitoring industrial processes in the food and biotechnology industries.[7] Food quality depends, to a large extent, on the content of nutrients and vitamins. Various enzymatic sensors for important compounds such as saccharides, lactic acid, malic acid, citric acid, and glutamic acid have been developed using the relevant enzymes. Of particular importance in the food industry is the control of pathogenic micro-organisms and microbial toxins in foodstuffs.[14] Chemical sensors for pathogens can be developed using either antibody–antigen recognition or by detection of specific DNA sequences. In agriculture, chemical sensors are employed in the monitoring of macronutrients such as nitrate, phosphate and potassium ions.[15] Biotechnology uses biological systems, living organisms, or derivatives thereof (e.g., enzymes or living cells) to process raw materials. Various chemical sensors are used to monitor process parameters such as pH, dissolved oxygen, carbon dioxide, and bio-

organic compounds such as saccharides and amino acids.[16] Typical applications of chemical sensors in biotechnology are found in the fermentation industry and in the production of certain antibiotics.

1.2.2.4 Chemical Sensors for Defence Applications

Defence in general, and against terror attacks in particular, is a matter of great concern that has prompted the development of chemical sensors for fast *in situ* detection of explosives and warfare agents such as pathogenic micro-organisms and toxic gases.[7] Explosives can be traced using sensors specific to the explosive vapours, which have been developed using natural and synthetic affinity recognition reagents, enzymes and whole cells.[17] Biological warfare agents include living organisms and viruses or infectious material derived from them, which could be used for hostile purposes. Such agents can multiply in the attacked host and cause disease or death. Various types of chemical sensor for the detection of biological warfare agents have been developed using recognition mechanisms such as affinity recognition by antibodies or synthetic materials, recognition by enzymes or whole cells, and the tracing of pathogen DNA by means of a complementary DNA sequence.[18]

1.3 The Importance of Boron

Boron is found in many everyday applications, from cleaning materials to glass, and is of increasing importance in the world of chemical synthesis and sensing.[19] Boron compounds already have many uses in organic synthesis; boron is an important component in reducing agents, e.g. sodium borohydride and borane. In the asymmetric reduction of ketones with the CBS catalyst, boron plays a dual role, acting as both a hydride source and a Lewis acid. This Lewis acidic character comes from the empty p orbital on the boron atom, and allows the use of boron compounds (such as boron trifluoride) as Lewis acid catalysts. Boron is most commonly utilised by the synthetic community in the form of boronic acids or esters.[19] These boron-containing species are key organic building blocks and also important cross coupling partners in palladium catalysed Suzuki–Miyaura reactions. Boronic acids and esters have been widely employed in self-assembly and supramolecular chemistry, and the reversible binding of diols with boronic acids to form boronic esters has been exploited in the development of new chemical sensors for carbohydrates, including glucose.

1.4 Boron Chemistry

All of the work within this thesis is related to boron chemistry. Boron, found in the first row of group 13, has a ground state configuration of $1s^2\ 2s^2\ 2p^1$. The three valence electrons are afforded very little shielding from the nucleus and have high ionisation energies, which is a major factor in distinguishing the bonding of boron from the rest of the group 13 elements.[20] Boron, the only non-metal of group 13, forms solely covalent bonds and its chemical bonding has greater similarities to carbon. Boron's electronegativity ($\chi = 2.0$) is also comparable with that of carbon ($\chi = 2.5$) and hydrogen ($\chi = 2.2$) but it is notably more electropositive than both these elements which means that on forming covalent bonds with these elements, the boron centre is left electron deficient.[20] In this type of compound, the boron is sp^2 hybridised and consequently has a trigonal planar shape with an R-B-R bond angle of 120 °. An empty p orbital which is not involved in bonding sits perpendicular to the trigonal plane (Figure 1).

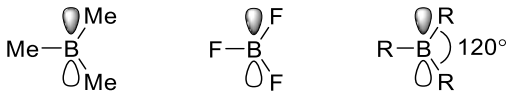

Figure 1. Examples of organoboron compounds. R = H, Me, Cl, Br, OH.

The presence of this vacant p orbital means that boron compounds can readily interact with electron-rich species, thus forming neutral species (adducts) by reaction with a Lewis base, or negatively charged species (borates) by reaction with a nucleophile. Both species contain tetrahedral boron sp^3 atoms (Scheme 2).[20] The trigonal boron species can then be considered as neutral equivalents of carbocations, and tetrahedral boron species as mimics of sp^3 hybridised carbon compounds. This capacity of boron to form trigonal and tetrahedral species is a constant in the mechanisms of the reactions in which boron is involved.

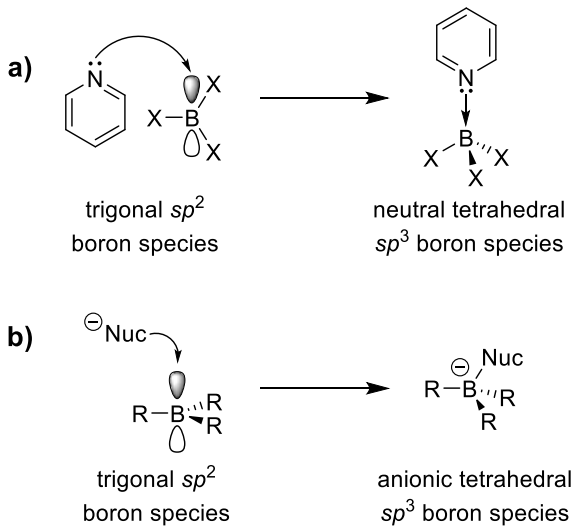

Scheme 2. a) Conversion of a sp^2 trigonal boron species to a neutral sp^3 tetrahedral boron species by association with the Lewis base pyridine; b) Conversion of a sp^2 trigonal boron species to an anionic sp^3 tetrahedral boron species by reaction with a nucleophile.

1.5 Introduction to Boronic Acids

Structurally, boronic acids are trivalent boron-containing organic compounds that possess one alkyl substituent and two hydroxyl groups on the boron atom.[21] With only six valence electrons and a resulting deficiency of two electrons, the sp^2 hybridised boron atom possesses a vacant p orbital. This empty orbital is orthogonal to the three substituents, which are orientated in a trigonal planar geometry. Their unique properties as mild Lewis acids, coupled with their stability and ease of handling, makes boronic acids a particularly attractive class of synthetic intermediates.

The origins of boronic acid based receptor design can be traced back to the seminal work of Lorand and Edwards.[22] In a study to clarify the disputed structure of the phenylboronate anion, a range of polyols were added to solutions of phenylboronic acid. The pH was adjusted so that there was an equal speciation of phenylboronic acid in its neutral and anionic forms; the pH matching the pK_a. The pH of the system decreased as the diol was added, allowing binding constants to be determined through the technique of pH depression. From these experiments, Lorand and Edwards concluded that the structure of the phenylboronate anion has a tetrahedral, rather than trigonal structure.

Alkyl- and arylboronic acids have both been accessible for over 150 years, and are commonly prepared *via* the reaction of organometallic reagents (Grignard or

organolithium reagents) with trialkyl borates.[2] The interactions of boronic acids with saccharides and anions have been extensively studied, and boronic acids have been utilised for many applications (Figure 2). Boronic acid-containing molecules have found use in a wide range of important applications, including optical and electrochemical sensors for a wide range of biologically relevant materials, separation devices for diol-functionalised biomaterials, and therapeutic uses for the treatment or prevention of disorders such as diabetes.[23] The key interaction of boronic acids with diols leads to utilisation in various areas including biological labelling and protein manipulation,[24] with the reversibility of this interaction leading to the development of a range of self-organising and self-healing systems in the field of materials chemistry.[25]

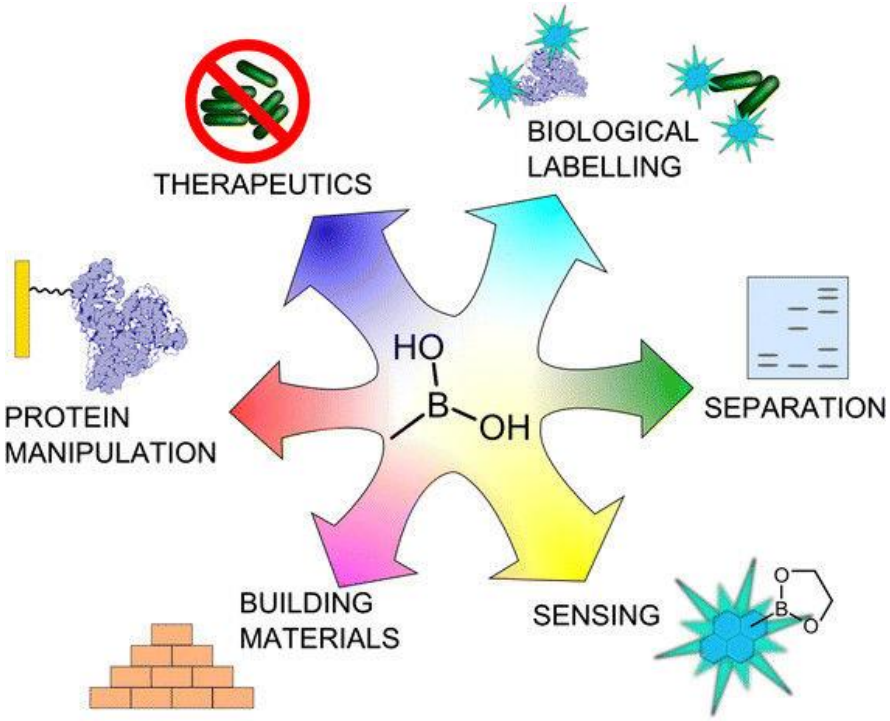

Figure 2. Diverse usage and applications of boronic acids.[24]

The chemistry of boronic acid compounds dates back to 1860 when the first preparation and isolation of a boronic acid was reported by Frankland.[26] Most of the properties of boronic acids are derived from the presence of the two labile hydroxyl groups. For instance, boronic acids readily undergo spontaneous dehydration, resulting in cyclic boroxines (Figure 3). The process is reversible, therefore boronic acids and boroxines can be used interchangeably in most cases.[21] As a result of the reversible reaction with other hydroxyl compounds, the corresponding boronic esters are formed. In the case of *cis*-1,2 and -1,3 diols, the most stable five- or six-membered cyclic esters are formed.

Boronic esters do not form oligomeric anhydrides and are therefore often preferred as synthetic intermediates. Benzoxaboroles are a distinct class of boronic compounds, and can be thought of as internal hemiesters of 2-(hydroxymethyl)phenylboronic acids, recently discovered as biologically active compounds and promising molecular receptors.

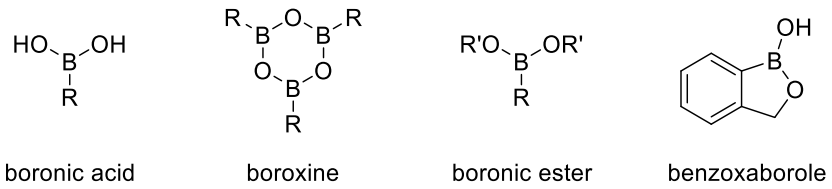

Figure 3. Structures of some common organoboron compounds.

Boronic acids as well as their esters are compounds of increasing interest due to their widespread application in organic as well as analytical chemistry.[21] Many boronic acids are now commercially available due to their use as Suzuki coupling agents. In some cases, boronic esters are more widely used than the corresponding boronic acids, due to their increased stability as well as improved solubility in organic solvents.

1.5.1 Boron-Diol Interactions

Boronic acids, especially phenylboronic acid and its derivatives, have been widely used as sensing tools for polyhydroxylated compounds such as saccharides in aqueous media.[27] Boron-diol reactions are rapid under basic aqueous conditions, affording cyclic boronate esters. The first study of the interaction between boronic acids and polyols in water was conducted by Lorand and Edwards in 1959.[22] It was found that in solutions of high pH, boronate ester formation is favourable due to the high concentration of boronate ions (Scheme 3). The favourable association at high pH as compared to neutral conditions was attributed to release of angle strain upon formation of hydroxyboronate complexes of 1,2-diols. This results from rehybridization of boron from sp^2 to sp^3.

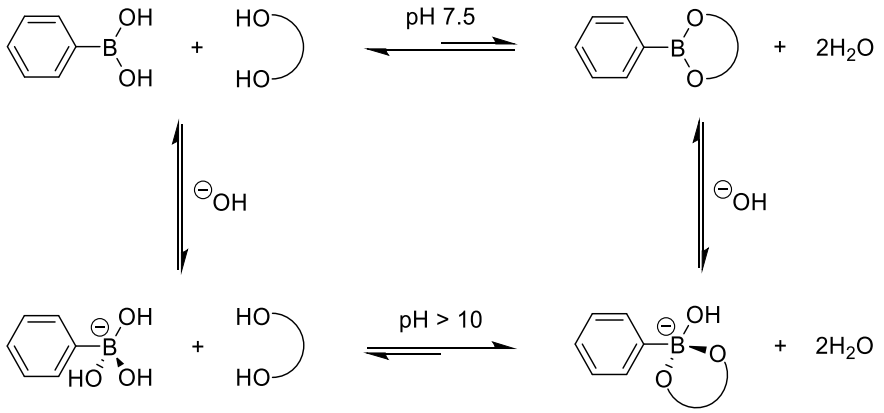

Scheme 3. Equilibrium between boronic acids and diols in aqueous medium.

Since this seminal report, several groups have investigated the details of the equilibria between boronic acids and diols. From these studies, it is evident that these equilibria are sensitive to the structure and stereochemistry of the diol. Whilst six-membered cyclic boronic esters can be formed with 1,3-diols, the stability of these diesters is lower than their five-membered analogues formed with 1,2-diols.[28] Although the boronic acid-diol interaction is covalent, it is reversible and in rapid equilibrium and therefore can be treated analogously to non-covalent recognition systems involving hydrogen bonds.[29] The fast and stable bond formation between boronic acids and diols to form boronate esters can also be utilised to build reversible molecular assemblies. The reversibility of the interaction allows for the formation of the most stable structures. The dynamic covalent functionality of boronic acids with structure-directing potential has led to the development of a variety of self-organising systems.[28,29] Most of the analytical applications of boronic acids, including sugar sensing, are due to their reversible interaction with hydroxyl compounds with formation of the corresponding boronic esters.

1.5.2 Boron-Nitrogen Interactions

Dative nitrogen-boron interactions were first reported when a complex between ammonia and trimethylborane was discovered in 1862.[30] The recognition of saccharides through boronic acid or ester complex formation often relies on an ancillary interaction between the Lewis acidic boronic acid and a proximal tertiary amine (Lewis base). The nitrogen boron (N-B) bond and its nature have been much disputed (especially in aqueous environments), but it is clear that an interaction of some kind exists which offers two advantages.[31] First, it was proposed by Wulff that a reduction in boronic acid

pK_a results from a boron-nitrogen interaction,[32] facilitating binding at neutral pH, thus, extending the pH range over which these sensors can operate, therefore expanding the scope of applications. Second, a narrowing of the O-B-O bond angle upon complex formation with a diol leads to an increase in boron's Lewis acidity. The increase in acidity of the Lewis acidic boron enhances the N-B interaction which, in certain systems, can modulate the fluorescence of nearby fluorophores, which is extremely useful in the design and application of chemosensors.[28]

The strength of a N-B bond depends greatly on the substituents at both atoms; electron-withdrawing groups increase the Lewis acidity of the boron atom, whilst electron-donating groups increase the Lewis basicity of nitrogen.[5] When considering the bond strength, it is necessary to balance these electronic factors against the steric effects of the same substituents.

The *N*-methyl-*o*-(phenylboronic acid)-*N*-benzylamine **1** system has been investigated separately by Wulff, Anslyn and within the T. D. James group.[31-33] Scheme 4 depicts a general model where, the acyclic forms (**1** and **2**) contain no N-B interaction and at the other extreme the cyclic forms (**3** and **4**) contain a full N-B interaction, with the species existing in equilibrium. Species **5** involves a protonated nitrogen, therefore the ammonium cation prevents any kind of N-B interaction. The energy of the N-B interaction has been calculated to be between 15 and 25 kJ mol^{-1} in *N*-methyl-*o*-(phenylboronic acid)-*N*-benzylamine, which is about the same energy as that of a hydrogen bond.[5] The strength of this interaction is a central feature in many fluorescent photoinduced electron transfer (PET) sensors, where the N-B interaction plays a crucial role in the signalling of the binding event. If the N-B interaction were much weaker, there would be no significant intramolecular N-B interaction to disrupt. On the other hand, if the N-B interaction were much stronger, then the binding of a diol would not be able to disrupt the N-B interaction sufficiently to result in a change in fluorescence.

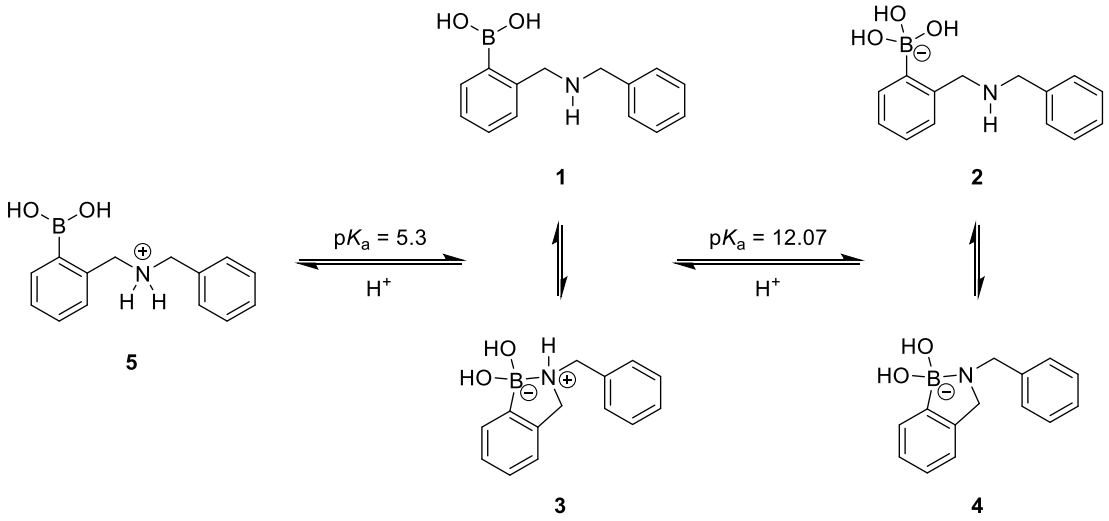

Scheme 4. The extent of interaction between nitrogen and boron is illustrated within the upper and lower bounds of possible coordination, depicted as the cyclic and acyclic forms.[31]

Anslyn *et al*. have carried out in depth structural investigations of N-B interactions in *o*-(*N*,*N*-dialkyl aminomethyl) arylboronates.[34] ^{11}B NMR spectroscopy and X-ray data have revealed that in an aprotic solvent, the dative N-B bond is usually present. However, in protic media, solvent insertion of the N-B interaction occurs, affording a hydrogen-bonded zwitterionic species. Therefore, the N-B interaction in protic media such as water or methanol should not be represented as **3**, but as the solvent-inserted form **6** (Figure 4).

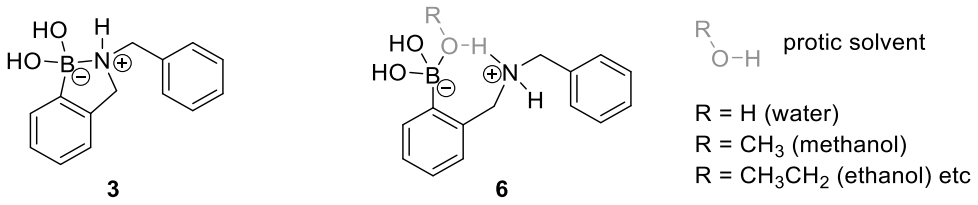

Figure 4. N-B interactions in *o*-(*N*,*N*-dialkyl aminomethyl) arylboronates in protic and aprotic media.

1.5.3 Boron-Anion Interactions

The relatively weak Lewis acidity of the boron centre creates a wealth of synthetic chemistry, but also allows boron to act as a receptor for hard anions, particularly, fluoride, cyanide and hydroxide.[3] A significant contribution to anion recognition chemistry came in 1967 when Shriver and Biallas identified the complex formed between the bidentate Lewis acid **7** and the methoxide anion (Figure 5).[35] This was the first known example of a bisboron compound binding an anion.

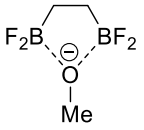

7

Figure 5. Complex formed between a between a bidentate Lewis acid and the methoxide anion.

Rather than serving as proton donors like most carboxylic acids, boronic acids act primarily as Lewis acids, due to the vacant p orbital on the boron centre.[23] Boronic acids often form complexes with Lewis bases such as fluoride or hydroxide anions, or electron-donating centres such as nitrogen or oxygen. Upon complexation, the hybridisation of the boron centre shifts from sp^2 to sp^3, with the boronic acid becoming a tetrahedral, anionic species (Scheme 5).

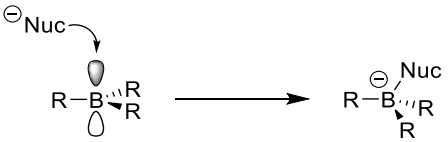

Scheme 5. The change in geometry at the boron centre when the vacant p orbital is filled by an attacking nucleophile.

Boronic acids also show significant affinity for other nucleophiles such as α-hydroxy-carboxylic acids and dicarboxylic acids. Boron, due to its Lewis acidic nature, forms coordinate bonds with a range of heteroatoms including oxygen, nitrogen, sulfur and phosphorus. Such compounds have widespread use in organic synthesis.[28]

Boronic acid-based fluorescent probes have been developed as sensors for fluoride ions as a result of the fact that trivalent boron forms strong covalent bonds with this ion.[36] Because the B-O bond in arylboronic acids is labile under protic conditions, in the presence of fluoride a series of equilibria is established (Scheme 6), in which boron participates in a series of OH^-/F^- exchange processes.[37]

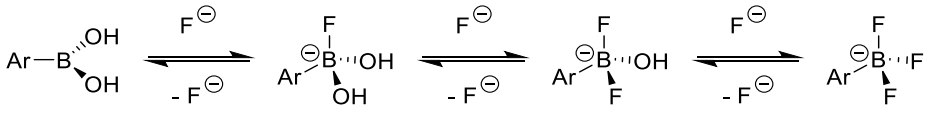

Scheme 6. Equilibrium between arylboronic acid and trifluoroborates.

1.6 Introduction to Benzoxaboroles

Benzoxaboroles can be thought of as internal esters of the corresponding *ortho*-hydroxymethylphenylboronic acids. Benzoxaboroles were first synthesised and characterised by Torssell in 1957.[38] The structure consists of a benzene ring, fused with an oxaborole heterocycle. The oxaborole ring was found to be very stable, and the boron-carbon bond was found to have very high hydrolytic resistance compared to the corresponding boronic acids.[39] However, this class of compounds remained largely ignored up until 2006, when the exceptional sugar-binding properties of benzoxaborole **8** (Figure 6) at physiological conditions was described.[40,41] The increasing interest in this class of compounds is primarily due to their biological activity, with 5-fluorobenzoxaborole (**9**, AN2690, tavaborole) being discovered as a potent antifungal agent for the treatment of onychomycosis (an infection of toes and fingernails), which was subsequently approved by the FDA in 2014.[42] A quick review of the literature reveals the recent and rapid emergence of this class of compounds; a comprehensive review published in 2009 described the structures of 65 known benzoxaboroles, whereas more than 500 novel structures had been described in the literature by 2015.[43] Benzoxaboroles display unique chemical properties, especially in comparison to their acyclic boronic acid counterparts.

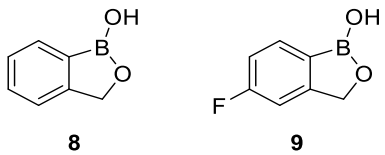

8 **9**

Figure 6. The structures of benzoxaborole and 5-fluorobenzoxaborole (AN2690).

Benzoxaboroles **10** combine structural features of both boronic acids **11** and boronic esters **12** (Figure 7). The presence of a free hydroxyl group as well as a relatively strong Lewis acidic centre on the heterocyclic boron atom results in the exceptional properties of benzoxaboroles.[43]

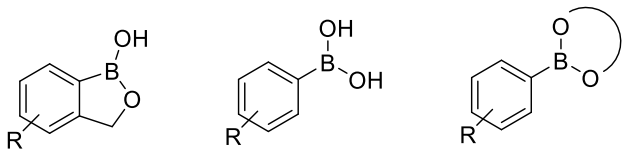

10 **11** **12**

Figure 7. General structure of benzoxaboroles, phenylboronic acids, and their cyclic esters.

All boronic acids are Lewis acids where the neutral form adopts a trigonal planar geometry, while the corresponding conjugate base is tetrahedral with the negative charge formally located on the boron atom (Scheme 7).[44] The addition of water with the accompanying loss of a proton is responsible for their acid/base properties. Benzoxaboroles also undergo the same change in hybridisation of boron from sp^2 hybridised to sp^3 hybridised, where the structure of boron is changed from its uncharged, trigonal planar form to an anionic, tetrahedral structure. This transformation releases the ring strain of the cyclic ester of the benzoxaborole. Consequently, benzoxaboroles tend to exist in charged (hydroxylated) forms under basic conditions.[45] The primary physiochemical difference observed between benzoxaboroles and phenylboronic acids is the difference in pK_a; benzoxaboroles have a pK_a around 7-8, 1-2 units lower than the corresponding phenylboronic acids (Scheme 7). The source of this difference is the ring strain that is induced by the five-membered oxaborole ring when the boron atom has trigonal planar geometry. Upon addition of water, the ring strain is relieved, leading to the observed pK_a depression.[44]

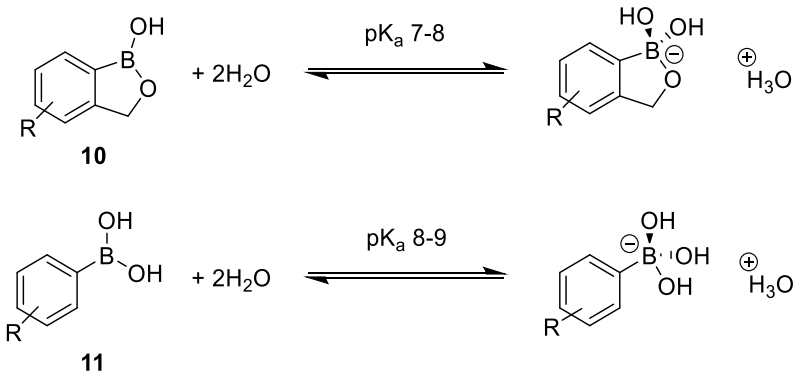

Scheme 7. The pK_a values of benzoxaboroles compared to that of phenylboronic acids.

Similarly to phenylboronic acids and their diol esters, benzoxaboroles behave as Lewis acids rather than Brønsted acids. Lewis acidity is one of the most important physicochemical properties of boronic molecules. Benzoxaboroles generally display higher acidity than the corresponding phenylboronic acids,[46] which is explained by the ring strain generated in the five-membered heterocyclic ring. The enhanced Lewis acidity of benzoxaboroles compared with phenylboronic acids results in about 50% of the anionic form being present in aqueous solution at physiological pH, which leads to their higher water solubility and significantly better pharmacokinetic properties than those of phenylboronic acids.[47]

Examination of pK_a values of benzoxaborole vs. benzoxaborin **13** (Figure 8) reveals that the pK_a value of 8.4 for **13** falls closer to the value of 8.8 for phenylboronic acid than that of 7.3 for benzoxaborole.[48] This is consistent with the idea that the ring strain in the 5-membered oxaborole ring distorts the geometry about the boron atom leading to a lowered pK_a. The 6-membered ring of benzoxaborin does not induce this distortion and therefore results in a higher pK_a value. The 0.4 pK_a unit difference between **13** and phenylboronic acid may be explained by the reduced flexibility of the intramolecular monoboronic ester, which prevents optimal B-O conjugation in **13** and consequently increases the boron atom's electronic deficiency.

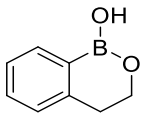

13

Figure 8. The structure of benzoxaborin.

Examination of substituent effects of the aromatic ring of benzoxaboroles follow a Hammett relationship with respect to the measured pK_a value of the compounds. These substituent effects are also shown to extend to the sugar binding properties of these compounds under physiologically relevant conditions.[48]

1.6.1 Stability of Benzoxaboroles

Benzoxaboroles can be considered as internal esters of the corresponding *ortho*-hydroxymethylphenylboronic acids. Compared to other esters of boronic acids, the stability of the ring B-O bond is very high.[49] Benzoxaboroles are completely resistant to hydrolysis, whereas the corresponding *ortho*-hydroxymethylphenylboronic acids can dehydrate spontaneously in water to form benzoxaboroles.[50] The B-O bond of benzoxaboroles is difficult to hydrolyse, and the B-C bond of benzoxaboroles is also more stable than that of the corresponding phenylboronic acids. Benzoxaborole can be recovered unchanged after refluxing with 10% HCl for three hours,[51] and can also be recovered almost quantitatively after refluxing with 15% NaOH for three hours.[52] By contrast, *para*-tolueneboronic acid was hydrolysed to toluene and boric acid after refluxing with 10% HCl for three hours.[53]

Another piece of evidence of the high stability of the oxaborole ring is the formation of 1,3-dihydro-1,3-dihydroxybenzoxaboroles from the corresponding 2-formylphenylboronic acids (Scheme 8).[54] Two forms exist in a tautomeric equilibrium, with no need for water elimination to provide a driving force for cyclisation. Variable temperature ^{1}H NMR spectroscopy was used to determine equilibrium constants, with the equilibrium shift found to be dependent on the substituents on the phenyl ring.

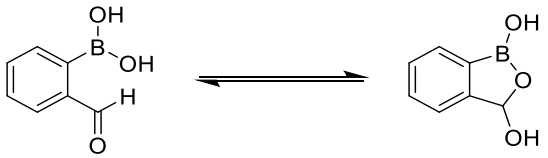

Scheme 8. The tautomeric rearrangement of 2-formylphenylboronic acids.

The stability of the benzoxaborole core allows for various modifications under a wide range of reaction conditions. For instance, benzoxaborole can be nitrated with fuming nitric acid to yield 6-nitrobenzoxaborole, which can subsequently be reduced to 6-aminobenzoxaborole under hydrogen in the presence of Raney nickel.[55] Benzoxaboroles are also stable towards oxidation with chromium(VI) oxide without any damage to the core, and can also tolerate reduction with lithium aluminium hydride.[51]

1.6.2 Reactivity of Benzoxaboroles

The reactivity of benzoxaboroles is similar to that of the corresponding boronic acids. When heated under vacuum, benzoxaboroles will dehydrate quantitatively to form a linear anhydride (Scheme 9).[39,56]

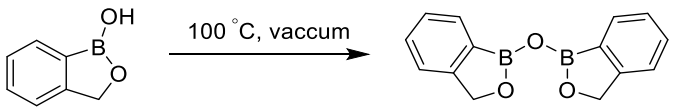

Scheme 9. Dehydration of benzoxaboroles to form anhydrides.

In the presence of alcohols benzoxaboroles will react to form monoesters, which will spontaneously hydrolyse on contact with air (Scheme 10).[39] A more stable ester is formed with ethanolamine (**14**) due to the intramolecular complexation of boron with a nitrogen atom.[49]

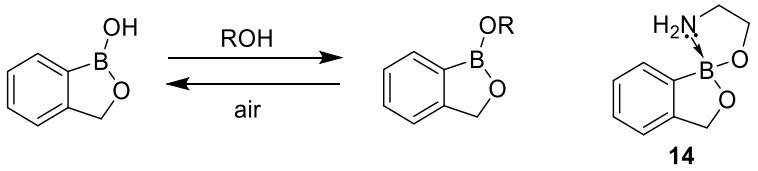

Scheme 10. Reaction of benzoxaboroles to form monoesters.

The nucleophilicity of the hydroxyl group was found to be poor, with chloro- and alkyl-substituted benzoxaboroles isolated in poor yields (Scheme 11).[56]

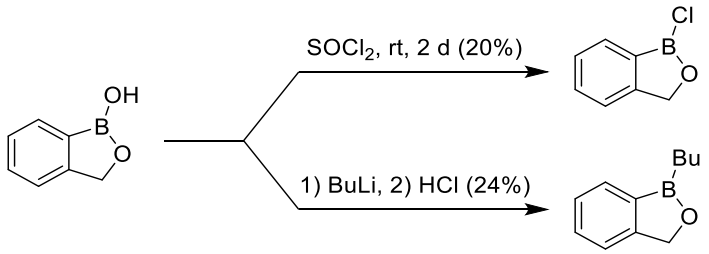

Scheme 11. Low reactivity of the B-OH bond.

Benzoxaboroles can be oxidised by hydrogen peroxide to form the corresponding phenols (Scheme 12).[57]

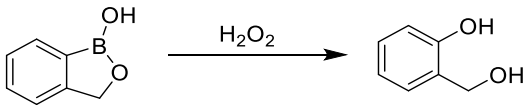

Scheme 12. The reaction of benzoxaboroles with hydrogen peroxide.

The B-C bonds of benzoxaboroles also react with alkyl halides in the Suzuki-Miyaura cross coupling reaction to form biaryls with a hydroxymethyl group at the *ortho* position (Scheme 13).[58,59]

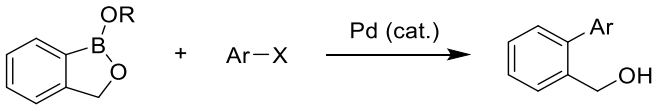

Scheme 13. Suzuki reaction with benzoxaboroles. R = H or ^{i}Pr, X = Br or I.

The B-C bond of benzoxaboroles can also be catalytically reacted with carbon monoxide or isocyanides to give lactones or cyclic imidates respectively (Scheme 14).[58] A Hayashi-Miyaura coupling between a benzoxaborole and methyl vinyl ketone can be used for the synthesis of a keto-substituted benzyl alcohol (Scheme 14).

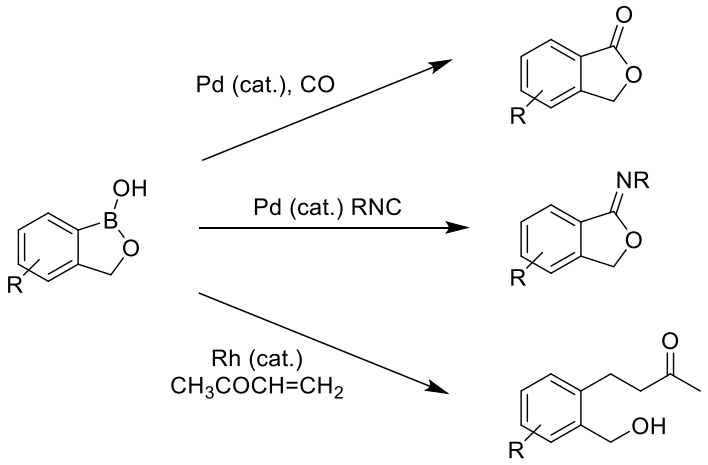

Scheme 14. Reactions involving catalytic cleavage of the B-C bond.

One important property of benzoxaboroles is their ability to efficiently bind diols such as those found in sugars (i.e. glucose, ribose and fructose) and 1,2 aromatic diols (i.e. catechol) in aqueous media at neutral pH.[44] For these reactions, the underlying chemistry consists of a sequential two-step process (Scheme 15) that forms the cyclic boronate ester. The first step is an intermolecular esterification reaction, followed by intramolecular ring closure to form the tetrahedral boronate adduct. Due to the differences in pK_a values, benzoxaboroles show an optimal affinity for diol binding around neutral pH, whereas phenylboronic acid species generally show optimal binding of diols at an increased pH of around 10-11.[44] This affinity and specificity for binding diol motifs has been extensively exploited for applications including sugar sensing, the enrichment of glycosylated proteins and therapeutics.

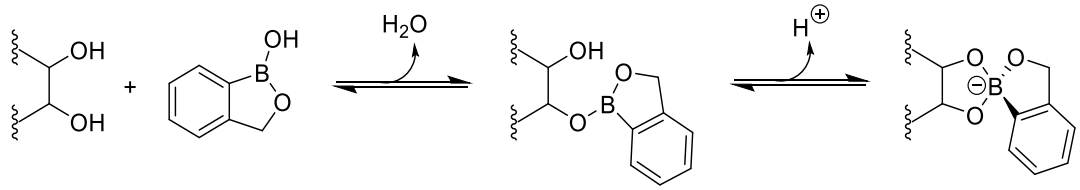

Scheme 15. Formation of a tetrahedral adduct between a benzoxaborole and a diol.

1.7 The Structures of Benzoxaboroles and Boronic Acids

Currently, crystal structures of very few benzoxaboroles have been fully characterised. As is the case with phenylboronic acids, the basic structural motif consists of a dimer containing two intermolecular hydrogen bonds (**15**, Figure 9). Benzoxaboroles contain only one hydroxyl group on the boron atom, and hence there is no possibility of lateral hydrogen bonds leading to the formation of infinite 2D or 3D networks, as is the case with phenylboronic acids (**16**, Figure 9).[60] In benzoxaboroles the boron centre is always trigonal, and the BOO fragment is always coplanar with the phenyl ring, unlike the case with phenylboronic acids. One of the B-O bonds is involved in the formation of a five-membered oxaborole ring, consequently leading to a slight exaggeration in the distortion of the bond lengths and bond angles around the boron atom. The length of the exocyclic B-O bond is shorter than the endocyclic one (with mean values of 1.350 and 1.394 Å respectively), and the exocyclic C-B-O angle is bigger than the endocyclic one (with mean values of 133.1° and 108.6° respectively), which is the source of ring strain of the five-membered oxaborole.[50] These geometric restraints reduce the diversity of possible crystal structures that can be formed. Substitution of the phenyl ring and/or the methylene carbon of the oxaborole ring can influence the intermolecular interactions by both steric and electric effects, so more complicated patterns are involved for substituted benzoxaboroles.[61,62]

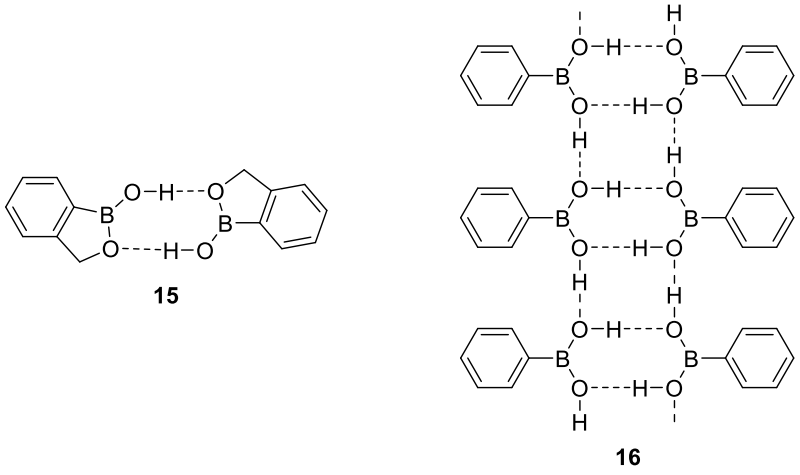

Figure 9. The crystal lattice of benzoxaborole compared to that of phenylboronic acid.

1.8 Summary of Introduction

A chemical sensor is a device that transforms chemical information into an analytically useful signal. To be classified as a sensor, the system must incorporate a mechanism that can report the recognition event to the macroscopic world. Chemosensors incorporate a synthetically prepared element for recognition, and are often designed entirely from first principles. Some of the most important synthetic sensors are optical systems, utilising UV-Vis, fluorescence and phosphorescence properties. The development of strategies for the selective binding of target molecules by rationally designed synthetic receptors remains a sought-after goal. The research conducted in this field is driven by the need to monitor compounds of industrial, environmental and biological significance.

Boron is found in many everyday applications, and is of increasing importance in the world of chemical synthesis and sensing. Boron is most commonly utilised by the synthetic community in the form of boronic acids or esters. Their unique properties as mild Lewis acids, coupled with their stability and ease of handling makes boronic acids a particularly attractive class of synthetic intermediates. Boronic acids and esters have been widely employed in self-assembly and supramolecular chemistry, and the reversible binding of diols with boronic acids to form boronic esters has been exploited in the development of new chemical sensors for carbohydrates, including glucose. Boronic acid-containing molecules have found uses in a wide range of important applications, including optical and electrochemical sensors for a wide range of biologically relevant materials, separation devices for diol-functionalised biomaterials, and therapeutic uses for the treatment or prevention of disorders such as diabetes.

Benzoxaboroles can be thought of as internal esters of the corresponding *ortho*-hydroxymethylphenylboronic acids. Benzoxaboroles show very high hydrolytic resistance compared to the corresponding boronic acids and have shown much potential as improved sugar binding agents compared to their traditional boronic acids counterparts. Benzoxaboroles are versatile scaffolds, playing important roles in organic synthesis, molecular recognition and supramolecular chemistry.

1.9 Project Aims

1.9.1 Chapter 2 - The Development of a Synthetic Route for Benzoxaborole-Functionalised Monomers for Applications in Membrane Separations

The initial overall aim of my PhD was to develop a polymer membrane system which could be used for the separation of useful compounds from waste grape biomass and the removal of fluoride from drinking water. This was an interdisciplinary project requiring both synthesis and separation technologies. The project aimed to alleviate the adverse environmental impact of the wine industry by providing new routes to convert the waste biomass into economically viable chemical product streams and provide a cheap and simple method for the detection and removal of fluoride from drinking water. Before the polymer membrane could be synthesised, a new synthetic route for the large scale synthesis of the benzoxaborole-containing monomer needed to be developed.

The aim of the project was to develop a reliable and high-yielding synthesis of benzoxaborole compounds, in particular the BA-NH_2 building block. A synthetic route to this key intermediate has already been published (Scheme 16),[63] however this pathway incorporates many steps and the use of toxic and flammable reagents. The project aimed to increase the overall yield and make the reactions more environmentally friendly by using catalytic processes rather than stoichiometric ones, as well as using greener reagents and solvents for the transformations and minimising chemical waste. So far, various methods have been developed for the construction of the benzoxaborole core, however, most of the current approaches suffer from limited substrate scope or the lack of readily available precursors, as well as tedious synthetic procedures.[64] Often, the existing literature methodologies for the synthesis of these boroles are not amenable to large scale synthesis.[59] Therefore, the project aimed to develop a synthetic route from readily available precursors that was suitable for large scale synthesis.

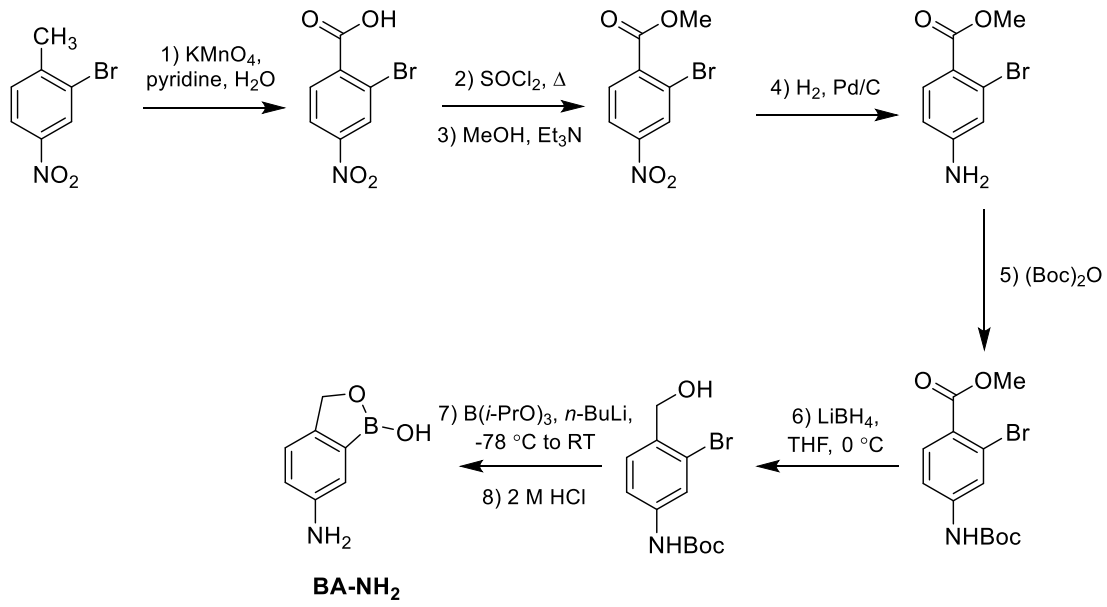

Scheme 16. Previously published synthesis of the BA-NH_2 building block.

Unforeseen events beyond our control in our collaborator's lab prevented copolymerisation and polymer grafting reactions from being carried out to prepare membrane materials at this time. Consequently, a new benzoxaborole based project was commenced, using benzoxaborole-functionalised polymer gels for the recognition of saccharides.

1.9.2 Chapter 3 - Dye Displacement Assay for Saccharide Detection with Boronic Acid Based Hydrogels

Previous work in the T.D. James group has demonstrated that boronic acid-functionalised hydrogels show a good binding affinity for fructose.[65] After reading papers by Hall and co-workers which reported that benzoxaboroles show an enhanced affinity for saccharides compared to traditional boronic acids,[40,41] it was hypothesised that incorporating the benzoxaborole functionality into hydrogels would further increase their sugar binding ability. It has also been reported that benzoxaboroles are able to complex non-reducing hexopyranoside sugars in solution, unlike traditional boronic acids.[40,41] Therefore we wanted to investigate whether benzoxaboroles were still capable of complexing non-reducing sugars when incorporated into a hydrogel structure. The overall aim of this project was to synthesise hydrogels which display an enhanced binding affinity for monosaccharide sugars compared to those previously prepared by the group.

1.9.3 Chapter 4 - The Synthesis of Fluorescent Probes for the Detection of Hydrogen Peroxide

Reactive oxygen species and reactive nitrogen species are important mediators in the pathological processes of many diseases including cerebral and cardiovascular diseases, inflammatory diseases, neurodegenerative diseases, diabetes and cancer. Because of their broad physiological and pathological consequences, the development of new methods for the detection of reactive oxygen species and reactive nitrogen species are required. The aim of this project was to synthesise a range of boronic acid pinacol ester-based fluorescent probes for the detection of hydrogen peroxide. A range of stilbene based boronic acid pinacol ester probes were synthesised and their fluorescence properties were investigated, along with a novel diphenyl oxazole based probe.

2 The Development of a Synthetic Route for Benzoxaborole-Functionalised Monomers for Applications in Membrane Separations

2.1 Introduction

2.1.1 Synthesis of Benzoxaboroles

Benzoxaboroles are internal esters of the corresponding *ortho*-boronobenzyl alcohols.[50] These alcohols are unstable and their dehydration is so easy that it will proceed even during crystallization from water. Subsequently a majority of synthetic methods for the formation of benzoxaboroles are based on either the introduction of a hydroxymethyl group to a boronic acid molecule; or the introduction of a boronic group to a benzyl alcohol. Depending on the specific conditions and functional groups present, appropriate protection of functional groups is necessary.

2.1.1.1 Functionalization of Boronic Acids and Derivatives

Unsubstituted benzoxaborole can be obtained from 2-methylphenylboronic acid in a multistep synthesis (Scheme 17).[38,55,66] The first step involves bromination of 2-methylphenylboronic acid using *N*-bromosuccinimide. Subsequent hydrolysis of this intermediate gives the benzyl alcohol, which is unstable and will spontaneously undergo intramolecular esterification to give benzoxaborole.

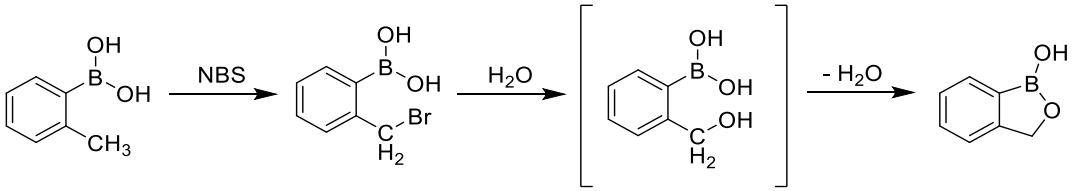

Scheme 17. Synthesis of benzoxaborole from 2-methylphenylboronic acid.

Benzoxaboroles with substitution at the 3-position can be obtained by the reaction of *ortho*-formylphenylboronic acid with nucleophiles.[67] Malonic acid, nitromethane and sodium cyanide have been used to form benzoxaboroles with carboxylic acid, nitro and cyanide substituents on the oxaborole ring respectively (Scheme 18). Reactions with secondary amines will lead to benzoxaboroles with an amino group at the 3-position.[68]

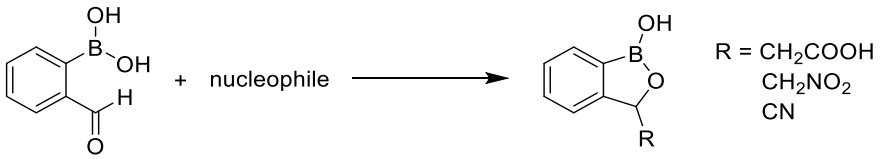

Scheme 18. Synthesis of benzoxaboroles from 2-formylphenylboronic acid.

More recently a large variety of novel 3-substituted benzoxaboroles have been synthesised by Kumar *et al*. Several benzoxaborole derivatives were synthesised from 2-formylphenylboronic acid utilising the Baylis-Hillman reaction, Barbier allylation, Passerini reaction and aldol reaction protocols as the key step.[69] The Barbier allylation reaction was used for the coupling of aryl bromides with boronoaldehydes in the presence of zinc and saturated ammonium chloride to form a variety of benzoxaboroles in good yields (**17**, Scheme 19). The Passerini reaction was utilised to synthesise α-amido benzoxaboroles by the reaction of boronoaldehydes with isonitriles (**18**, Scheme 19). α-acrylate substituted benzoxaboroles can be formed *via* the Baylis-Hillman reaction. The reaction is a highly atom efficient and environmentally benign carbon-carbon bond forming reaction that forms highly functionalised allylic compounds upon condensation of acrylates with aldehydes, using stoichiometric amounts of DABCO as a base (**19**, Scheme 19). Some aldol reactions were also investigated for the formation of β-keto substituted benzoxaboroles, but a large amount of unreacted starting material was recovered in all cases.[69]

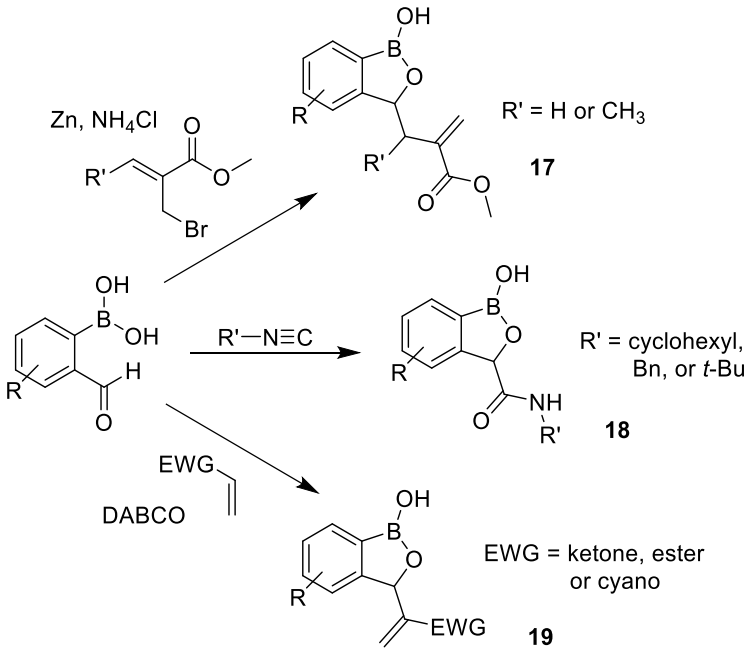

Scheme 19. Synthesis of benzoxaboroles from 2-formylphenylboronic acid using Baylis-Hillman reaction, Barbier allylation and Passerini reactions.

2.1.1.2 Functionalization of Benzyl Alcohols and Derivatives

The most common substrates for metalation reactions leading to benzoxaboroles are *ortho*-bromobenzyl alcohols.[50] Reaction of *ortho*-bromobenzyl alcohol with butyllithium yields the corresponding phenyllithium compounds.[56,68,70] The phenyllithium intermediate can then be reacted with triisopropyl borate to give the corresponding boronic ester, followed by hydrolysis to give the free boronic acid. This intermediate is unstable and will dehydrate spontaneously to give a benzoxaborole (Scheme 20).

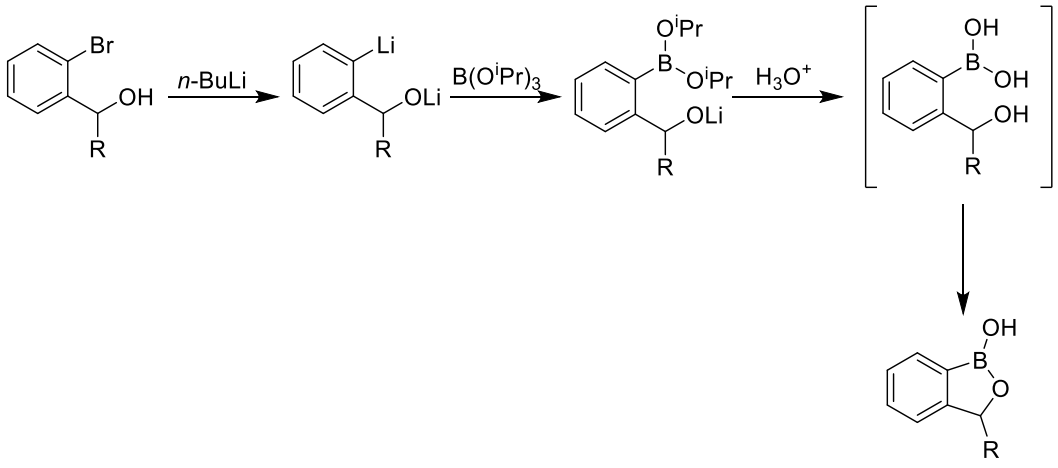

Scheme 20. Synthesis of benzoxaboroles from *ortho*-bromobenzyl alcohols.

Nicolaou and co-workers have converted 3,5-dimethoxybenzyl alcohol into the corresponding benzoxaborole by *N*-iodosuccinimide (NIS) iodination, followed by reaction with *n*-butyllithium and trimethoxyborate (Scheme 21).[71] Hydrolysis of the methoxyborate ester with hydrochloric acid generates the boronic acid, with the unstable intermediate then undergoing spontaneous dehydration to form the benzoxaborole.

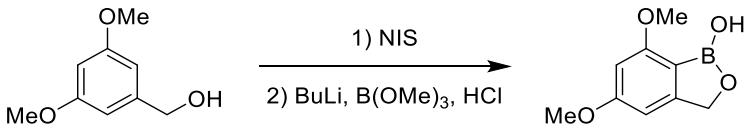

Scheme 21. Synthesis of benzoxaboroles from 2,5-dimethoxybenzyl alcohol.

2.1.1.3 Other Methods for the Synthesis of Benzoxaboroles

Another method of forming benzoxaboroles involves forming the C-B bond *via* a direct Suzuki-Miyaura coupling of bis(pinacolato)diboron to the aryl halide (Scheme 22).[72] Reaction of the pinacol intermediate with sodium borohydride reduces the aldehyde functionality to an alcohol, and subsequent treatment with hydrochloric acid removes the pinacol group to give the free boronic acid. This intermediate is unstable and spontaneously undergoes dehydration leading to the formation of a benzoxaborole.

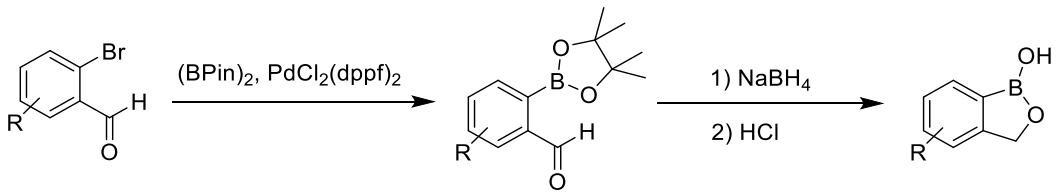

Scheme 22. Synthesis of benzoxaboroles by the Suzuki-Miyaura reaction.

The ruthenium-catalysed cyclotrimerization of the appropriate alkynes can be used for the formation of 5,7-substituted-disubstituted benzoxaboroles (Scheme 23).[58] The Cp*RuCl catalysed regioselective [2 + 2 + 2] cyclotrimerization of alkynylboronates, propargyl alcohol and terminal alkynes, proceeds through unsymmetrical diynes with a temporal C-B-O linkage cyclic to give arylboronate products as single regioisomers.

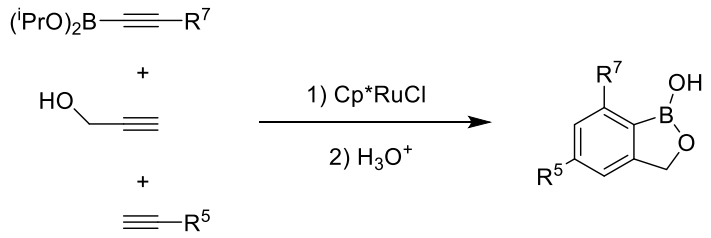

Scheme 23. Synthesis of benzoxaboroles by catalytic cyclotrimerization of alkynes.

Grassberger synthesised benzoxaboroles by hydrolysing 1,2-dihydro-1-hydroxy-2,3,1-benzodiazaborines to the corresponding benzoxaboroles in the presence of aqueous sodium hydroxide (Scheme 24).[57]

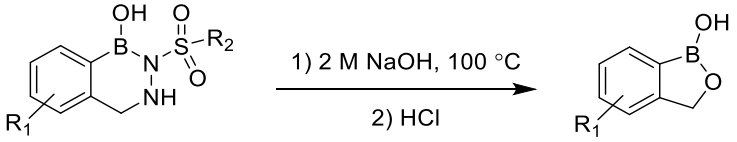

Scheme 24. Synthesis of benzoxaboroles by hydrolysis of 1,2-dihydro-1-hydroxy-2,3,1-benzodiazaborines.

Typically, introduction of the benzoxaborole heterocycle has been carried out at a late stage of a multi-step reaction synthesis, due to the inherent reactivity of boron's empty p orbital and complications in isolation and purification.[44] Recently, the Raines group has developed a divalent, charge-neutral protecting group designed specifically for benzoxaboroles.[73] 1-Dimethylamino-8-methylaminonaphthalene, was used to protect benzoxaboroles (Figure 10) in high yields, after azeotropic water removal. The resulting complexes can be readily cleaved *via* treatment with aqueous acid, yet are stable under basic and strongly reducing conditions. Further benefits of this protecting group are its compatibility with chromatographic separation and visible fluorescence upon long wavelength UV illumination. This protecting group significantly extends the scope of transformations that can be carried out on benzoxaboroles, therefore increasing their synthetic and application potential.

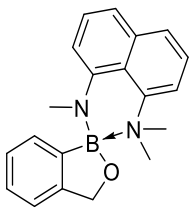

Figure 10. 1-Dimethylamino-8-methylaminonaphthalene derivative of benzoxaborole.

2.1.2 Applications of Benzoxaboroles

2.1.2.1 Medicinal Applications of Benzoxaboroles

Benzoxaboroles show a variety of antibacterial,[47] antiviral,[74] anti-parasitic[75] and anti-inflammatory activities,[52] with several benzoxaboroles currently undergoing clinical trials.[76] The low bio-toxicity of benzoxaboroles combined with their high target specificity make them very attractive as therapeutic agents.[44] 5-fluorobenzoxaborole (**9**, AN2690, tavaborole) is the first well studied benzoxaborole antifungal agent.[77] It effectively penetrates the nail plate and nail bed, and was approved by the FDA in 2014 for the topical treatment of onychomycosis.[42] Benzoxaboroles show great therapeutic potential, they have proved to be very safe and can provide novel pharmaceuticals for the treatment of diseases where resistance is emerging to existing drugs.

2.1.2.2 Applications of Benzoxaboroles in Organic Synthesis

One of the most important synthetic applications of benzoxaboroles is their use in Suzuki-Miyaura coupling.[59] In this reaction, benzoxaboroles or their esters are reacted with aryl halides to give *ortho*-aryl-substituted benzyl alcohols in high yields. For example, a 5,7-dimethyoxy-substituted benzoxaborole derivative was used in the total synthesis of Vancomycin by Nicolaou *et al*., wherein a benzoxaborole was cross coupled with an aryl iodide to obtain the benzyl alcohol intermediate for the total synthesis of vancomycin (Scheme 25).[71]

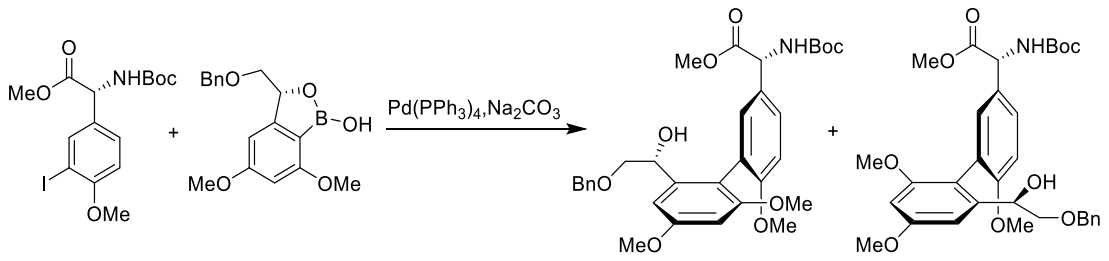

Scheme 25. A benzoxaborole derivative applied in the total synthesis of vancomycin.

2.1.2.3 Applications of Benzoxaboroles as Molecular Receptors

Unlike boronic acids, whose ability to bind polyols was widely investigated,[27] initially benzoxaboroles were only found to bind monoalcohols. Benzoxaboroles were not discovered to be an improved class of sugar-binding compounds until almost 20 years after their discovery.[41] Benzoxaboroles have many advantages such as good solubility in water, without the need for a co-solvent. They bind glycosides under physiologically relevant conditions and have been used for the design of oligomeric sensors for selective recognition of sugars, especially cell-surface glyconjugates.[40] Benzoxaboroles have great potential as a promising group of carbohydrate chemosensors.

Many of the applications of benzoxaboroles in molecular recognition involve the development of improved carbohydrate sensors. Many researchers are taking advantage of benzoxaborole's high affinity for sugar molecules at physiological pH. One way to enhance this affinity is the focus on multi-valency, where two or more binding units are arrayed with a specific geometry. Hall and co-workers have applied their discovery of efficient saccharide binding by benzoxaboroles to the construction of a peptidyl bis-benzoxaborole library that could be used as a synthetic receptor (Figure 11).[78] A rationally-designed library of synthetic receptors was targeted against an important tumour-associated carbohydrate antigen, the Thomsen-Friedenreich (TF) disaccharide. Because the TF antigen contains two diol units that bind preferentially with benzoxaboroles, two benzoxaborole units were included in the receptors. The receptors studied were found to have moderate binding affinity comparable to some lectins, but further studies are needed to exploit multivalency effects with oligomeric receptors and assess their efficiency in the labelling of TF-specific tumour cell lines.

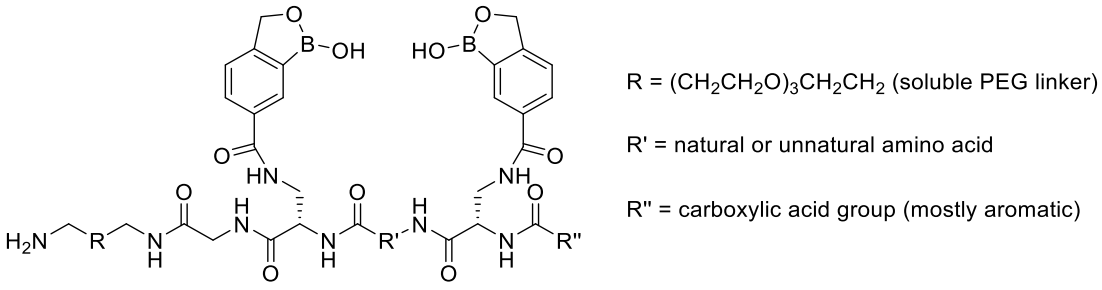

Figure 11. Design of peptidyl benzoxaborole disaccharide receptor library.

2.1.2.4 Applications of Benzoxaboroles in Materials Chemistry

The high affinity of benzoxaboroles for sugars and other diols under neutral aqueous conditions has also started to be utilised by materials scientists. Liu and co-workers have reported a method to attach benzoxaboroles to the surface of a monolithic capillary column for the chromatographic separation of various diols.[79] In their previous work using phenylboronic acid as the surface functionality, the authors were frustrated with the need for alkaline conditions.[80] Subsequently, 6-carboxy-benzoxaborole was used to functionalise methylene bisacrylamide/glycidyl methacrylate polymer capillary monoliths *via* amide bond formation (Figure 12). The columns prepared provided efficient chromatographic separation of a variety of nucleosides as well as efficient retention of model glycoproteins at neutral pH. These columns may also prove useful in the selective enrichment of nucleosides and glycosylated proteins.

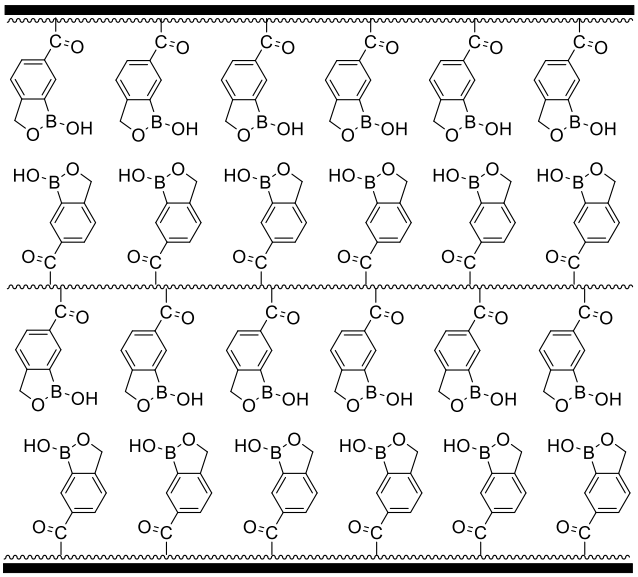

Figure 12. Benzoxaborole incorporation for affinity chromatography on monolithic capillary column.

A similar approach has been applied to the rapid enrichment of proteins that have been post-translationally glycosylated.[81] Beginning with a magnetic microsphere core coated with a shell of cross-linked poly(acrylic acid), standard amide bond formation chemistry was used to functionalise the surface of the beads with 6-aminobenzoxaborole (Figure 13). Once prepared, these beads allowed the easy enrichment of model glycoproteins from various complex biological media. Due to their magnetic properties, washing and recovery of the beads is highly efficient. By taking advantage of the reversible nature

of the complex formation between sugars and benzoxaboroles, the proteins may be easily released from the beads simply by lowering the pH of the solution.

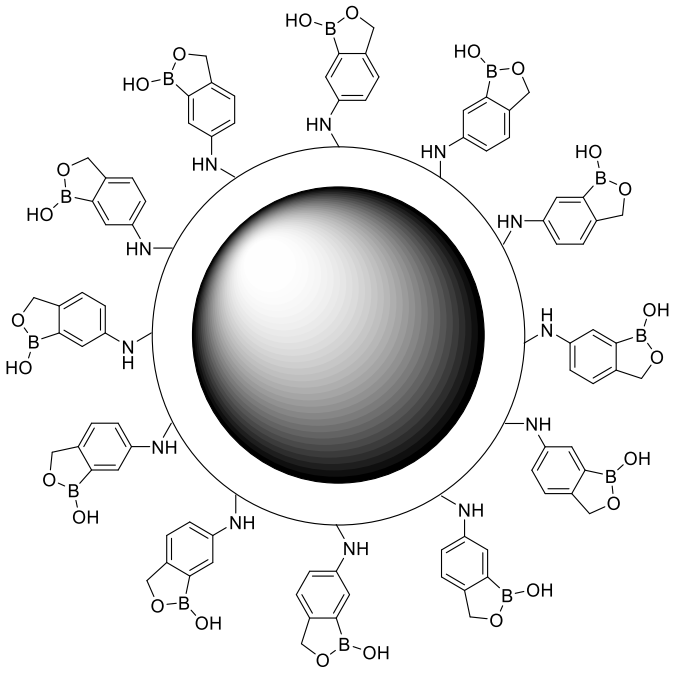

Figure 13. Glycoprotein enrichment with magnetic core-shell microspheres.

Besides their applications in chromatography and glycoprotein binding, benzoxaboroles have also been incorporated into smart materials, which can respond to environmental cues with changes in their physical properties. Kim *et al*. have developed a stimuli-responsive polymer, where the stimuli of interest was the presence of simple sugars. Synthesis of a 6-vinyl substituted benzoxaborole allowed for the direct incorporation of the benzoxaborole group into the polymer itself *via* reversible addition-fragmentation and chain transfer (RAFT) polymerisation.[82] The co-polymers produced were found to have unique properties including sugar binding and self-assembly into macromolecular vesicle-like structures called polymerosomes. It was found that the presence of sugars at neutral pH triggered the disassembly of these structures. The authors then investigated the encapsulation of insulin within these polymerosomes, and found that they could release the enclosed insulin in the presence of sugar. Materials such as these could prove useful as drug delivery systems for the treatment of sugar-related diseases.

2.1.3 Introduction to Membranes

From a chemical engineering point of view, membranes are defined as a selective barrier which separates a mixed fluid stream into two separate streams, by restricting the transport of the constituent chemical species either by size exclusion, or diffusion and partitioning by a selectivity of differing chemical properties.[83] Membranes now play an important role in many of the world's major industries including; dairy, food and beverage, chemical manufacture and wastewater treatment. The use of membranes has also revolutionised sustainable practices in some industrial sectors by allowing the recovery and reuse of previously wasted materials.[84] This practice enables these industries to be more environmentally sustainable by reducing the amount of waste produced, and more cost effective as less of these high value materials are needed.

Membrane processes require modest energy consumption compared with other more conventional separation techniques such as distillation,[83] making them an attractive alternative when considering greener technologies. Membranes also have other advantages over conventional separation techniques such as the generation of no additional waste products, lower running costs, and they also allow for greater flexibility as the membrane is 'tailor-made' to meet individual requirements.

Membrane separation processes involve the permeation of liquids or gases through a selective barrier under a specific driving force such as pressure or concentration. A membrane selectively splits a feed into two streams (Figure 14).[83] Porosity can be introduced into a membrane by extracting one component of a polymer blend, swelling the polymer in a solvent and then rapidly volatizing the solvent, or by etching techniques.[85] Porous membranes can also be synthesised using nanoparticles as pore templates, which can be extracted after fabrication of the polymeric materials.[86]

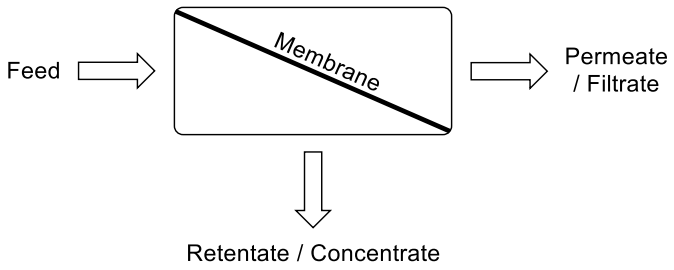

Figure 14. Basic membrane schematic.

The retentate or concentrate is the fraction that does not pass through the membrane, *i.e.* the portion retained. This consists of solutes that cannot be passed through the membrane, as well as solvent that does not have sufficient time or driving force to pass through the membrane. The permeate or filtrate is the fraction that passes through the membrane. This consists of the solvent and solutes that are able to pass through the membrane.

The ability of membranes to control the rate of permeation of different chemical species is what enables them to function for separations. For membranes to be useful for commercial separation processes, they must have a high selectivity, high mechanical stability, complete tolerance to feed stream components and tolerance to temperature variations.[83] Membranes, however, do have limited lifetimes and must be replaced periodically.

There are two main modes of filtration used in membrane processes: dead-end filtration (Figure 15a) and cross-flow filtration (Figure 15b).[83] In dead-end filtration, the feed flow is perpendicular to the membrane. As there is no retentate flow in this process, retentate builds up against the surface of the membrane until no more permeate can be collected. Therefore, these systems require regular backwashing, cleaning and replacement of membranes in order to overcome this fouling. Dead-end membranes, however, can better guarantee a complete rejection of molecules from the feed stream, since all flow must pass through the membrane. They are used in many industrial processes where guaranteed rejection of key species is required, such as the desalination of water.

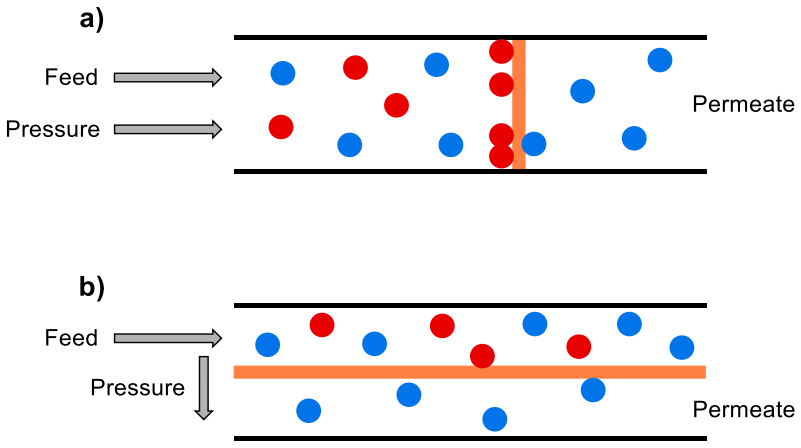

Figure 15. Schematic of a) dead-end membrane filtration processes and b) cross-flow membrane filtration processes.

In cross-flow filtration, the membrane lies parallel to the flow of the feed and not all of the solvent passes through the membrane. In contrast to dead-end filtration, this allows flow of the retentate stream across the surface of the membrane, minimising concentration polarisation and fouling of the membrane. Higher feed rates can therefore be used to control fouling. Cross-flow systems are more commonly used in industrial processes due to this potential for fouling control.

Membranes are used in a wide range of chemical processes. One of the major uses of membranes is the desalination of water by reverse osmosis. Reverse osmosis has been used to produce clean water through desalination, and has been applied in particular to the desalination of sea water in some of the largest scale applications of membrane technology worldwide.[87] Another use of membranes is for the recovery of high value components from multi-component mixtures, especially when temperature sensitive components are present such as biomolecules, active pharmaceutical ingredients and homogeneous transition metal based catalysts. Examples include the recovery of dilute biofuels from fermentation broths and the recovery of whey protein from milk.[83] Since a membrane is a barrier, wastewater can also be very effectively cleaned using membrane processes. If the water is to be reused, nanofiltration and/or reverse osmosis can be used as selective barriers to remove practically all pollutants, whilst allowing the clean water to permeate. This has been applied in treating food and beverage wastewaters,[88] oily waste and wastewater streams,[89] and the removal of emerging contaminants such as endocrine disrupting compounds, pesticides and pharmaceuticals.[90]

Membrane separations have become a new essential unit operation for effecting selective, low temperature separations either where other unit operations are not suitable for achieving a separation and/or as a lower energy, lower waste replacement for more conventional separations.

2.1.4 The Chemical and Biological Importance of Fluoride

Fluoride is the smallest anion and, due to its extreme hardness, often displays slightly different properties to the rest of the halides.[3] The real-time monitoring of fluoride ion concentration in aqueous and physiological media is of vital importance. Methods for the quantitative detection of fluoride over a large concentration range are required, due to the various environments in which fluoride is thought to have detrimental effects.

The role of fluoride in dental health appears to be one of balance. Fluoride is crucial in forming and preserving tooth enamel, however, exposure to higher levels can result in dental fluorosis. Ingestion of excess fluoride, most commonly in drinking-water, can cause fluorosis which affects the teeth and bones.[91] Long-term ingestion of large amounts of fluoride can lead to potentially severe skeletal problems. Chronic high-level exposure to fluoride can lead to skeletal fluorosis, where fluoride accumulates in the bone progressively over many years. The early symptoms of skeletal fluorosis, include stiffness and pain in the joints. In severe cases, the bone structure may change and ligaments may calcify, resulting in the impairment of muscles and pain. Acute systematic fluoride poisoning can result in kidney failure,[92] as well as systemic hypocalcaemia, cardiac dysrhythmias and cardiovascular collapse.[93]

Fluoride in water is mostly of geological origin. Known fluoride belts on land include: one that stretches from Syria through Jordan, Egypt, Libya, Algeria, Sudan and Kenya, and another that stretches from Turkey through Iraq, Iran, Afghanistan, India, northern Thailand and China.[94] In these areas fluorosis has been reported. Acute high-level exposure to fluoride is rare and usually due to accidental contamination of drinking-water or due to fires or explosions. Moderate-level chronic exposure (above the World Health Organisation guideline value for fluoride in water of 1.5 mg/L)[95] is more common. Removal of excessive fluoride from drinking-water is difficult and expensive. The preferred option is to find a supply of safe drinking-water with safe fluoride levels. Where access to safe water is already limited, de-fluoridation may be the only solution.

2.1.5 The Chemical and Biological Importance of Waste Grape Biomass

Grapes are one of the major global horticultural crops with an estimated production of 69.1 million tonnes during 2012, of which approximately 80% were wine grapes.[96] Grape marc (or pomace) is a by-product of wine industry. Grape marc consists mainly of peels (skins), seeds and stems and accounts for about 20–25% of the weight of the grapes crushed for wine production.[97] Grape seed is rich in extractable phenolic antioxidants such as phenolic acid, flavonoids such as catechin **20**, procyanidins and resveratrol **21**, while grape skins contain abundant anthocyanins such as **22** (Figure 16). The composition of grape marc is related to the grape variety, the method of processing, environmental conditions and the ratio of skin:seeds:stem.[98] Unlike other agricultural by-products, grape biomass waste has limited use as an animal feed stock due to its poor nutrient value and low digestibility (due to the high concentration of tannins and polyphenols). The polyphenols also slow down microbial utilisation of this biomass. A majority of these winery biomass wastes therefore end up as landfill.[96]

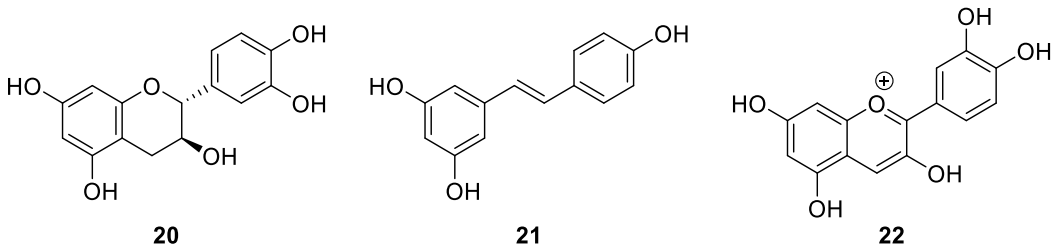

Figure 16. Examples of some of the polyphenol compounds found within grape marc.

The health benefits of grape marc polyphenols are of great interest of researchers, the food industry and nutraceutical industry. Antioxidant activity is the most notable bioactivity of phenolic compounds from grape marc.[97] The antioxidative characteristics have been widely studied, including scavenging of free radicals, inhibition of lipid oxidation and reduction in hydroperoxide formation.[99] Numerous studies have demonstrated that grape seed phenolics have many health benefits such as antimutagenic and anticarcinogenic activity,[100] antioxidant and anti-inflammatory activities,[101] prevention of cardiovascular diseases,[102] and can delay the onset of age-related markers.[103] Resveratrol is another important polyphenol found in grape skins and seeds. Resveratrol, which is rich in grape skin, has been reported to have strong antifungal and antibacterial activities.[97] In addition to antioxidant activities and therapeutic functions, many plant phenolic extracts have been shown to have

antimicrobial activity against specific strains of bacteria such as *Streptococcus mutans*, *Staphylococcus aureus*, *Escherichia coli* and *Candida albicans*.[104,105] Therefore, polyphenols extracted from grape marc have the potential to be used for food preservation and medicinal purposes to suppress the growth of pathogenic bacteria and prevent oxidation of lipids. Some polyphenols have long been used in food products. For example, anthocyanins from grapes and berries are used as food colourants.[97]

Due to the diverse potential applications for the polyphenol compounds found in waste grape biomass, there is the need for new routes for these 'waste' products to be converted into useful products. Benzoxaborole-containing membranes could be used to extract these polyphenol compounds from an aqueous stream of waste grape biomass, as benzoxaboroles are reported to show strong binding to many diols, a functionality found in many of these compounds (Figure 16).[106]

2.1.6 Summary of Introduction

Benzoxaboroles are internal esters of the corresponding *o*-boronobenzyl alcohols. A majority of synthetic methods for the formation of benzoxaboroles are based on either the introduction of a hydroxymethyl group to a boronic acid, or the introduction of a boronic group to a benzyl alcohol. Benzoxaboroles show great therapeutic potential, they have proved to be very safe and can provide novel pharmaceuticals for use against diseases where resistance is emerging to existing approaches. Benzoxaboroles are also being used as molecular receptors for the enhanced binding of sugars, and show potential as sensors for cell-surface glyconjugates. The high affinity of benzoxaboroles for diols has also been utilised by materials scientists in the development of benzoxaborole-functionalised monolithic capillary columns for chromatographic separations, as well as sugar responsive polymers.

Membrane separation processes involve the permeation of liquids through a selective barrier under a specific driving force. Membranes play an important role in many of the world's major industries including dairy, food and beverage, chemical manufacture and wastewater treatment. Incorporation of the benzoxaborole functionality into polymer membranes could lead to a new class of membranes with different chemical properties. Due to the strong affinity of boronic acids for diols and fluoride, these membranes could find many applications such as the separation of polyols from an aqueous stream of waste grape biomass or the removal of fluoride from drinking water.

2.2 Results and Discussion

2.2.1 Synthesis of Benzoxaboroles with Substitution on the Oxaborole Ring

Benzoxaboroles can be thought of as internal esters of the corresponding phenylboronic acids, therefore phenylboronic acids are commonly employed as starting materials for the synthesis of benzoxaboroles. Most benzoxaboroles have substitution on the phenyl ring, modification of the free position of the oxaborole ring is much less common.[76] Using 2-formylphenylboronic acid as the starting material, the aldehyde is susceptible to nucleophilic attack, activating its oxygen atom and then resulting in intramolecular nucleophilic attack at the boron atom. This attack closes the ring, leading to the formation of a benzoxaborole with a new substituent on the carbon atom of the oxaborole ring. These reactions proceed with high atom efficiency, and therefore can provide a reasonably green method for the formation of benzoxaboroles. Therefore, 2-formylphenylboronic acid was reacted with malonic acid in the presence of pyridine (Scheme 26).

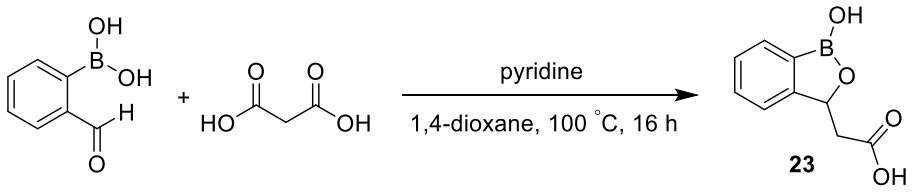

Scheme 26. Reaction of 2-formylphenylboronic acid with malonic acid.

Initial deprotonation of malonic acid at the α-position by pyridine activates the nucleophile, leading to subsequent nucleophilic attack at the aldehyde of 2-formylphenylboronic acid (Scheme 27). The aldehyde oxygen is now activated, leading to an intramolecular nucleophilic attack at the boron atom, and thus formation of the oxaborole ring. The intermediate dicarboxylic acid then undergoes thermal decomposition upon heating to form the monocarboxylic acid product **23** with the loss of a molecule of carbon dioxide.[49]

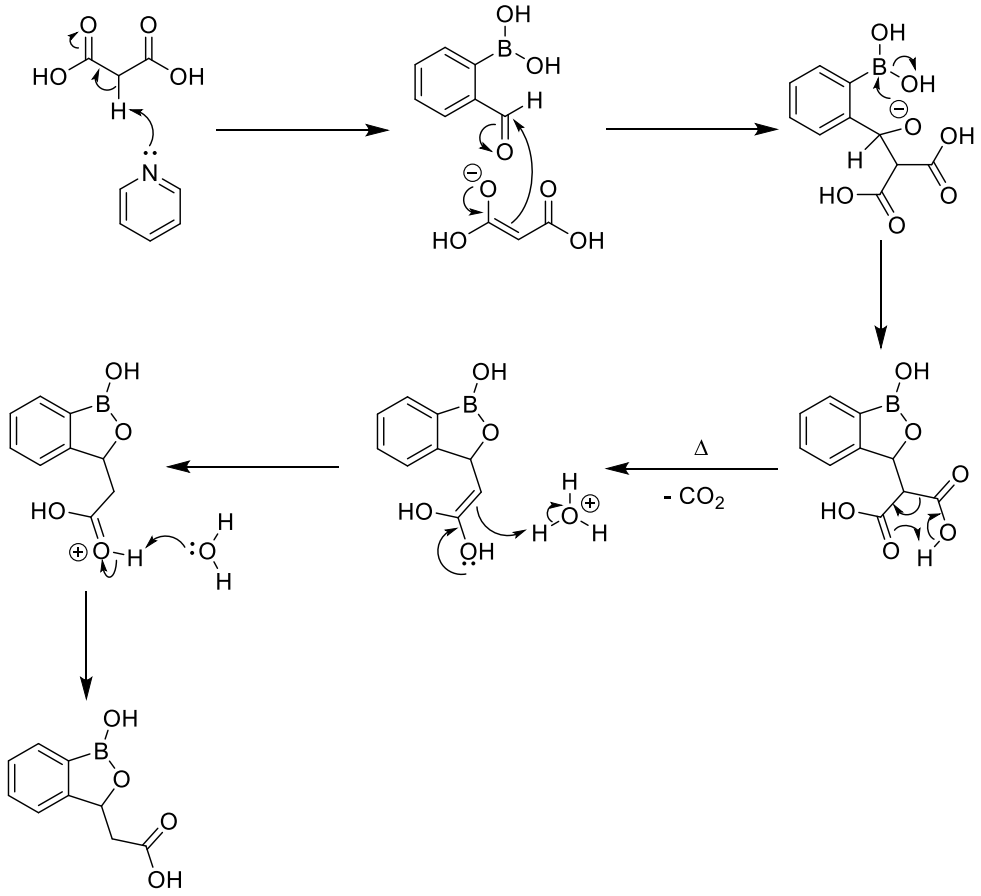

Scheme 27. Mechanism for the reaction between 2-formylphenylboronic acid and malonic acid.

The ^{1}H NMR spectrum of the crude reaction mixture confirmed the presence of the desired product, along with large amounts of unreacted starting materials and other impurities. The crude reaction product was only partially soluble in a small number of solvents, so purification by recrystallization could not be achieved. Column chromatography would also have proven unsuccessful, as the spot corresponding to the desired product remained on the baseline of the TLC plate in a large number of solvent systems of increasing polarity screened for the separation. This is due to the strong interaction of the free carboxylic acid groups with the silica gel.

After isolation of the monocarboxylic acid product **23**, this intermediate would have been subjected to a coupling reaction with an allyl amine derivative to give an alkenyl product such as that shown in Scheme 28. This intermediate could then have been used as the monomer for subsequent polymerisation for the formation of membranes.

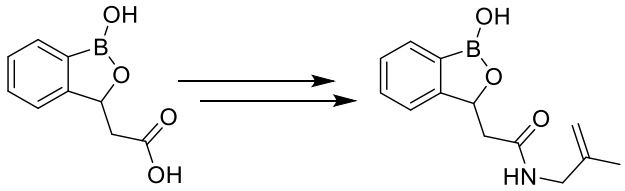

Scheme 28. Initially planned functionalization of monocarboxylic acid.

As the isolation of the free monocarboxylic acid product **23** proved unsuccessful, it was postulated that if a derivative was formed where there were no free carboxylic acid groups, this should allow for easier separation of the product as purification by column chromatography should be possible. The protecting functionality could then be removed after purification, leading to the formation of a clean product. With this in mind, 2-formylphenylboronic acid was reacted with dibenzyl malonate (Scheme 29).

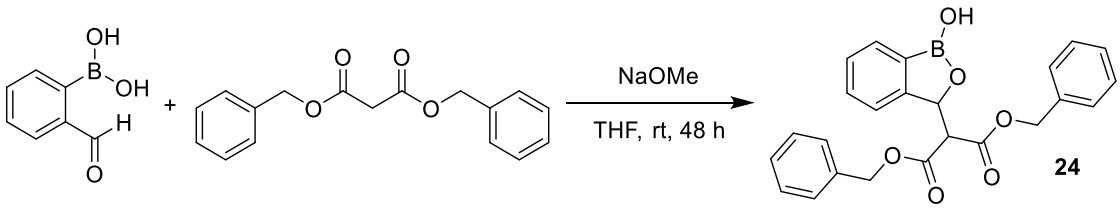

Scheme 29. Reaction of 2-formylphenylboronic acid with dibenzyl malonate.

The dibenzyl malonate is deprotonated at the α-position by sodium methoxide, activating it for nucleophilic attack of the 2-formylphenylboronic acid. The activated oxygen of the aldehyde then attacks the boron atom leading to the formation of the oxaborole ring (Scheme 30).

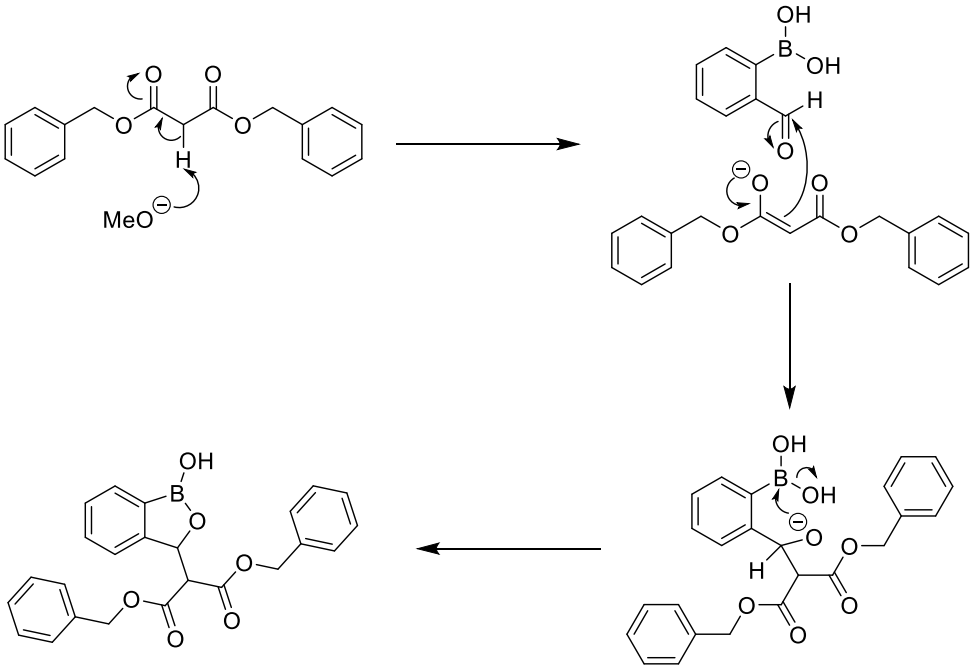

Scheme 30. Mechanism for the formation of dibenzyl 2-(1-hydroxy-1,3-dihydrobenzo[*c*][1,2]oxaborol-3-yl)malonate **24**.

A ^{1}H NMR spectrum of the crude reaction mixture confirmed the presence of the desired product, along with unreacted excess dibenzyl malonate. As there are no free carboxylic acid groups present, the product does not interact strongly with silica gel and is therefore easily purified in high yields by flash column chromatography.

Removal of the benzyl groups to yield the dicarboxylic acid **25** was then attempted. It was postulated that reaction of the dibenzyl malonate-substituted product **24** with palladium on carbon and hydrogen gas would yield the dicarboxylic acid product **25**, which could then undergo subsequent thermal decarboxylation to give the desired monocarboxylic acid product **23** (Scheme 31).

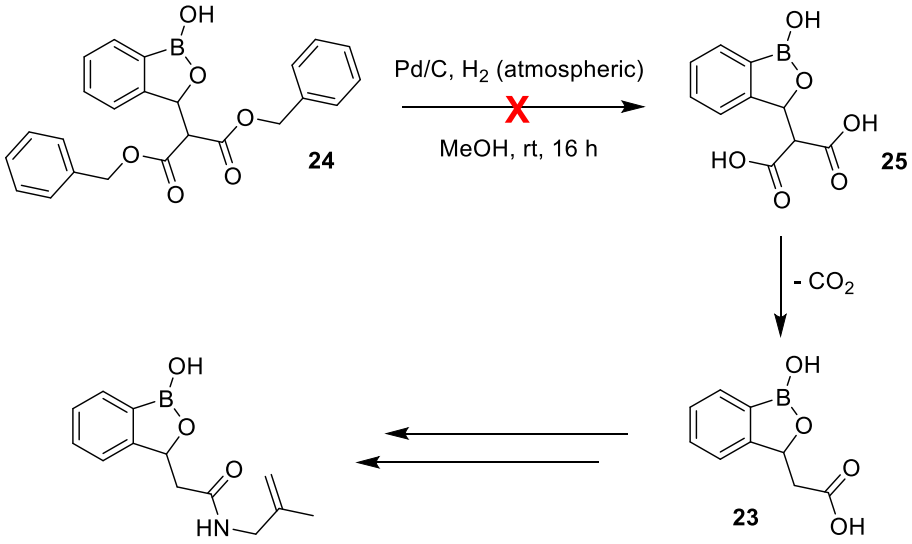

Scheme 31. Planned debenzylation of **24**.

The dibenzyl malonate-substituted product **24** was reacted with palladium on carbon and hydrogen gas and left to stir overnight. ^{1}H NMR spectroscopic analysis of the crude reaction product in DMSO-d_6 showed neither of the characteristic methylene peaks at δ 5.21 and 4.99 ppm of the benzyl groups, suggesting that they had been successfully removed. However, the crude ^{1}H NMR spectrum also showed no peak around δ 9.39 ppm corresponding to the OH group of the oxaborole ring, which is always visible in NMR spectra of this class of compounds in DMSO. The peak at δ 5.75 ppm corresponding to the CH proton of the oxaborole ring was also not present, suggesting that the oxaborole ring was destroyed. It was postulated that the hydrogenation reaction had been left for too long, so the reaction time was reduced to 1 hour, then 30 minutes. Again, the ^{1}H NMR spectrum of the crude reaction product suggested that the oxaborole ring had been destroyed. It is hypothesised that the dibenzyl malonate-substituted product is being hydrolysed back to the starting 2-formylphenylboronic acid and dibenzyl malonate, which subsequently react with the palladium on carbon and hydrogen gas to form 2-(hydroxymethyl)phenylboronic acid and malonic acid respectively (Scheme 32).

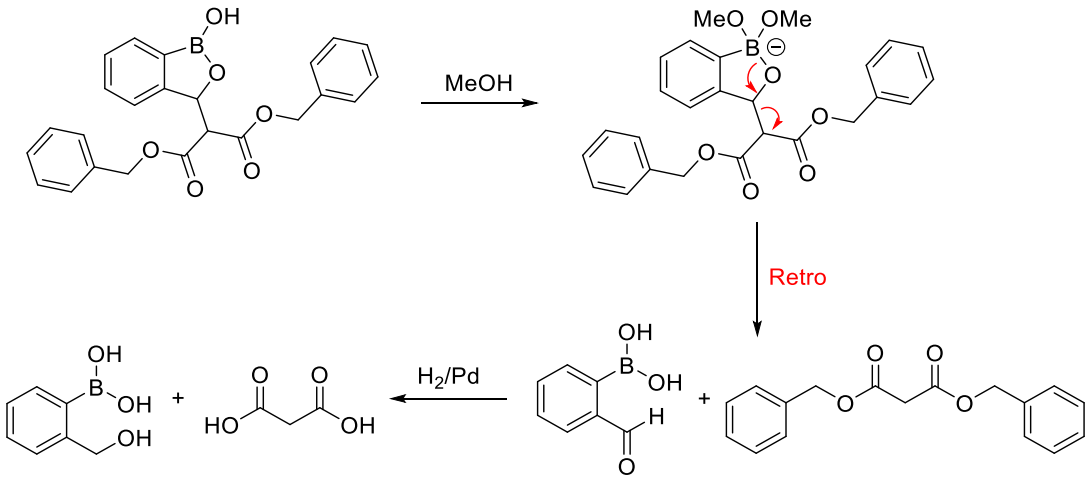

Scheme 32. Hypothesised reaction between dibenzyl malonate-substituted product and Pd/C.

Palladium hydroxide on carbon, generally known as Pearlman's catalyst, is used in various hydrogenation and hydrogenolysis reactions, and is also used as a debenzylation agent.[107] The catalyst is particularly active for *N*- or *O*-debenzylation, and has proven successful even where other palladium on carbon catalysts have failed.[108] In addition, the catalyst can tolerate an electron-withdrawing group on the aromatic ring and is also effective for sterically hindered substrates. Palladium hydroxide on carbon ($Pd(OH)_2/C$) and hydrogen were reacted with the dibenzyl malonate-substituted product **24** (Scheme 33) in a further attempt to remove the benzyl groups. The reaction was left to stir at room temperature for 1 hour. The crude ^1H NMR spectrum of the reaction mixture showed that the benzyl groups had been removed, but once again the oxaborole ring has been destroyed.

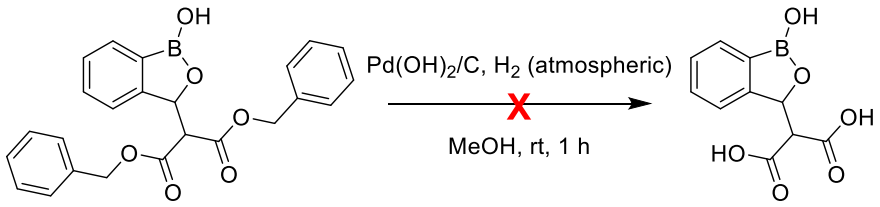

Scheme 33. Failed debenzylation of **24** with Pearlman's catalyst.

There are several reports in the literature of hydrogenation reactions carried out on benzoxaboroles, suggesting that the oxaborole ring should be stable under these conditions.[109,110] Indeed, the oxaborole core is stable under hydrogenation conditions with palladium on carbon; these conditions were used for the reduction of a nitro-

substituted benzoxaborole to an amino-substituted benzoxaborole, as discussed in the next section of this report.

After several different debenzylation reactions using palladium on carbon and hydrogen failed to yield the desired product, base-catalysed hydrolysis of the esters was attempted instead. The dibenzyl malonate-substituted product **24** was dissolved in a small volume of methanol and treated with 2 M NaOH overnight. A ^{1}H NMR spectrum of the reaction product showed that once again the oxaborole fragment had been destroyed. The reaction was repeated with the less basic lithium hydroxide and shorter reaction times, again without success. The crude ^{1}H NMR spectrum showed a small peak at δ 10.12 ppm had started to appear which could correspond to the aldehyde proton of the starting 2-formylphenylboronic acid, supporting the hypothesis that the benzoxaborole ring has been hydrolysed back to the starting 2-formylphenylboronic acid and dibenzyl malonate (Scheme 34). The literature reports that benzoxaboroles are resistant to hydrolysis and can be recovered almost quantitatively after refluxing with 15% NaOH for three hours,[53] therefore it was surprising that the benzoxaborole ring was destroyed.

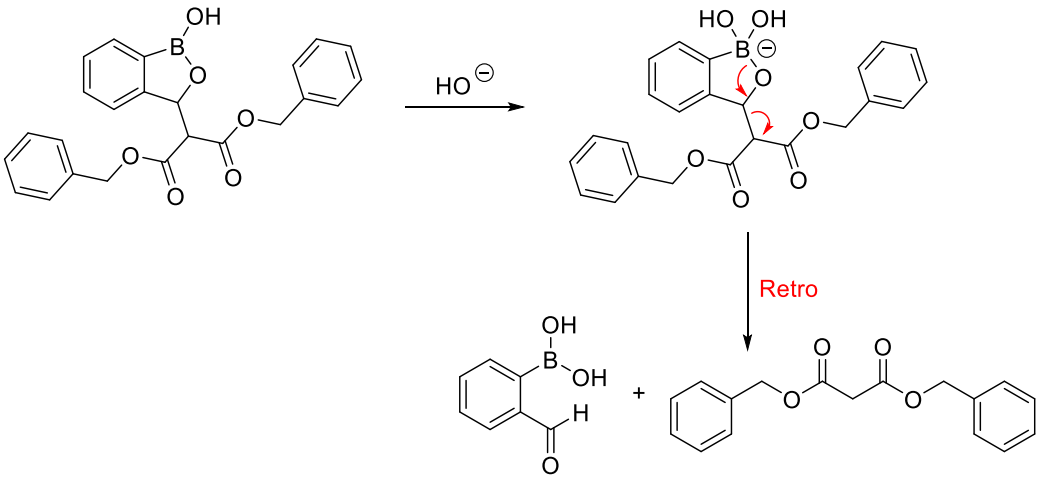

Scheme 34. Proposed hydrolysis of dibenzyl malonate-substituted product.

As removal of the benzyl groups of the dibenzyl malonate-substituted benzoxaborole **24** was proving difficult, a diethyl malonate-substituted derivative **26** was synthesised instead (Scheme 35).

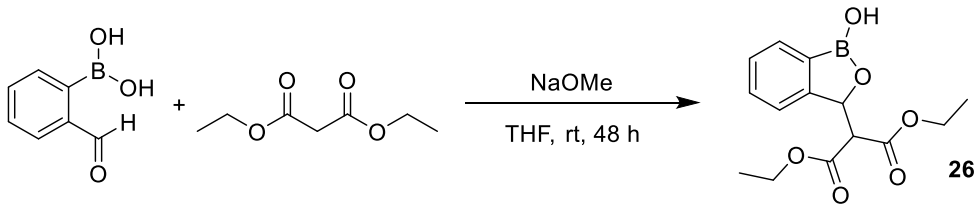

Scheme 35. Reaction of 2-formylphenylboronic acid with diethyl malonate.

The reaction proceeds *via* the same mechanism as the analogous reaction between 2-formylphenylboronic acid and dibenzyl malonate. Base-catalysed hydrolysis of the ester bonds was also attempted for the diethyl malonate-substituted product **26**, again without success.

At this point, since functionalization of the oxaborole ring had proved unsuccessful, attention was focused on the synthesis of benzoxaborole derivatives with substituents on the phenyl ring.

2.2.2 Synthesis of Benzoxaboroles with Substitution on the Phenyl Ring

Again using 2-formylphenylboronic acid as the starting material, benzoxaborole derivatives were synthesised with functionalization on the phenyl ring. The benzoxaborole core **8** was formed by treating 2-formylphenylboronic acid with sodium borohydride (Scheme 36).

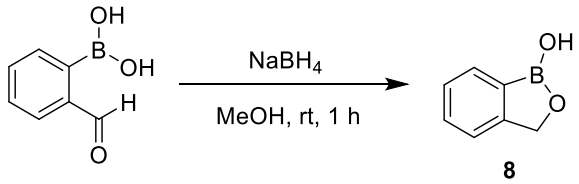

Scheme 36. Reaction of 2-formylphenyl boronic acid with sodium borohydride.

The sodium borohydride reduces the aldehyde of the 2-formylphenylboronic acid to an alcohol, the intermediate formed is highly unstable and immediately cyclises to form the oxaborole ring with the loss of a molecule of water (Scheme 37).

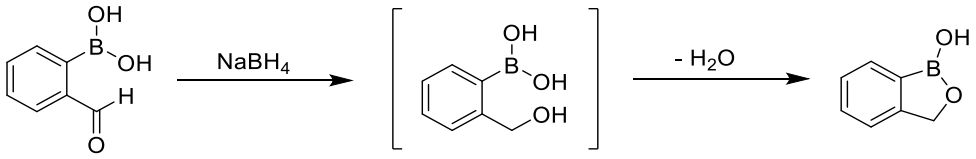

Scheme 37. Reaction of 2-formylphenylboronic acid with sodium borohydride to form benzoxaborole.

The reaction proceeds easily and cleanly at room temperature in an almost quantitative yield (99.8%), and no purification of the product is required.

The benzoxaborole core **8** can easily be nitrated *via* reaction with fuming nitric acid to give 6-nitrobenzoxaborole **27** (Scheme 38).

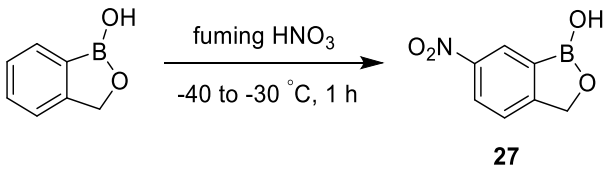

Scheme 38. Nitration of benzoxaborole with fuming nitric acid.

A proportion of the nitric acid undergoes self-dehydration giving rise to the nitronium ion, a nitrate ion and water (Scheme 39).[111] It is the nitronium ion which is the reactive species, which is attacked by the phenyl ring of benzoxaborole in an electrophilic aromatic substitution reaction. The intermediate carbocation (of which only one

resonance form is shown) is deprotonated by a molecule of water to give the nitro-substituted product.

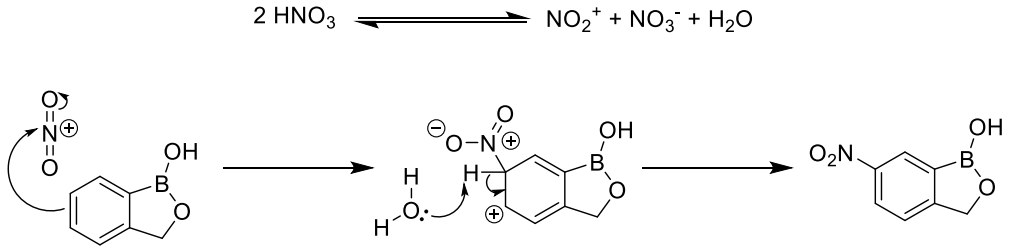

Scheme 39. Mechanism for nitration of benzoxaborole with fuming nitric acid.

The crude reaction product can be recrystallised from hot ethanol to give the purified product as a pale yellow powder in a reasonable yield of 66%. The product is formed as one regioisomer, with nitration at the 6-position, as observed by Snyder,[55] Jiang,[112] and Jonnalagadda.[113] This was confirmed by ^{1}H NMR spectroscopic analysis.

The nitro group can easily be reduced to an amine by a hydrogenation reaction using palladium on carbon and hydrogen gas (Scheme 40).

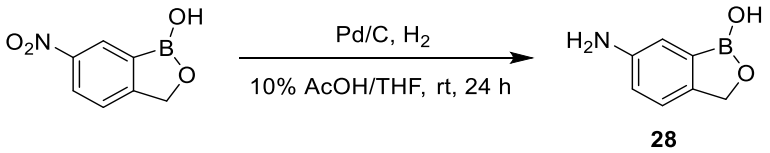

Scheme 40. Reduction of nitrobenzoxaborole to aminobenzoxaborole with palladium on carbon and hydrogen gas.

The reaction proceeds easily at room temperature, proving that the benzoxaborole core is stable to hydrogenation conditions with palladium on carbon and hydrogen. The amino-substituted product **28** is formed in good yields of 78% without the need for further purification.

Ammonium formate was also investigated as a hydrogen source. In the presence of a palladium catalyst the ammonium formate decomposes to give ammonia, carbon dioxide and hydrogen.[114] Many reported procedures using ammonium formate as a hydrogen transfer agent in the presence of a palladium on carbon catalyst report that the reaction requires refluxing in methanol,[115] however for the reduction of 6-nitrobenzoxaborole **27** to 6-aminobenzoxaborole **28** the reaction was found to proceed at room temperature when left to stir overnight.

The modified hydrogenation conditions utilising ammonium formate as the hydrogen source makes the reaction more amenable to scale up, which would be important when the reaction is carried out on a larger scale for the synthesis of considerable quantities of the monomer 6-methacrylamidebenzoxaborole **29**. The amount of hydrogen that can fit into a balloon limits the scale on which the reaction can be run, or requires the use of a pressurised reaction system. The amount of ammonium formate used can be easily increased, overcoming this problem.

Once the hydrogenation reaction for the preparation of 6-aminobenzoxaborole **28** had been optimised, attention was focused on the conversion of this product into 6-methacrylamidebenzoxaborole **29**. 6-methacrylamidebenzoxaborole **29** was synthesised *via* a coupling reaction between 6-aminobenzoxaborole **28** and methacrylic acid, utilising HBTU as the coupling reagent (Scheme 41).

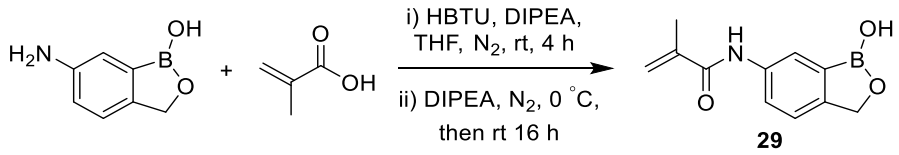

Scheme 41. Synthesis of 6-methacrylamidebenzoxaborole **29** with methacrylic acid.

The reaction proceeds *via* the mechanism shown in Scheme 42. In the first step the *N*,*N*-diisopropylethylamine (DIPEA) deprotonates the methacrylic acid. The resulting carboxylate anion then attacks the electron deficient carbon atom of HBTU, leading to the formation of a tetrahedral intermediate. The iminium ion is then reformed, resulting in cleavage of the HOBt group. The resulting HOBt anion then reacts with the newly formed activated methacrylic acid-derived intermediate to form an OBt-activated ester. The 6-aminobenzoxaborole reacts with the OBt-activated ester to form the protonated 6-methacrylamidebenzoxaborole product, along with HOBt, DIPEA then removes a proton to give the final 6-methacrylamidebenzoxaborole product.

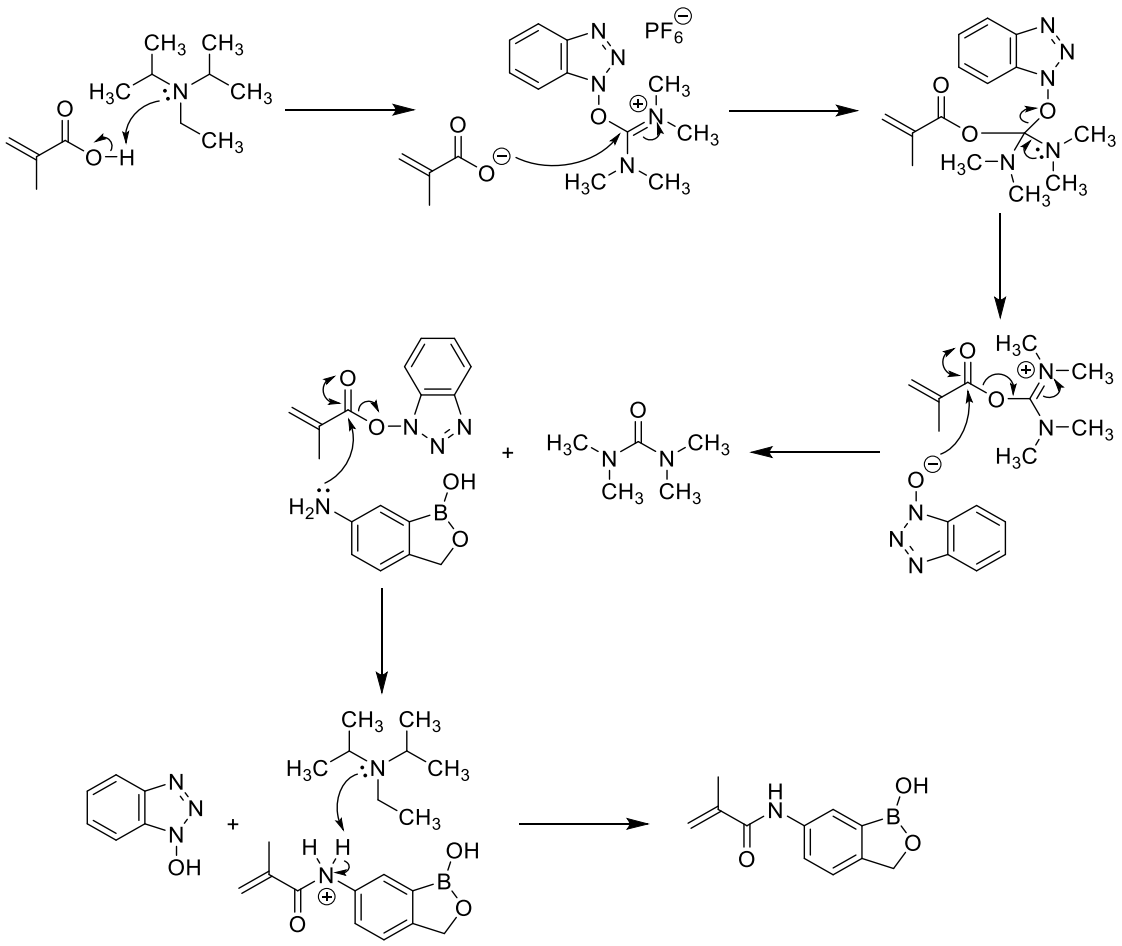

Scheme 42. Mechanism of the coupling reaction between methacrylic acid and 6-aminobenzoxaborole.

A ^{1}H NMR spectrum of the crude reaction mixture showed the presence of the desired 6-methacrylamidebenzoxaborole product, which could be easily separated by column chromatography to give the desired product as a pale brown powder in 86% yield.

While the HBTU coupling reaction works well to give the desired 6-methacrylamidebenzoxaborole product, it is not particularly sustainable as it requires stoichiometric amounts of expensive coupling reagents and generates large quantities of waste. Purification is achieved by flash column chromatography, which isn't well suited to large scale synthesis. Also, issues arising from unwanted polymerisation occurred when the reaction was scaled up. As larger amounts of product were produced, polymerisation was found to occur during the purification process.

A literature procedure reported that the 6-methacrylamidebenzoxaborole product could be produced from reaction of 6-aminobenzoxaborole with methacryloyl chloride, utilising sodium hydroxide as the base.[116] The literature reports acidifying the reaction

mixture slowly at 0 °C with concentrated HCl in order to precipitate out the desired product. However, this was attempted several times, each time the product polymerised in solution and precipitated out in large clumps, even when very dilute HCl was used. The use of weaker acids was also investigated, again without success. Synthetic procedures for the preparation of acrylamido boronic acid monomers have also previously been reported to have issues associated with unwanted polymerisation.[117]

A more extensive analysis of the literature was carried out and a procedure was found for the reaction of 6-aminobenzoxaborole with acryloyl chloride, avoiding the use of acid to precipitate out the desired product.[112] 6-Aminobenzoxaborole and sodium hydrogen carbonate were dissolved in a 1:1 mixture of THF and water and cooled down to 0 °C. Methacryloyl chloride was then added *via* syringe pump over a period of one hour (Scheme 43).

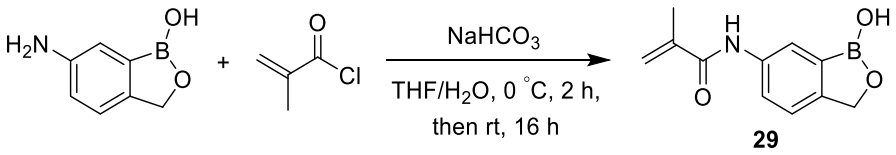

Scheme 43. Synthesis of 6-methacrylamidebenzoxaborole **29** with methacryloyl chloride.

The reaction proceeds *via* the nucleophilic addition elimination mechanism shown in Scheme 44. The 6-aminobenzoxaborole attacks the carbonyl carbon of the methacryloyl chloride, resulting in subsequent loss of a chloride ion. Loss of a proton then leads to the formation of the 6-methacrylamidebenzoxaborole product.

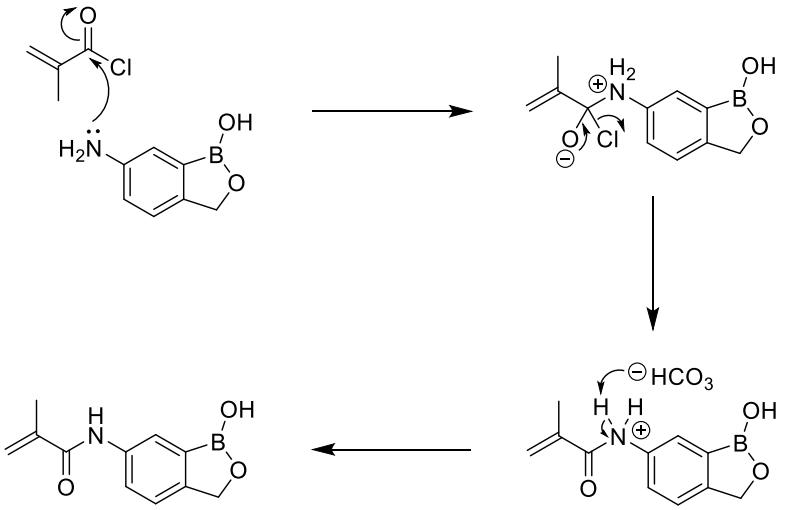

Scheme 44. Mechanism for the reaction between methacrylic acid and 6-aminobenzoxaborole.

A crude reaction product was obtained after THF was evaporated. After an aqueous work up, the product was concentrated under reduced pressure, to give a pale brown solid in 82% yield. As this method for the synthesis of 6-methacrylamidebenzoxaborole avoids the use of stoichiometric amounts of coupling reagents, it is much better suited to large scale synthesis.

Overall, a new synthetic route to the benzoxaborole monomer 6-methacrylamidebenzoxaborole **29** has been developed, giving the product in 43% yield over the four steps (Scheme 45). The 6-aminobenzoxaborole intermediate **28** is produced in 52% yield, which is much higher than the previously published synthetic route which gave this product in 27% yield. This route therefore fulfils the aim of this project by providing a synthetic route starting from readily available precursors which is suitable for larger scale synthesis, giving the desired product in higher yields compared to previously published syntheses.

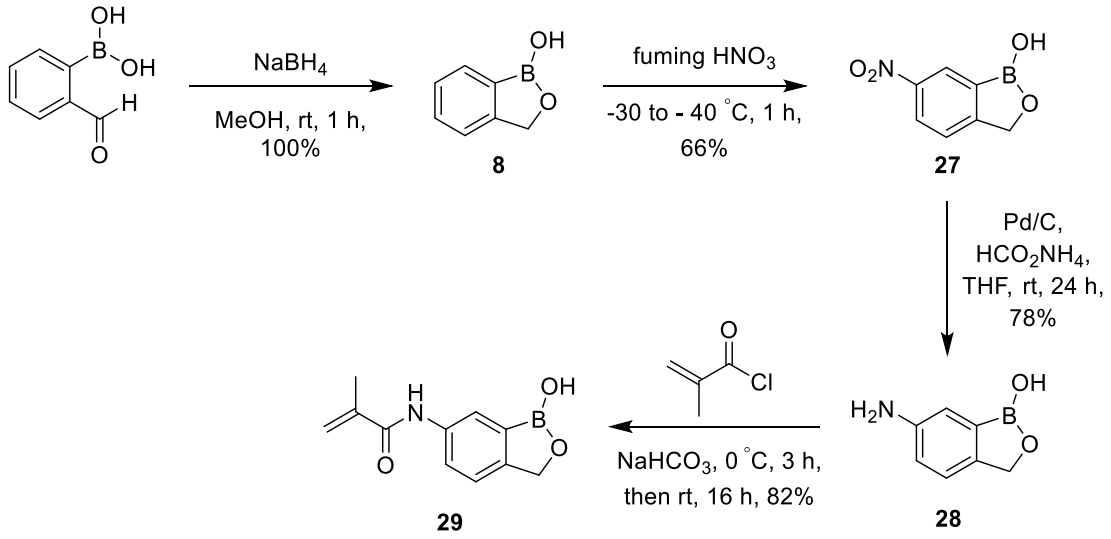

Scheme 45. Overall synthetic route to the benzoxaborole monomer 6-methacrylamidebenzoxaborole.

2.3 Conclusions

The aim of this project was the development of a new synthetic route to the benzoxaborole monomer 6-methacrylamidebenzoxaborole. The previously published synthesis of the 6-aminobenxozaborole compound involved six steps and the use of toxic and flammable reagents, and provided a low overall yield of 27%. The new synthetic route provides the 6-aminobenzoxaborole compound in three steps in an overall yield of 52%, an additional step can be incorporated for the conversion of this compound into the monomer 6-methacrylamidebenzoxaborole giving the product in an overall yield of 43%.

The synthesis of benzoxaboroles with substitution on the oxaborole ring proved unsuccessful due to issues with purification or debenzylation. The synthesis of benzoxaboroles with substitution on the phenyl ring proved more successful. The benzoxaborole core can be easily formed by reacting 2-formylphenylboronic acid with sodium borohydride. This benzoxaborole can be easily nitrated using fuming nitric acid, and a subsequent reduction with palladium on carbon and hydrogen gas gives the 6-aminobenzoxaborole. Subsequent reaction with methacryloyl chloride gives 6-methacrylamidebenzoxaborole. The reaction conditions have been modified to make the synthesis more suitable for scale up, which will be important for the synthesis of large quantities of the monomer for the production of polymer membranes.

Unforeseen events beyond our control in our collaborator's lab prevented copolymerisation and polymer grafting reactions from being carried out to prepare membrane materials at this time. Consequently, a new benzoxaborole based project was commenced, using benzoxaborole-functionalised polymer gels for the recognition of saccharides, the results of which are described in the following chapter.

2.4 Future Work

Now that a synthetic route to the benzoxaborole monomer 6-methacrylamidebenzoxaborole has been developed, future work should focus on the incorporation of this monomer into membrane materials. Initial studies should involve the incorporation of the benzoxaborole functionality into existing membranes. It is envisaged that this could be done by a direct coupling of the 6-aminobenzoxaborole with sulfonic acid groups on the membrane surface (Scheme 46).

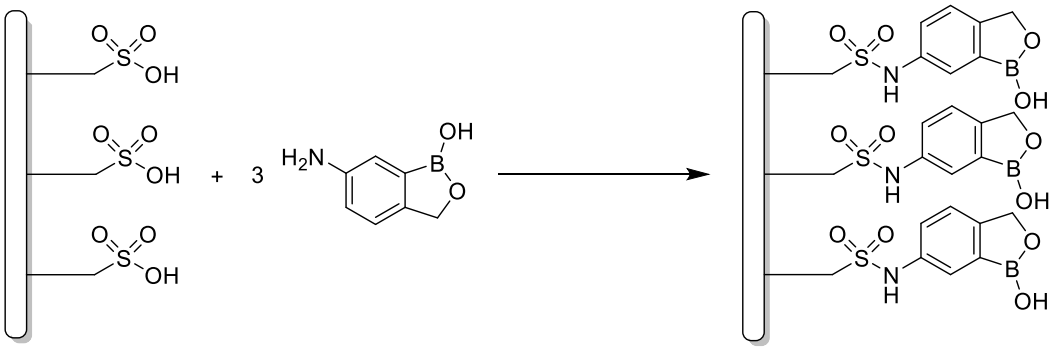

Scheme 46. Planned functionalization of sulfonic acid membranes with 6-aminobenzoxaborole.

The use of various polyethylene glycol (PEG) linkers should also be investigated, in order to increase the distance between the benzoxaborole functionality and the membrane surface. Polyethylene glycol is one of the most widely used biocompatible polymers. PEG linkers have been chosen to be investigated as they have high hydrophilicity and will therefore be readily solvated, decreasing aggregation and increasing the distance between the benzoxaborole core and the bulk of the polymer. The use of hydrophobic linkers would encourage the benzoxaborole functionality to sit closer to the bulk of the polymer, away from the water. Studies should be carried out to determine the optimal stoichiometry between the PEG linker and benzoxaborole core and the optimal levels of the benzoxaborole core incorporated into the membrane structure.

Once initial functionalization studies have been carried out on existing membranes, the polymerisation of the 6-methacrylamidebenzoxaborole monomer for the production of polymer membranes should be investigated. 6-Methacrylamidebenzoxaborole polymers have previously been synthesised by Reversible Addition-Fragmentation chain Transfer (RAFT) polymerisation with the use of various co-monomers.[118] Co-monomers such as styrene and acrylamide should be investigated for co-

polymerisation with 6-methacrylamidebenzoxaborole for the production of polymer membranes.

Once formed, the polymer membranes should be screened for their ability to selectively extract phenolic natural products from aqueous extracts of grape biomass and also for their ability to remove fluoride from water. Simple filtration techniques should be employed in order to evaluate the most selective and effective process suitable for the isolation of phenolic natural products and the fluoride anion.

3 Dye Displacement Assay for Saccharide Detection with Boronic Acid Based Hydrogels

3.1 Introduction

3.1.1 Introduction to Saccharides and Carbohydrates

Carbohydrates are one of the four major classes of organic compounds in living cells. They provide the main source of energy for our bodies, are building blocks for polysaccharides, and components of other molecules such as DNA, RNA, glycolipids, glycoproteins *etc*.[2] Carbohydrates include monosaccharides (e.g. glucose) and disaccharides (e.g. sucrose) which are often called sugars, and large carbohydrate molecules (e.g. starch and cellulose), known as polysaccharides. Saccharides, which are the product of photosynthesis, account for the most abundant class of organic compounds on the surface of the earth. In their most ubiquitous roles, they provide nature with structural rigidity, in the form of cellulose, and they also provide the energy store, in the form of starch and glycogen, that sustains life.[119]

As well as being abundant, these compounds are also incredibly versatile. Oligosaccharides are involved in protein targeting and folding, as well as controlling the cell recognition events for inflammation, infection and immunity.[120] The monitoring of D-glucose is particularly important from a medical perspective, since D-glucose provides the metabolic energy for most cells within higher organisms. In humans, a breakdown in the pathways of D-glucose transport has been linked to several conditions including cancer,[121] cystic fibrosis,[122] and renal glycosuria,[123] however by far the most prevalent condition arising from the ineffective transport of D-glucose is diabetes mellitus.[124] Because of the important role that sugars play in the progression of various diseases, they are attractive targets for artificial receptors. If receptors can be designed to selectively recognise and report the presence of particular sugars then they could be employed as powerful tools in biological diagnostics and imaging.

3.1.2 Structure of Saccharides

The simplest carbohydrates are monosaccharides, consisting of single polyhydroxyl aldehyde or ketone units. These monosaccharides can form disaccharides, oligosaccharides and polysaccharides through glycosidic bonds. According to the position of the carbonyl group, monosaccharides are classified as aldoses or ketoses. The detection of saccharides presents a challenge due to their structural complexity. The linear form of D-glucose for example contains four stereocentres, giving rise to many stereoisomers.[27] In aqueous solution, the situation is even more complex. Saccharides with four carbons or more tend to form cyclic structures, in which the carbonyl group forms a covalent bond with a hydroxyl group along the chain. Cleavage of the hemiacetal ring causes interconversion between the pyranose and furanose ring forms *via* an acyclic intermediate, and inversion of configuration at the anomeric centre gives rise to α- and β-anomers, which can alter the optical rotation of its solutions (Figure 17). These properties substantially increase the number of possible structures that may be formed, making saccharides difficult to differentiate from each other. In addition, receptors for saccharides may be heavily solvated in water, with differentiation between water and hydroxyl groups of the saccharides presenting a difficult challenge.

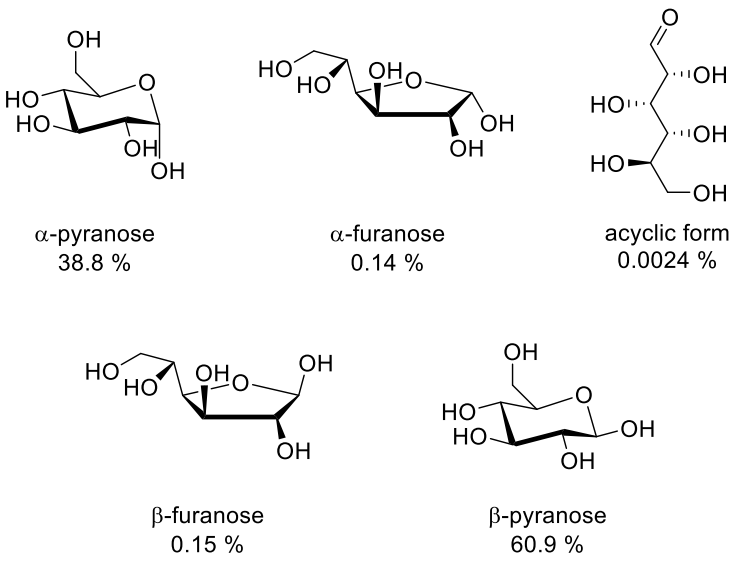

Figure 17. D-glucose in its various cyclic and acyclic forms and the percentage composition at equilibrium of each form of the sugar in D_2O at 27 °C.[125]

3.1.3 Complexation of Boronic Acids with Saccharides

The primary interaction of a boronic acid with a diol is covalent and involves the rapid and reversible formation of a cyclic boronate ester. The array of hydroxyl groups present on saccharides provides an ideal scaffold for these interactions and has led to the development of a range of boronic acid based sensors for saccharides.[5]

The first quantitative investigation into the interactions between boronic acids and polyols was carried out in 1959 by Lorand and Edwards.[22] In a study to clarify the structure of the much disputed phenylboronate anion a range of polyols were added to solutions of phenylboronic acid. As the polyols were added the pH decreased, allowing binding constants to be calculated using the technique of pH depression. From these experiments, it was concluded that the conjugate base of phenylboronic acid has a tetrahedral, rather than trigonal structure. The dissociation of a hydrogen ion from phenylboronic acid occurs from the interaction of the boron atom with a molecule of water. As the phenylboronic acid and water react, a hydrated proton is liberated, thereby defining the acidity constant, K_a, as shown in Scheme 47.[126] Whist one explicitly associated water molecule is shown, it should be noted that water is in rapid exchange with the boron atom. The reported p*K*a's of phenylboronic acid are between ~8.7 and 8.9,[127-129] with a recent in depth study refining this value to 8.70 in water at 25 °C.[31]

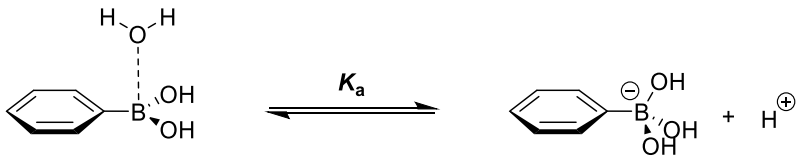

Scheme 47. Acid-conjugate base equilibrium for phenylboronic acid in water.

Boronic acids have been reported to interact rapidly and reversibly with dicarboxylic acids, α-hydroxy carboxylic acids and diols to form esters in aqueous media.[5] The most common interaction is with 1,2- and 1,3-diols to form five- and six-membered rings respectively (Scheme 48). The kinetics of this interconversion are fastest in aqueous basic media where the boron is present in its tetrahedral, anionic form. Typically, differences in rate of 10^4 are observed between boron in its trigonal and tetrahedral forms.[130]

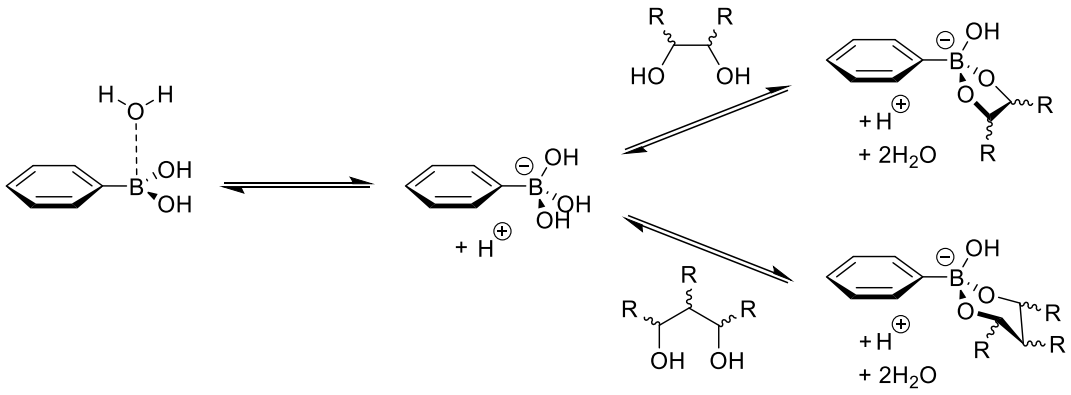

Scheme 48. Interaction of the phenylboronate anion with 1,2- and 1,3-diols.

Whilst the boronate anion does account for the strongest binding of diols in aqueous media, the interaction between diols and the neutral boronic acid should not be ignored.[27] Taking into consideration these interactions, the equilibria in Scheme 48 can be expanded to form a thermodynamic cycle, as shown in Scheme 49.

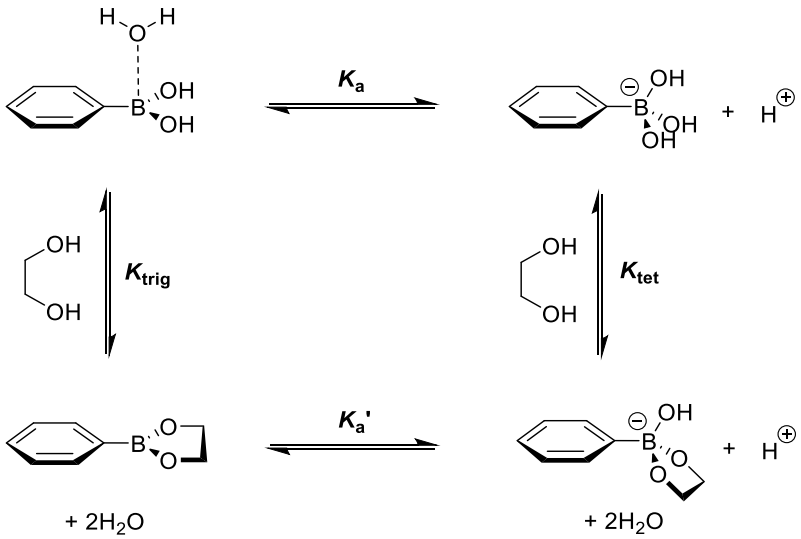

Scheme 49. The equilibria for boronate ester formation to generate a thermodynamic cycle.

Considering Scheme 49, the formation of the diol-boronate anion complex is defined as K_{tet} and the formation of the diol-neutral boronic acid complex is K_{trig}, where it is observed that $K_{tet} > K_{trig}$. Differences of up to five orders of magnitude are commonplace for this difference in binding constants between K_{tet} and K_{trig}.[31] The neutral boronic acid also becomes more acidic upon binding. The acidity of the bound complex is defined by K_a', where it is observed that $pK_a > pK_a$'. For example, the pK_a of phenylboronic acid is 9.0 in 0.1 M NaCl 1:2 (v/v) methanol/water, under the same conditions the pK_a' of

phenylboronic acid bound to fructose is 5.2. In other words, the boronic ester is more acidic than the boronic acid.[31]

3.1.4 The Preference of Monoboronic Acids for D-Fructose

The β-D-fructofuranose form of D-fructose contains a syn-periplanar anomeric hydroxyl group that accounts for 25% of the equilibrated forms of D-fructose in deuterated water at 31 °C (Figure 18).[131] This value contrasts with the amount of α-D-glucofuranose at equilibrium, which accounts for just 0.14% of D-glucose in deuterated water at 27 °C.[125] This correlates to the stability constants reported by Lorand and Edwards in the presence of phenylboronic acid of 4400 M^{-1} with D-fructose and 110 M^{-1} with D-glucose.[22]

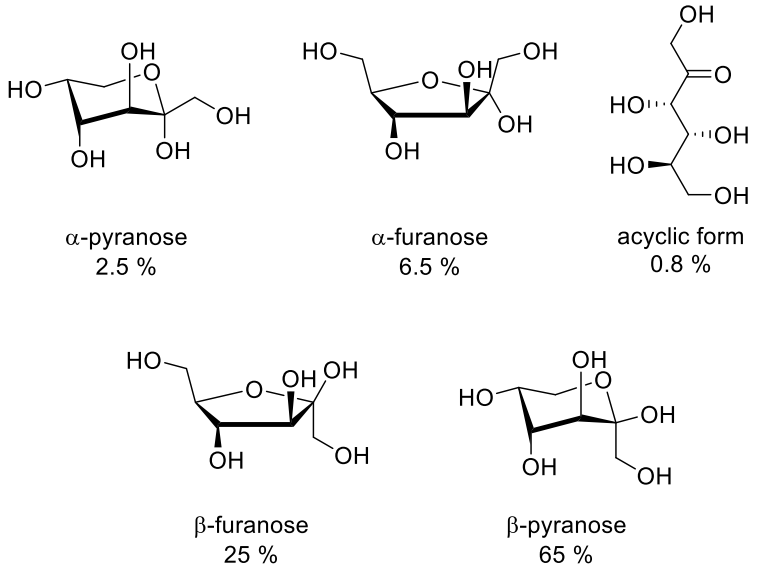

Figure 18. D-fructose in its various cyclic and acyclic forms and the percentage composition at equilibrium of each form of the sugar in D_2O at 31 °C.

A simple statistical trend appears to exist between the natural speciation of saccharide forms containing the syn-periplanar anomeric hydroxyl pair arrangement and their observed stability constants with monoboronic acids. However, this is only a statistical rule-of-thumb guide, due to the complexity and multiple number of binding motifs possible; the furanose form of a saccharide may not necessarily always be the one favoured for binding.[5]

3.1.5 Diabetes Mellitus

Diabetes refers to a medical condition where a patient lacks sufficient control of blood glucose levels, which can lead to serious complications such as heart disease, stroke, kidney and nerve damage, limb amputation and blindness.[132] These diabetic-related conditions occur due to uncontrolled blood glucose concentrations over a prolonged period of time, therefore it is essential that patients are diagnosed, treated and monitored to maintain blood glucose levels within healthy limits. Treatment of diabetes involves a combination of diet control, exercise, medication, home blood glucose testing and insulin injections.[133] However, current treatments rely heavily on informed patient compliance and there is much scope for improvement.

The aim of all diabetic treatments is to maintain a patient's blood glucose levels within healthy physiological limits. Non-diabetic blood glucose concentrations are usually in the range 4-7 mM.[27] This is normally achieved by twice-daily invasive blood analysis (e.g. painful finger-prick blood collection) using testing strips and glucose monitoring systems that require external calibration at least once a day.[134] The development of calibration-free devices for blood glucose monitoring is potentially ground-breaking since it would remove the need for painful finger-prick blood tests and remove human error associated with current calibration processes. In addition, this would also bring the possibility of developing a closed-loop artificial pancreas for automated regulation of blood glucose levels one step closer.[2]

Diabetes is a serious condition that can affect many parts of the body and is linked with a range of serious illnesses including heart disease and stroke, kidney failure, blindness and lower limb amputation. Diabetes can also trigger hypoglycaemia and hyperglycemic crisis,[135] high blood pressure and high blood low-density lipoprotein,[136] and people suffering with diabetes may develop other conditions such as nerve disease, non-alcoholic fatty liver disease, gum disease, depression, hearing loss and complications during pregnancy.[2] The prevalence of diabetes for all age-groups worldwide was estimated to be 2.8% in 2000 and is expected to rise to 4.4% by 2030. The total number of people with diabetes is projected to rise from 171 million in 2000 to 366 million in 2030.[124]

3.1.6 Home Blood Glucose Monitoring

Commercially, the preferred tools for sensing complex molecular species have relied on the high specificity displayed by antibodies and enzymes. Most clinical systems that are currently available for monitoring blood glucose levels rely on the glucose oxidase enzyme (GOx).[137] The majority of these home blood glucose monitoring systems rely on the invasive withdrawal of blood, followed by application of the sample onto an enzymatic test strip allowing GOx to catalyse the oxidation of glucose to gluconic acid (Scheme 50).[137] Early glucose monitors measured the production of hydrogen peroxide by oxidation at a single working electrode. At a constant voltage, the current generated across the cell is proportional to the concentration of hydrogen peroxide, which in turn is proportional to the concentration of glucose in the sample under investigation.

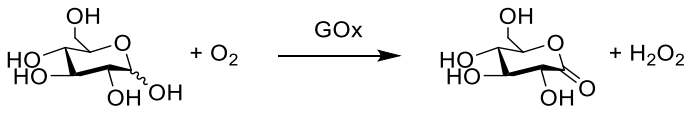

Scheme 50. Oxidation of D-glucose to D-gluconolactone (the ring-closed form of D-gluconic acid) in the presence of GOx.

The development of affordable home blood glucose monitoring systems has undoubtedly improved the quality of life experienced by diabetics. However, there are several limitations with this enzymatic approach. The systems have to be stored appropriately, they are specific only for a few saccharides, and in most cases they become unstable under harsh conditions and hence cannot be sterilised.[27] Considering these flaws, it is likely that non-enzymatic glucose sensors will become the next generation of glucose sensors for analytical applications. The holy grail of glucose sensing is the design of a continuous monitoring system, where the measurement of blood glucose levels could automatically trigger the release of insulin when an healthy concentration of glucose is exceeded.[138] Much work has been focused on the development of synthetic sensors with the capacity to monitor saccharides under a broad range of environmental conditions, allowing access to a wider range of diagnostic applications.

3.1.7 Synthetic Sensors for Saccharides

3.1.7.1 Non-Boronic Acid Saccharide Sensors

Many synthetic sensors for neutral guests rely on non-covalent interactions such as hydrogen bonding. However, in aqueous systems the neutral guests may become heavily solvated. Whilst biological systems have the ability to expel water from their binding pockets to bind with the analyte using non-covalent interactions, synthetic monomeric receptors have not yet been reported where hydrogen bonding between the receptor and the analyte has been able to compete with bulk water for low concentrations of monosaccharides.[139]

The first synthetic saccharide receptor **30** was reported by Aoyama *et al.* in 1988 (Figure 19).[140] The bowl-shaped calixarene was too small to encapsulate saccharides but was reported to form a 2:1 sandwich complex to bind the methyl β-D-glucoside enantiomer. It was initially proposed that recognition occurred in a face-to-face arrangement of hydrogen bonds between **30** and sugar hydroxy groups in a manner that closely resembles the optimal self-assembly of water molecules. However, the development of advanced NMR spectroscopic techniques has since allowed Rebek *et al.* to demonstrate that **30** assembles into a hexameric capsule with 6:3 receptor/substrate stoichiometry in solution.[141] From a practical perspective, the system is not particularly useful since to form complexes of saccharides in water, high concentrations of saccharides were required.

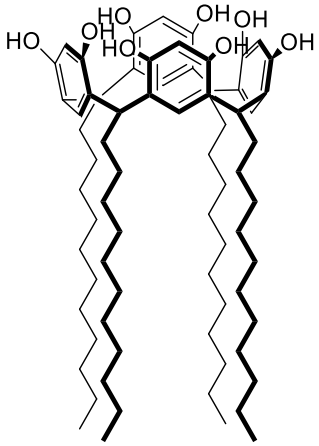

30

Figure 19. The structure of the first synthetic saccharide sensor.

Davis and Wareham have designed the octaamide sensor **31 (**Figure 20**)**.[142] The rigid architecture mimics nature in that the binding pocket is designed to completely encapsulate a saccharide substrate. The planar hydrophobic surfaces of the dual biaryl groups provide apolar contacts, and an array of amides provides favourable hydrogen-bonding interactions with hydroxyl groups of the saccharide. However, even with such an elegant design, the reported stability constants for **31** in deuterated chloroform are significantly reduced upon addition of competitive co-solvents. More recently, the dodecacarboxylate version of this receptor **32** has been developed and is reported to bind D-glucose in water with a stability constant of 9.5 M^{-1}.[143] This is much better than the previous system, but the binding is still too weak in water for these systems to be useful in detecting saccharides in biological systems.

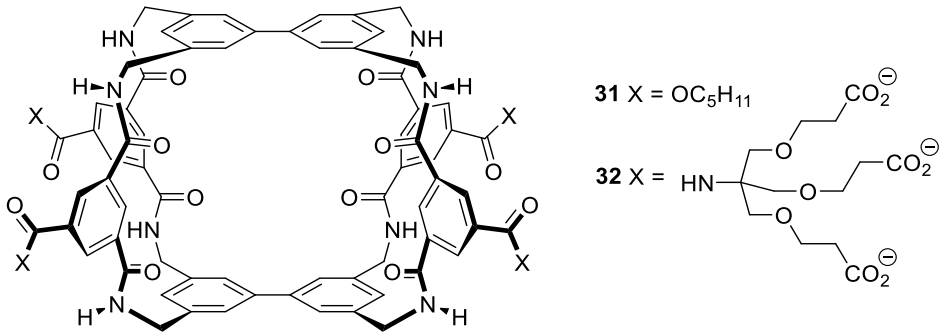

Figure 20. Octaamide sensors for saccharide detection.

Diederich and co-workers have utilised a binaphthalene-derived macrocycle appended with internal phosphate groups to provide a ring of hydrogen-bonding sites within a central recognition cavity (Figure 21).[144-146] Sensor **33** was shown to have good selectivity for saccharides such as octyl β-D-glycopyranoside. The calculated interphosphate distance of 7.2 Å was designed to accommodate monosaccharides exclusively. A stability constant of 5200 M^{-1} was reported for the complexation on sensor **33** with octyl β-D-glucopyranoside in 8:2 deuterated acetonitrile/deuterated methanol.[146]

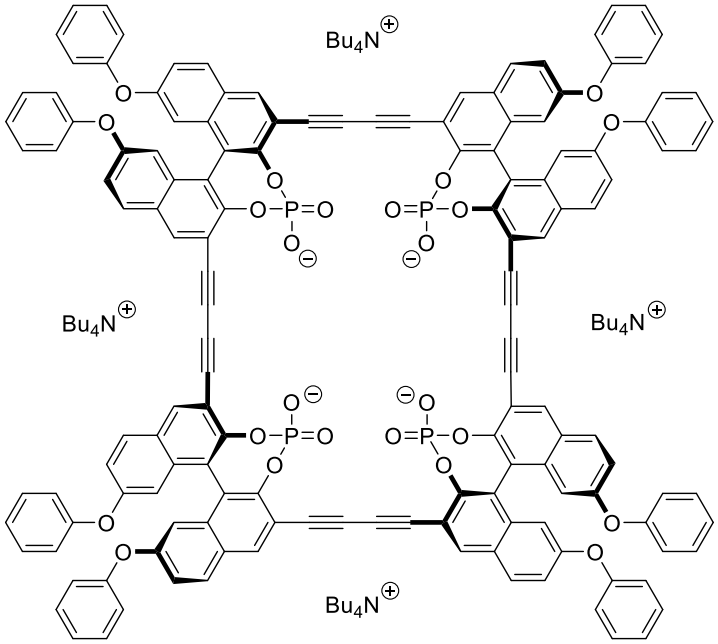

33

Figure 21. Binaphthalene-derived macrocyclic receptor for saccharide detection.

The major obstacle for all the synthetic receptors described above is solvent competition. In aqueous systems, neutral guests may become heavily solvated, therefore the sensors are unable to monitor glucose in media of specific interest such as blood, urine, tear fluid, beverages *etc*. Because monitoring saccharide interactions in water with these receptors is difficult, they are typically evaluated in aprotic solvents such as chloroform.[27] The use of aprotic solvents means that simple saccharides cannot be used because they are insoluble, leading to the use of O-alkylated saccharides. The covalent interaction between boronic acids and saccharides is hugely advantageous in overcoming this problem.

3.1.7.2 Fluorescent Boronic Acid Saccharide Sensors

The use of boronic acids in the development of fluorescent sensors for saccharides is a relatively young area of research. The first fluorescence-based saccharide sensor using boronic acids was reported by Yoon and Czarnik in 1992.[147] The excited state internal charge transfer (ICT, see section 4.1.2 for more on fluorescence mechanisms) sensor **34** consists of a boronic acid linked directly to a fluorescent anthracene unit (Figure 22). Addition of saccharides to **34** resulted in a 30% decrease in fluorescence emission intensity, believed to be caused by changes in the electronic properties accompanying rehybridization at the boron from sp^2 to sp^3.

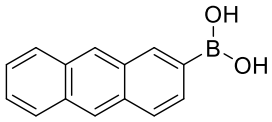

34

Figure 22. Structure of the first fluorescence-based saccharide sensor.

Boronic acid-based ICT sensors are strongly affected by pH, which must be considered for development of the sensors for real-world applications.[2] Photoinduced electron transfer (PET) sensors, are probably the most important class of boronic acid-based fluorescence sensors, as significantly, these sensors are not affected by changes in pH. Interaction of tertiary amines (Lewis bases) with the boron of *o*-methylphenylboronic acids (Lewis acids) removes the pH sensitivity of the boronic acid as well as producing fluorescent sensors for saccharides. Sensor **35** was developed within the Shinkai group as a saccharide sensor, displaying a remarkable fluorescence enhancement over a large pH range in aqueous media upon saccharide binding.[148] The monoboronic acid sensor **35**, which showed selectivity for fructose, was enhanced by introduction of a second receptor to prepare the diboronic acid sensor **36** (Figure 23).[149] This system retained the advantage of utilising PET to produce an off-on response upon binding of saccharides and introduced a potential selective recognition site. The structure proved very successful, with the two boronic acid groups producing a selective binding pocket for glucose.

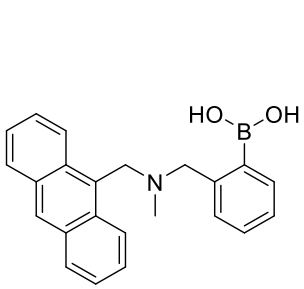

35

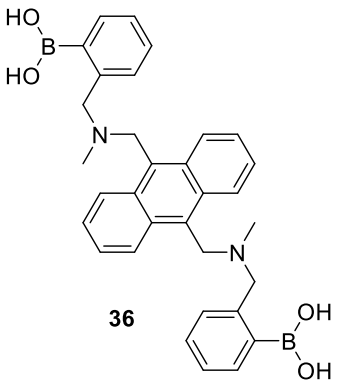

36

Figure 23. Mono- and diboronic acid PET sensors for saccharides.

Research has shown that boronic acid-based sensor systems require more than one receptor to achieve saccharide selectivity.[2] Simplified receptor design can be achieved by use of two boronic acid receptors in a modular system, where the linker and fluorophore units are varied independently. Modular system **37**, with two boronic acid

groups and a linker allows the spacing between the boronic acids to be easily changed (Figure 24). For example, sensor **38** with a flexible six-carbon linker was selective for D-glucose.[150] A switch to galactose selectivity was observed with an increase of the linker length, for example *n*-heptylene and *n*-octylene. The basic design concept of the modular sensor system **37** has been further developed by Glysure Ltd. into a fully functional continuous fibre optic sensor for the continuous glucose monitoring of patients in intensive care units.[2]

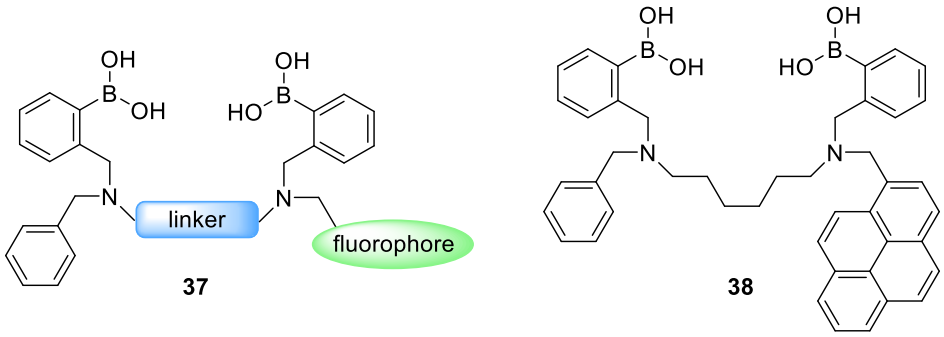

Figure 24. Modular fluorescent sensor systems.

3.1.7.3 Colorimetric Boronic Acid Saccharide Sensors

Sensors for saccharides that produce a colorimetric response are of particular interest for practical applications, for example, if a system can produce a large colour change, then it could be used to help develop a diagnostic test paper for saccharides, comparable to universal indicator paper used to determine pH.[2] This type of sensor would eliminate the need for specialist equipment for monitoring blood glucose levels, and would be particularly beneficial to diabetics in developing countries.

Boronic acid azo dyes have been used in the treatment of cancer for many years, by a technique called boron neutron capture therapy.[151] However, it was not until the 1990s that related dyes were investigated for saccharide binding. Shinkai *et al*. investigated diazo chromophores with boronic acid groups which aggregate in water, **39** (Figure 25). Upon binding with saccharides the system disaggregated and changed colour from yellow to orange.[152] The disaggregation is due to saccharide complexation causing an increase in hydrophilicity of the complex. Anslyn has also recently reported that this disaggregation mechanism is responsible for the observed increase in fluorescence emission intensity upon binding of *ortho*-aminomethylphenylboronic acid to fructose.[153]

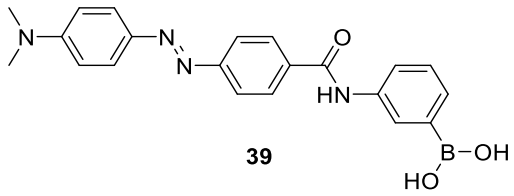

39

Figure 25. Boronic acid azo dye for saccharide sensing.

Sandanayake and Shinkai have developed an internal charge transfer sensor **40**, utilising an intramolecular interaction between the neighbouring amine and the boronic acid unit to produce colour changes upon addition of saccharides (Figure 26).[154] The electron-rich amine produces a basic environment in close proximity to the electron-deficient boron atom, enhancing the interaction between the boronic acid and saccharides, and reducing the working pH of the sensor. The electronic changes caused by this reduction in the pK_a of the boronic acid upon saccharide binding results in a spectral change in the attached ICT chromophore and is detected as a colour change. The observed stability constant for sensor **40** with D-fructose at pH 7.6 in water was 138 M^{-1}, however a binding constant with D-glucose could not be recorded due to negligible spectral changes.

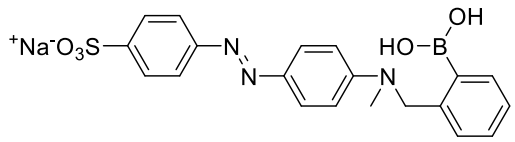

40

Figure 26. ICT boronic acid azo dye for saccharide sensing.

James *et al*. have prepared diazoboronic acid sensor **41** which produces a large naked-eye colour change from purple to red upon saccharide binding (Figure 27).[155] For the diazoboronic acid sensor **40** described above, at intermediate pH an N-B interaction exists, however this interaction is not observed at high or low pH. For sensor **41**, the presence of an anilinic hydrogen makes the system particularly interesting, since it can form different species at high pH. At pH 11.32 in the absence of saccharides, sensor **41** is purple, upon addition of saccharides the colour changes to red. In the presence of saccharides, the N-B interaction becomes stronger, making the N-H proton more acidic. At pH 11.32 the saccharide-boronate complex results in the red species with a N-B bond *via* loss of a water molecule. These observations explain why sensor **40** does not

produce a visible colour change upon saccharide binding, with no anilinic proton there is no possibility for dehydration and therefore no large spectral shift is observed.

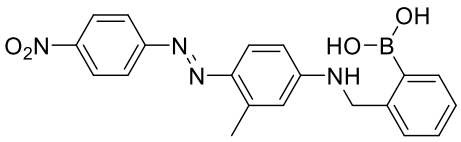

41

Figure 27. Improved boronic acid azo dye for saccharide sensing.

3.1.7.4 Boronic Acid-Based Indicator Displacement Assays

The previous sections describe the use of boronic acids in the development of integrated molecular sensors. The most widely used approach for chemosensors is the indicator-spacer-receptor approach, where the indicator (a chromophore or fluorophore) is covalently attached to the receptor through a spacer (Figure 28a).[156] Commonly with organic structures, introduction of an analyte that binds to the receptor would produce measurable changes in fluorescence or absorbance. Although popular, this approach does have its limitations. Attachment of the receptor to the indicator may require difficult syntheses. An alternative approach that avoids this problem is the indicator displacement assay.

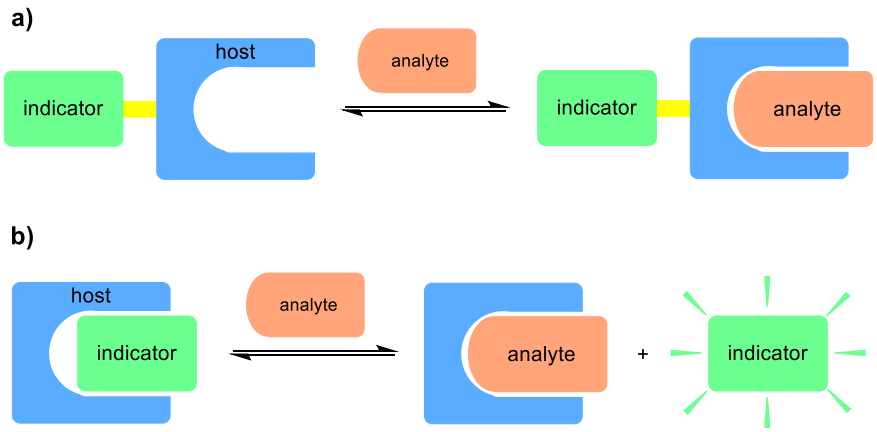

Figure 28. Schematic of a) Traditional chemosensing assay and b) indicator displacement assay.

An indictor displacement assay (IDA) involves initial binding of the indicator to the host, forming a complex in solution. Upon introduction of an analyte, the indicator is displaced from the host *via* thermodynamically controlled competition of the analyte and the indicator for the host (Figure 28b). Displacement of the indicator from the binding cavity of the host results in a change in the detector output. For a colorimetric

indicator, the visible spectra can be collected as the analyte is titrated into the solution of the host-guest complex. The amount of displaced indicator is linearly related to the amount of analyte introduced. The major requirement for an indicator displacement assay is that the affinity between the indicator and the receptor is comparable to that between the analyte and the receptor.[156] Common interactions between the indicator or analyte and the host are hydrogen bonding, electrostatic interactions and complexation with metal centres. Pioneering work in this area includes the influential protocols of Anslyn and co-workers,[156] Buryak and Severin,[157] and Singaram and co-workers,[158] all of which are excellent examples of supramolecular sensing.

The indicator displacement assay offers many advantages over traditional sensing assays. First, because the receptor is not covalently attached to the indicator, it is possible to use several different indicators for the same receptor. Second, as the method does not require the indicator to be covalently attached to the receptor, attention can be focused on the design of the host first, and an indicator can be chosen later. Third, the assay works well in both organic and aqueous solvents, therefore one can tune the solvent system to obtain the desired K_a values of the indicator and the analyte. However, the major disadvantage of this technique is that it is not amenable to imaging tissue or whole cells, because the displaced indicator is present everywhere in solution, not just isolated to the receptor.[159]

Indicator displacement assays have been used to sense both cations and anions, however the majority of IDAs have been for anions.[156] Anions play fundamental roles in many phenomena, including biological processes such as the transport of hormones, protein biosynthesis, DNA regulation and the activity of enzymes. IDAs are particularly useful for anion sensing because many indicators themselves are anions and therefore have a natural affinity for receptors that are designed to bind to other anions.

One very elegant system utilising boronic acid receptors has been published by Anslyn and co-workers. The C_3 symmetric tripodal boronic acid **42** has been developed as a D-glucose 6-phosphate-selective receptor (Figure 29).[160] Binding of D-glucose 6-phosphate **44** was measured by the competitive displacement of 5-carboxyfluorescein **45**. The addition of D-glucose 6-phosphate led to a decrease in the absorption band at 494 nm, allowing for the concentration of D-glucose 6-phosphate to be measured.

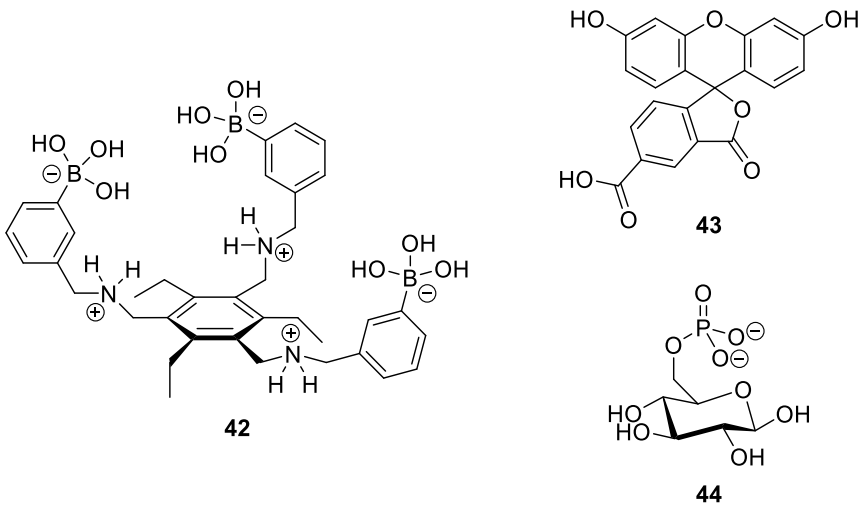

Figure 29. Indicator displacement assay for detection of D-glucose 6-phosphate.

Anslyn *et al*. also developed an assay for the sensing of tartrate **47** using a colorimetric indicator (Figure 30). Receptor **45** was designed to bind tartrate, which is a common natural product found in grape-derived beverages such as wine and juice.[161] Because tartrate comprises of two carboxylates and a diol functionality, the binding sites needed to be chosen accordingly. The chosen chromophore, alizarin complexone **46**, possesses similar functionalities to tartrate. Various beverages were analysed for their total concentration of tartrate and malate. Wines and grape juices were analysed with the complex of **45** and **46**, and the values obtained were in good agreement with values independently determined by NMR spectroscopy. Sensor **45** has also been used to evaluate malate in pinot noir grapes.[162]

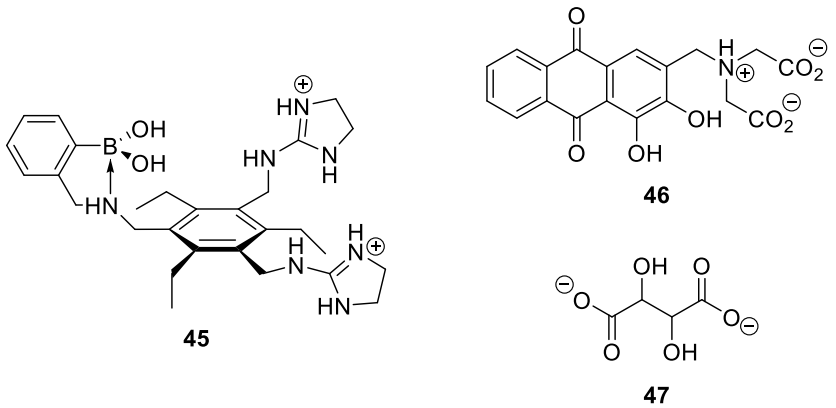

Figure 30. Indicator displacement assay for detection of tartrate.

Anslyn *et al.* have also developed an indicator displacement assay to monitor glucose oxidase activity in blood serum by detecting gluconic acid, produced from the oxidation of glucose by glucose oxidase.[163] A colorimetric response to gluconic acid **50** was produced using an indicator displacement assay with receptor **48** and pyrocatechol violet **49** as the indicator (Figure 31). Upon introduction of gluconic acid, because of its stronger interaction with receptor **48**, pyrocatechol violet was displaced from the receptor pocket. This produced a large spectral response, demonstrating that it is possible to monitor this product of glucose oxidase. Little or no displacement of the indicator occurs upon the addition of glucose, demonstrating that gluconic acid can be detected in the presence of glucose or other sugars. The sensing ensemble was successfully applied to determine the glucose concentration in human blood serum, offering a facile, colorimetric, sensitive and accurate glucose test.

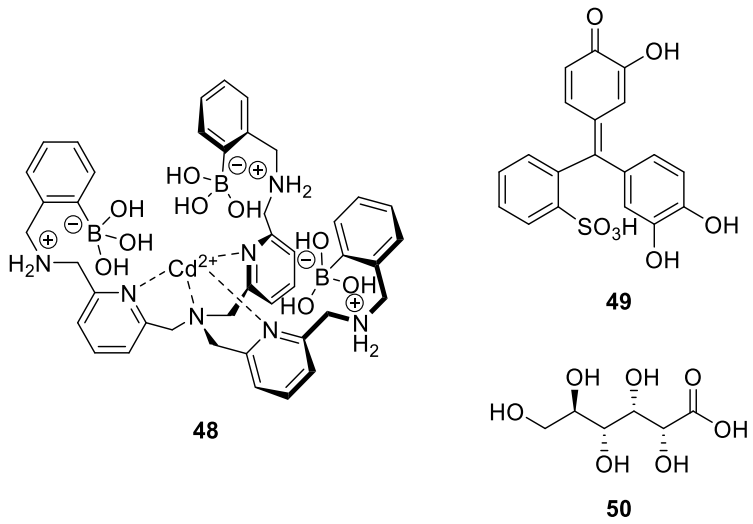

Figure 31. Indicator displacement assay for detection of gluconic acid.

Wang and co-workers have shown that Alizarin Red S (ARS) and phenylboronic acid (PBA) can be used in competitive dye displacement assays for saccharides (Scheme 51).[127,164,165] The system takes advantage of the known interaction of ARS with boronic acids, and was found to be D-fructose selective. The ARS dye displayed a dramatic change in fluorescence intensity upon binding to a boronic acid, allowing the study of carbohydrate-boronic acid interactions both qualitatively and quantitatively.

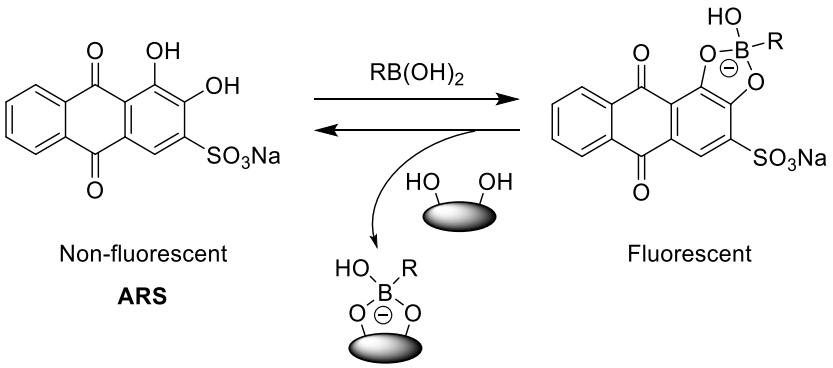

Scheme 51. Competitive binding of a boronic acid with alizarin red S and a *cis*-diol.

James *et al*. have developed a D-glucose selective fluorescent indicator displacement assay utilising alizarin red S.[166] The diboronic acid receptor **51** and ARS displays a 6-fold enhancement in binding for D-glucose over the simple PBA system (Figure 32). The observed change in absorbance and fluorescence represents the release of free ARS as the saccharide competes for the boronic acid in solution. Cooperative binding of the two boronic acid groups is clearly observed, indicated by the difference in stability constants for PBA and **51**. Receptor **51** can also be used at 10 times lower concentrations than the simple PBA system.

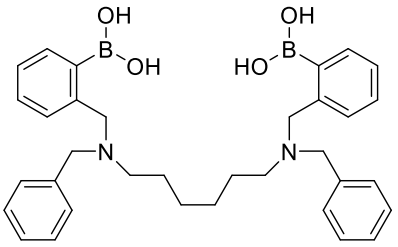

51

Figure 32. Indicator displacement assay for D-glucose detection.

3.1.8 Introduction to Hydrogels

Hydrogels are three-dimensional, hydrophilic, polymeric networks, which are crosslinked *via* covalent or noncovalent interactions and are capable of holding large amounts of water or biological fluids.[167] Their ability to absorb water arises from hydrophilic functional groups attached to the polymeric backbone, while their resistance to dissolution arises from cross-links between network chains. There is much interest in the potential biomedical applications of hydrogels; they are homogeneous soft materials with similar physical properties to soft tissues, and they have shown promise in a number of areas including sensors, separation systems and biomaterials.[168]

Unlike low molecular weight compounds, and uncrosslinked polymers, hydrogels swell but do not dissolve in aqueous solutions. Like solid materials they can retain their shape in solution, in spite of the fact that the weight of water absorbed by the gel is usually much higher than the weight of the polymeric matrix.[25]

According to the nature of cross-linkers, hydrogels are generally classified as physical or chemical hydrogels.[169] As the name suggests, physical hydrogels are cross-linked by physical methods, namely non-covalent interactions such as hydrogen bonds, van der Waals forces, hydrophobic interactions, π-π stacking or ionic interactions.[170] Such hydrogels, also called supramolecular hydrogels often utilise sol-gel transitions as the signal reporter for sensing. Chemical hydrogels are cross-linked by covalent bonds between the polymer strands, these gels are generally not able to go through sol-gel transitions, but have a stronger mechanical strength.

Recently, significant efforts have focused on stimuli-responsive hydrogels due to their ability to respond to external triggers such as pH,[171] temperature,[118] and light,[172] making them a class of important biomaterials for applications in medicine and tissue engineering. These "smart" hydrogels with stimuli-responsive properties such as sol-gel phase transitions can offer many advantages over conventional hydrogels, with many potential applications in the development of drug delivery systems, wound dressings, superabsorbents, and tissue engineering.[172]

3.1.8.1 Boronic Acid-Containing Hydrogels

Boronic acid-containing hydrogels combine the merits of both boronic acids and hydrogels. The introduction of boronic acid provides the hydrogel with new functions, such as glucose responsivity, reversibility and self-healing. The three-dimensional networks and swelling properties of hydrogels are also important for the implementation of many functions of the boronic acid.[25] Because of their sensitivity to glucose and other saccharides, boronic acid-containing hydrogels have been utilised for various applications such as glucose sensing and self-regulated insulin release.

3.1.8.2 Synthesis and Properties of Boronic Acid-Containing Hydrogels

One way to synthesise hydrogels is to polymerise a boronic acid-containing monomer, e.g. 3-acrylamidophenylboronic acid, with a co-monomer, e.g. *N*-isopropylacrylamide, in the presence of a crosslinker, e.g. *N*,*N'*methylenebisacrylamide (route 1 in Scheme 52). The choice of co-monomer can influence the hydrophilicity of the resulting gel and can also be used to introduce other functionality. Alternatively, boronic acid functional groups can be introduced by grafting the groups onto pre-formed polymeric networks, usually *via* carbodiimide chemistry (route 2 in Scheme 52). These synthetic routes produce hydrogels with pendant phenylboronic acid groups. Because of these phenylboronic acid groups, these hydrogels can exhibit glucose-dependant swelling behaviour, which is a major property of these gels.[25]

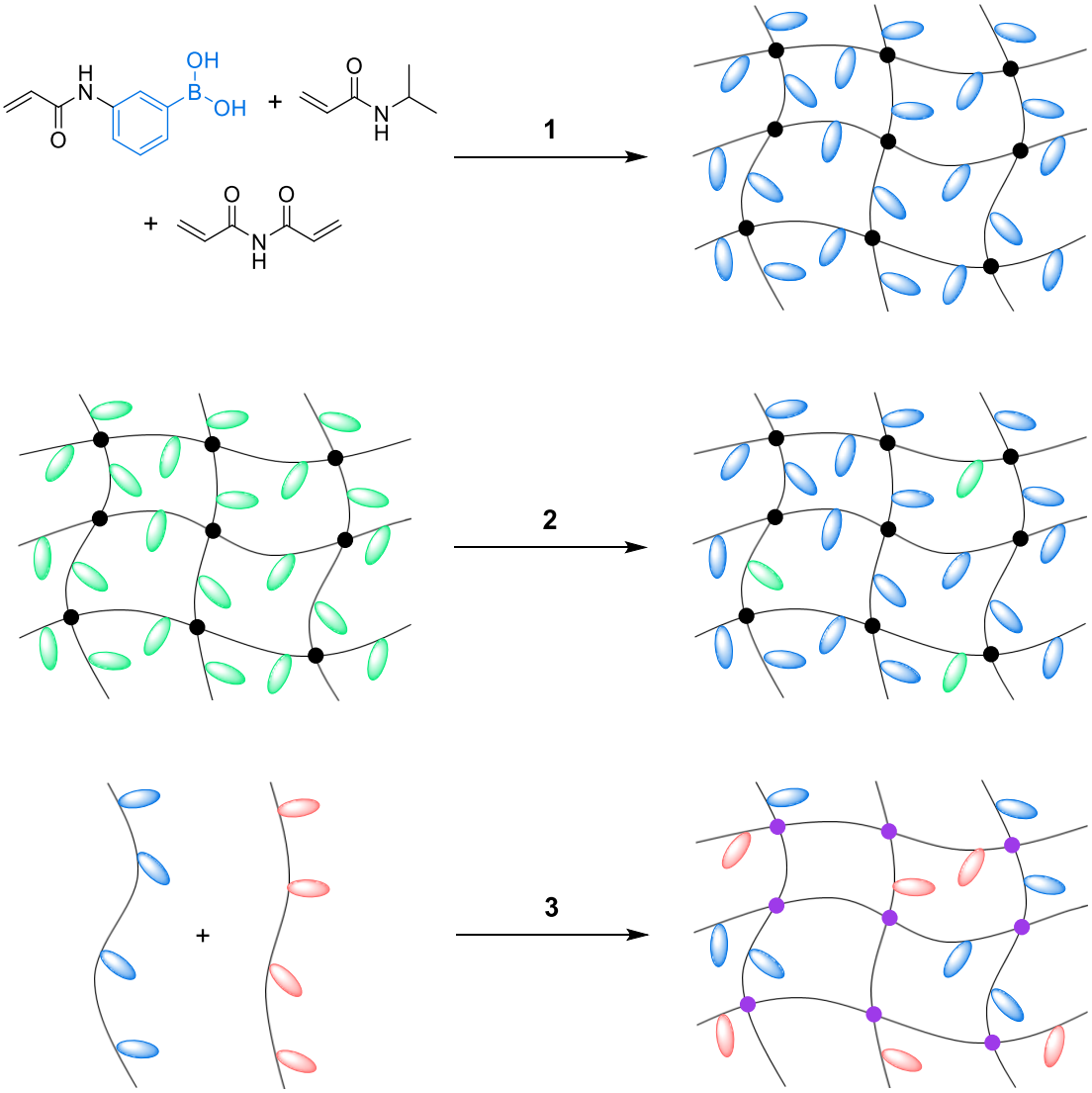

Scheme 52. Three routes to synthesize boronic acid-containing hydrogels. 1) Polymerisation of a boronic acid-containing monomer in the presence of a co-monomer and crosslinker; 2) Modification of a pre-formed network with boronic acid groups; 3) Complexation between a boronic acid-containing polymer and a diol-containing polymer.

In some cases, the addition of glucose induces a deswelling, instead of swelling, of the boronic acid-containing hydrogels. Glucose can simultaneously bind with two boronates in the hydrogel, increasing the crosslinking density of the hydrogel and thus reducing the degree of swelling. Asher *et al*. have reported a contraction of hydrogels when the glucose concentration is increased from 0 to 5 mM, suggesting that the 1:2 binding is dominant. However, increasing the glucose concentration further results in a reswelling of the gel, indicating that 1:1 binding is dominant.[173]

Another type of boronic acid-containing hydrogel can be synthesised using route 3 as shown in Scheme 52. In this route, crosslinking is achieved *via* the formation of the boronate ester bonds between a phenylboronic acid-containing polymer and a polymer with diol groups.[174] Because of the reversibility of the reaction between boronic acids and diols, the network of boronic acid-polyol gels is transient. The gel network can restructure dynamically and self-heal after mechanical disruption. This is very different from the gels synthesised using routes 1 and 2, which are permanent and do not allow for restructuring.

The binding affinity of a diol with a boronic acid is dictated by a number of factors including boronic acid pK_a, diol acidity, solution pH, solution composition, and the dihedral angle of the incoming diol.[23] In an aqueous environment, the free diol is in equilibrium with the bound diol in the boronate ester. Because of this exchange, materials prepared from boronate esters constantly undergo dynamic rearrangement and are considered "dynamic covalent" structures.[175] In boronate ester hydrogels, this covalent character leads to unique mechanical properties.

Hydrogels cross-linked *via* boronate esters are not permanently rigid, but can creep under their own weight. This creep is the result of the inevitable rearrangement of the boronate esters, in which the esters disassociate to yield the free boronic acids and diols, with the functional groups potentially diffusing away from each other before re-forming the boronate esters with newly adjacent diols.[23] While this creep is a potentially unwanted physical property for some applications, the exchange between boronate esters allows for materials to exhibit "self-healing" behaviour. Damage to the material can be repaired through the formation of new dynamic covalent bonds, without the need for external stimuli.

Messersmith *et al*. have developed pH responsive self-healing hydrogels based on boronate-catechol complexation.[168] The hydrogel formed at alkaline pH underwent a phase change to a liquid after adjusting the pH to 3.0 using HCl. The gel to sol transition is accompanied by a colour change from red to yellow, attributed to disassociation of the borate-catechol complex. At pH 9 the polymer gel could be cut into two pieces, fused together again and then stretched without fracture. This self-healing mechanism displayed is believed to be due to the dynamically reversible complexation between the boronic acid and catechol, upon return of the fractured surfaces together, free boronic

acid and catechol groups should be capable of complexing with each other at the interface to reform the polymer network (Figure 33).

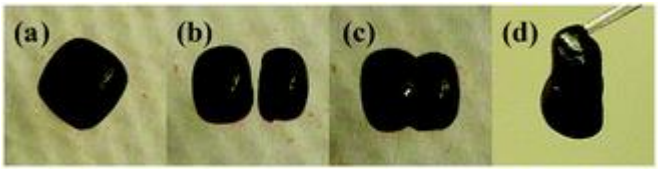

Figure 33. Self-healing properties of the polymer gel formed from boronate-catechol complexation at pH 9. The gel was formed into a cube (a), cut into two pieces (b), fused together (c), and then stretched without fracture 30 s after fusion (d).[168]

3.1.8.3 Glucose-Responsive Hydrogels and Their Applications

Because of their responsivity to glucose and other saccharides, boronic acid-containing hydrogels have been used for various applications including glucose sensing and self-regulated insulin release.[25] Hydrogels can be used as sensing materials in sensor design by coupling with various signal transduction methods, including electrochemical, optical, and mechanical ones.

The first glucose responsive hydrogel was prepared by Kataoka and co-workers, displaying an abrupt change in the degree of swelling at a critical glucose concentration in aqueous media.[176] When the phenylboronic acid groups within the hydrogel bind with a saccharide, the negatively charged boronate complex is formed. Upon addition of glucose, more of these anionic boronate complexes are formed, which are more hydrophilic than the uncharged boronic acid, making the polymer more soluble and resulting in the release of encapsulated insulin. Almost no insulin was released from the gel when the concentration of glucose was below 1 g/L. When the gels were immersed in buffer containing 3 g/L of glucose a large amount of insulin was released, demonstrating the presence of a threshold concentration of glucose to trigger insulin release from the gel.

Lei *et al*. have designed glucose sensors by coupling the glucose-induced swelling or shrinking of phenylboronic acid based hydrogels with pressure transducers.[177] The hydrogel is confined between a stiff nanoporous membrane and a thin glass diaphragm. In the presence of glucose, the hydrogel swells and deflects the glass diaphragm, resulting in resonant frequency changes which can be detected by a hand-held interrogating unit. The sensor is implantable in the subcutaneous tissue, allowing for

wireless glucose detection. However, the response rate is quite slow and the hydrogel also responds to other sugars.

Narain and co-workers have synthesised glyco-based polymers and copolymers with linear and hyperbranched structures for several applications.[118] Co-polymers containing 6-methacrylamido-1,2-benzoxaborole were mixed with the glycopolymers to spontaneously form hydrogels, the interaction of 6-methacrylamido-1,2-benzoxaborole with hydroxyl groups of the sugars allowed such cross-linking of the polymer chains (Figure 34). This cross-linking results in controllable gelation of the polymers. The gels were found to be responsive to different types of external stimuli, specifically temperature, pH and glucose concentration. It was discovered that when the gel is exposed to glucose or low pH, the inter-chain cross-links are disrupted and the gel disassociates. This responsive gelation system has the potential to be very useful for the encapsulation of therapeutic drugs and their slow release could be triggered by changes in temperature, pH and glucose concentration.

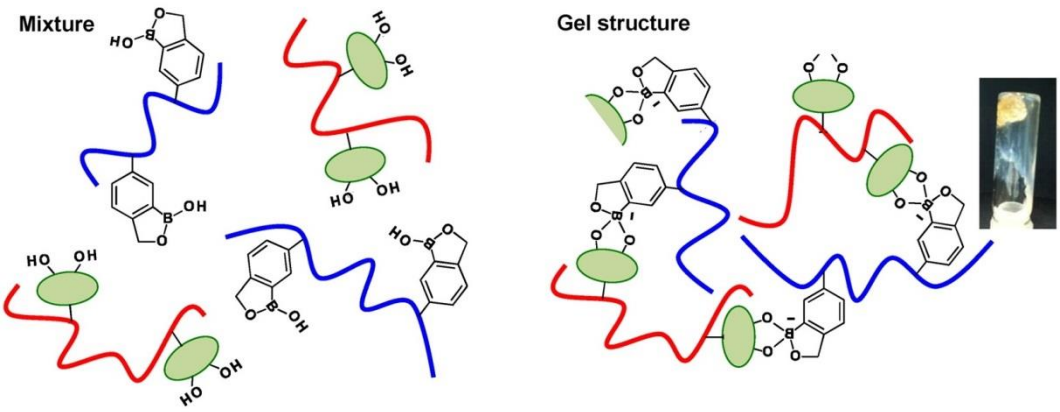

Figure 34. Gel formation *via* benzoxaborole-diol interactions between 6-methacrylamido-1,2-benzoxaborole and glycopolymers.[118]

Stimuli-responsive block copolymers readily change their physical properties in response to external stimuli such as temperature, pH, and irradiation.[178] The stimulated change of chemical and physical properties causes the vesicular membrane consisting of stimuli-responsive block copolymers to become permeable. This results in release of the encapsulated cargo molecules from the polymerosomes only when the appropriate stimulus is applied. Therefore, polymerosomes made from self-assembly of stimuli-responsive block copolymers are promising containers for smart nanocontainers that can be used as drug delivery vehicles and bioreactors.[179]

Kim *et al*. have synthesized benzoxaborole-containing polymers, whose degree of polymerisation could be controlled to yield sugar-responsive block copolymers that self-assembled into a variety of structures including polymer vesicles (polymerosomes).[82] These benzoxaborole-containing polymers can bind reversibly to biologically important 1,2- and 1,3-diols such as monosaccharides and nucleotides.[28] This binding switches the solubility of boronic acid-containing polymers from insoluble to soluble in water, which can be translated into the monosaccharide-triggered swelling of hydrogels and disassembly of micelles and polymerosomes. Kim *et al*. have demonstrated the possibility of using polymerosomes as sugar-responsive delivery vehicles for insulin in neutral phosphate buffer (pH 7.4).[82] By utilising the sugar-responsive disassembly of polymerosomes, encapsulated insulin could be released from the polymerosomes under physiologically relevant pH conditions. Boronic acid and benzoxaborole-containing polymers therefore contain great potential for sensors and drug delivery systems for sugar-related human diseases such as diabetes.

Low molecular weight gelators are small molecules that self-assemble to form fibrous nanostructures, which can further associate into higher order structures.[180] One example of this type of molecule are dipeptide hydrogels. Gels are formed through a variety of methods including pH change[181] and enzyme catalysis.[182] The driving force for the formation of dipeptide gel networks is the formation of fibres by non-covalent forces such as hydrogen bonding, π-π stacking and hydrophobic interactions between peptides. Once self-assembly is triggered, the growth of fibres leads to a three-dimensional entangled network which traps water, resulting in gel formation.[183] Cameron *et al*. have shown that the pH drop associated with the binding of fructose to phenylboronic acid can be used to trigger dipeptide gel formation. The pK_a of boronic acid drops after a diol is bound, leading to a greater amount of the anionic boronate complex and free hydrogen ions in solution, lowering the pH. Stable gels were formed at a range of fructose concentrations, demonstrating that it is possible to control gel formation using a saccharide trigger. Such saccharide-triggered gel formation has many potential applications including smart wound dressings, where saccharide release will trigger the formation of a gel barrier or coating.[184]

A major objective for the development of boronic-acid containing hydrogels is the construction of glucose sensing and self-regulated insulin release systems. Although a

lot of ground-breaking progress has been achieved, there are still some barriers that need to be overcome before their real application. Some barriers such as the lack of sensitivity for glucose originate from the boronic acid group. Other issues such as slow response rates and concerns about biodegradability originate from the hydrogel network.[25] These problems may be overcome *via* the rational design of these hydrogels. The applications of boronic-acid containing hydrogels will not be limited to glucose sensing. Carbohydrates and their derivatives, including many important biomolecules, play key roles in the immune system. With the ability to bind these biologically important molecules, it is highly likely that boronic acid-containing hydrogels will find many more applications in biomedical areas in the future.

3.1.9 Benzoxaboroles – An Improved Class of Sugar Binding Agents

The selective recognition of carbohydrates under physiological conditions remains as one of the biggest challenges in chemical biology. While the use of boronic acids is regarded as one of the most promising approaches for the recognition of carbohydrates in water,[185] it is not without severe limitations. Boronic acids do not bind to non-reducing sugars and glycosides, which account for a large proportion of biologically important oligosaccharides found in the form of cell-surface glycoconjugates.[41] The "Wulff-type" *ortho*-dialkylaminomethyl arylboronic acids,[32] currently the established standard for the recognition of simple reducing sugars, tend to have limited solubility in aqueous solutions. Hall *et al*. have reported that *ortho*-hydroxyalkyl arylboronic acids, also known as benzoxaboroles, bind to monosaccharides such as fructose and glucose with higher affinity compared to Wulff-type boronic acids in neutral water, and also show an increased solubility profile.[41] It was also reported that this new class of boronic acids are capable of complexing non-reducing glycopyranosides.

Although a number of synthetic receptors have been described for the recognition of complex carbohydrates in organic solvents,[139] it is notoriously difficult to achieve the same success under physiological conditions.[186] The essence of the problem lies in large part with the competition between the multiple hydroxyl groups on the carbohydrates and the overwhelming presence of the bulk solvent, water. Any approach to the recognition of carbohydrates in water should take advantage of the intrinsic geometrical orientation of the sugar's hydroxyl groups on the rigid oxacarbocyclic skeleton.

Norrild and co-workers have confirmed that glucose binds to boronic acids in water in its weakly populated furanose form, rather than its pyranose form (Scheme 53).[187] This behaviour is generally ascribed to geometrical preferences in the resulting boronate complexes. Rigid and coplanar vicinal diols such as the syn 1,2-diols of furanoses are strongly preferred because they minimise angle strain in the resulting boronate ester. The formation of a coplanar boronate with the nonplanar vicinal diols of a hexopyranose induces an unfavourable conformational change to pucker the sugar ring.[188]

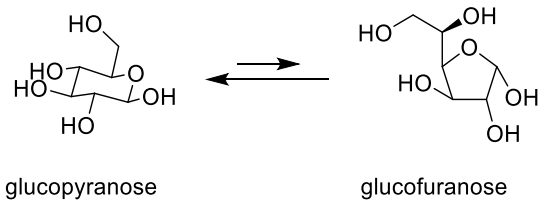

Scheme 53. Pyranose and furanose forms of glucose.

Further work by Hall *et al*. towards the discovery of glycopyranoside-binding boronic acids was based on taking advantage of bifunctional interactions, that is, covalent boronic ester formation complemented by secondary interactions from a suitable *ortho* substituent on the arylboronic acid template. More than a dozen arylboronic acids were screened in water at neutral pH, with benzoxaborole **8** standing out by displaying strong binding to both fructose and glucose.[40] Modest binding to the model hexopyranoside methyl α-D-glucopyranoside was also observed. Several possible factors could explain the capability of benzoxaborole to complex glycopyranosides under physiological conditions. One of the most important factors in carbohydrate recognition with boronic acids concerns the Lewis acidity of the boronic acid. Generally, the most acidic boronic acids usually provide tighter complexation. A pK_a value of 7.2 was measured for benzoxaborole **8** by ^{11}B NMR spectroscopic analysis. This relatively low value is likely due to the strained nature of the boroxole unit, and the favourable rehybridization that accompanies the formation of a tetrahedral hydroxyboronate complex. The pK_a of its one-carbon homologue benzoxaborin **13 (**Figure 35**)** was found to be 8.4, slightly more acidic than phenylboronic acid with a pK_a value of 8.8. Both benzoxaborin **13** and phenylboronic acid failed to show any complexation with methyl α-D-glucopyranoside. These results indicate that the low pK_a of benzoxaborole plays an important role in its hexopyranoside-binding ability. Other factors than Lewis acidity must be involved however, because the very acidic Wulff-type boronic acid **52** (pK_a ~6.7)[40] does not show

any complexation to glycopyranosides. Other factors such as intramolecular hydrogen bonding with other pyranoside hydroxyl groups in the resulting anionic complex are likely a contributing factor.

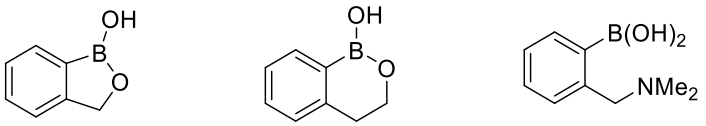

8 **13** **52**

Figure 35. Benzoxaborole, its one-carbon homologue benzoxaborin and Wulff-type boronic acids evaluated for sugar complexation.

3.1.10 Summary of Introduction

Beyond the challenges of sugar recognition in water, chemists face the difficulty of designing receptors capable of differentiating between sugars with very similar chemical structures. The development of rationally designed synthetic receptors for selective binding of saccharides remains one of chemistry's most sought after goals. Research in this field is driven by the need to monitor saccharides of industrial, environmental and biological significance. The rapid and reversible interaction between boronic acids and diols offers an excellent platform for saccharide recognition, and many sensors have been developed incorporating this interaction into the fundamental design concept. Boronic acid-containing hydrogels combine the merits of both boronic acids and hydrogels. The introduction of boronic acid groups provides the hydrogel with new properties, such as glucose responsivity and self-healing. The three-dimensional networks and swelling properties of hydrogels are also important for the implementation of many functions of the boronic acid. Because of their sensitivity to glucose and other saccharides, boronic acid-containing hydrogels can be utilised for various applications such as glucose sensing and self-regulated insulin release.

3.2 Previous Work in the Group

Previous work in the group showed that hydrogel spheres incorporating boronate units were able to function as saccharide sensors.[65] An alizarin red S (ARS) dye displacement assay utilising the strong affinity of boronic acids for saccharides was the basis of these hydrogel sensors. A range of polyacrylamide hydrogels were prepared, consisting of water, acrylamide **53**, methylene bisacrylamide **54**, and *meta* substituted phenyl boronate methacrylamides **55a-d**, along with the corresponding blank gels containing additional acrylamide in place of the boronate (Scheme 54).

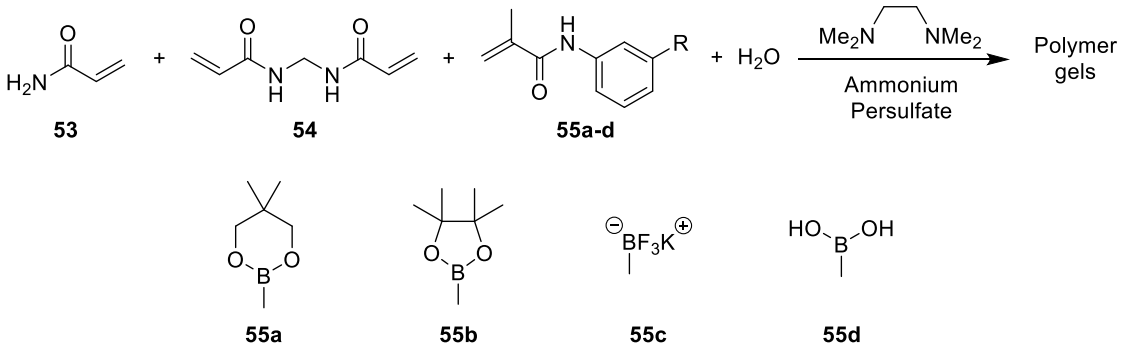

Scheme 54. Preparation of borogels and blank gels.

Prior to treatment with ARS, the borogels appeared colourless (as did the blank gel, not shown). Treatment of the blank gel and borogels with ARS solution resulted in red and orange slabs respectively (Figure 36).

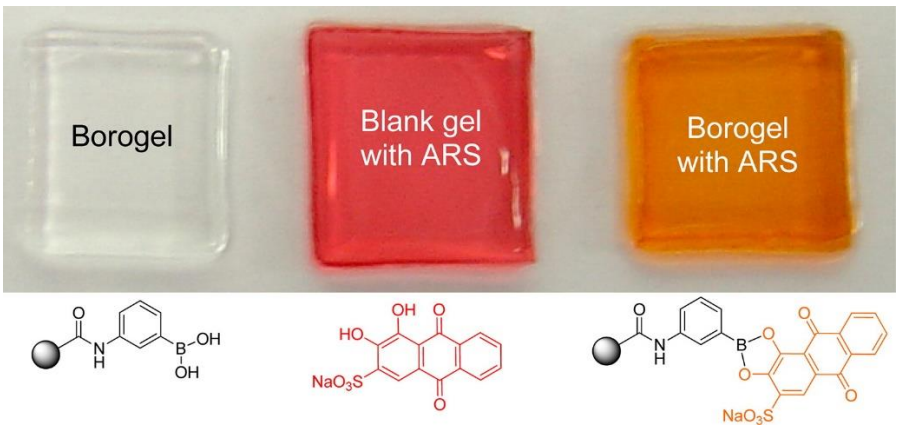

Figure 36. Gel slabs: Borogel (left); blank gel plus alizarin red S (middle) and borogel plus alizarin red S (right).[189]

A hypsochromic shift is indicative of ARS binding to boron; ARS develops an orange colour upon binding to boron. Whilst dye displacement assays on gel slabs provided

qualitative information, quantitative information was obtained from gel spheres of 5 mm diameter, cast from a bespoke mould. These spheres were then exposed to 2.5×10^{-4} M ARS solution, and the corresponding boronic esters were formed. Once excess dye had been removed by washing, the spheres were exposed to increasing concentrations of fructose. In the dye release assay, an excess of fructose analyte will displace ARS from boron, leading to an increase in absorbance at 513 nm in solution. Figure 37 shows the release of ARS into solution for the different borogel and blank spheres as the fructose concentration is increased. Blank gels gave up a small amount of dye upon addition of fructose, presumed to be that which was held in the polyacrylamide gel matrix by non-covalent interactions. The boronic acid pinacol ester **55b** functionalised gel showed the greatest dye release under the conditions employed.

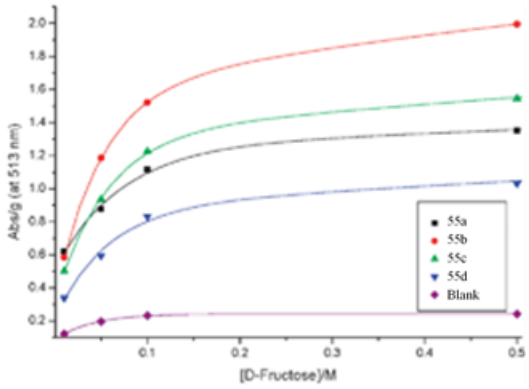

Figure 37. Fructose mediated ARS dye displacement assay, data points obtained 30 minutes after fructose addition.[65]

After reading papers by Hall and co-workers which reported that benzoxaboroles show an enhanced affinity for saccharides compared to traditional boronic acids,[40,41] it was hypothesised that incorporating the benzoxaborole functionality into hydrogels would further increase their sugar binding ability. Previous studies only looked at the binding affinity for D-fructose, therefore we wanted to expand the scope of the study by looking at the binding affinity of other monosaccharide sugars. It has also been reported that benzoxaboroles are able to complex non-reducing hexopyranoside sugars in solution, unlike traditional boronic acids.[40,41] Therefore we wanted to investigate whether benzoxaboroles were still capable of complexing non-reducing sugars when incorporated into a hydrogel structure. The overall aim of this project was to synthesise hydrogels which display an enhanced binding affinity for monosaccharide sugars compared to those previously prepared by the group.

3.3 Results and Discussion

Building on previous work, new hydrogels were prepared containing the benzoxaborole monomer **29**. Hydrogels containing the phenylboronic acid pinacol ester **55b** were also synthesised for comparison, as gels containing this boron functional group displayed the strongest binding to fructose in previous studies.[65] Blank hydrogels were also prepared for baseline comparison.

3.3.1 Synthesis of Boron-Containing Monomers

The 6-methacryloylamino benzoxaborole monomer **29** was synthesised as described in Chapter 2. The 3-methacyryloylamino phenylboronic acid pinacol ester **55b** was synthesised from 3-aminophenylboronic acid pinacol ester **56** *via* reaction with methacryloyl chloride, as shown in Scheme 55.

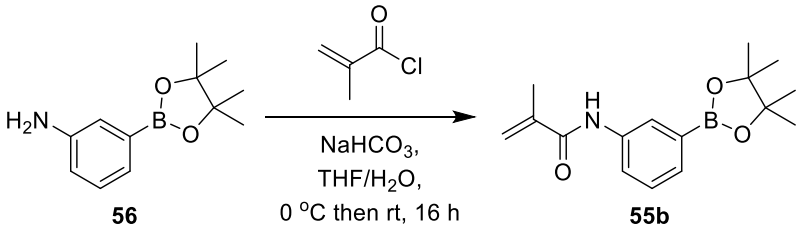

Scheme 55. Synthesis of 3-methacryloylamino phenylboronic acid pinacol ester.

The crude product was recrystallized from DCM/hexane to give pure **55b** as a white powdery solid. The presence of the desired product was confirmed by ^{1}H, ^{13}C and ^{11}B NMR spectroscopic analysis and mass spectrometry.

3.3.2 Hydrogel Preparation

A series of polyacrylamide hydrogels were synthesised consisting of water (60% w/w), acrylamide (**53**, 38% w/w), methylene bisacrylamide (**54**, 1% w/w) and either 3-methacyryloylamino phenylboronic acid pinacol ester (**55b**, 1% w/w) or 6-methacryloylamino benzoxaborole (**29**, 1% w/w). Blank gels were also prepared containing additional acrylamide in the place of the boronate compound (1% w/w), Scheme 56. Full details of hydrogel preparation are given in the experimental chapter (section 5.5.2). After the mixture was set, the hydrogels were carefully removed from the moulds, and their weights were recorded. The gels were stored in phosphate buffer (pH 7.3) in order to prevent drying.

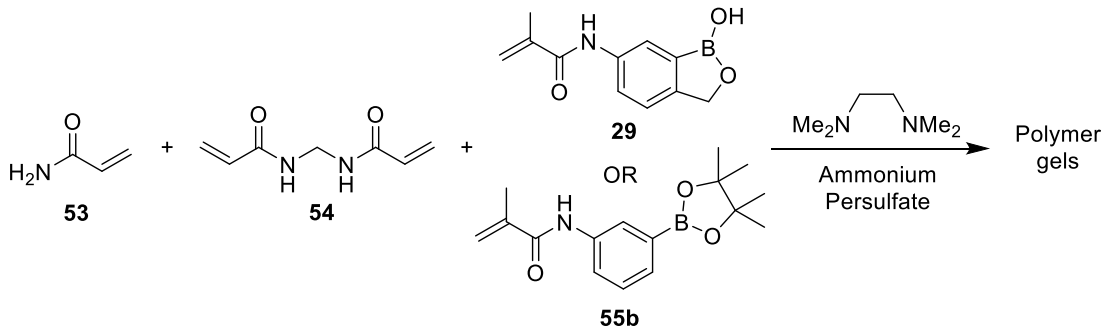

Scheme 56. Preparation of boronate hydrogels.

3.3.3 Gel Swelling Studies

In order to investigate factors that could affect the volume of the hydrogels, gel swelling studies were carried out. Blank, benzoxaborole-functionalised and phenylboronic acid pinacol ester-functionalised hydrogels were immersed overnight in pure water, pH 7.3 phosphate buffer, pH 8.5 phosphate buffer, pH 10 phosphate buffer, pH 8.21 phosphate buffer (containing 52.1 wt. % methanol) and pH 10 phosphate buffer (containing 52.1 wt. % methanol). Equilibrium swelling studies were carried out at room temperature. The hydrogels were weighed before and after immobilisation in the various buffers. Percentage change values are given in Tables 1-3 for blank, benzoxaborole-functionalised and phenylboronic acid pinacol ester-functionalised hydrogels, for full tables see Appendix 1. Photographs were taken of the gels before and after the swelling studies for comparative purposes (Figures 38 and 39).

Table 1. Percentage weight changes for blank hydrogels after immobilisation in various buffers.

Buffer	**Repeat 1 % change**	**Repeat 2 % change**	**Repeat 3 % change**	**Average % change**
Pure water	+36	+38	+36	+37
pH 7.3 phosphate	+39	+42	+38	+39
pH 8.5 phosphate	+38	+42	+39	+40
pH 10 phosphate	+39	+41	+39	+39
pH 8.21 phosphate (with MeOH)	-37	-38	-37	-37
pH 10 phosphate (with MeOH)	-38	-36	-37	-37

Table 2. Percentage weight changes for benzoxaborole-functionalised hydrogels after immobilisation in various buffers.

Buffer	**Repeat 1 % change**	**Repeat 2 % change**	**Repeat 3 % change**	**Average % change**
Pure water	+47	+46	+45	+46
pH 7.3 phosphate	+44	+47	+44	+45
pH 8.5 phosphate	+43	+45	+44	+44
pH 10 phosphate	+44	+46	+46	+45
pH 8.21 phosphate (with MeOH)	-38	-41	-38	-39
pH 10 phosphate (with MeOH)	-37	-40	-39	-39

Table 3. Percentage weight changes for phenylboronic acid pinacol ester-functionalised hydrogels after immobilisation in various buffers.

Buffer	**Repeat 1 % change**	**Repeat 2 % change**	**Repeat 3 % change**	**Average % change**
Pure water	+42	+43	+41	+42
pH 7.3 phosphate	+37	+40	+40	+39
pH 8.5 phosphate	+39	+42	+39	+40
pH 10 phosphate	+39	+42	+39	+40
pH 8.21 phosphate (with MeOH)	-36	-38	-37	-37
pH 10 phosphate (with MeOH)	-36	-36	-37	-36

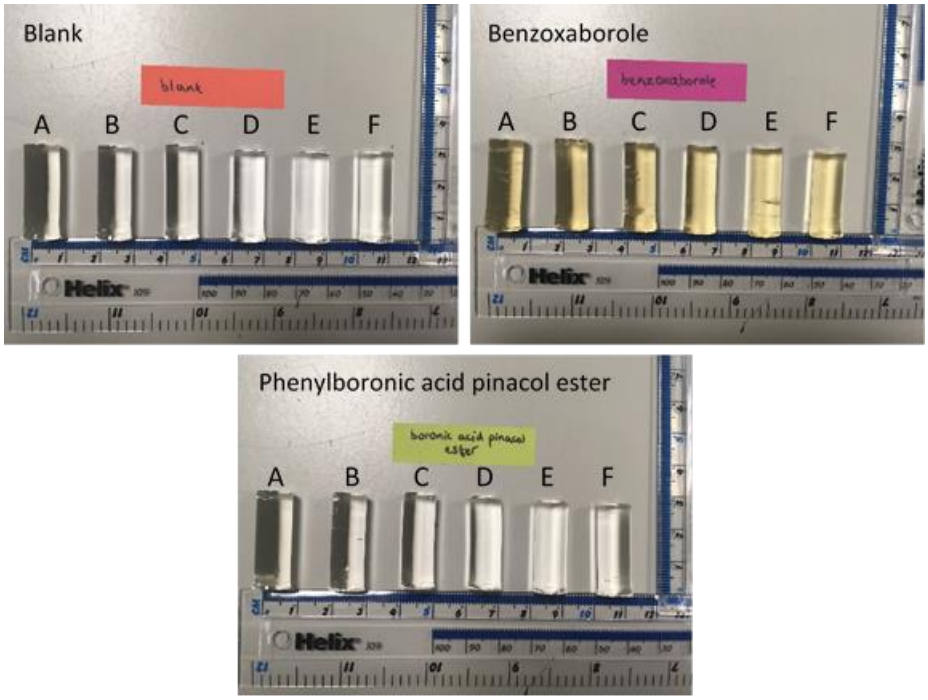

Figure 38. Hydrogels before immobilisation in a) pure water, b) pH 7.3 phosphate buffer, c) pH 8.5 phosphate buffer, d) pH 10 phosphate buffer, e) pH 8.21 phosphate buffer (52.1 wt. % MeOH), f) pH 10 phosphate buffer (52.1 wt. % MeOH).

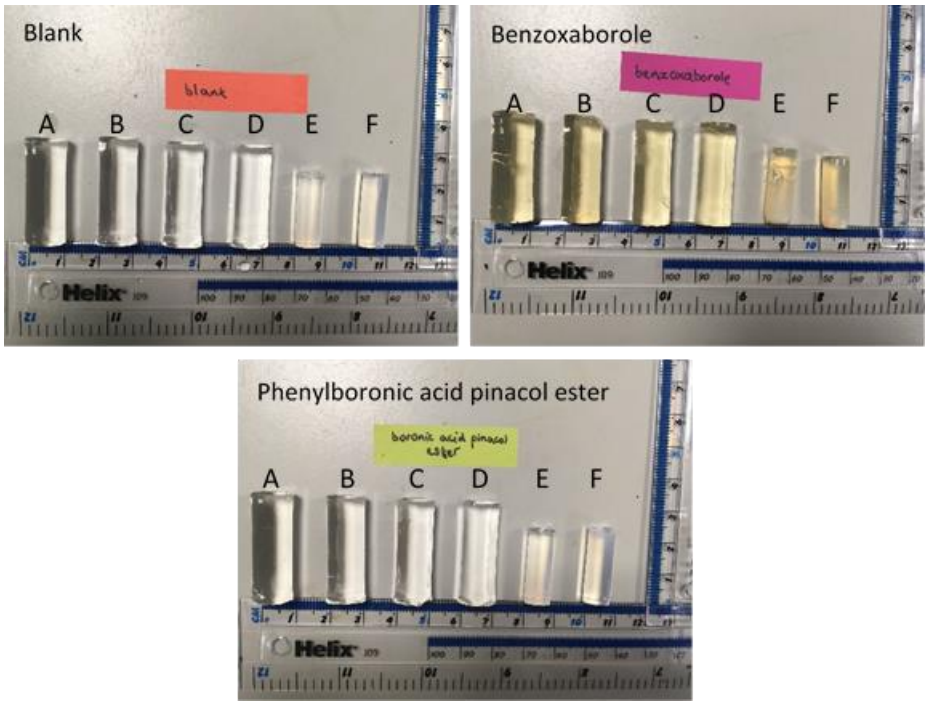

Figure 39. Hydrogels after immobilisation in a) pure water, b) pH 7.3 phosphate buffer, c) pH 8.5 phosphate buffer, d) pH 10 phosphate buffer, e) pH 8.21 phosphate buffer (52.1 wt. % MeOH), f) pH 10 phosphate buffer (52.1 wt. % MeOH).

In all water based buffers, an increase in swelling for all hydrogels was observed. Increasing the pH would be expected to increase the degree of swelling for the boron-functionalised hydrogels. With increasing pH, more hydroxide ions are present, which convert the trigonal boron atom to the charged tetrahedral form. When attached to a hydrogel, these negatively charged boron groups give rise to an osmotic swelling force causing the hydrogel to expand. The negatively charged boronate moiety draws in counterions from the surrounding solution, and the resulting excess of mobile ions inside the hydrogel generates an osmotic influx of water, causing the hydrogels to swell.[190] Also, the stabilized charge may alter the polarity and enhance the hydrophilicity of the boronic acid, promoting swelling. However, a significant increase in swelling was not observed with increasing pH, this may be due to the low proportion of the boron-containing monomers (only 1%). Interestingly, the benzoxaborole-functionalised hydrogels did swell slightly more than the phenylboronic acid pinacol ester-functionalised hydrogels. This is hypothesised to be due to the lower pK_a of the benzoxaborole, meaning that there are more negatively charged boronate groups within the benzoxaborole hydrogel, leading to an increase in swelling.

All of the hydrogels shrunk to approximately the same extent in both of the phosphate buffers containing 52.1 weight % methanol. This is due to methanol drawing out water from the hydrogel, causing the gel to contract. Even at high pH values which would be expected to result in swelling of the gel, shrinking of the hydrogels was observed. Therefore, buffer solutions without organic solvents were used for the following experiments.

3.3.4 Dye Displacement Assay

The dye displacement assay utilising alizarin red S (ARS) as an optical reporter developed by Wang and co-workers[164] was used in the following experiments. Benkovic and co-workers have shown that it is primarily the mono-phenolate form of ARS that interacts with the neutral, trigonal boronic acid species. Other reaction pathways are possible arising from the less nucleophilic undeprotonated ARS diol or the anionic, tetrahedral boronic acid, although these pathways are less favoured due to charge-charge repulsion at high pH.[191] The reaction pathway is shown in Scheme 57. The ARS changes colour from bright red in solution to orange when bound to boron. Colourless hydrogels immersed in ARS solution turned orange upon binding of ARS to boron functional groups within the gel.

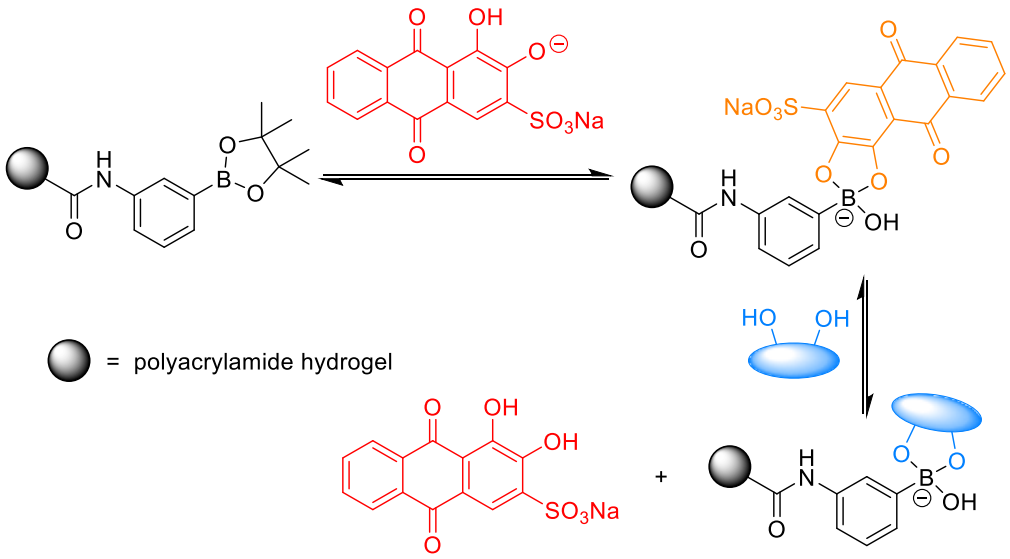

Scheme 57. Dye displacement assay with phenylboronic acid pinacol ester-functionalised hydrogel.

The ARS dye-saturated hydrogels are then washed in phosphate buffer to remove any non-specifically bound dye. Phosphate buffer-washed hydrogels were then exposed to increasing concentrations of various sugars. An excess of the saccharide analyte should displace the ARS dye from the boron into solution. This displacement of ARS back into solution caused the colourless phosphate buffer solution to turn pink (Figure 40). The amount of dye displaced could be measured quantitatively by measuring the increase in absorbance at 513 nm of the solution. The amount of dye displaced from the boron corresponds directly to the amount of saccharide analyte that has been bound.

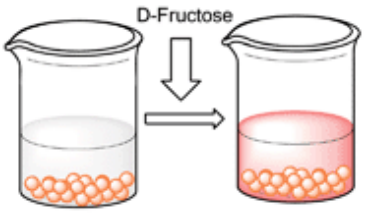

Figure 40. Colour change of the solution as ARS dye is displaced.

The binding of ARS to benzoxaboroles occurs *via* the same mechanism as the reaction with phenylboronic acid (Scheme 58). Again, the most preferential pathway is the reaction between the ARS mono-phenolate and the neutral, trigonal benzoxaborole.[106] Optimal binding for both phenylboronic acids and benzoxaboroles was achieved at near neutral pH.

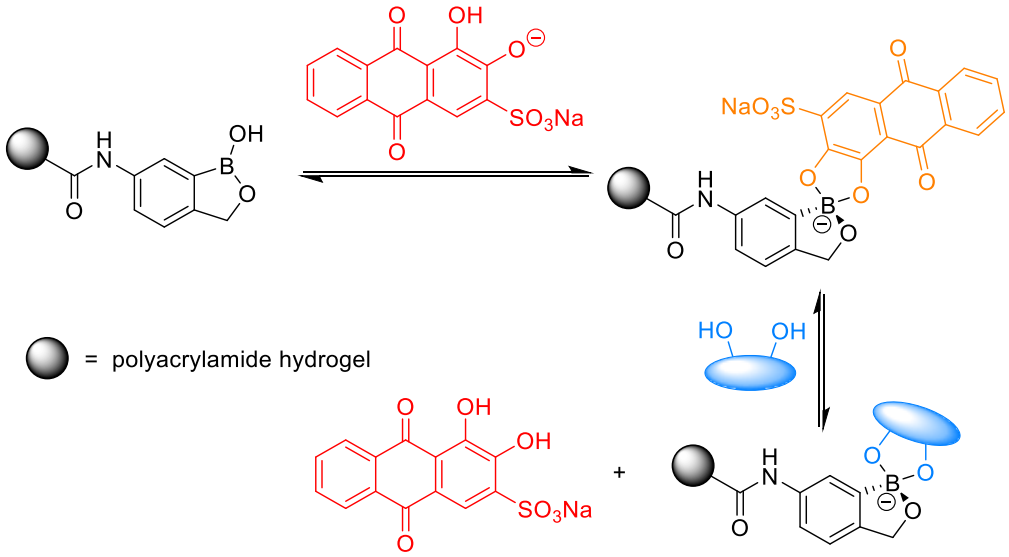

Scheme 58. Dye displacement assay with benzoxaborole-functionalised hydrogel.

3.3.5 Qualitative Binding Studies

As for the previous study, qualitative data could be obtained by examining the colour changes of the hydrogels upon ARS binding. Before addition of ARS, the blank and phenylboronic acid pinacol ester (PBA) gels were both colourless, while the benzoxaborole (BOB) gel had a faint brown tint to it (Figure 41).

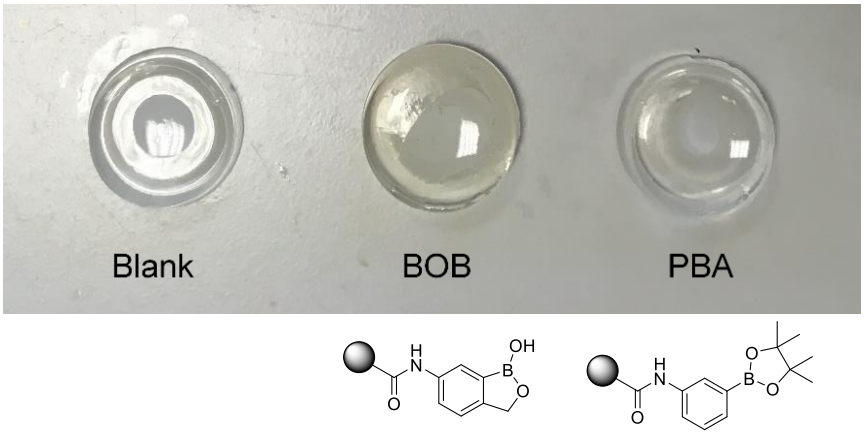

Figure 41. Gel slabs prior to treatment with alizarin red S.

Treatment of the blank gel with ARS solution (pH 7.3) resulted in red slabs, due to some ARS dye held in the polyacrylamide gel matrix by non-covalent interactions. The benzoxaborole and phenylboronic acid pinacol ester gels both turned orange on addition of ARS (Figure 42). A hypsochromic shift is indicative of ARS binding to boron, free dye in solution is red, but develops an orange colour upon binding to boron, providing visual conformation that ARS is bound to boron. Gel slabs were then placed in phosphate buffer in order to wash out any non-specifically bound dye. The orange colour for the borogels persisted after washing (not shown), whilst the blank gel was pink, due to a small amount of non-specifically bound dye remaining.

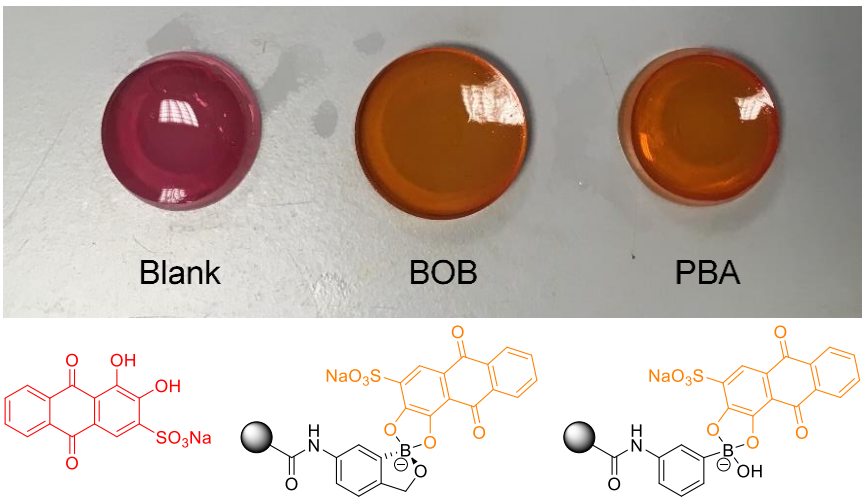

Figure 42. Gel slabs treated with alizarin red S.

Following phosphate buffer washing, the borogel slabs were orange whilst the blank gels were pale pink. The boron-containing gels now include the ARS-boronic ester conjugate and a small amount of non-specifically bound dye remains in all gels including the blank. The gels were then placed in a phosphate buffer solution containing fructose. In the dye release assay, an excess of fructose analyte should displace ARS from the boron, leading to an increase in the amount of dye in solution. As the dye is displaced into solution, the amount of dye within the gel decreases. After exposure to fructose all gels are pale pink, showing that all ARS has been displaced from the boron but a small amount of dye remains non-specifically bound within the pores of the gel (Figure 43).

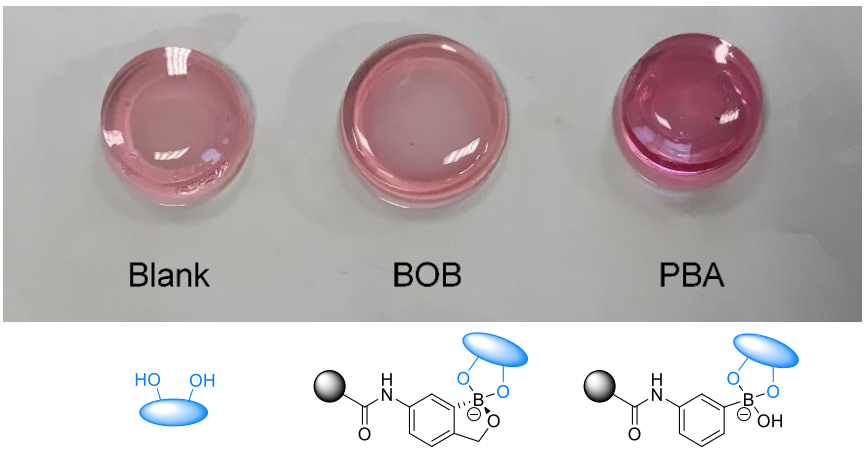

Figure 43. Gel slabs after exposure to fructose. The pink colour persists due to a small amount of non-specifically bound ARS dye.

3.3.6 Quantitative Binding Studies

3.3.6.1 Method Development

The previous results reported by James *et al*. utilised hydrogel spheres of 5 mm in diameter cast from a bespoke mould.[65] Whilst this method was successful, it does suffer from several limitations. Other researchers wishing to replicate the results in their own studies would have to have their own moulds produced *via* expensive techniques such as 3D printing. Also, any modifications to the size or shape of the hydrogels would require new moulds to be printed. In addition, ridges and cylindrical protrusions arise from the casting process, leading to irregular shaped gels which could influence diffusion within the gel. In this study, hydrogels were prepared in plastic disposable syringes. These syringes are available in a variety of volumes and shapes, allowing for hydrogels with a diverse range of shapes and sizes to be produced. This method also allows for excellent reproducibility when synthesising a series of gels for an experiment; when the polymer solution is taken up into the syringe, the volume increments on the side of the syringe can be used to ensure that all gels are the same volume. The size of the polymer gels produced can easily be modified by increasing or decreasing the amount of polymer solution taken up into the syringe. The syringes can then be inverted and left to set. Once set, the gels are easily removed from their moulds by cutting off the end of the syringe, then using the plunger to push the hydrogel out. More information on the syringe method for polymerisation can be found in the experimental section.

3.3.6.2 Dye Displacement Assays with Monosaccharides

Initial experiments were carried out with a single hydrogel cylinder, with a mass of approximately 0.5 g. The hydrogel cylinder was immersed in 2.0×10^{-4} M ARS solution (made up in pH 7.3 phosphate buffer) and stirred at 100 rpm. At specified time intervals, aliquots were taken and the absorbance recorded at 513 nm. No degradation of the polymer gels occurred. The decrease in absorbance at 513 nm corresponds to the amount of dye taken up by the hydrogel cylinder. A meaningful comparison between different hydrogels can be made by plotting absorbance of the solution per unit mass of gel (Abs per g), versus time for dye uptake. A comparison between the phenylboronic acid pinacol ester-functionalised hydrogel (abbreviated to PBA on graph below) and blank hydrogel is shown in Figure 44. After five hours, the gels have almost become

dye saturated, but the absorbance is still showing a slight decrease. The phenylboronic acid pinacol ester-functionalised hydrogel was now orange, while the blank hydrogel was a dark shade of pink. The blank hydrogel took up significantly less dye than the phenylboronic acid pinacol ester-functionalised hydrogel.

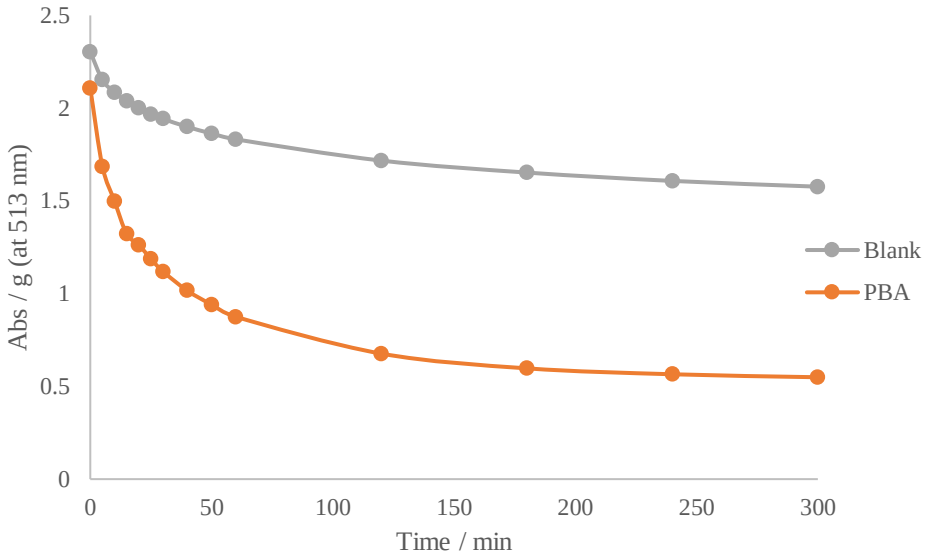

Figure 44. Dye uptake per unit mass of gel versus time for larger hydrogel cylinders.

Hydrogel cylinders were then placed in phosphate buffer (pH 7.3) and stirred at 100 rpm in order to wash out any non-specifically bound dye. Both the blank and phenylboronic acid pinacol ester-functionalised hydrogels released approximately the same amount of dye per gram of gel (Figure 45). After two hours, the absorbance of the rinsing solution is still increasing, indicating that non-specifically bound dye is still being washed out.

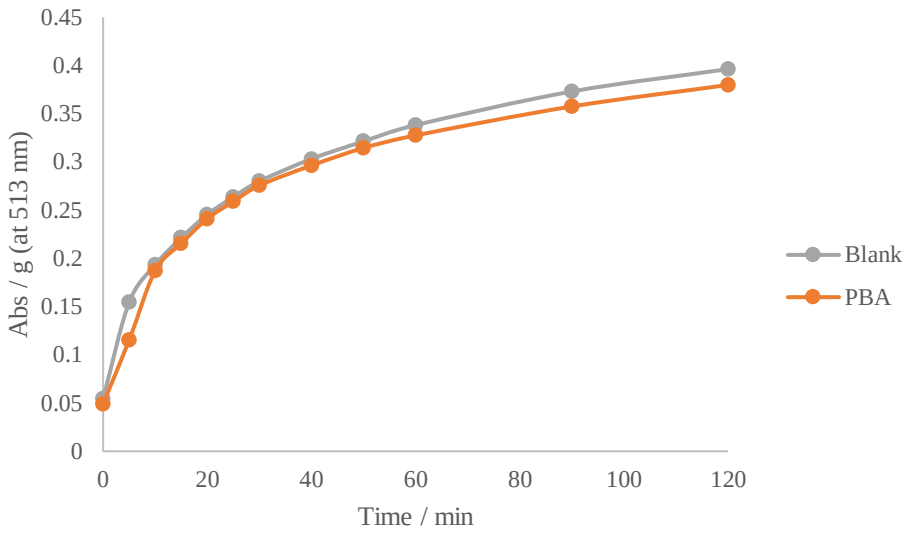

Figure 45. Dye released per unit mass of gel versus time for larger hydrogel cylinders upon washing in phosphate buffer.

The phosphate buffer-washed hydrogels were then exposed to increasing concentrations of fructose. In order to limit concentration effects, solid portions of D-fructose were added that rapidly dissolved in the buffer solution. Hydrogel cylinders were stirred in the fructose solution at 100 rpm for 30 minutes before measurements were taken. In the dye-release assay, an excess of fructose should displace the ARS dye from boron, leading to an increased absorbance at 513 nm in solution. Figure 46 shows the release of ARS into solution for the blank and phenylboronic acid pinacol ester-functionalised hydrogels as the concentration of fructose is increased. The blank gel released a small amount of dye upon fructose addition, which was presumed to be that held in the gel matrix by non-covalent interactions. The phenylboronic acid pinacol ester-functionalised hydrogel released a much larger amount of dye, due to an increased amount of dye being held within the gel *via* covalent interactions with boron. At a 1 M concentration of D-fructose, the absorbance at 513 nm of the solution is still increasing, indicating that ARS dye is still being displaced.

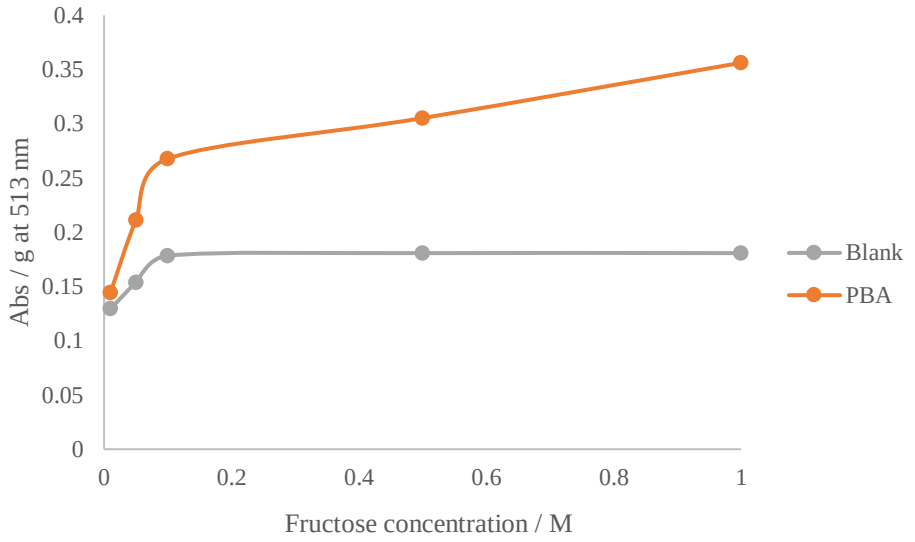

Figure 46. Fructose mediated ARS dye displacement assay for larger hydrogels. Data points obtained 30 minutes after fructose addition.

For the dye uptake graphs for hydrogels of approximately 0.5 g mass, the absorption per gram of the solution is still decreasing, even after five hours, suggesting that dye uptake is not complete. The absorbance of the solution at 513 nm is still increasing for the washing phase after two hours, suggesting that there is still non-covalently bound dye within the gel to be displaced. The graph showing dye displacement upon fructose addition still displays a steep increase in absorption at 513 nm, even after increasing the concentration of fructose to 1 M, which is twice as high as the concentration of fructose needed to displace all of the ARS dye in previous experiments.[65] It is likely that the single, larger hydrogel cylinders are suffering from a very slow rate of diffusion, due to their low surface area to volume ratio. This is confirmed by the observation that after the dye-displacement assay with fructose, whilst the edges of the phenylboronic acid pinacol ester-functionalised hydrogel are pink, the centre of the gel remains orange, showing that the fructose has not had sufficient time to diffuse through the hydrogel and displace the ARS dye. One way to overcome this problem would be to run the dye uptake and release experiments for a longer time period. However, this would drastically reduce the rate at which data could be obtained. It was therefore decided that it would be much more favourable to decrease the size of the hydrogels, allowing for faster diffusion within the gel. For future experiments, five smaller hydrogels, each of approximately 0.1 g in mass were used, giving the same total mass as for previous experiments.

The dye uptake experiment was repeated with the smaller hydrogel cylinders. Again, a comparison could be made by plotting absorbance of the solution per unit mass of gels versus time for dye uptake (Figure 47). Compared to the dye uptake experiment with the larger hydrogel cylinders, approximately the same amount of dye is absorbed overall, however the initial rate of dye uptake is slightly faster. After five hours, the gel cylinders have become dye saturated and the absorption at 513 nm did not decrease any further. The benzoxaborole-functionalised hydrogels took up a similar amount of dye to the phenylboronic acid pinacol ester-functionalised hydrogels, and again the blank hydrogels took up significantly less.

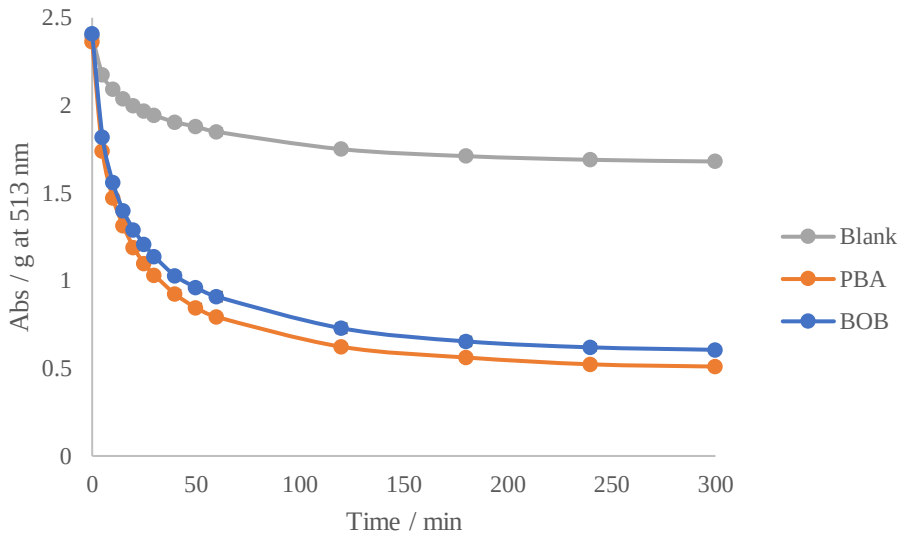

Figure 47. Dye uptake per unit mass of gels versus time for smaller hydrogel cylinders. Data points are an average of at least two experiments. Error bars show standard error.

Again, the hydrogel cylinders were placed in phosphate buffer (pH 7.3) and stirred at 100 rpm in order to wash out any non-specifically bound dye. The benzoxaborole-functionalised hydrogels released a similar amount of dye to the phenylboronic acid pinacol ester-functionalised hydrogels, whilst the blank hydrogels released slightly more (Figure 48). After two hours, there was a negligible further increase in dye concentration in solution.

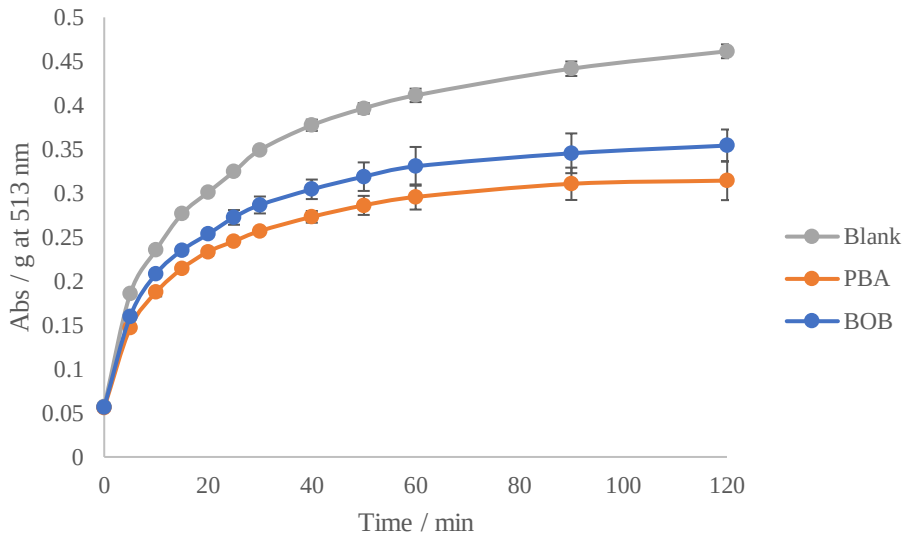

Figure 48. Dye released per unit mass of gels versus time for smaller hydrogel cylinders. Data points are an average of at least two experiments. Error bars show standard error.

The phosphate buffer-washed hydrogels were once again exposed to increasing concentrations of fructose. In order to generate more data points, additional fructose concentrations were studied. Hydrogel cylinders were stirred in the fructose solution at 100 rpm for 30 minutes before measurements were taken. Figure 49 shows the release of ARS into solution for the hydrogels as the concentration of fructose is increased. The blank gels released a small amount of dye upon fructose addition, presumably due to dye held in the gel matrix by non-covalent interactions. The phenylboronic acid pinacol ester-functionalised hydrogels released a much larger amount of dye, but the largest amount of dye was released by the benzoxaborole-functionalised hydrogels. Benzoxaboroles have been reported to have a higher binding affinity for saccharides in solution phase studies,[40] and it was found that they also displayed enhanced binding when incorporated into a hydrogel structure. At a 1 M concentration of D-fructose, the absorbance at 513 nm of the solution has reached a plateau. The smaller size of the hydrogel cylinders enables faster diffusion of fructose through the gel, the centre-of the boron-functionalised hydrogels are pink after fructose addition, showing that all of the ARS dye has been displaced by the fructose.

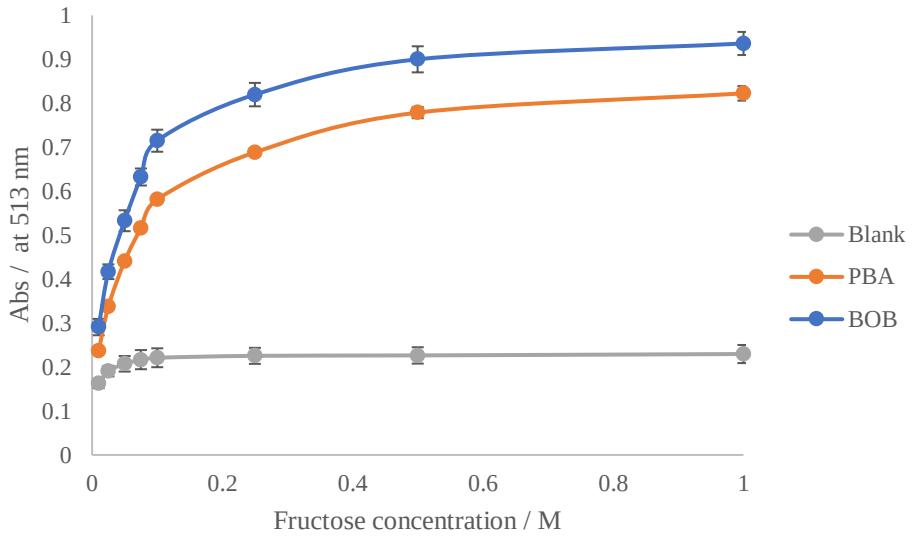

Figure 49. Fructose mediated ARS dye displacement assay for smaller hydrogels. Data points obtained 30 minutes after fructose addition and are an average of at least two experiments. Error bars show standard error.

The dye displacement assay was then repeated with D-galactose. A fresh set of hydrogels were saturated with ARS dye and then rinsed with phosphate buffer. Hydrogel cylinders were stirred in increasing concentrations of galactose solution at 100 rpm for 30 minutes before measurements were taken. Figure 50 shows the release of ARS into solution for the hydrogels as the concentration of galactose is increased. The blank gels released a small amount of dye upon galactose addition, due to dye held in the gel matrix by non-covalent interactions. The phenylboronic acid pinacol ester-functionalised hydrogels and benzoxaborole-functionalised hydrogels both released significantly less dye than in the previous experiment with fructose, but relative to the blank, the benzoxaborole-functionalised hydrogel shows a smaller decrease in binding affinity compared to the phenylboronic acid pinacol ester-functionalised hydrogel.

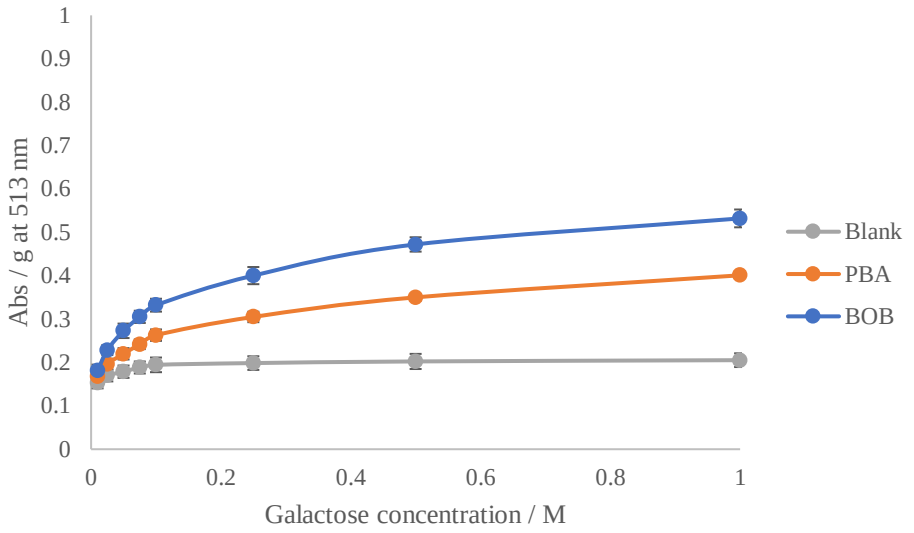

Figure 50. Galactose mediated ARS dye displacement assay for smaller hydrogels. Data points obtained 30 minutes after galactose addition and are an average of at least two experiments. Error bars show standard error.

The dye displacement assay was then repeated with D-mannose. A fresh set of hydrogels were stirred in increasing concentrations of mannose solution at 100 rpm for 30 minutes before measurements were taken. Figure 51 shows the release of ARS into solution for the hydrogels as the concentration of mannose is increased. The blank gels released a small amount of dye upon mannose addition, due to dye held in the gel matrix by non-covalent interactions. The phenylboronic acid pinacol ester-functionalised hydrogels released a similar amount of dye upon addition of mannose as was released upon addition of galactose. On the other hand, the benzoxaborole-functionalised hydrogel released a slightly larger amount of dye upon addition of mannose, compared to the amount of dye released on addition of galactose. Again, relative to the blank, the benzoxaborole-functionalised hydrogel shows a smaller decrease in binding affinity compared to the phenylboronic acid pinacol ester-functionalised hydrogel.

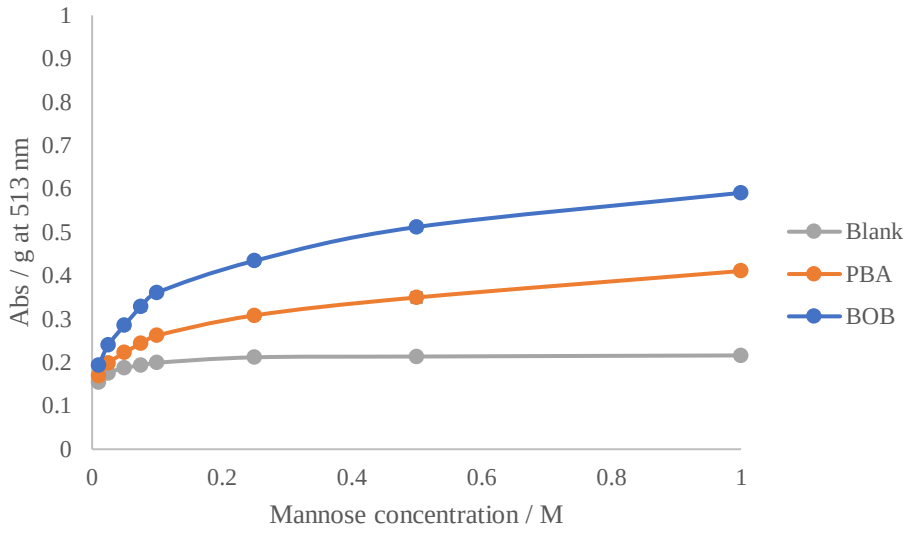

Figure 51. Mannose mediated ARS dye displacement assay for smaller hydrogels. Data points obtained 30 minutes after mannose addition and are an average of at least two experiments. Error bars show standard error.

The dye displacement assay was then repeated with D-glucose. A fresh set of hydrogels were stirred in increasing concentrations of glucose solution at 100 rpm for 30 minutes before measurements were taken. Figure 52 shows the release of ARS into solution for the hydrogels as the concentration of glucose is increased. The blank gels released a small amount of dye upon glucose addition, due to dye held in the gel matrix by non-covalent interactions. The phenylboronic acid pinacol ester-functionalised hydrogels released the smallest amount of dye compared to the previously studied sugars, as was expected. The benzoxaborole-functionalised hydrogels also released a smaller amount of dye, but once again saw a smaller decrease in binding affinity compared to the phenylboronic acid pinacol ester-functionalised hydrogels.

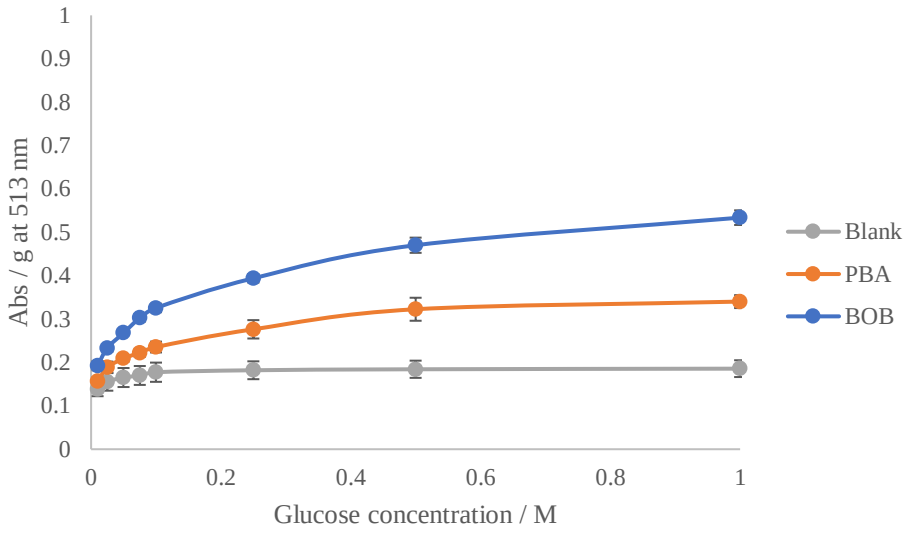

Figure 52. Glucose mediated ARS dye displacement assay for smaller hydrogels. Data points obtained 30 minutes after glucose addition and are an average of at least two experiments. Error bars show standard error.

As a general trend, the binding affinity for both the phenylboronic acid pinacol ester-functionalised and benzoxaborole-functionalised hydrogels for saccharides followed the order fructose > galactose > mannose > glucose, matching the order of stability constants reported for phenylboronic acid by Lorand and Edwards.[22] The benzoxaborole-functionalised hydrogel showed enhanced binding compared to the phenylboronic acid pinacol ester-functionalised hydrogel for all reducing hexose sugars investigated. Interestingly, the difference in binding affinities between the benzoxaborole-functionalised and phenylboronic acid pinacol ester-functionalised hydrogels increased as the overall binding affinities decreased, as exemplified by Table 4. If the benzoxaborole-functionalised hydrogel is used as a benchmark for comparison, the relative binding affinity of the phenylboronic acid pinacol ester-functionalised hydrogel decreases as the overall binding affinities decrease. For studies with fructose, the binding affinity of the phenylboronic acid pinacol ester-functionalised hydrogel was 88% of the binding affinity for the benzoxaborole-functionalised hydrogel. For galactose, the relative binding was 75%, for mannose the relative binding was 70% and for glucose the relative binding was 64%. In other words, the benzoxaborole-functionalised hydrogels do not display as dramatic decrease in their binding affinity down the sugar series compared to the phenylboronic acid pinacol ester-functionalised hydrogels.

Table 4. Relative absorbance values of dye displacement assays with all hydrogels compared to the benzoxaborole-functionalised hydrogels for monosaccharide sugars at a final concentration of 1 M.

Gel	Fructose		Galactose		Mannose		Glucose	
	Abs / g at 513 nm	% Abs (relative to BOB)	Abs / g at 513 nm	% Abs (relative to BOB)	Abs / g at 513 nm	% Abs (relative to BOB)	Abs / g at 513 nm	% Abs (relative to BOB)
BOB	0.9360	100	0.5320	100	0.5909	100	0.5337	100
PBA	0.8225	88	0.4009	75	0.4108	70	0.3403	64
Blank	0.2296	25	0.2052	39	0.2162	37	0.1857	35

3.3.6.3 Dye Displacement Assays with Non-Reducing Monosaccharides

After the successful binding of a range of reducing sugars to the benzoxaborole-functionalised hydrogels, attention was then focused on the binding of non-reducing sugars. Hall and co-workers have reported that benzoxaboroles are capable of complexing a range of glycopyranosides efficiently in neutral water, unlike normal boronic acids.[40] Unlike phenylboronic acids, which bind to reducing sugars such as glucose in their weakly populated furanose form, benzoxaboroles are able to complex non-reducing sugars in their pyranoside form. For hexopyranosides such as galactopyranosides, the preferred binding mode is through a *cis*-3,4-diol. Complexation of glucopyranosides is through their 4,6-diol unit (Figure 53).

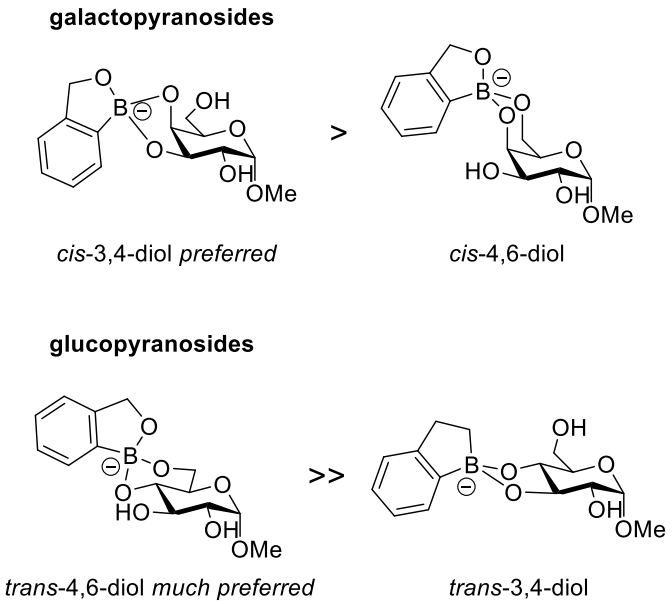

Figure 53. Favoured diol binding modes between benzoxaborole and glycopyranosides.

The relatively high Lewis acidity is likely a factor for this exceptional carbohydrate binding behaviour, along with subtle factors such as intramolecular hydrogen bonds with other hydroxyl groups on the sugar in the resulting anionic complex.

With this in mind, the dye displacement assay was then repeated using methyl α-D-glucopyranoside. A fresh set of hydrogels were stirred in increasing concentrations of methyl α-D-glucopyranoside solution at 100 rpm for 30 minutes before measurements were taken. Figure 54 shows the release of ARS into solution for the hydrogels as the concentration of methyl α-D-glucopyranoside is increased.

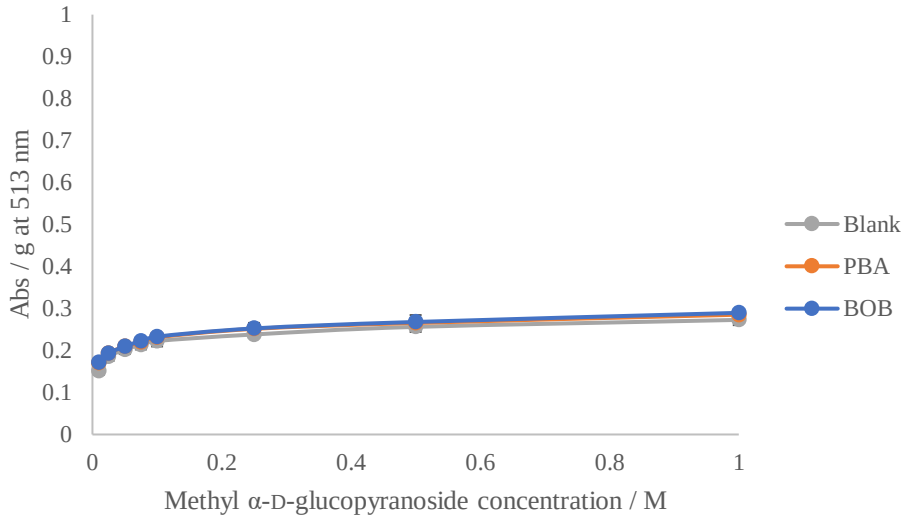

Figure 54. Methyl α-D-glucopyranoside mediated ARS dye displacement assay for smaller hydrogels. Data points obtained 30 minutes after methyl α-D-glucopyranoside addition and are an average of at least two experiments. Error bars show standard error.

The blank, benzoxaborole-functionalised and phenylboronic acid pinacol ester-functionalised hydrogels all only gave up a small amount dye upon addition of methyl α-D-glucopyranoside, presumed to be that held in the hydrogel matrix by non-covalent interactions. The binding of non-reducing sugars such as methyl α-D-glucopyranoside to benzoxaboroles is reported to be weaker than that of reducing sugars such as glucose.[40] Previous calculations of binding constants by Hall and co-workers were carried out in solution phase studies, and it is likely that the binding constants are even lower when the benzoxaborole is contained within a hydrogel matrix. This low binding affinity means that the methyl α-D-glucopyranoside is unable to complex efficiently with the benzoxaborole in order to displace the ARS dye into solution.

3.4 Conclusions

A series of blank, benzoxaborole-functionalised and phenylboronic acid pinacol ester-functionalised hydrogels were prepared and their relative saccharide binding affinities were determined. The benzoxaborole-functionalised hydrogels showed enhanced binding affinity for all the reducing monosaccharide sugars studied. The enhanced binding to D-glucose relative to the previously synthesised phenylboronic acid pinacol ester-functionalised hydrogels is of particular importance, due its implications in type 2 diabetes and the need for methods of detection for this particular sugar. However, both the benzoxaborole-functionalised and phenylboronic acid pinacol ester-functionalised hydrogels are D-fructose selective, showing a higher affinity for D-fructose compared to all other monosaccharides studied.

The ability of benzoxaboroles to complex non-reducing sugars when incorporated into a hydrogel matrix was also investigated. In solution, these compounds have been reported to complex hexopyranosides,[40] however the binding affinity is low compared to reducing sugars such as D-glucose. It was found that when incorporated into a hydrogel structure, no complexation to the non-reducing sugar methyl α-D-glucopyranoside was observed, with the same amount of dye displaced into solution as was observed for the blank hydrogel. The low binding constants calculated in solution must be even lower when the benzoxaborole functionality is incorporated into a hydrogel matrix.

3.5 Future Work

Whilst the benzoxaborole-functionalised hydrogels displayed an enhanced binding affinity for all of the reducing monosaccharide sugars studied, there is still scope to improve this binding affinity further, particularly for sugars such as D-glucose which displayed weaker binding. For boronic acid-based sensor systems, research has shown that more than one boronic acid unit is required to achieve saccharide selectivity.[2] The same idea could be incorporated into the development of a di-benzoxaborole-functionalised monomer. By incorporation of a second benzoxaborole group into the monomer, selectivity for a particular sugar may be achieved through two-point binding. One possible structure for such a monomer is given in Figure 55. Whilst use of a 6-carbon linker gave selective binding for D-glucose in the diboronic acid system,[150] the length of the linker may need to be tuned for a di-benzoxaborole system due to a different spatial arrangement of the boron functional groups.

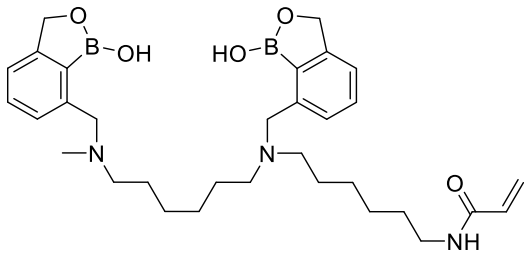

Figure 55. Proposed structure for a di-benzoxaborole-functionalised monomer

Previous work in the T. D. James group has led to the development of a reaction-based indicator displacement assay for the selective colorimetric and fluorometric detection of peroxynitrite.[192] Sensing systems were formed from the self-assembly of aromatic boronic acids with alizarin red S *in situ* for the selective detection of peroxynitrite. Addition of reactive oxygen species to this sensing complex led to the hydrolysis of the boronic acid compound to the corresponding phenol, and subsequent release of ARS. This resulted in spectral changes in both the fluorescence and absorbance spectrums; a decrease in intensity was observed when ARS is released from the boron. The same concept could be applied to the hydrogels utilised in this chapter. Previous work looked at the reaction-based indicator displacement assay in solution phase studies, but there is scope for this assay to be expanded to hydrogel-based systems.

Based on the same concept as the dye displacement assay for saccharide detection described in this chapter, a reaction-based indicator displacement assay could be utilised for the detection of reactive oxygen species or reactive nitrogen species (ROS or RNS). If boronic acid-functionalised hydrogels saturated with ARS dye were exposed to increasing concentrations of ROS such as hydrogen peroxide, the boronic acid group would be hydrolysed to a phenol, displacing the ARS dye into solution (Scheme 59). This would cause an increase in absorbance of the reaction solution, corresponding to the amount of ARS dye displaced, therefore the concentration of hydrogen peroxide could be determined.

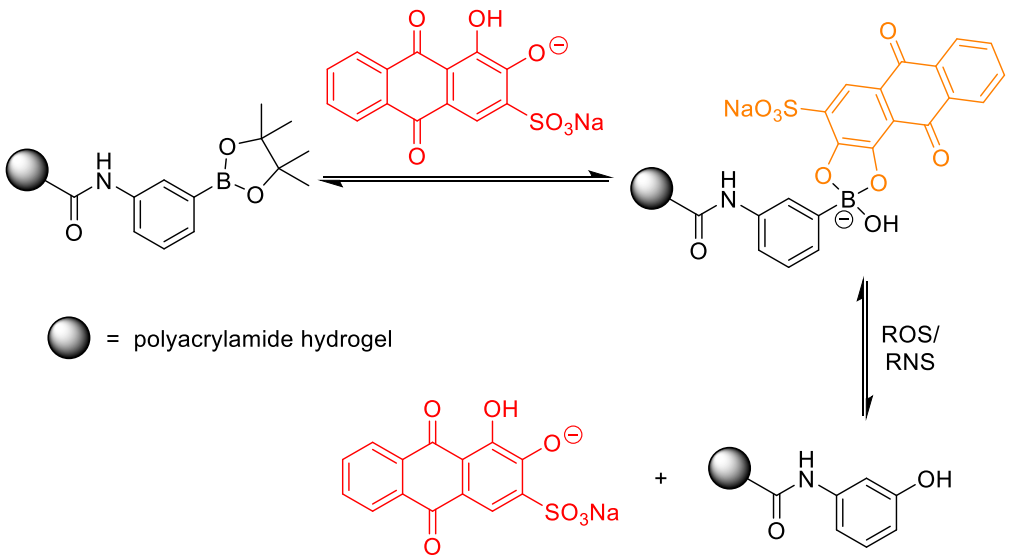

Scheme 59. Proposed reaction-based indicator displacement assay with boronic acid-functionalised hydrogels.

4 The Synthesis of Fluorescent Probes for the Detection of Hydrogen Peroxide

4.1 Introduction

4.1.1 Introduction to Fluorescence Spectroscopy

Luminescence is the emission of light from any substance, and occurs from electronically excited states. Luminescence is divided into two categories; fluorescence and phosphorescence, depending on the nature of the excited state. In fluorescence, which occurs in excited singlet states, the electron in the excited orbital is paired by opposite spin orientation to the electron in the ground state orbital. Return to the ground state is therefore spin allowed, and occurs rapidly by the emission of a photon. The emission rates of fluorescence are typically 10^8 s^{-1}, so that a typical fluorescence lifetime is approximately 10 ns.[193]

Phosphorescence is the emission of light from triplet excited states, in which the electron in the excited orbital has the same spin orientation as the electron in the ground state orbital. Transitions to the ground state are spin forbidden and therefore the emission rates are slow, 10^3 to 10^0 s^{-1}, so that phosphorescence lifetimes typically range from milliseconds to seconds. Following exposure to light, phosphorescent substances can glow for up to several minutes whilst the excited photon slowly returns to the ground state. Phosphorescence is not usually seen in fluid solutions at room temperature, due to the many deactivation processes that compete with emission, such as quenching processes and non-radiative decay.

The processes that occur between the absorption and emission of light are usually illustrated by a Jablonski diagram.[194] A typical Jablonski diagram is shown in Figure 56. The singlet ground, first and second electronic states are depicted by S_0, S_1, and S_2 respectively. A number of vibrational energy levels exist within each of these electronic energy levels, denoted by 0, 1, 2, *etc*. The transitions between states are depicted as vertical lines to illustrate the instantaneous nature of light absorption. Following light absorption several processes usually occur. A fluorophore is often excited to a higher vibrational level of either S_1 or S_2. Molecules rapidly relax to the lowest vibrational level of S_1, with a few rare exceptions, *via* internal conversion. This process generally

occurs within 10^{-12} s or less. Since fluorescence lifetimes are typically 10^{-8} s, internal conversion is generally complete prior to emission, therefore fluorescence emission generally occurs from the lowest energy vibrational state of S_1.

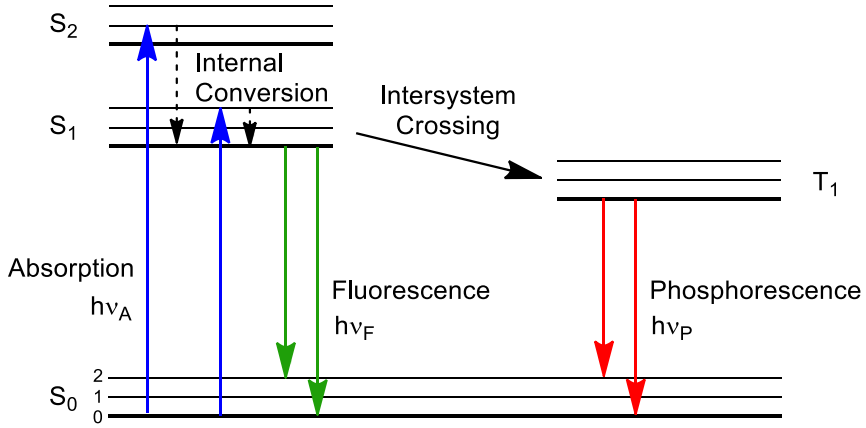

Figure 56. Jablonski diagram showing various energy transitions.

Return to the ground state typically occurs to a higher excited vibrational ground state level, which then quickly reaches thermal equilibrium. As a consequence of emission to higher vibrational ground states, the emission spectrum is typically a mirror image of the absorption spectrum of the $S_0 \rightarrow S_1$ transition. The spacing of the vibrational energy levels of the excited states is similar to that of the ground state, and consequently the vibrational structures seen in the absorption and the emission spectra are similar.

Molecules in the S_1 state can also undergo a spin conversion to the first triplet state, T_1. Emission from this triplet state is termed phosphorescence, and is generally shifted to longer wavelengths (lower energy) relative to fluorescence. This conversion from S_1 to T_1 is called intersystem crossing. Transition from T_1 to the singlet ground state is forbidden, and as a result the rate constants for triplet emission are several orders of magnitude smaller than those for fluorescence, resulting in the longer lifetimes observed for phosphorescence emission.

The phenomenon of fluorescence displays a number of general characteristics. Exceptions are known, but these are infrequent. Examination of the Jablonski diagram reveals that the energy of the emission is typically less than that of absorption; therefore fluorescence typically occurs at lower energies or longer wavelengths. This is known as the Stokes shift. One common cause for the Stokes shift is the rapid decay to the lowest vibrational level of S_1. Also, fluorophores generally decay to higher vibrational

levels of S_0, resulting in further loss of excitation energy by thermalization of the excess vibrational energy.

Another general property of fluorescence is that the same fluorescence emission spectrum is generally observed irrespective of the excitation wavelength, known as Kasha's rule.[195] Upon excitation to higher electronic and vibrational levels, the excess energy is quickly dissipated, leaving the fluorophore in the lowest vibrational level of S_1. Because of this rapid relaxation, emission spectra are usually independent of the excitation wavelength, although there are exceptions to this rule. For many fluorophores the absorption spectrum is a mirror image of the emission spectrum. The generally symmetric nature of these spectra is a result of the same transitions being involved in both absorption and emission, and the similar vibrational energy levels of S_0 and S_1.

4.1.2 Different Types of Fluorescence

As discussed above, the concept of fluorescence is characterised as the emission of energy when electrons from the excited state return to the ground state. The initial promotion of electrons can happen in several ways, leading to a number of different fluorescent mechanisms, some of which are discussed below.

4.1.2.1 Förster Resonance Energy Transfer (FRET)

The acronym FRET is commonly presented as 'Fluorescence Resonance Energy Transfer', however, this is not correct since this general mechanism of energy transfer in the excited state does not necessarily involve fluorescence. Therefore, according to recommendations approved by IUPAC and in recognition of the first theoretical description of this mechanism by Förster, the term 'Förster resonance energy transfer' is commonly used.[196] FRET occurs between two dye molecules that are sufficiently close in space, when the distance between them is less than 10 nm. The process occurs whenever the emission spectrum of a fluorophore, called the donor, overlaps with the absorption spectrum of another molecule, the acceptor (Figure 57).[193] The energy flows from the donor to the acceptor *via* non-radiative transfer, due to the dipole-dipole resonance interaction between them. The acceptor can be excited by this transferred energy and emit light. When such communication between excited and unexcited molecules exists, upon excitation of the donor its emission is quenched, and instead emission of the acceptor is increased. When this coupling is absent, only the emission

of the donor is observed.[196] The FRET effect depends strongly upon the distance between the donor and the acceptor. If the distance is short and the donor is excited, it can transfer the energy of electronic excitation to the acceptor, resulting in emission of fluorescence from the acceptor, if it is not quenched. The acceptor can be non-fluorescent and can only provide the quenching effect of the donor emission. Because FRET efficiency is steeply dependant on the distance separating the FRET pair and the relative orientation of the fluorophores, FRET can be used to detect changes in protein-protein interactions that arise from changes in affinity between the two proteins or changes in the conformation of their binding.[197]

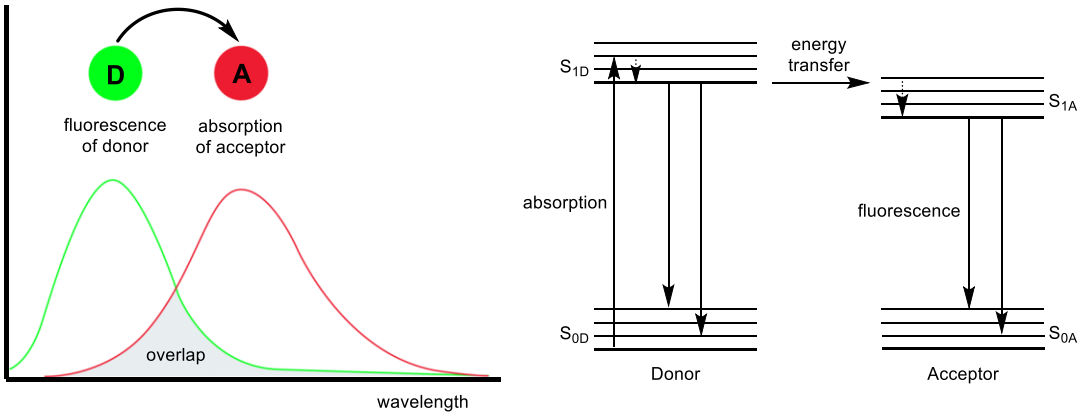

Figure 57. Spectral overlap for FRET and Jablonski diagram showing FRET processes.

4.1.2.2 Photoinduced Electron Transfer (PET)

Photoinduced electron transfer is the process by which an electron moves from one orbital to another. Important requirements for this reaction are the closeness in space of the two sites and matching their oxidation-reduction potentials.[196] The distances for this reaction are much shorter than those for FRET processes. PET can be facilitated by covalent bonding between a receptor and a fluorophore *via* a spacer (Figure 58). This 'fluorophore-spacer-receptor' format encapsulates the design of fluorescent PET sensors.[198]

Figure 58. The 'fluorophore-spacer-receptor' format of fluorescent PET sensors.

Figure 59a expands on this idea. In its 'off' state, when an incoming photon is absorbed ($h\nu_{Abs}$), the fluorophore component of the fluorophore-spacer-receptor system is energized. PET from the receptor to the fluorophore (or vice versa) is driven by this excitation, provided that the excitation energy is sufficient to perform the one-electron oxidation of the receptor and the one-electron reduction of the fluorophore.[199] In this case no fluorescence is observed from the fluorophore because its excitation has been dissipated *via* the PET process. Usually, the molecular system rapidly returns to the starting situation with a reverse electron transfer without further photonic assistance. In its 'on' state, excitation of the fluorophore results in fluorescence only because the PET process is arrested by the arrival of the analyte at the receptor site. If a cationic target is considered, the one-electron oxidation of the receptor when it is occupied is energetically much more expensive than before and so the PET process stops. An electrostatic attraction between the cationic target and the electron prevents its photoinduced transfer. This leads to the unused excitation energy in the fluorophore being returned as a fluorescence photon ($h\nu_{Flu}$).

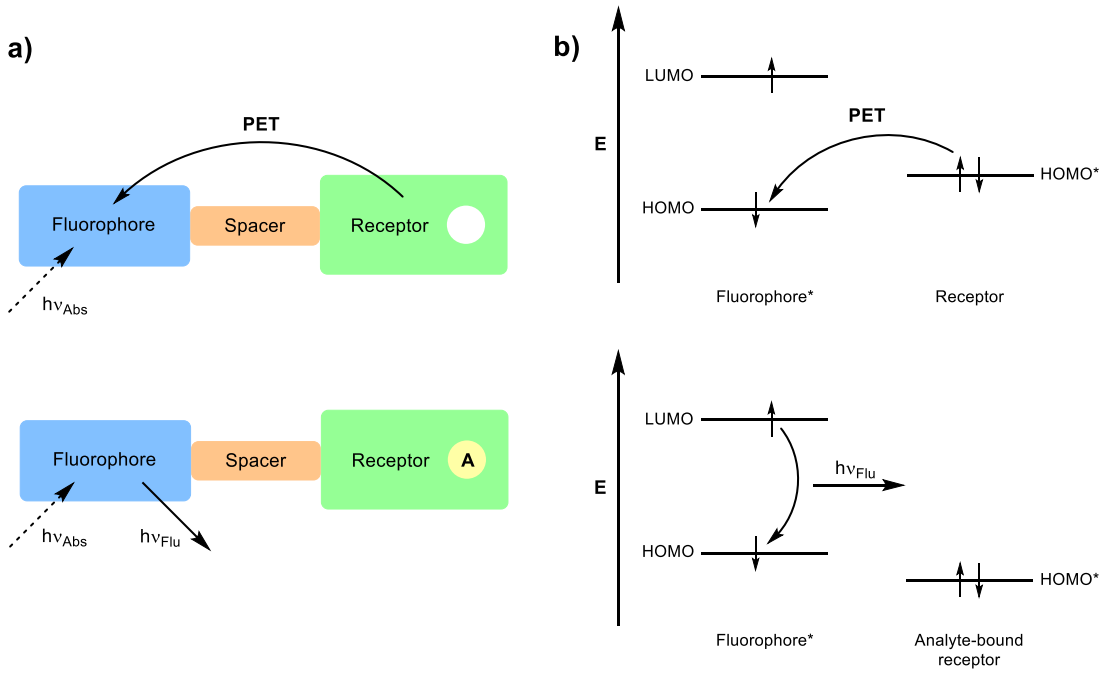

Figure 59. a) Signal transduction in PET sensors acting as an 'off-on' fluorescent switch. b) Molecular orbital energy diagrams showing the relative energetic dispositions of the frontier orbitals of the fluorophore and the receptor in its analyte-free and bound state.

This process can also be explained with the aid of molecular orbital energy diagrams (Figure 59b). For the 'off' state, the highest occupied molecular orbital (HOMO) of the

receptor is higher in energy than the HOMO of the fluorophore. Upon excitation, the fluorescence is quenched by the transfer of an electron from the HOMO of the receptor to the HOMO of the fluorophore.[198] In the 'on' state once the analyte is bound, the analyte-bound receptor's HOMO is stabilized and lies below the HOMO of the fluorophore, the thermodynamics for PET are no longer favourable and fluorescence is observed. As well as the 'off-on' PET fluorescent switches described here, 'on-off' molecular fluorescent switches are also possible.[199,200]

4.1.2.3 Internal Charge Transfer (ICT)

Internal charge transfer, sometimes referred to as intramolecular charge transfer, is also an electron transfer. In ICT the charge transfer is always intramolecular within the same electronic system or between systems with a high level of electronic conjugation, and the fluorophore and receptor usually overlap (eliminating the need for the spacer required in PET systems, Figure 60).[201] PET and ICT are easily distinguished by their absorption and emission spectra. In PET, strong quenching occurs without spectral shifts. In contrast, in ICT processes, both the normal (or locally excited, LE) state and the ICT state are fluorescent, displaying different intensities. In addition, their excitation and emission spectra usually exhibit significant wavelength shifts, depending on the local environment.[196] Although changes in emission intensity are often observed in parallel with changes in the emission wavelength, the principal designed mode of action for ICT sensors is to signal substrate binding *via* a shift in the emission wavelength.[27]

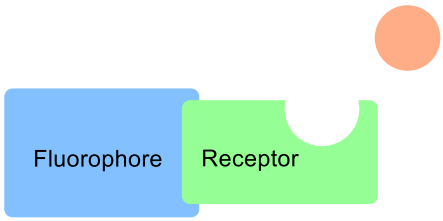

Figure 60. Schematic representation of the overlapped fluorophore-receptor design for fluorescent ICT sensors.

Commonly, ICT states are observed when a molecule contains both an electron-donating group and an electron-withdrawing group. If these groups are located at opposite ends of a molecule, an electronic polarization is induced. In the excited state, the electron donor becomes a stronger donor and the electron acceptor a stronger acceptor, subsequently the electronic polarization is substantially increased in the

excited state.[196] The enhanced dipole moment interacts with dipoles in the solvent medium, resulting in strong Stokes shifts. A change in the medium conditions can result in a switch from the locally excited state to the ICT state. Fluorescence from the normal, or locally excited (LE), state is commonly observed in solvents with lower polarity, at lower temperatures. An increase in solvent polarity and/or temperature causes fluorescence to occur from the ICT state. In polar solvents, these shifts become larger because the solute-solvent dipole interactions are stronger.[196] The ICT states are very sensitive to electric field effects and, therefore, to the presence of nearby charges.

This switching between LE and ICT states can be brought about by binding an ion to either the electron donor or acceptor site. When an electron-donor is attached to the receptor, binding of a cation will reduce the electron-donating character of the group. Owing to the resulting reduction of electronic conjugation, a blue shift occurs in the absorption spectra, together with a decrease of the molar extinction (Figure 61). Conversely, when an electron-acceptor is attached to the receptor, binding of a cation will enhance the electron-withdrawing character of the group. This resultant increase in electronic conjugation will lead to a red shift in the absorption spectrum and the molar extinction is increased.[196] Binding of an anion would produce the opposite effect.

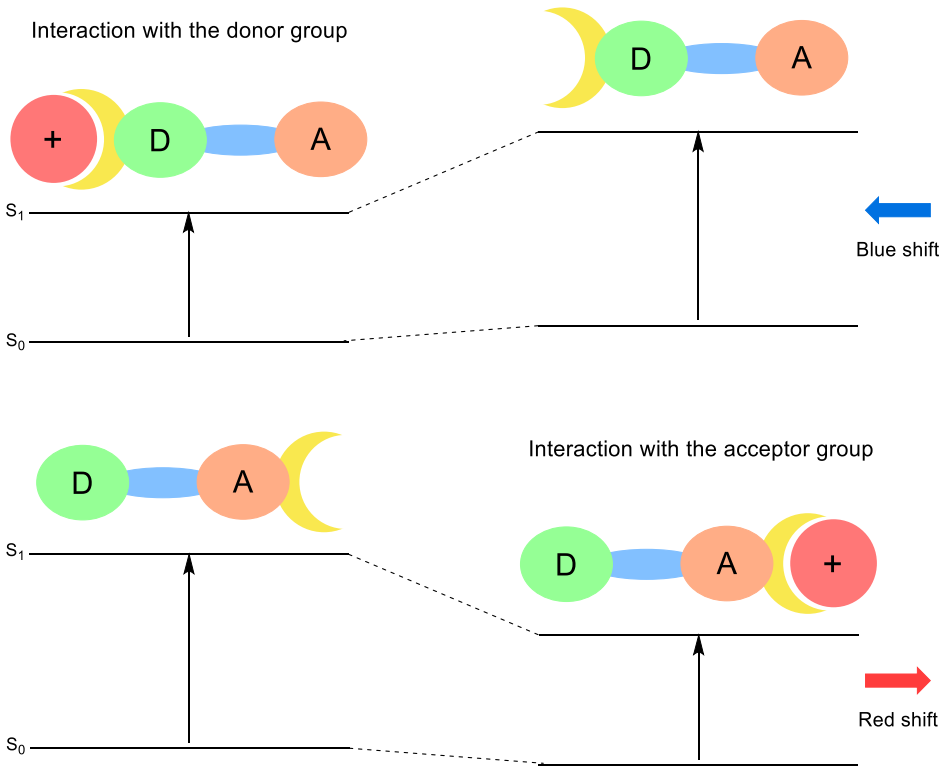

Figure 61. Spectral shifts of ICT sensors resulting from interaction of a bound cation with an electron-donating (D) or electron-withdrawing (A) group.

The electronic conjugation of compounds exhibiting ICT emission can also be modified. This can be done by changing the planarity between the electron-donor and acceptor fragments, since planar structures result in the best π-π electronic coupling. A single bond rotation in the excited state leads to an entirely charge separated state. Such disruptions of planarity with the appearance of ICT emission is well studied, and such states are known as twisted intramolecular charge transfer (TICT) states.[202]

4.1.3 Fluorescent Sensors

There are several analytical techniques for reporting molecular recognition, including Nuclear Magnetic Resonance (NMR), Circular Dichroism (CD), and UV-Vis, phosphorescence and fluorescence spectroscopy. Fluorescence spectroscopy possesses many advantages, which has seen it rise to the forefront of most sensor research. Fluorescence has great potential for *in vivo* analyte monitoring and is an extremely sensitive technique, with the capability to detect even a single photon in solution.[3]

Fluorescent sensors can be separated into two classes. 'Off-on' sensors produce an increase in fluorescence intensity upon analyte binding. This can occur for several

reasons, for example the cleavage of bonds or the opening of a ring in the molecule.[203] 'On-off' sensors result in a decrease in fluorescence intensity upon analyte binding. This change in fluorescent intensity upon analyte binding is a vital characteristic required for fluorescent sensors. Another vital property of fluorescent sensors is the shift in wavelength of the fluorescence upon binding with an analyte. This shift in wavelength could be a red shift (increasing wavelength), corresponding to a decrease in the energy of emission, or a blue shift (decreasing wavelength), corresponding to an increase in the energy of the emission.

4.1.4 The Use of Boron in Fluorescent Sensor Design

The origins of boronic acid based receptor design can be traced back to the fundamental work of Lorand and Edwards, when they used the pH drop observed on addition of saccharides to determine their association constants.[22] Boron is an element that has been widely used in sensor design. This is largely due to the fact that boronic acids can react reversibly with a range of other species to form boronate complexes. The boronic acid can react with a molecule to be detected to generate a species that produces some sort of response. The reversibility of this binding allows the original boronic acid species to be regenerated, therefore allowing further binding and signalling to occur.[189] Under certain conditions, this reversible binding can create fluorescence signals, particularly with arylboronic acids and esters. This fluorescence can occur *via* a photo-induced electron transfer (PET) mechanism, involving the transfer of electrons from an electron donor to an electron acceptor *via* a fluorophore, for example a pi-system.[204]

The reversible binding of analytes to boronic acids and esters can be exploited for the detection of hydrogen peroxide. Hydrogen peroxide reacts with aryl boronic acids and esters to produce phenols and the corresponding boric acid (Scheme 60).[205] Due to its empty 2*p* orbital, the boron atom of the trigonal planar boronic acid or ester is electrophilic and is attacked by the hydroperoxide anion to give a tetrahedral boronate anion. In the second step, R group migration occurs to the oxygen atom of hydroperoxide, liberating a hydroxide anion. This step occurs with retention of configuration at the migrating carbon atom. Migration of all the boron R groups occurs, until only a trialkoxyborane remains. If the boronic acids or esters contain a fluorophore within their structure, fluorescence signals can be produced due to the donation of electrons from the phenolic oxygen into the fluorophore.[206] Many sensors for reactive

oxygen species and reactive nitrogen species have been developed based on this oxidative removal of the boronic acid group.[206-210] This mechanism is the basis of the fluorescent probes synthesised in this chapter.

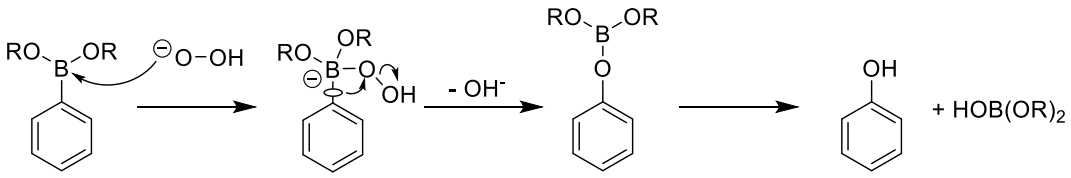

Scheme 60. Reaction of a boronic acid (R = H) or ester (R = alkyl) with H_2O_2.

4.1.5 Introduction to Reactive Oxygen Species and Reactive Nitrogen Species

Free radicals and related species have received much attention in recent years. Free radicals are one of the important mediators in the pathological processes of many diseases including cerebral and cardiovascular diseases, inflammatory diseases, neurodegenerative diseases, diabetes and cancer.[211] They include reactive oxygen species (ROS) and reactive nitrogen species (RNS). The term reactive oxygen species is a blanket term for the metabolites of standard diatomic oxygen and includes hydroxyl radicals ($HO^{\cdot}$), superoxide anion radicals ($O_2^{\cdot -}$), singlet oxygen ($^1O_2$), hydrogen peroxide (H_2O_2), peroxyl radicals ($ROO^{\cdot}$), ozone (O_3) and hypochlorous acid (HOCl). Reactive nitrogen species include nitric oxide (NO), nitroxyl (HNO) and peroxynitrite ($ONOO^-$). Both ROS and RNS have well-recognized beneficial and deleterious effects depending upon their concentrations. Reactive oxygen species and reactive nitrogen species are formed as natural by-products of the metabolism of oxygen or nitrogen, and play an important role in cellular signalling. During times of environmental stress, e.g. heat or UV exposure, the levels of ROS and RNS can increase dramatically. They can also be generated from interactions with exogenous sources such as xenobiotic compounds.[212] The increased production of these molecules leads to oxidative stress-mediated damage to lipids, proteins and DNA, culminating in pathological conditions and aging.[213] This necessitated the evolution of antioxidant systems to protect against over-oxidation and to combat reactive oxygen species.

4.1.5.1 Reactive Oxygen Species Production

Free radicals including ROS are the basic units of oxidative stress. Many sources of these free radicals have been discovered, which can be classified into endogenous and exogenous sources (Figure 62). Exogenous sources primarily include ionization radiations, drugs, pollutants, xenobiotics and toxins. The endogenous sources and mechanisms involved are much more complex.

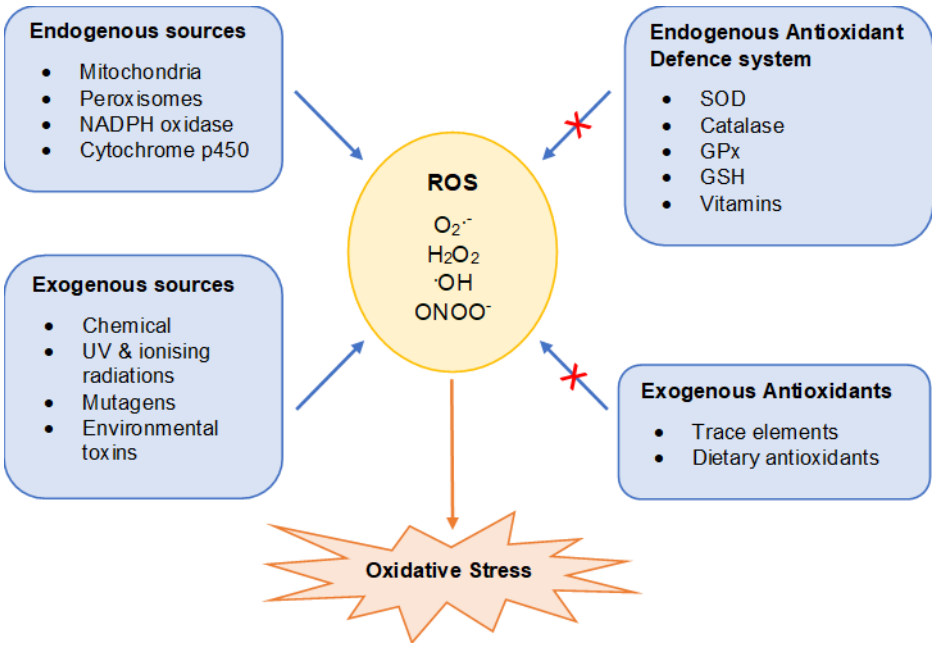

Figure 62. Sources of reactive oxygen species leading to induction of oxidative stress.

The most important and key source of ROS production and hence oxidative stress are mitochondria.[214] Mechanistically, ROS production occurs during the physiological process of ATP generation. During this process, molecular ground-state oxygen can be activated to form singlet oxygen by means of energy transfer, or by electron transfer forming the superoxide anion radical.[215] Subsequently, the superoxide anion radical can be converted into other ROS and RNS by a cascade of other enzyme-catalysed and spontaneous reactions.

Although the mitochondrial respiratory chain is the major source of superoxide anion radicals, these molecular species can also be generated by one-electron reduction of oxygen by several different oxidases under certain conditions.[216] These oxidases include NADPH oxidase (NOX family) and xanthine oxidase which are localized to various cellular membranes. NOX proteins are classically known as important ROS producers for the phagocytic killing of pathogens during the immune response.[208]

In addition to these ROS sources, a plethora of other "radical" enzymes present in many cell types and tissues contribute towards oxidative stress. These include mixed-function oxidases of the endoplasmic reticulum,[208] the cytosolic enzymes such as lipoxygenases or cyclooxygenases, the peroxisomal enzymes, and even DNA methylating enzymes and enzymes involved in the synthesis of hormones and neurotransmitters.[213]

4.1.5.2 Reactive Oxygen Species as a Source of Cellular Damage

ROS are generated by all of the aerobic cells involved in routine physiological processes, and the maintenance of a reduced cellular environment is essential for cell wellbeing. Within cells there is a careful balance between the level of oxidants and the availability of cellular antioxidants to combat them. At low physiological concentrations, these reactive oxidants have positive effects and act selectively. Besides being metabolic intermediates, they are also involved in gene regulation, cellular growth, and signal transduction cascades.[217-219] Furthermore, they play an essential role in the microbial defence and immunological surveillance. However, if the concentration of these highly reactive species increases and they are not quenched by antioxidant species or other scavenging molecules, then they are free to react with multiple cellular components to a damaging degree.[220]

When ROS overwhelm the cellular antioxidant defence system, whether through an increase in ROS levels or a decrease in the cellular antioxidant capacity, oxidative stress occurs. This oxidative stress results in direct or indirect ROS-mediated damage of nucleic acids, lipids and proteins, and has been implicated in neurodegeneration,[221] diabetes,[222] carcinogenesis[223] and aging.[224] As a consequence of ROS accumulation, oxidative stress increases exponentially with age, paralleled by a remarkable decline of the cell repair machinery.[225] Oxidative stress contributes to the pathogenesis of several cardiovascular, pulmonary and neuronal disorders common among elderly people, such as myocardial infarction, diabetes, atherosclerosis, chronic obstructive pulmonary disease or Alzheimer's disease.[226]

Which specific age-related diseases develop is dependent on where the oxidative damage takes place. There is an increasing focus on research in this area to enhance our understanding of the role that oxidative stress plays during the progression of these diseases, owing to current demographic trends and associated healthcare costs in Western societies.[226] Considering the number of pathogenic pathways which ROS

contribute to, it is clear that the species are vital medical targets in the area of diagnostic detection.

4.1.6 Sensors for Reactive Oxygen Species and Reactive Nitrogen Species

Since it has been established that they are responsible for multiple human diseases, ROS and RNS sensors have been proposed to be a useful diagnostic tool as their *in vivo* concentration is thought to be an indicator for a site of potential disease. A selective fluorescent sensor could be used to help understand the critical role of ROS/RNS and detect high concentrations of ROS or RNS within a cell, producing a useful diagnostics tool for gaining further knowledge about the links between ROS/RNS and disease. Multiple studies have examined the use of antioxidants to reduce particularly high concentrations of ROS, however large doses of supplementary antioxidants do not necessarily prevent oxidative aging *in vivo*.[227] The development of selective fluorescent sensors is showing progress in their ability to quantitatively and selectively detect free radical species *in vitro*,[209] however further applications of these sensors may be hindered by the difficulties of detecting ROS *in vivo*.[228]

Fluorescent probes are required to be biorthogonal, meaning that they do not disrupt normal cellular functions. The sensor must also be sensitive and specific to a single ROS or RNS and be able to pass through cellular membranes. Additionally, the sensor is required to be viable at neutral, physiological pH.[229] The fulfilment of all of these parameters is required to produce a successful sensor, demonstrating the necessity of this field of research.

The development of fluorescent sensors for the detection of ROS is not a new area of research. Dichlorodihydrofluorescein probes were first used to detect reactive oxygen species half a century ago.[230] These probes are based on the oxidation of dichlorodihydrofluorescein **57** to its fluorescent analogue **58** (Scheme 61), which was initially thought to be a relatively specific indicator of H_2O_2 formation and has been used extensively in the detection of oxidants produced during the respiratory burst in inflammatory cells.[231] However, further research has revealed that these compounds lack selectivity and may require a catalyst for reaction. Despite these drawbacks, dichlorodihydrofluorescein probes have been used in well over 2000 studies.[232] Because of the multiple pathways that can lead to dichlorodihydrofluorescein fluorescence, this

assay may best be applied as a qualitative marker of cellular oxidant stress rather than a precise indicator of rates of H_2O_2 formation.[231]

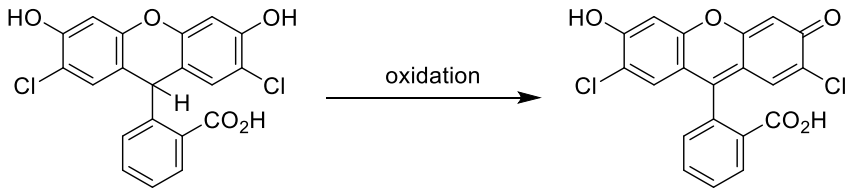

57 58

Scheme 61. Oxidation of dichlorodihydrofluorescein probe for ROS detection.

The selectivity of the ROS/RNS probes is arguably the most difficult criteria to fulfil due to the distinct similarity in the shape and size of all ROS and RNS species. The use of reaction based sensors can help overcome this issue. The discovery of functional groups which react differently with different ROS and RNS species can be effectively integrated into a fluorophore to increase the selectivity of a sensor.

Because of the broad physiological and pathological consequences of ROS and RNS species and the chemical complexities associated with these reactive small molecules, new and better methods to monitor the origins and fates of ROS and RNS are required. Much progress has been made in the development of more selective sensors. The following sections give more detail on hydrogen peroxide, as well as fluorescent probes that have been developed for its detection.

4.1.6.1 Probes for Hydrogen Peroxide

Hydrogen peroxide (H_2O_2) is the simplest peroxide (a compound with an oxygen-oxygen single bond) and is a strong oxidising agent, which has been widely employed as a bleach and as a cleaning reagent to reduce Biological Oxygen Demand (BOD) and Chemical Oxygen Demand (COD) from industrial wastewater.[206] Hydrogen peroxide plays an important role as a signalling molecule in a variety of different biological processes, and is an important factor in the progression of diseases such as Alzheimer's disease[233] and cancer.[234] The importance of H_2O_2 has led to researchers seeking effective approaches for its detection. Fluorescent probes are well suited to meet the need for tools to map the spatial and temporal distribution of H_2O_2 in living cells. However, the major challenge for practical H_2O_2 sensing in biological environments is

creating water-soluble systems that respond to H_2O_2 selectively over competing cellular ROS such as superoxide, nitric oxide, and lipid peroxides.[235]

Chang *et al*. have developed a range of probes for the selective detection of H_2O_2 based on the hydrogen peroxide-mediated conversion of arylboronates to phenols. Based on this strategy, Peroxyfluor-1 (PF1) **59** was developed as the first fluorescent probe for selective imaging of H_2O_2 in biological systems.[236] Installation of boronic ester groups at the 3' and 6' positions of an xanthene scaffold forces the probe to adopt a closed, colourless, and non-fluorescent lactone form. Upon treatment with H_2O_2, hydrolytic deprotection of the boronates subsequently generates the open, coloured and fluorescent fluorescein product (Scheme 62).[237] The probe was evaluated under simulated physiological conditions, and was shown to be non-fluorescent. The addition of H_2O_2 triggers a prompt fluorescence increase with concomitant growth of a visible wavelength band characteristic of fluorescein. The probe was also shown to be highly selective for H_2O_2 over other more oxidising ROS, this observed selectivity is due to the detection mechanism of the probe, which relies on chemoselective boronate deprotection rather than nonspecific oxidation to produce an optical response.

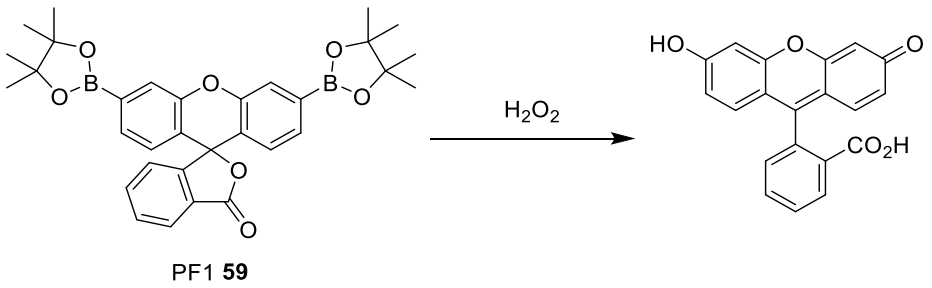

PF1 **59**

Scheme 62. Reaction of Peroxyfluor-1 with H_2O_2 to generate fluorescein.

Building on this work Chang *et al*. developed further Peroxysensor cell-permeable boronate-based probes for H_2O_2 detection, capable of imaging micromolar changes in H_2O_2 concentrations in living cells (Scheme 63).[235] Peroxyresorufin-1 (PR1) **60** and Peroxyxanthone-1 (PX1) **61** displayed a prompt increase in fluorescence upon reaction with H_2O_2 and again displayed high selectivity for H_2O_2 over other ROS. Taken together PR1, PF1 and PX1 represent a unique homologous series of red-, green-, and blue-fluorescent probes for H_2O_2, respectively, that operate by a boronate deprotection mechanism.

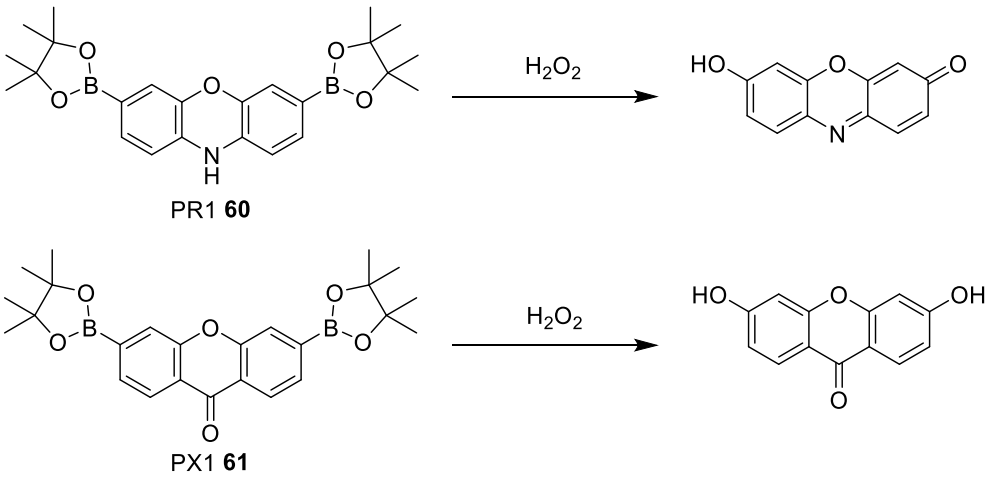

Scheme 63. Reaction of Peroxyresorufin-1 and Peroxyxanthone-1 with H_2O_2 to generate resorufin and 3,6-dihydroxyxanthone respectively.

As a further development of this work, Chang *et al*. developed the Ratio-Peroxyfluor-1 (RPF1) probe **62**, a ratiometric fluorescent reporter for H_2O_2 (Scheme 64). The probe displays good selectivity for H_2O_2 over other ROS in water, visible wavelength excitation and emission profiles, and is capable of detecting endogenous H_2O_2 production from viable mitochondria.[238] The ratiometric detection of H_2O_2 is based on modulating fluorescence resonance energy transfer in a two-fluorophore cassette consisting of a coumarin donor and a boronate-protected fluorescein acceptor linked by a rigid spacer. In the absence of H_2O_2, the boronate protecting groups force the acceptor to adopt a closed, colourless, and non-fluorescent lactone form. Spectral overlap between coumarin emission and fluorescein absorption is minimised, FRET is suppressed, and only blue donor emission is observed upon excitation of the coumarin chromophore. Upon reaction with H_2O_2 to generate the open, coloured, and fluorescent fluorescein moiety, the acceptor shows a strong absorption in the coumarin emission region. Spectroscopic overlap is enhanced, and excitation of the donor coumarin chromophore results in increased green fluorescein acceptor emission by FRET. Changes in H_2O_2 concentration can be detected by measuring the ratio of blue and green fluorescence intensities.

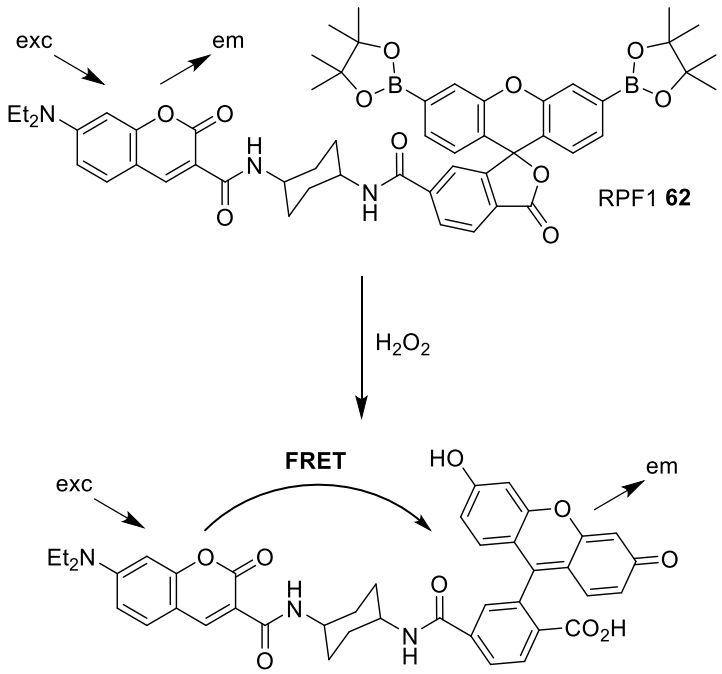

Scheme 64. Reaction of Ratio-Peroxyfluor-1 with H_2O_2.

Two further probes were developed by Chang *et al*. for detecting endogenous H_2O_2 produced for signalling in living cells. Previous work has shown that deprotection of aryl boronates to phenols provides a reaction-based approach to specific fluorescence detection of H_2O_2 over other ROS in situations of oxidative stress.[235,237] However, initial attempts to use these diboronate reagents to detect H_2O_2 under oxidative signalling conditions were unsuccessful.[239] Aiming to develop new chemical tools that are sensitive enough to report H_2O_2 production at physiological signalling levels while maintaining H_2O_2 specificity, attention was turned to dyes that could be activated by a single boronate deprotection. Peroxy Green-1 (PG1) **63** and Peroxy Crimson-1 (PC1) **64** (Scheme 65) were developed as boronate-based probes that have high selectivity for H_2O_2 and are capable of visualizing endogenous H_2O_2 produced in living cells by growth factor stimulation, including the first direct imaging of peroxide produced for brain cell signalling.[239] Fluorescence data showed that the monoboronate probe PG1 **63** undergoes the greatest absolute change in fluorescence turn-on upon reaction with H_2O_2 relative to the PC1, PR1 and PF1 probes.

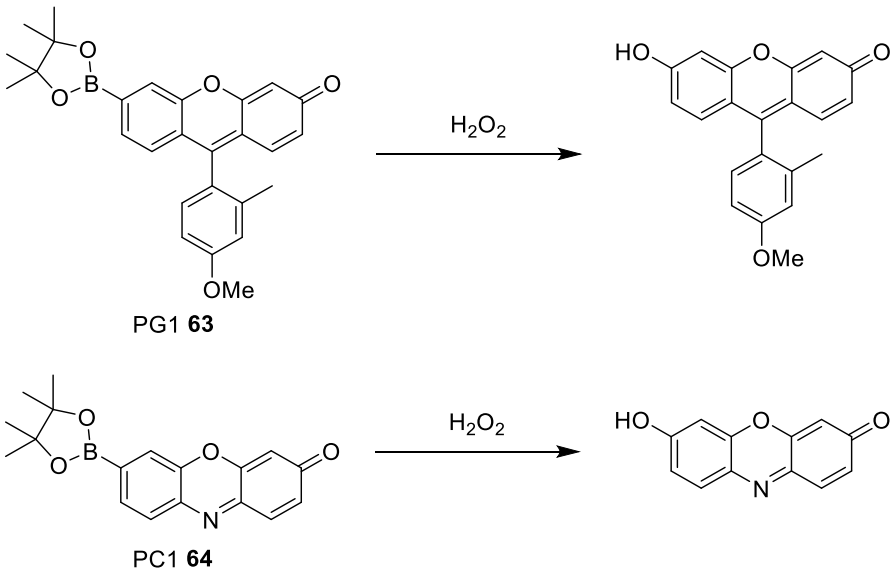

PG1 **63**

PC1 **64**

Scheme 65. Reaction of Peroxy Green-1 and Peroxy Crimson-1 with H_2O_2.

Chang *et al*. have also developed a further ratiometric probe for H_2O_2 detection in living cells based on the structural core of the fluorescent dye Lucifer yellow.[240] The ratiometric fluorescence detection of cellular H_2O_2 relies on controlling internal charge transfer within the dye platform to promote a change in emission colour upon reaction with H_2O_2. Modification of the electron-donating 4-amino donor on the 1,8-naphthalimide affects both ICT and emission colour, as making this substituent more electron deficient results in ICT-induced blue shifts in emission maxima. Modifying the 4-amino donor into an electron-withdrawing carbamate group that can be specifically decaged by H_2O_2 back to the amine provides a switch for ratiometric detection of H_2O_2. Reaction of Peroxy Lucifer-1 (PL1) **65** with H_2O_2 triggers chemoselective cleavage of the boronate-based carbamate protecting group to release the fluorescent dye (Scheme 66).

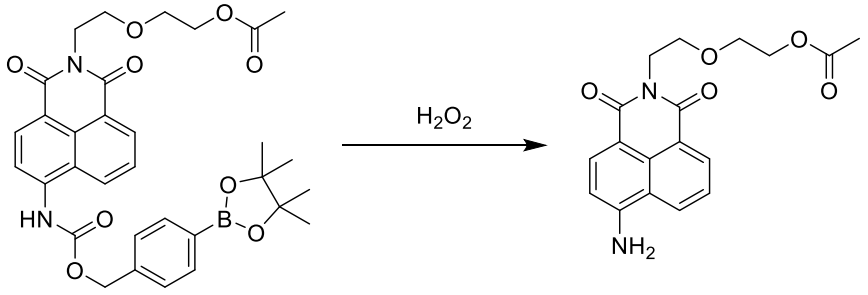

PL1 **65**

Scheme 66. Reaction of Peroxy Lucifer-1 with H_2O_2.

Further work by Chang *et al*. has led to the development of a nuclear-localized fluorescent probe for the detection of H_2O_2. Previous work by the group had shown the H_2O_2-mediated conversion of arylboronates to phenols provides a general reaction-based strategy for the selective and sensitive detection of cellular H_2O_2 in immune and neural signalling models, but the previous probes developed do not possess a preferred subcellular location.[209] The Nuclear Peroxy Emerald-1 (NucPE1) probe **66** was found to accumulate in the nuclei of live cells, without the need for additional targeting groups. Reaction of NucPE1 with H_2O_2 triggers a fluorescence increase upon its conversion to the fluorophore (Scheme 67) and was shown to be selective for H_2O_2 over a panel of biologically relevant ROS, including superoxide, nitric oxide and hydroxyl radicals.

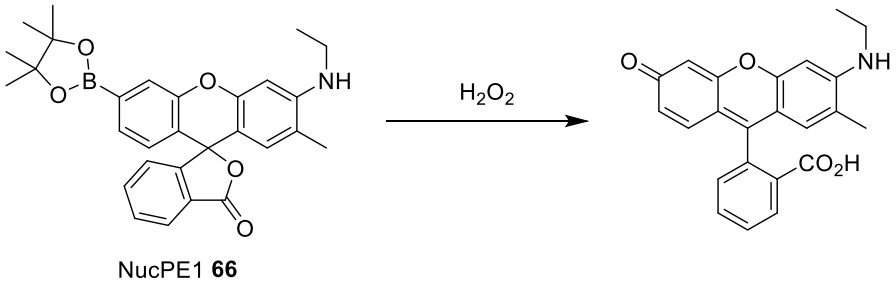

NucPE1 **66**

Scheme 67. Reaction of Nuclear Peroxy Emerald-1 with H_2O_2.

Boronate deprotection offers a general strategy for providing selective fluorescent probes for H_2O_2 in cellular environments. James *et al*. have employed boronic acids as sensors where the boron atom is directly attached to a fluorophore, leading to an integrated probe, and separated by a Lewis basic spacer leading to an insulated probe (Figure 63).[206] The reactions of the integrated boronate probe **67** and the insulated boronate probe **35** with H_2O_2 in the presence of D-fructose were investigated. It was reported that D-fructose effects the reaction of the integrated and insulated probes with H_2O_2 in opposite directions. The integrated boronate probe **67** showed enhanced reactivity with H_2O_2 in the presence of D-fructose, whilst the insulated boronate probe **35** displayed reduced reactivity with H_2O_2. The fluorescence of the insulated probe **35** is turned on by saccharide binding, since boronic ester formation causes an enhanced interaction between the neighbouring amine and the boron atom. This N-B interaction hinders the reaction between boron and H_2O_2 in the presence of saccharides.

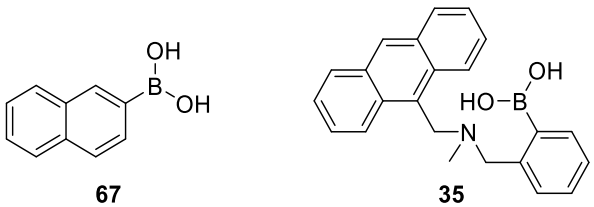

67 "Integrated" **35** "Insulated"

Figure 63. The structures of the "integrated" and "insulated" boronic acid probes.

4.1.7 Summary of Introduction

ROS and RNS have received much attention in recent years. They are important mediators in the pathological processes of many diseases including cerebral and cardiovascular diseases, inflammatory diseases, neurodegenerative diseases, diabetes and cancer. Because of the broad physiological and pathological consequences of ROS and RNS, the development of new and better methods for the detection and measurement of ROS and RNS both *in vivo* and *in vitro* is of great importance. Synthetic fluorescent probes have received great attention and achieved much success in the detection of certain reactive species with high selectivity and sensitivity. However, it should be noted that it is still a big challenge using traditional boronate-based chemosensors to distinguish between H_2O_2 and $ONOO^-$. There are still many challenges in the development of more effective fluorescent probes, with increased chemoselectivity, biocompatibility and bio-orthogonality.

The aim of this project was to synthesise a range of boronic acid pinacol ester-based fluorescent probes for the detection of hydrogen peroxide. Hydrogen peroxide reacts with boronic acid pinacol esters to generate the corresponding phenol, as shown in Scheme 60. If the boronic acid pinacol ester is attached to a fluorophore, then this conversion to a phenol can cause a change in the fluorescent characteristics of the probe. The probes synthesised in this chapter were designed on the basis of this mechanism. A range of electron-donating and electron-withdrawing substituents were chosen in order to investigate their effect upon the fluorescence of the probes. A fluorescent probe showing 'Off-On' fluorescence characteristics accompanied by a large wavelength shift upon reaction with hydrogen peroxide was desired, as this type of change is easiest to detect.

4.2 Results and Discussion

4.2.1 Synthesis of the Probes

Initially, four stilbene boronic acid pinacol esters were synthesised as fluorescent probes for the detection of hydrogen peroxide (Figure 64). These structures were chosen as synthetic targets based on a paper by Lakowicz *et al*. describing the spectral properties of the corresponding boronic acid compounds and their use as saccharide sensors.[241]

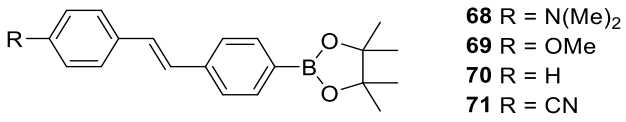

Figure 64. The structures of the initially synthesised arylboronic pinacol ester probes.

The synthesis involved a Horner-Wadsworth-Emmons (HWE) reaction to produce a bromo-substituted intermediate, which was then further reacted with bis(pinacolato)diboron (B_2pin_2) in a palladium-catalysed Suzuki reaction to form the pinacol ester probes. The synthetic route is discussed in further detail below.

4-bromobenzylbromide was first reacted with triethyl phosphite ($P(OEt)_3$) to form the phosphonate ester, which was deprotonated to afford an anion that was then reacted *in situ* with the corresponding substituted benzaldehyde (Scheme 68).

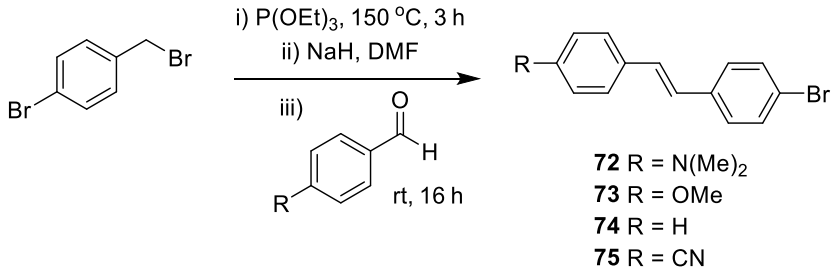

Scheme 68. HWE reaction between 4-bromobenzylbromide and the substituted aldehyde.

The reaction proceeds *via* the HWE mechanism shown in Scheme 69. 4-bromobenzylbromide first reacts with $P(OEt)_3$ to form the phosphonate ester. This is then deprotonated by sodium hydride (NaH) to form a phosphonate enolate, which will then attack the carbonyl of the substituted aldehyde to form an oxaphosphetane intermediate. A molecule of the phosphonate salt is then eliminated from the oxaphosphetane intermediate, generating the *trans* alkene product. The reversibility of

the addition step leads to the formation of the more thermodynamically stable *trans* alkene product.

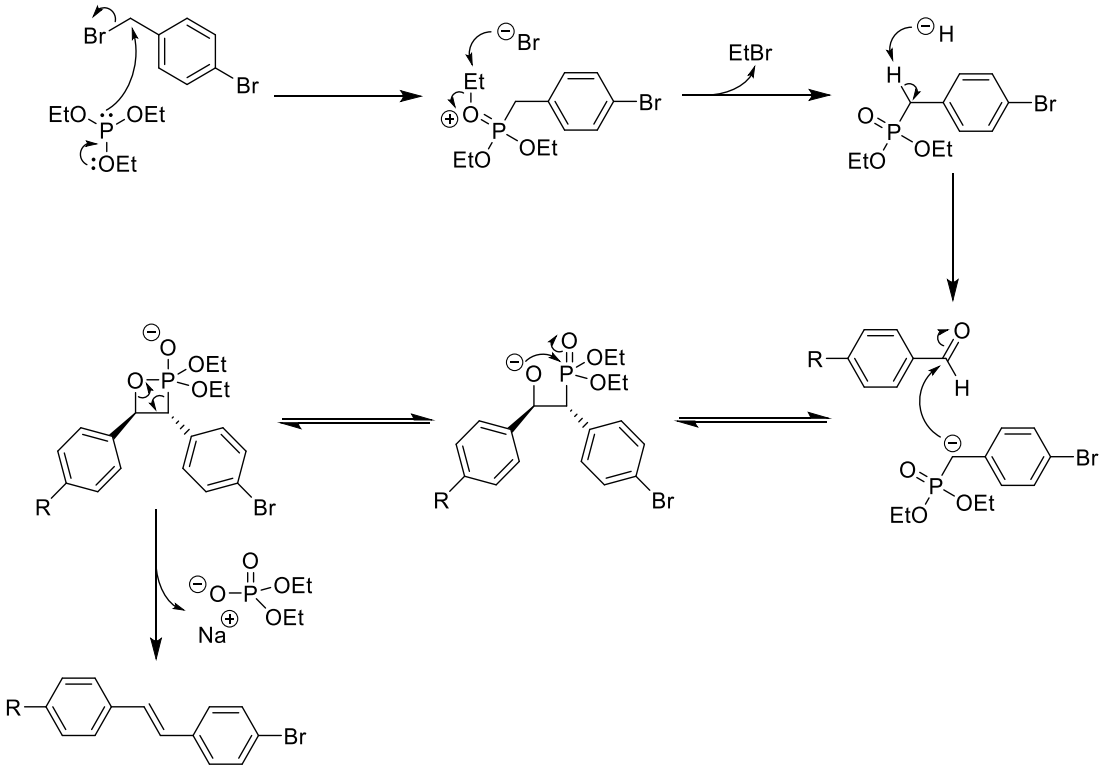

Scheme 69. Mechanism of the HWE reaction to form the bromo-substituted intermediate.

The product was confirmed to be the *trans* alkene by ^{1}H NMR spectroscopy. The coupling constants (*J*) of *trans* alkenyl protons tend to be in the range of 12-18 Hz, whereas those of *cis* alkenyl protons tend to be smaller, in the range of 6-12 Hz. The coupling constants observed of 16 Hz confirmed the formation of the expected *trans* alkene product. The phosphonate salt produced as a by-product of the reaction is water-soluble so is easily removed from the reaction mixture by an aqueous wash. The product was then purified by recrystallization, before being taken through to the next step.

Once the bromo-substituted stilbene product had been formed, it was subjected to a Suzuki reaction with bis(pinacolato)diboron (Scheme 70).

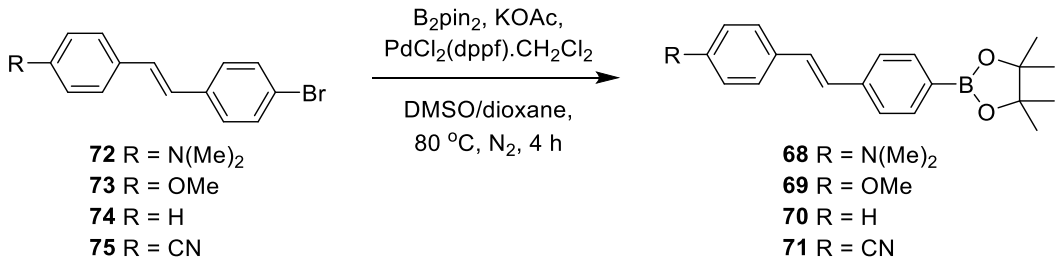

Scheme 70. Suzuki reaction of bromo-substituted intermediate to form the boronic acid pinacol ester.

The Suzuki reaction proceeds *via* the mechanism shown in Scheme 71. The first step involves oxidative addition. During this step, the palladium catalyst is oxidized from palladium(0) to palladium(II).[242] The palladium catalyst is inserted into the carbon-bromine bond to yield an organopalladium complex. In the second step, the bromine atom is exchanged for an acetate ligand, forming an (acetato)palladium(II) complex. The Pd-O bond, which consists of a hard Lewis base with a soft Lewis acid, is more reactive than a Pd-Br bond. In the third step, transmetallation, the acetate ligand is exchanged with one of the Bpin groups on the bis(pinacolato)diboron species to give the new palladium(II) complex. The final step is the reductive elimination step where the palladium(II) complex eliminates the product and regenerates the palladium(0) catalyst.

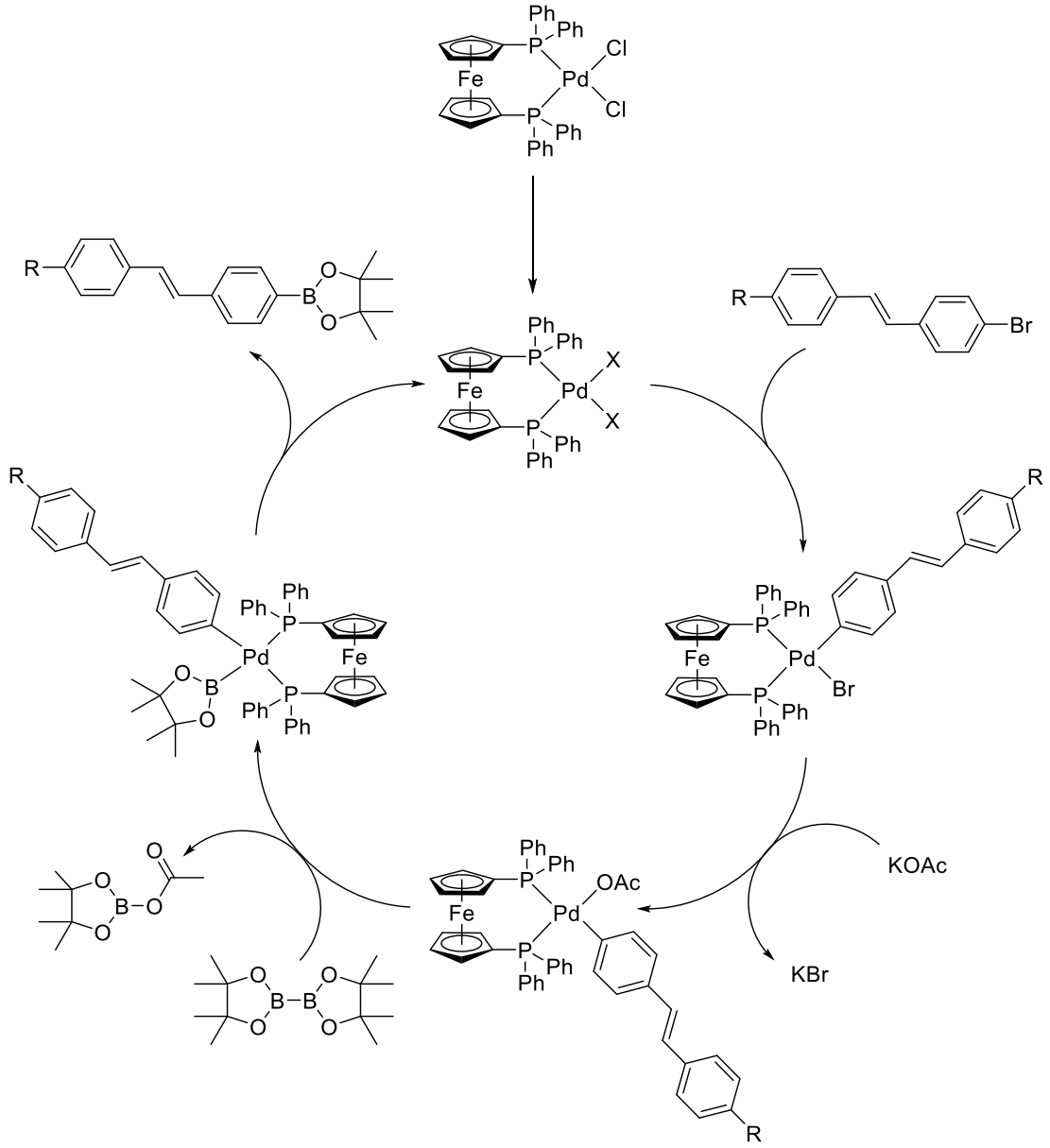

Scheme 71. Mechanism of the Suzuki reaction for the synthesis of pinacol ester probes.

Pure *trans* stilbene pinacol ester probes were obtained after an aqueous work up and purification by recrystallization from DCM and hexane to remove excess unreacted bis(pinacolato)diboron. ^{1}H, ^{13}C and ^{11}B NMR spectra and mass spectrometry confirmed the presence of the desired products.

Initial fluorescence analysis of the probes revealed that they all fluoresce in the wavelength range of 300 nm to 480 nm (fluorescence analysis of the probes is described in section 4.3.2). However, several proteins, coenzymes and other biological materials also fluoresce in the wavelength range of 250 nm to 500 nm.[243] These materials will generate background fluorescence and will therefore interfere with the analysis of the

probe if it fluoresces in the same wavelength range. The stilbene probes fluoresce in this range, so would not be suitable for use in cells.

Initial fluorescence studies showed that probe **68** with the electron-donating dimethylamino substituent displayed the biggest 'off-on' response upon reaction with hydrogen peroxide. A modified version of this probe was synthesised in an attempt to shift the fluorescence profiles to a longer wavelength, overcoming issues associated with background fluorescence of biological materials, allowing for the probe to be used within cells. The naphthalene stilbene probe **76** was chosen as a synthetic target (Figure 65), designed to have the same electron-donating properties as probe **68**, but with increased conjugation. It was hypothesised that the increased conjugation of the system would result in the electron density found within the fluorophores being spread out over a larger number of atoms. This would decrease the energy of the HOMO-LUMO gap overall, causing the molecule to fluoresce at longer wavelengths.

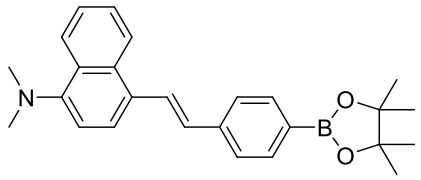

76

Figure 65. The structure of the naphthalene stilbene probe.

Probe **76** was synthesised by the same method used for the stilbene probes, with 4-dimethylamino-1-naphthaldehyde used as the substituted aldehyde in the HWE reaction. An extended reaction time for the Suzuki reaction (18 hours as compared to 4 hours for probe **68**) gave the naphthalene stilbene pinacol ester probe **76**.

Fluorescence studies revealed that although an increase in the wavelength of fluorescence was observed, the increase in conjugation affected the intensity of the florescence upon reaction with hydrogen peroxide, as probe **76** displayed 'on-off' characteristics upon reaction with H_2O_2. Also, the stilbene based probes have issues associated with low photostability, due to *trans-cis* isomerisation of the ethylene bridge joining the two benzene rings.[244]

In a further attempt to continue this work, a new fluorescent probe was synthesised. The dimethylamino oxazole probe **77** was chosen as a synthetic target (Figure 66). As this probe does not contain a bridging ethylene unit, *trans-cis* isomerisation is not possible,

leading to a probe with increased photostability. It was also hoped that the probe would display fluorescence profiles at longer wavelength, as the corresponding boronic acid analogue **78** is reported in the literature to have a maximum fluorescence intensity at 557 nm in its neutral form.[245]

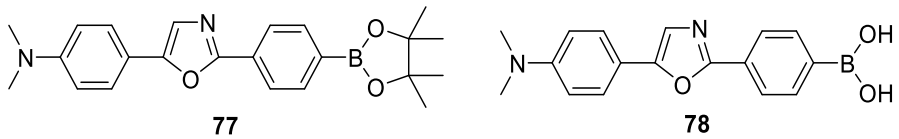

Figure 66. The structures of the boron pinacol ester target probe and previously reported boronic acid probe.

2-amino-4-dimethylaminoacetophenone hydrochloride was reacted with 4-bromobenzoyl chloride and anhydrous pyridine in anhydrous DCM to form amide **79** (Scheme 72).

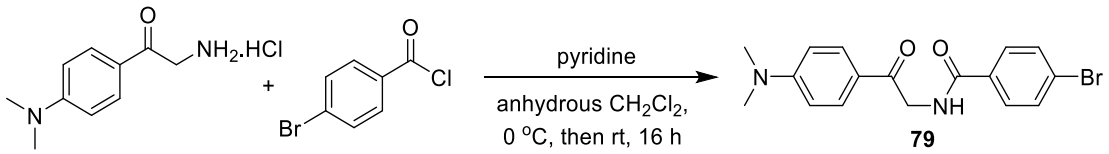

Scheme 72. Synthesis of 4-bromo-*N*-(2-(4-(dimethylamino)phenyl)-2-oxoethyl)benzamide intermediate.

The hydrochloride salt of the 2-amino-4-dimethylaminoacetophenone reacts with the pyridine to give the free amine, which subsequently attacks the carbonyl carbon of 4-bromobenzyl chloride to form the amide bond, with the loss of chlorine to form the desired amide (Scheme 73).

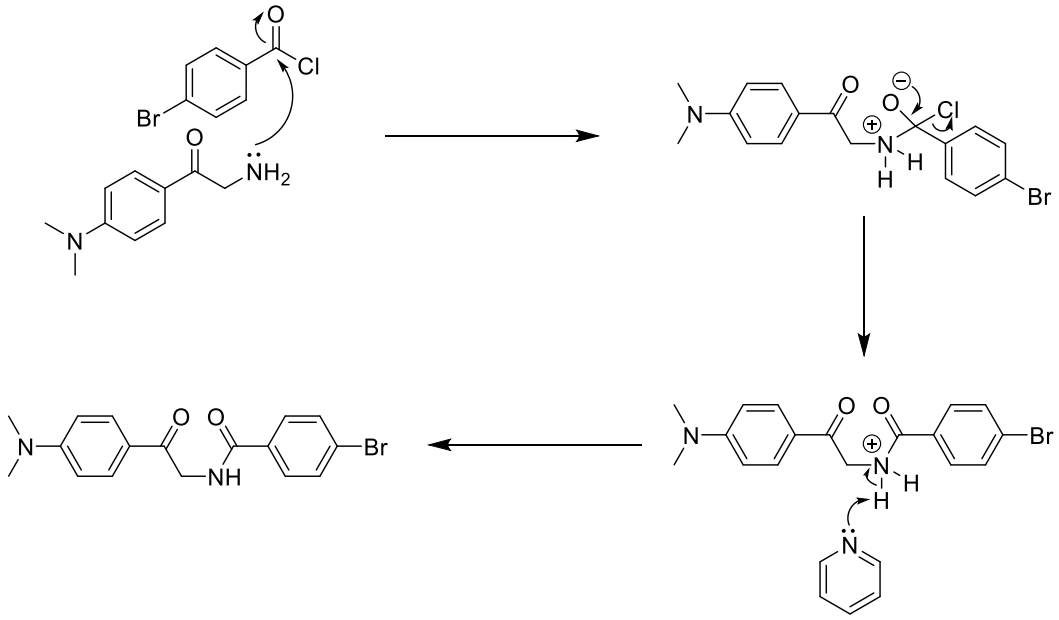

Scheme 73. Mechanism for the reaction between 2-amino-4-dimethylaminoacetophenone hydrochloride and 4-bromobenzoyl chloride.

After an aqueous work up which removed all of the unreacted 2-amino-4-dimethylaminoacetophenone hydrochloride, it could be seen in the ^{1}H NMR spectrum of the crude reaction product that there was a large amount of unreacted 4-bromobenzoyl chloride. An attempt was made to purify the crude product by washing with dilute sodium hydroxide to remove unreacted 4-bromobenzoyl chloride from the reaction mixture, however, this was shown to have no effect on the purity of the product and thus it was taken through, crude, to the next step.

From the reported literature procedure for the synthesis of probe **78**, it was reported that dehydration to form the diphenyloxazole was carried out by refluxing for 30 minutes in $POCl_3$.[245,246] The 4-bromo-*N*-(2-(4-(dimethylamino)phenyl)-2-oxoethyl)benzamide intermediate **79** was dissolved in $POCl_3$ and refluxed for 30 minutes as reported (Scheme 74), but failed to form the dehydrated product. The reaction was repeated several times without success.

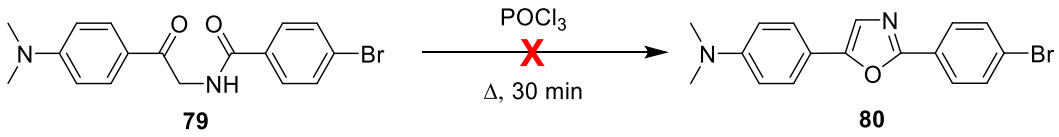

79 **80**

Scheme 74. Attempted dehydration in $POCl_3$.

After dehydration in $POCl_3$ failed, dehydration was attempted in concentrated sulfuric acid. The 4-bromo-*N*-(2-(4-(dimethylamino)phenyl)-2-oxoethyl)benzamide intermediate **79** was dissolved in concentrated H_2SO_4 and left to stir at room temperature for 24 hours (Scheme 75).

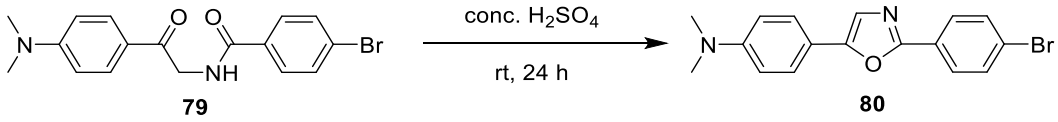

Scheme 75. Dehydration in conc. H_2SO_4 to form the diphenyloxazole intermediate.

The diphenyloxazole intermediate **80** is formed *via* the Robinson-Gabriel synthesis shown in Scheme 76. This reaction is commonly used for the formation of 2,5-diaryloxazoles. The first part of the reaction is cyclization of an acylaminoketone that contains all of the oxazole substituents. The second part is a dehydration, removing water from the molecule. Labelling studies have determined that the amide oxygen is the most Lewis basic and therefore is the one included in the oxazole.[247]

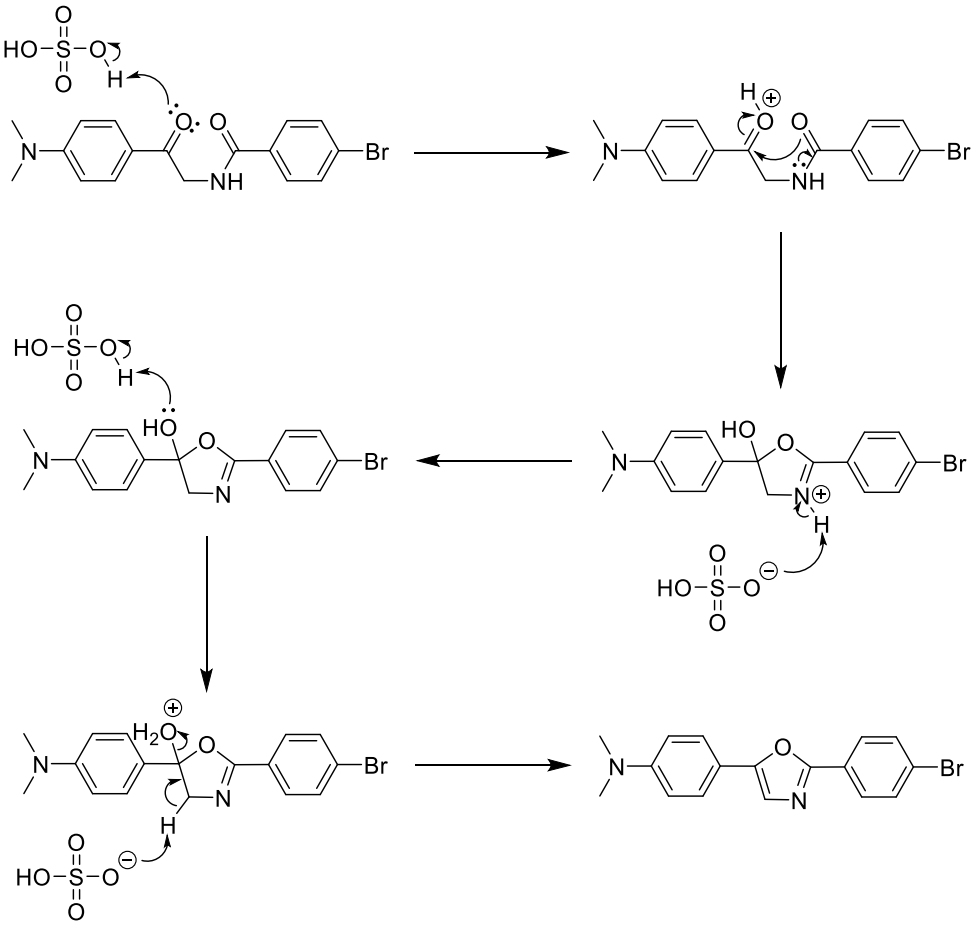

Scheme 76. Mechanism of the Robinson-Gabriel synthesis to form the diphenyloxazole intermediate.

The desired diphenyl oxazole product precipitated out along with unreacted 4-bromobenzylchloride leftover from the previous reaction when the reaction mixture was poured into ice water. After collecting the product by filtration, the crude product was dissolved in DCM and washed three times with 1 M sodium hydroxide in order to remove the unreacted 4-bromobenzoyl chloride. This gave the diphenyloxazole product **80** with high purity in a low yield of 34%.

Once the diphenyloxazole product had been formed, it was subjected to a Suzuki reaction with bis(pinacolato)diboron ($B_2(pin)_2$). The initial reaction was heated to 80 °C for 4 hours, as was the case for the previously synthesised stilbene probes.[248] However, when the reaction was worked up after 4 hours the crude ^{1}H NMR spectrum of the reaction product showed no methyl resonance corresponding to the Bpin group, indicating that the coupling reaction had failed. A subsequent reaction was heated to 80 °C overnight (Scheme 77), in which all of the starting material was reacted to give the desired product.

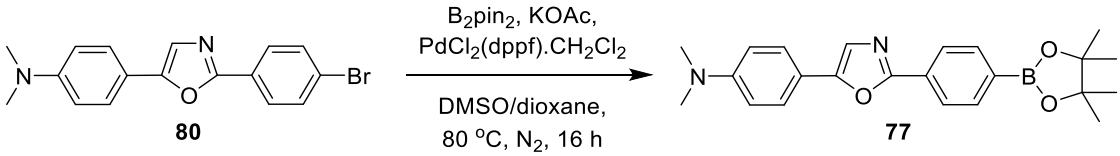

Scheme 77. Suzuki reaction of diphenyloxazole intermediate to form the boron pinacol ester.

The Suzuki reaction proceeds *via* the mechanism as that for the stilbene probes (Scheme 71). Pure diphenyloxazole probe **77** was obtained after an aqueous work up and purification by recrystallization from DCM and hexane to remove excess unreacted bis(pinacolato)diboron. ^{1}H, ^{13}C and ^{11}B NMR spectra and mass spectrometry confirmed the presence of the desired product.

4.2.2 UV-Vis and Fluorescence Analysis of the Synthesised Probes

Each probe was analysed *via* ultraviolet-visible (UV-Vis) spectroscopy in the presence and absence of hydrogen peroxide. This was used to determine how the absorbance and wavelength of maximum absorbance (λ_{max}) changed upon reaction of the probe with H_2O_2. The determined λ_{max} was used as the excitation wavelength for fluorescence analysis. Fluorescence analysis was then carried out on each probe, again in the absence and presence of H_2O_2. This was used to determine how the wavelength of maximum emission and the intensity of the emission changed upon the reaction of the probe with H_2O_2. This information was then used to evaluate whether the probe was suitable as a fluorescent probe for the detection of H_2O_2 and should be investigated further.

The Bpin substituent of the probes reacts with H_2O_2 to form the corresponding phenol, as shown in Scheme 60. This change in structure can alter the UV-Vis and fluorescence characteristics of the probe. This could involve a red (increase in nm) wavelength shift or a blue (decrease in nm) wavelength shift, and a change in absorbance/emission intensity. In the design of a fluorescent sensor, both a wavelength shift and a change in intensity upon binding with the analyte are vital for a probe to be successful. In an ideal situation, a wavelength shift will occur with an increase in fluorescence intensity as this is the easiest change to detect. The aim of this project was to synthesise 'Off-On' fluorescence probes, where the intensity of the emission increased upon reaction with hydrogen peroxide.

As discussed previously, six probes were synthesised. Four of these probes follow the same basic structure, each with a different R substituent. All of the probes contain aromatic rings which can act as fluorophores, and a Bpin moiety which acts as a receptor for H_2O_2. There is a high degree of conjugation in each of the probe structures. The nature of the R-substituent can alter the UV-Vis and fluorescence characteristics of the probe.

All of the synthesised probes in the neutral state contain an sp^2 hybridised boronic ester which shows acceptor group properties. In instances when an electron-donating substituent at the 4' position produces a system with a donor and an acceptor linked though a conjugated stilbene or oxazole scaffold, ICT has been reported to occur, lowering the energy of the excited state.[27]

The stilbene probes **68** and **69** containing electron-donating substituents and the oxazole probe **77** are able to fluctuate between two resonance states due to the electron donating nature of the terminal tertiary amine or methoxy group and the electron accepting trivalent boron atom (Scheme 78). The resonance involves the conversion of an sp^2 hybridised boron with an empty p orbital to an sp^3 hybridised boron anion. The anionic boron therefore no longer possesses electron accepting properties, lessening the internal charge transfer (ICT) and resulting in altered spectroscopic properties. This ICT results in a minor fluorescent emission.[241,245] This change in fluorescent intensity can be increased dramatically in the presence of hydrogen peroxide, as discussed in the next section.

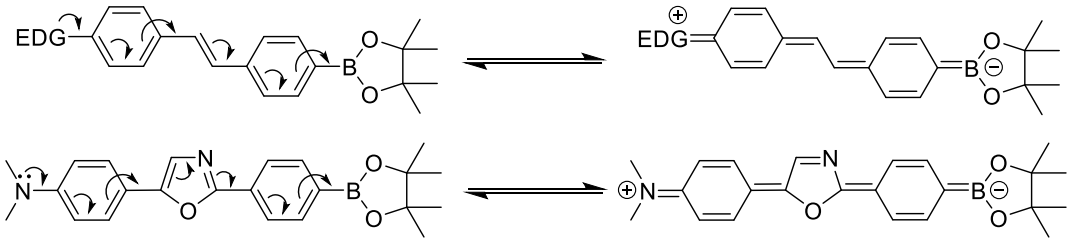

Scheme 78. Internal charge transfer mechanism in stilbene probes **68** and **69** and oxazole probe **77** from the electron-donating group to the electron-withdrawing boron group.

If the 4'-dimethylamino stilbene probe **68** is considered, the electron donating dimethylamino moiety is the donor group. When the boron atom is sp^2 hybridised and therefore an electron acceptor, excited-state ICT can occur between the dimethylamino donor and the boron acceptor, redshifting the emission wavelength of the boronic ester species. Upon reaction with H_2O_2, the boronic acid pinacol ester is converted to a phenol, and the electron-acceptor properties are lost (Scheme 79). This leads to a loss of the ICT effect in the excited state of the phenol species, resulting in a shift of the emission wavelength of the fluorophore to higher energy. This shift in the emission band is due to the inability of the phenol species to lower the energy of its excited state by a mechanism available to the boronic ester species, and as a consequence emission is observed from the locally excited (LE) species instead.

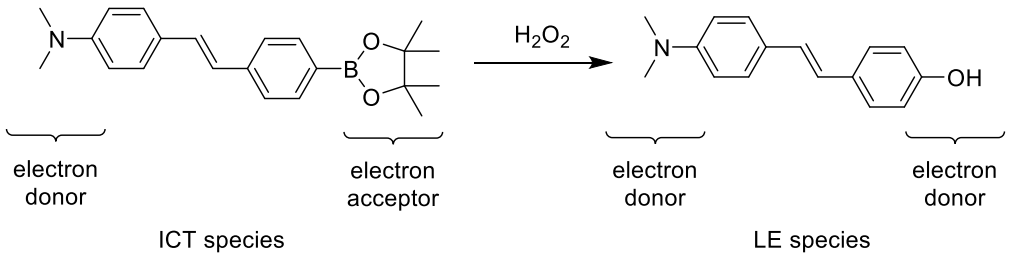

Scheme 79. ICT and LE species for probe **68**.

If the 4'-cyano stilbene probe **71** is considered, the electron-withdrawing cyano moiety is an acceptor group. When the boron atom is sp^2 hybridised and therefore also an electron acceptor, no excited-state ICT is feasible and we observe emission from the locally excited state (Scheme 80). Upon conversion of the boronic ester to the phenol *via* reaction with H_2O_2, the phenol is now a donor group, allowing ICT to occur between the phenol donor and cyano acceptor, red shifting the emission wavelength of the phenol species.

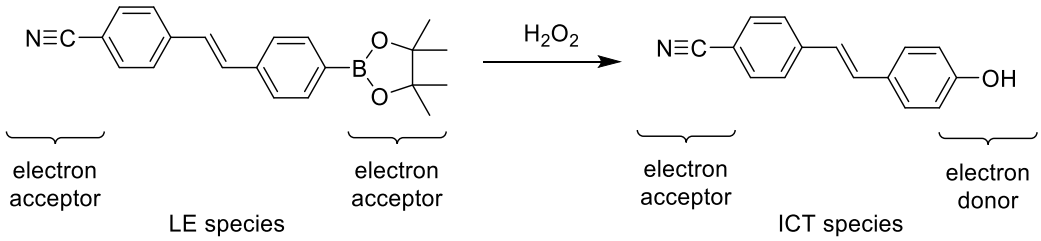

Scheme 80. LE and ICT species for probe **71**.

The change in absorbance in the UV-Vis analysis and the intensity increase or decrease of fluorescence emission is an intrinsic property of the molecule, dependent on the population of molecular energy levels. The direction and degree of change in absorbance and intensity upon reaction with H_2O_2 cannot easily be predicted,[249] so must be determined by experiment. The initial results of the UV-Vis and fluorescence analysis of each probe is discussed in the following sections.

4.2.2.1 Analysis of dimethylamino stilbene probe 68

The UV-Vis characteristics of probe **68** were investigated. The λ_{max} of probe **68** was found to be 354 nm. Upon reaction with H_2O_2, the λ_{max} of probe **68** was blue shifted from 354 nm to 332 nm. This was accompanied by a slight increase in absorbance, as shown in Figure 67.

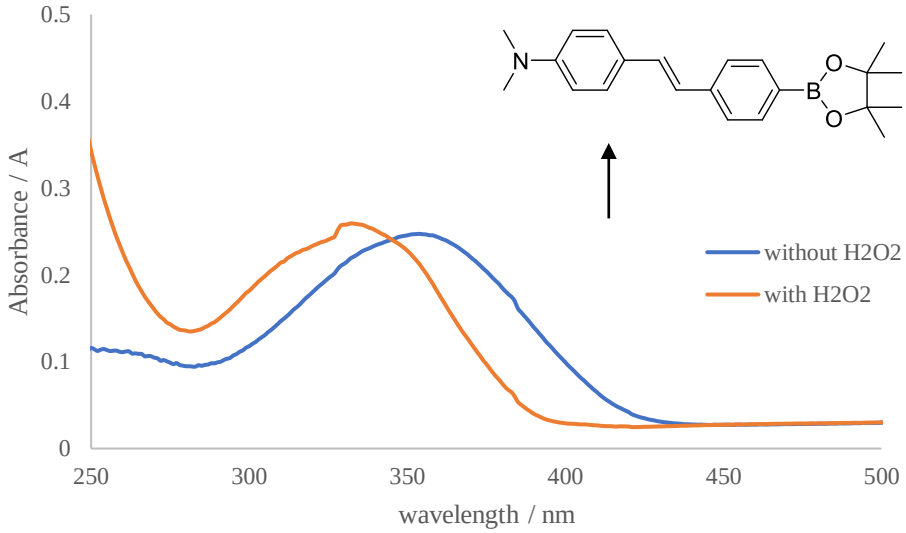

Figure 67. UV analysis of probe **68** in pH 8.21 buffer (52.1 wt.% MeOH). Probe **68**: 10 µM, H_2O_2: 13.1 mM, analysed 15 minutes after H_2O_2 addition.

The fluorescence characteristics of probe **68** were then investigated. The wavelength of maximum fluorescence emission of the probe was 488 nm. This emission was blue shifted from 488 nm to 444 nm upon reaction with H_2O_2, as shown in Figure 68. The intensity of this emission also increased. These spectroscopic changes observed are due to the conversion of the electron-withdrawing boronic ester to the electron-donating phenol. As the phenol species is formed, the system no longer contains an electron-withdrawing group, resulting in the removal of the charge-transfer nature of the excited state. As a result, the emission wavelength of the fluorophore is shifted to a higher energy. The inability of the phenol species to lower the energy of its excited state by an ICT mechanism causes a dramatic blue shift in the emission wavelength coupled with an increase in intensity of the emission.

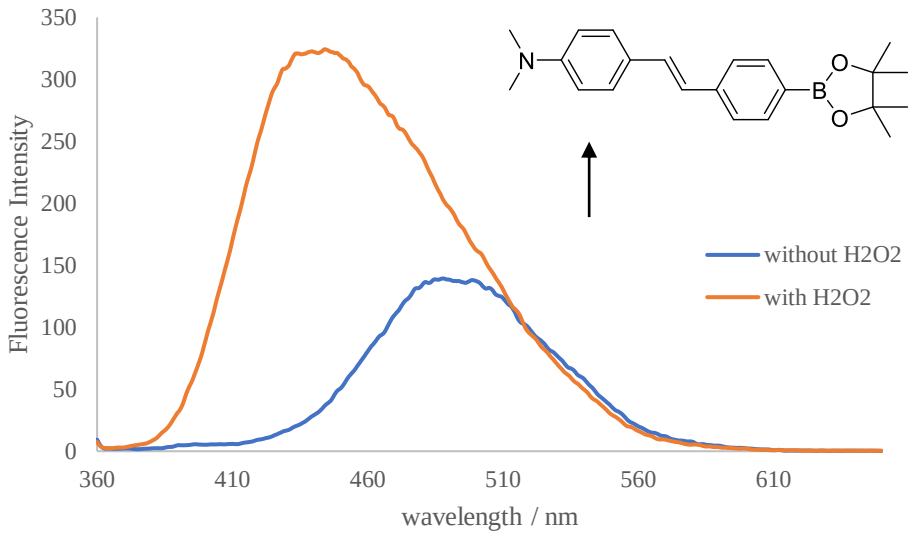

Figure 68. Fluorescence analysis of probe **68** in pH 8.21 buffer (52.1 wt.% MeOH). Probe **68**: 5 µM, H_2O_2: 2 mM, analysed 30 minutes after H_2O_2 addition. Excitation wavelength: 350 nm; slit widths: excitation: 10 nm, emission: 3 nm.

Before reaction with H_2O_2, electron donation can occur from the dimethylamino group along the length of the molecule to the electron-accepting Bpin group. After reaction with H_2O_2 to generate the phenol, both the dimethylamino group and the phenol donate electrons into the aromatic fluorophore, increasing the electron density of the system (Scheme 81). The sensor changes from having weak fluorescence induced by a Push-Pull ICT mechanism into a Push-Push sensor showing increased fluorescence intensity. The Push-Push mechanism increases quantum fluorescence by significantly increasing the electron density within the π system.

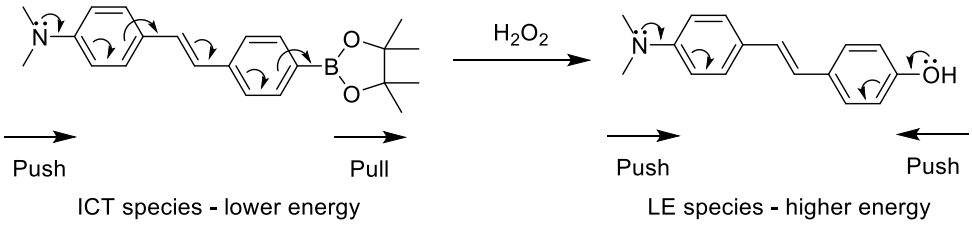

Scheme 81. ICT and LE states of dimethylamino stilbene probe **68**.

4.2.2.2 Analysis of methoxy stilbene probe 69

The UV-Vis characteristics of probe **69** were analysed. The λ_{max} of probe **69** was found to be 329 nm. Upon reaction with H_2O_2, the λ_{max} of probe **69** was blue shifted from 329 nm to 295 nm. This was accompanied by a slight increase in absorbance, as shown in Figure 69.

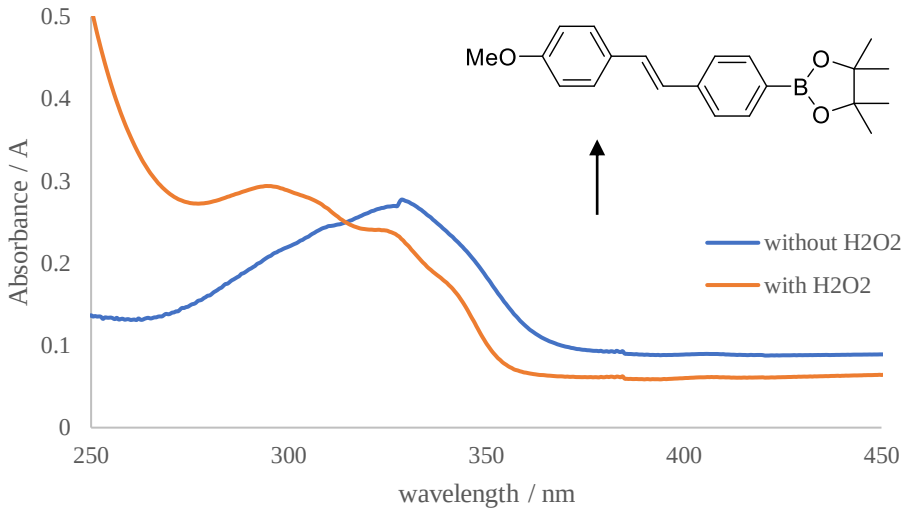

Figure 69. UV analysis of probe **69** in pH 8.21 buffer (52.1 wt.% MeOH). Probe **69**: 10 µM, H_2O_2: 13.1 mM, analysed 15 minutes after H_2O_2 addition.

The fluorescence characteristics of probe **69** were then analysed. The wavelength of maximum fluorescence emission of probe **69** was 405 nm. This wavelength was blue shifted from 405 nm to 380 nm upon reaction with H_2O_2, as shown in Figure 70. The intensity of this emission also increased. Again, these spectroscopic changes observed are due to the conversion of the electron-withdrawing boronic ester to the electron-donating phenol. As the phenol species is formed, the loss of the electron-withdrawing properties from the boron results in the removal of the charge-transfer nature of the excited state, resulting in the emission wavelength of the fluorophore being shifted to a higher energy. This is similar to the blue shift in fluorescence observed for the dimethylamino stilbene probe. The blue shift is smaller for the methoxy stilbene probe, this is due to the methoxy group being a weaker electron-donating group compared to the dimethylamino group, resulting in a slightly weaker ICT effect.

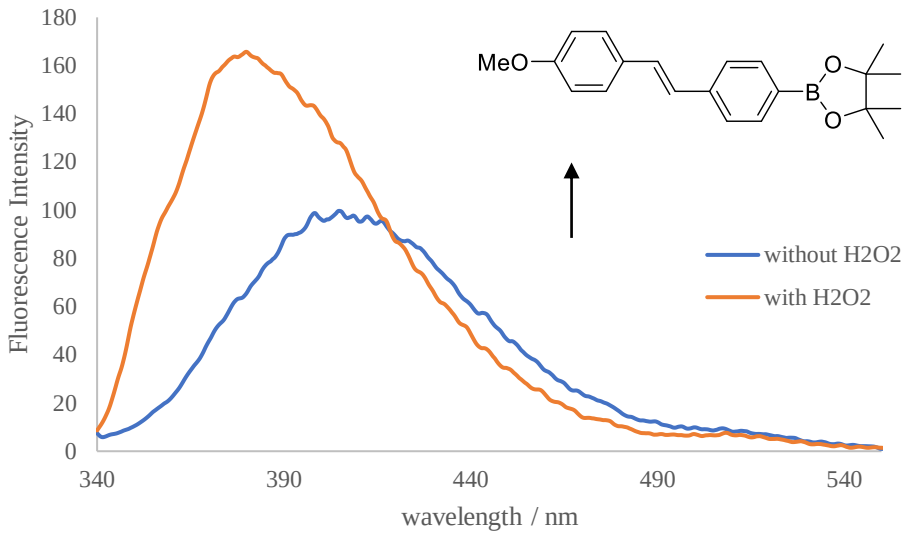

Figure 70. Fluorescence analysis of probe **69** in pH 8.21 buffer (52.1 wt.% MeOH). Probe **69**: 5 µM, H_2O_2: 2 mM, analysed 30 minutes after H_2O_2 addition. Excitation wavelength: 330 nm; slit widths: excitation: 10 nm, emission: 3 nm.

Before reaction with H_2O_2, electron donation can occur from the methoxy group along the length of the molecule to the electron-accepting Bpin group. After reaction with H_2O_2 to generate the phenol, both the methoxy group and the phenol donate electrons into the aromatic fluorophore, increasing the electron density of the system (Scheme 82). The sensor changes from having weak fluorescence induced by a Push-Pull ICT mechanism into a Push-Push sensor showing increased fluorescence intensity. The Push-Push mechanism increases quantum fluorescence by significantly increasing the electron density within the π system.

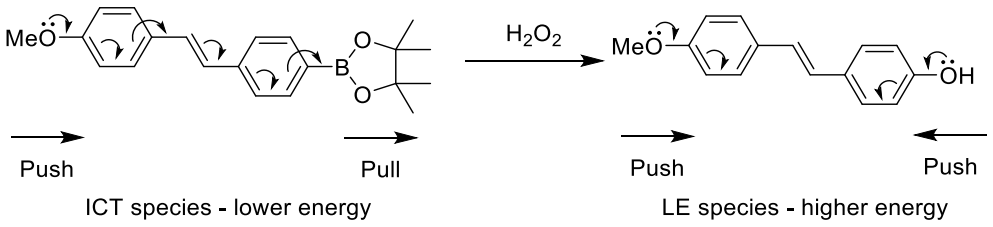

Scheme 82. ICT and LE states of methoxy stilbene probe **69**.

4.2.2.3 Analysis of unsubstituted stilbene probe 70

The UV-Vis characteristics of probe **70** were investigated. The λ_{max} of probe **70** was found to be 317 nm. Upon reaction with H_2O_2, the λ_{max} of probe **70** was blue shifted from 317 nm to 302 nm. This was accompanied by a decrease in absorbance, as shown in Figure 71.

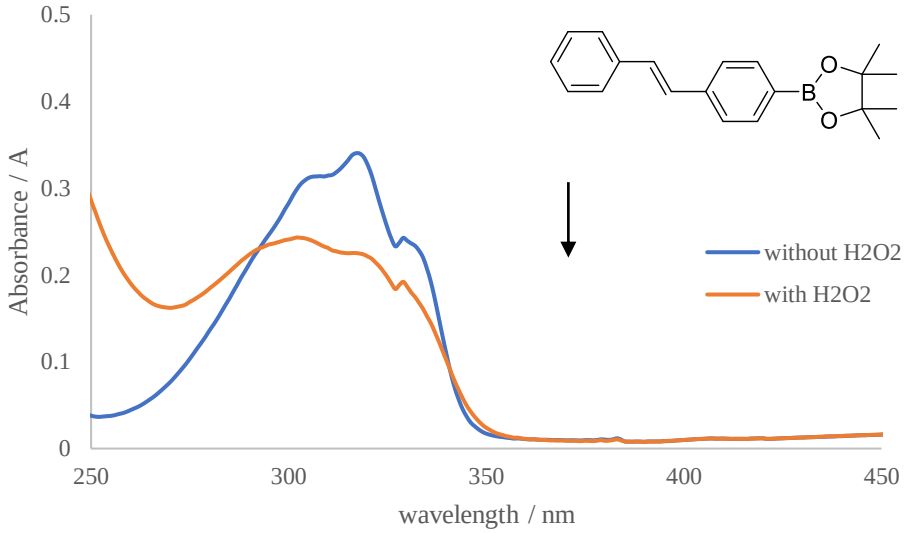

Figure 71. UV analysis of probe **70** in pH 8.21 buffer (52.1 wt.% MeOH). Probe **70**: 10 µM, H_2O_2: 13.1 mM, analysed 15 minutes after H_2O_2 addition.

The fluorescence characteristics of probe **70** were then investigated. The wavelength of maximum fluorescence emission of probe **70** was 365.5 nm. This emission was blue shifted from 365.5 nm to 360.5 nm upon reaction with H_2O_2, as shown in Figure 72. The intensity of the emission decreased upon reaction with H_2O_2. The change in fluorescence characteristics arises from the conversion of the boronic ester to the phenol. As the probe has no other substituents, excited state ICT is not possible for either species. Lakowicz *et al.* have suggested that the loss of the empty p orbital of the boron atom could result in a partial loss of the resonance between the aromatic system and the boronic acid group,[241] which could be responsible for the changes in fluorescence observed.

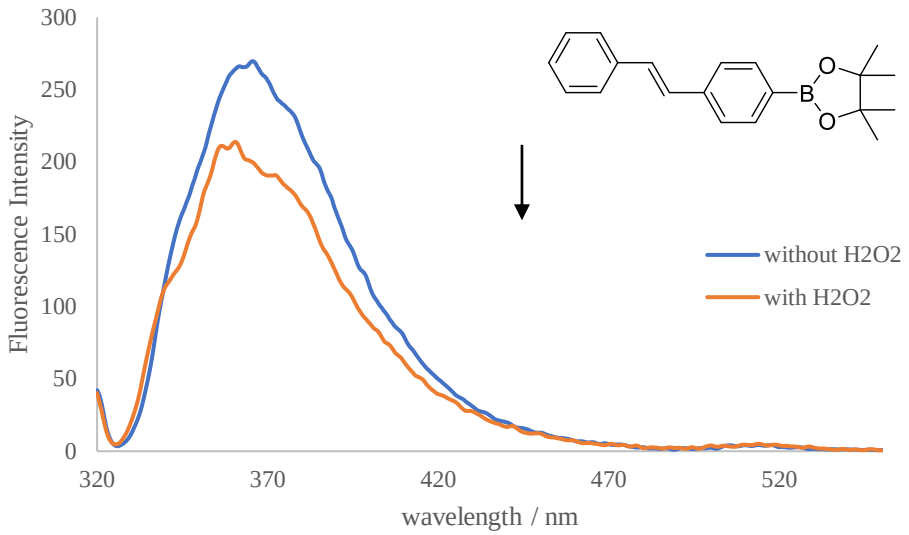

Figure 72. Fluorescence analysis of probe **70** in pH 8.21 buffer (52.1 wt.% MeOH). Probe **70**: 5 µM, H_2O_2: 2 mM, analysed 30 minutes after H_2O_2 addition. Excitation wavelength: 315 nm; slit widths: excitation: 10 nm, emission: 3 nm.

4.2.2.4 Analysis of cyano stilbene probe 71

The UV-Vis characteristics of probe **71** were analysed. The λ_{max} of probe **71** was found to be 328 nm. Upon reaction with H_2O_2, the λ_{max} of probe **71** underwent a very slight red shift from 328 nm to 332 nm. This was accompanied by a decrease in absorbance, as shown in Figure 73.

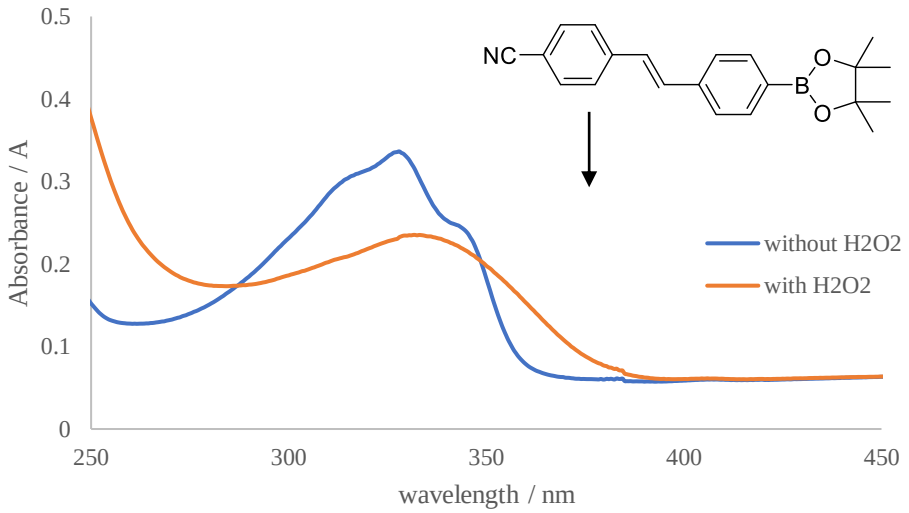

Figure 73. UV analysis of probe **71** in pH 8.21 buffer (52.1 wt.% MeOH). Probe **71**: 10 µM, H_2O_2: 13.1 mM, analysed 15 minutes after H_2O_2 addition.

The fluorescence characteristics of probe **71** were then investigated. The wavelength of maximum fluorescence emission of probe **71** was 377.5 nm. This emission was red shifted from 377.5 nm to 385.5 nm upon reaction with H_2O_2, as shown in Figure 74. These spectral changes observed are due to the conversion of the electron-withdrawing boronic ester to the electron-donating phenol. Before reaction with H_2O_2, the cyano stilbene probe contains two electron-withdrawing groups, so no ICT effect is possible, and fluorescence emission is observed from the locally excited state. As the phenol species is formed, the introduction of an electron-donating group results in the charge-transfer effect of the excited state, and as a result the emission wavelength of the fluorophore is shifted to a lower energy. The ability of the phenol species to lower the energy of its excited state by an ICT mechanism causes a redshift in the emission wavelength coupled with a decrease in intensity of the emission.

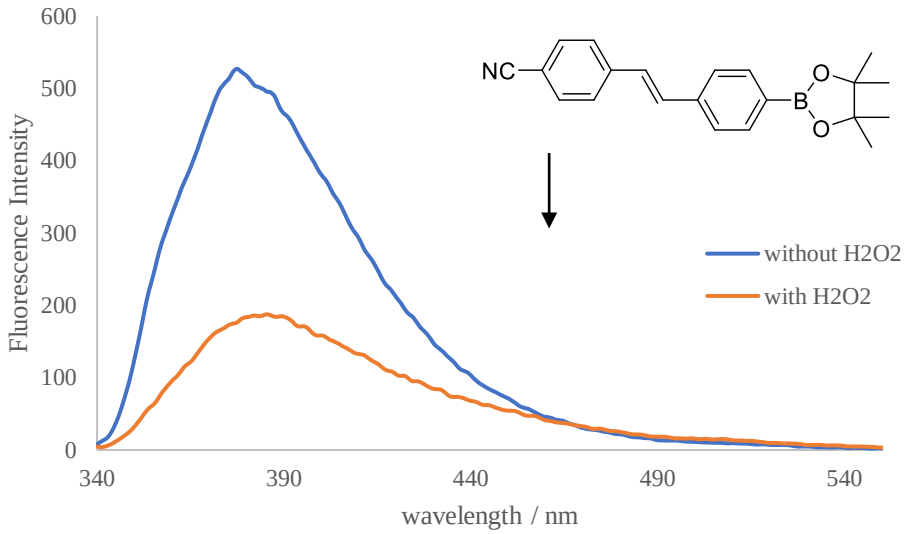

Figure 74. Fluorescence analysis of probe **71** in pH 8.21 buffer (52.1 wt.% MeOH). Probe **71**: 5 µM, H_2O_2: 2 mM, analysed 30 minutes after H_2O_2 addition. Excitation wavelength: 330 nm; slit widths: excitation: 10 nm, emission: 3 nm.

Before reaction with H_2O_2 the fluorophores are relatively electron poor. As the Bpin substituent is converted into a phenol, an electron withdrawing mechanism is set up (Scheme 83). The electrons donated into the aromatic ring from the phenol are delocalised across the whole system, including the electron withdrawing group. The sensor changes from having moderate fluorescence induced by a Pull-Pull mechanism to a Push-Pull internal charge transfer (ICT) sensor showing decreased fluorescence due to stabilization of the ICT state.

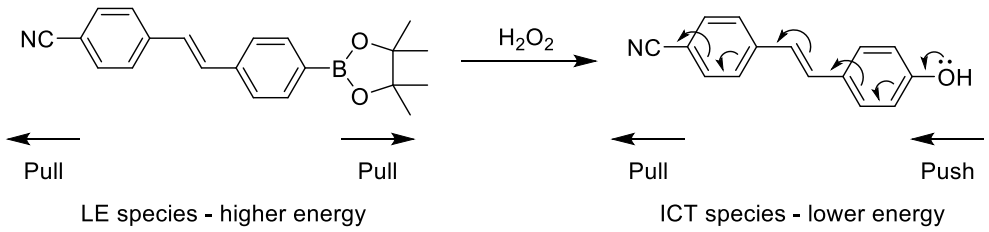

Scheme 83. LE and ICT states for cyano stilbene probe **71**.

4.2.2.5 Summary of Stilbene Probes 68-71

From analysis of the first four probes, the dimethylamino stilbene probe **68** showed the most potential as an 'Off-On' fluorescent probe for the detection of hydrogen peroxide (Table 5). The dimethylamino probe **68** and the methoxy probe **69** both showed 'Off-On' fluorescence characteristics upon reaction with H_2O_2, however a greater change in wavelength of the maximum emission intensity was observed for the dimethylamino probe. This difference in wavelength shift corresponds to the relative electron-donating abilities of the substituents of the aromatic ring. The dimethylamino substituent on probe **68** is a stronger electron donating group than the methoxy substituent of probe **69**, as a result there is a larger blue shift in fluorescence emission due to perturbation of a stronger ICT state. The unsubstituted stilbene probe **70** and cyano stilbene probe **71** both displayed a decrease in fluorescence intensity upon reaction with H_2O_2.

Table 5. Summary of fluorescence analysis of stilbene probes **68-71**.

Probe	Fluorescence λ_{max} without H_2O_2	Fluorescence λ_{max} with H_2O_2	Change in λ_{max}	Intensity change
68 dimethylamino	488 nm	444 nm	Blue shift 44 nm	Increase
69 methoxy	405 nm	380 nm	Blue shift 25 nm	Increase
70 unsubstituted	365.5 nm	360.5 nm	Blue shift 5 nm	Decrease
71 cyano	377.5 nm	385.5 nm	Red shift 8 nm	Decrease

All the probes investigated fluoresce in the wavelength range of 300 nm to 480 nm. However, several proteins, coenzymes and other biological materials also fluoresce in the wavelength range of 250 nm to 500 nm.[243] These materials will generate background fluorescence and will therefore interfere with the analysis of the probe if it fluoresces in the same wavelength range. The stilbene probes fluoresce in this range, so would not be suitable for use in cells.

As the dimethylamino stilbene probe **68** displayed the biggest 'off-on' response upon reaction with hydrogen peroxide, a modified version of this probe was synthesised in an attempt to shift the fluorescence profiles to a longer wavelength, overcoming issues associated with background fluorescence of biological materials, allowing for the probe to be used within cells. The dimethylamino naphthalene stilbene probe **76** was designed to have the same electron-donating properties as probe **68**, but with increased conjugation. It was hypothesised that the increased conjugation of the system would result in the electron density found within the fluorophores being spread out over a larger number of atoms. This would overall decrease the energy of the HOMO-LUMO gap, causing the molecule to fluoresce at longer wavelengths.

4.2.2.6 Analysis of dimethylamino naphthalene stilbene probe 76

The UV-Vis characteristics of probe **76** were investigated. The λ_{max} of probe **76** was found to be 357 nm. Upon reaction with H_2O_2, the λ_{max} of probe **76** was blue shifted from 357 nm to 351 nm. This was accompanied by a slight decrease in absorbance, as shown in Figure 75.

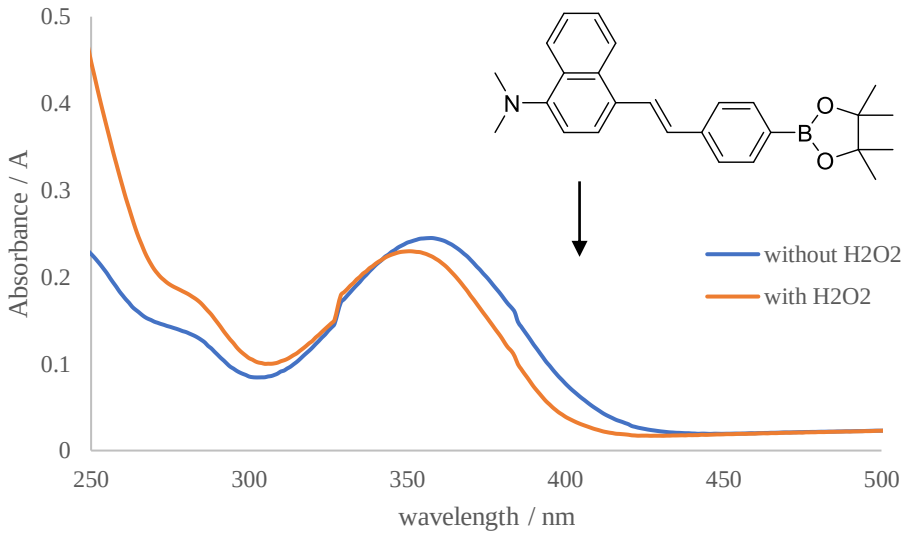

Figure 75. UV analysis of probe **76** in pH 8.21 buffer (52.1 wt.% MeOH). Probe **76**: 10 µM, H_2O_2: 13.1 mM, analysed 15 minutes after H_2O_2 addition.

The fluorescence characteristics of probe **76** were then investigated. The wavelength of maximum fluorescence emission of probe **76** was 517 nm. This emission was blue shifted from 517 nm to 510 nm upon reaction with H_2O_2, as shown in Figure 76. These spectroscopic changes observed are due to the conversion of the electron-withdrawing

boronic ester to the electron-donating phenol. As the phenol species is formed, the system no longer contains an electron-withdrawing group, resulting in the removal of the charge-transfer nature of the excited state. As a result, the emission wavelength of the fluorophore is shifted to a higher energy. The inability of the phenol species to lower the energy of its excited state by an ICT mechanism causes a blue shift in the emission wavelength coupled with a decrease in intensity of the emission. The intensity of this emission decreased, unlike the intensity of the dimethylamino stilbene probe **68** which displayed an increase in fluorescence intensity upon reaction with H_2O_2. Lakowicz *et al*. have reported smaller increases in fluorescence intensity as the linker length of probes increases.[250] These observations suggest that as the molecular length increases, the loss of the electron-withdrawing property of the boronic acid group leads to smaller spectral changes, suggesting that charge transfer is less important as linker length increases. Although the linker length is the same in the dimethylamino probe **68** and dimethylamino naphthalene stilbene probe **76**, a similar effect could be observed due to the increased conjugation upon introduction of the naphthalene ring. The cross-conjugation introduced by the naphthalene ring system is not very effective in increasing delocalization as the ICT mechanism runs along the length of the molecule.

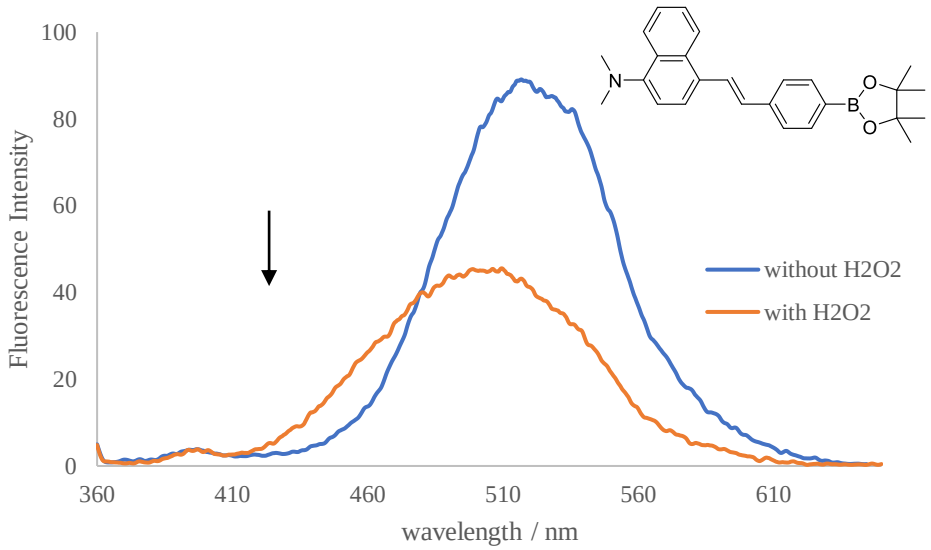

Figure 76. Fluorescence analysis of probe **76** in pH 8.21 buffer (52.1 wt.% MeOH). Probe **76**: 5 µM, H_2O_2: 2 mM, analysed 30 minutes after H_2O_2 addition. Excitation wavelength: 350 nm; slit widths: excitation: 10 nm, emission: 3 nm.

The overall wavelengths of fluorescence emission in the absence and presence of H_2O_2 of probe **76** were red shifted to longer wavelengths in comparison to probe **68**, due to

the increased conjugation of the molecule. Probe **76** however still maintained the blue shift characteristics of probe **68** upon reaction with H_2O_2. The increase in conjugation seems to have also affected the intensity of the fluorescence upon reaction with H_2O_2 as probe **76** now displays 'On-Off' characteristics in the presence of H_2O_2.

The stilbene based probes also suffer from low photostability due to *trans-cis* isomerisation of the ethylene bridge joining the two benzene rings (Scheme 84).[244,251] After electronic excitation, the molecule undergoes rotation about its ethylene bond. When rotated through about 90° from either the *cis* or *trans* conformation, stilbene arrives at a minimum of potential energy, from which it decays to the ground state through nonadiabatic transitions. After reaching the ground state, the molecule can follow a trajectory which leads to the formation of a product, or a trajectory which leads back to the reactant. Isomerization of stilbene can start from either the *cis* or the *trans* geometry.[252]

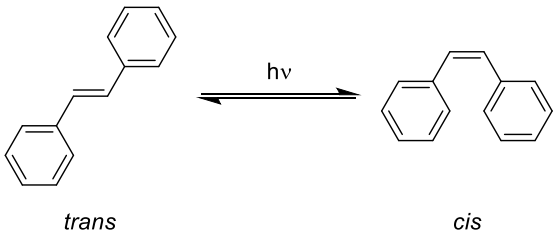

Scheme 84. *Trans-cis* photoisomerisation of stilbenes.

Due to the issues associated with low photostability of the stilbenes, the dimethylamino oxazole probe **77** was synthesised. As this probe does not contain a bridging ethylene unit, *cis-trans* isomerisation is not possible, leading to a probe with in increased photostability. The strongly electron-donating dimethylamino group was again incorporated into the sensor design.

4.2.2.7 Analysis of dimethylamino oxazole probe 77

The UV-Vis characteristics of probe **77** were investigated. The λ_{max} of probe **77** was found to be 347 nm. Upon reaction with H_2O_2, the λ_{max} of probe **77** was blue shifted from 347 nm to 334 nm. This was accompanied by a slight increase in absorbance, as shown in Figure 77.

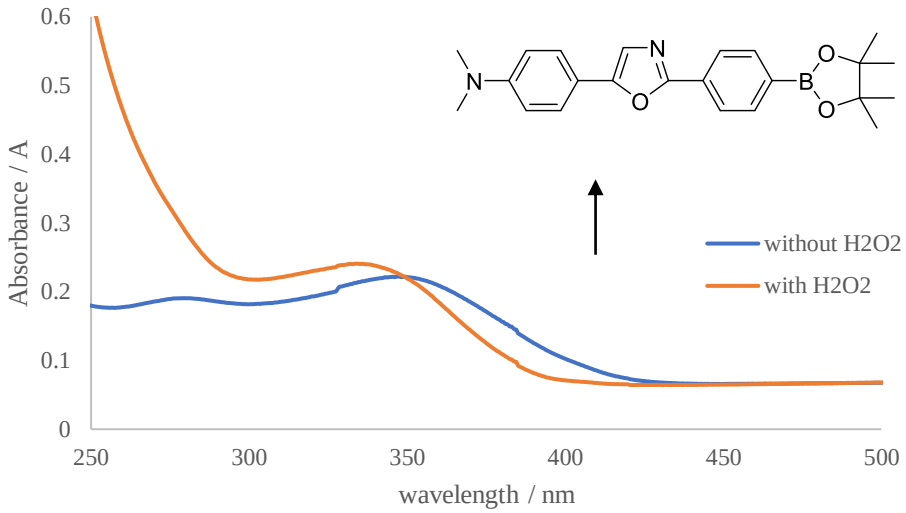

Figure 77. UV analysis of probe **77** in pH 8.21 buffer (52.1 wt.% MeOH). Probe **77**: 10 µM, H_2O_2: 13.1 mM, analysed 15 minutes after H_2O_2 addition.

The fluorescence characteristics of probe **77** were then investigated. The wavelength of maximum fluorescence emission of the probe was 472 nm. This emission underwent a small blue shift from 472 nm to 468.5 nm upon reaction with H_2O_2, as shown in Figure 78. A large increase in fluorescence intensity is also observed. These spectral changes observed are due to the conversion of the electron-withdrawing boronic ester to the electron-donating phenol. As the phenol species is formed, the system no longer contains an electron-withdrawing group resulting in the removal of the charge-transfer nature of the excited state and as a result the emission wavelength of the fluorophore is shifted to a higher energy. The inability of the phenol species to lower the energy of its excited state by an ICT mechanism causes a blue shift in the emission wavelength coupled with an increase in intensity of the emission.

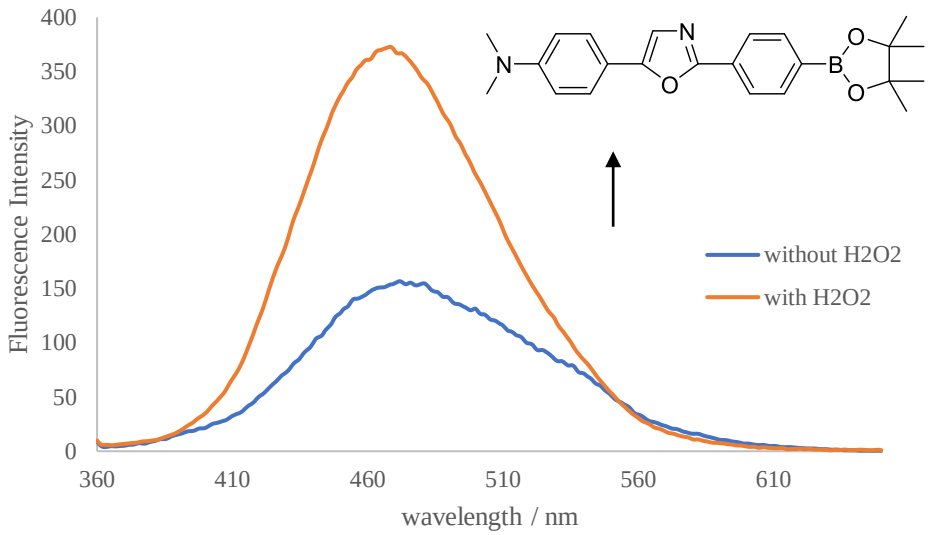

Figure 78. Fluorescence analysis of probe **77** in pH 8.21 buffer (52.1 wt.% MeOH). Probe **77**: 1 µM, H_2O_2: 2 mM, analysed 30 minutes after H_2O_2 addition. Excitation wavelength: 350 nm; slit widths: excitation: 10 nm, emission: 3 nm.

Before reaction with H_2O_2, electron donation can occur from the dimethylamino group along the length of the molecule to the electron-accepting Bpin group. After reaction with H_2O_2 to generate the phenol, both the dimethylamino group and the phenol donate electrons into the aromatic fluorophore, increasing the electron density of the system (Scheme 85). The sensor changes from having weak fluorescence induced by a Push-Pull ICT mechanism into a Push-Push sensor showing increased fluorescence intensity. The Push-Push mechanism increases fluorescence intensity by significantly increasing the electron density within the π system.

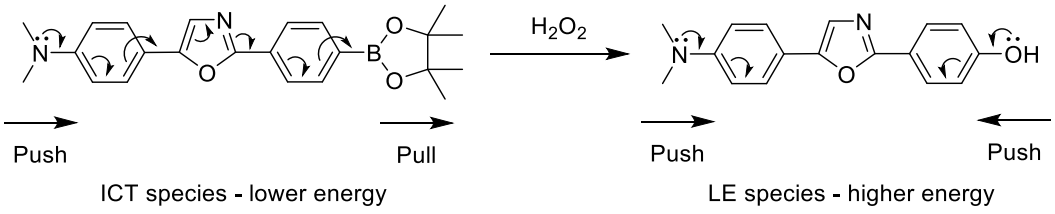

Scheme 85. ICT and LE states of dimethylamino oxazole probe **77**.

The dimethylamino oxazole probe **77** displayed the desired 'Off-On' fluorescence response upon reaction with hydrogen peroxide, and showed the biggest increase in fluorescence compared to the previously synthesised probes. The dimethylamino oxazole probe also does not suffer from low photostability, unlike the stilbene probes.

Once the suitability of the probe had been determined as a fluorescent sensor for H_2O_2, further fluorescence experiments were carried out.

To accurately determine the sensitivity of probe **77** towards H_2O_2, the time taken for the probe to fully react with H_2O_2 needs to be determined. This information can be obtained by monitoring the emission peak at a specific wavelength over a period of time, known as a time drive. A time drive is able to determine the completion of a reaction by monitoring the fluorescent intensity at the maximum emission wavelength of probe **77** in the 'On' state. As oxidation of the boronic acid group to the phenol results in a shift in maximum emission wavelength to 468 nm, as the reaction proceeds the intensity of the fluorescence at 468 nm will increase up until a point where it remains constant, once the reaction is complete. The time drive shows this as a plot of intensity at 468 nm against time, Figure 79.

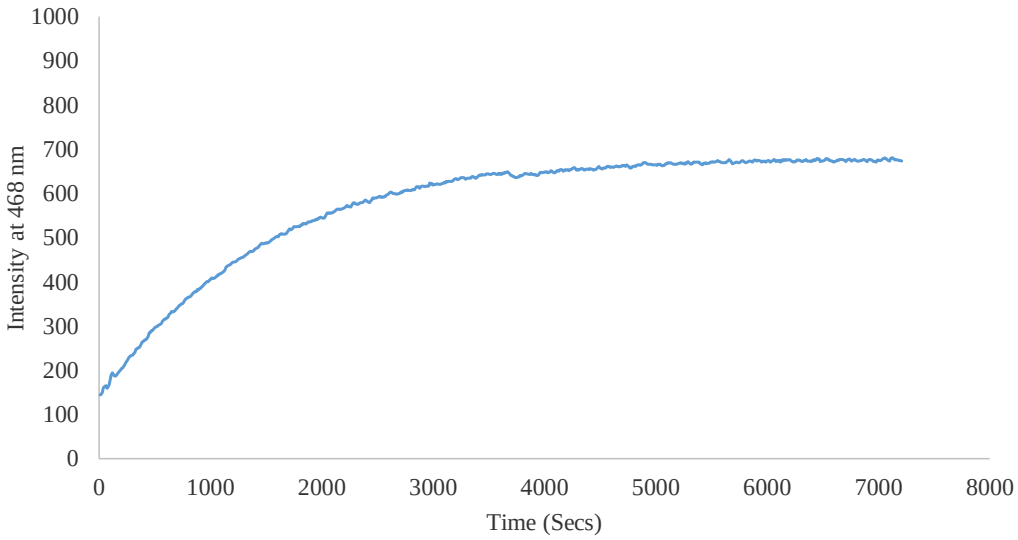

Figure 79. Time drive of probe **77** (10 nM) and H_2O_2 (4.1 mM) in pH 7.14 PBS buffer. Intensity is measured at 468 nm, excitation wavelength 350 nm. Graph does not go through (0,0) as probe displays some fluorescence in the absence of H_2O_2.

The time drive shows an initially fast increase in fluorescence intensity at 468 nm, with the rate slowly decreasing until it reaches a plateau. The reaction was almost at completion after 1 hour (3600 seconds). To accompany the time drive, the emission peaks were recorded for an identical sample at 5 minute intervals, showing the increase in fluorescence over time (Figure 80).

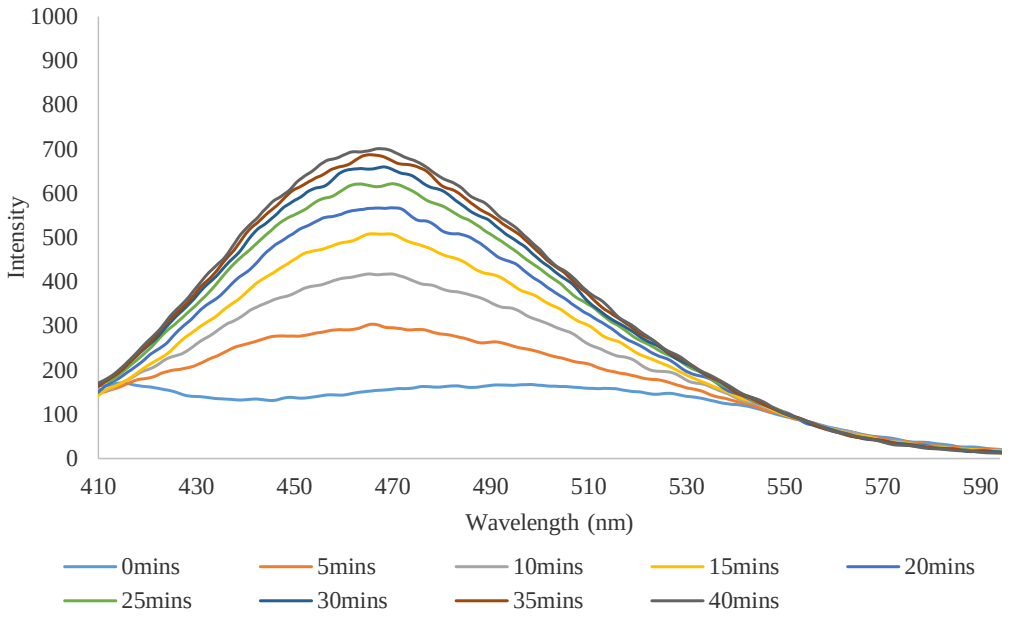

Figure 80. Fluorescent spectra showing increase in emission intensity over time. Probe **77** (10 nM) and H_2O_2 (4.3 mM) in pH 7.14 PBS buffer, analysed at 5 minute intervals. Excitation wavelength 350 nm.

Titration curves are required to gather information about the sensitivity and the limits of detection (LOD) of probe **77**. Both the sensitivity and the limit of detection are important parameters required to assess sensor viability.

An initial titration curve was obtained for probe **77** with a range of H_2O_2 concentrations from 0 mM – 12 mM (Figure 81). To ensure that all of the emission peaks for this wide range of H_2O_2 concentrations remained within the measurable intensity range (0-1000), a concentration of 20 nM was chosen for the sensor.

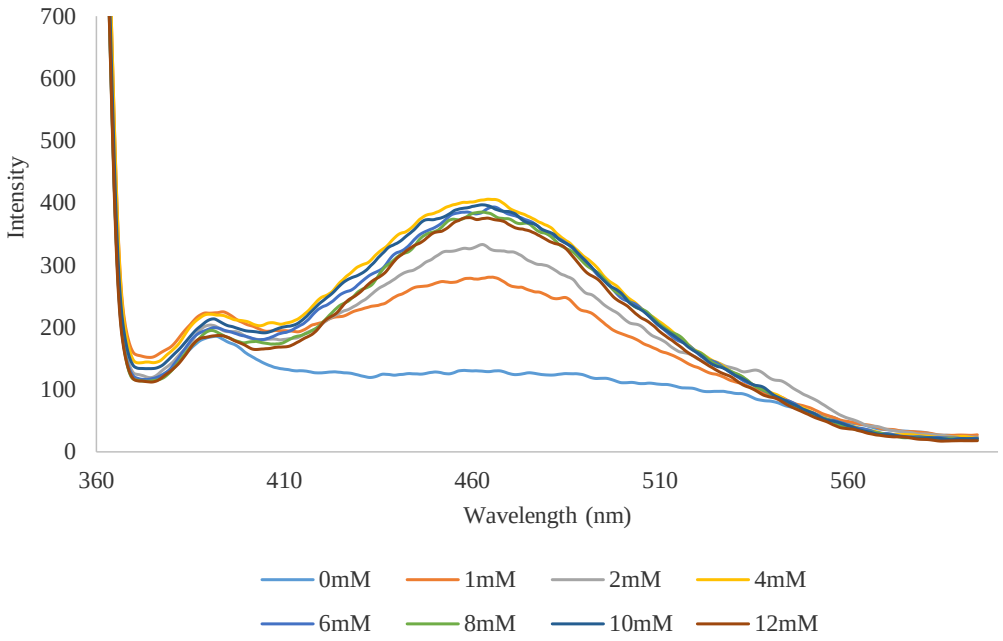

Figure 81. Fluorescent spectra showing changes in emission intensity as H_2O_2 concentration is increased. Probe **77** (20 nM) with H_2O_2 (0 mM – 12 mM) in pH 7.14 PBS buffer, analysed 40 minutes after H_2O_2 was introduced. Excitation wavelength 350 nm.

The emission spectra in Figure 81 indicates that after the addition of 4 mM H_2O_2 the fluorescent intensity of probe **77** increased no further. This suggests that 4 mM of H_2O_2 is a sufficient quantity to allow the complete conversion of boronic acid to phenol in probe **77**. Once this initial range of H_2O_2 concentrations had been established, the procedure was adapted to add H_2O_2 in smaller increments cumulatively to a single cuvette after a ten minute time period. Before the addition of further H_2O_2 the sample was analysed on the fluorimeter (Figure 82). The concentration of probe **77** was also increased slightly to 30 nM.

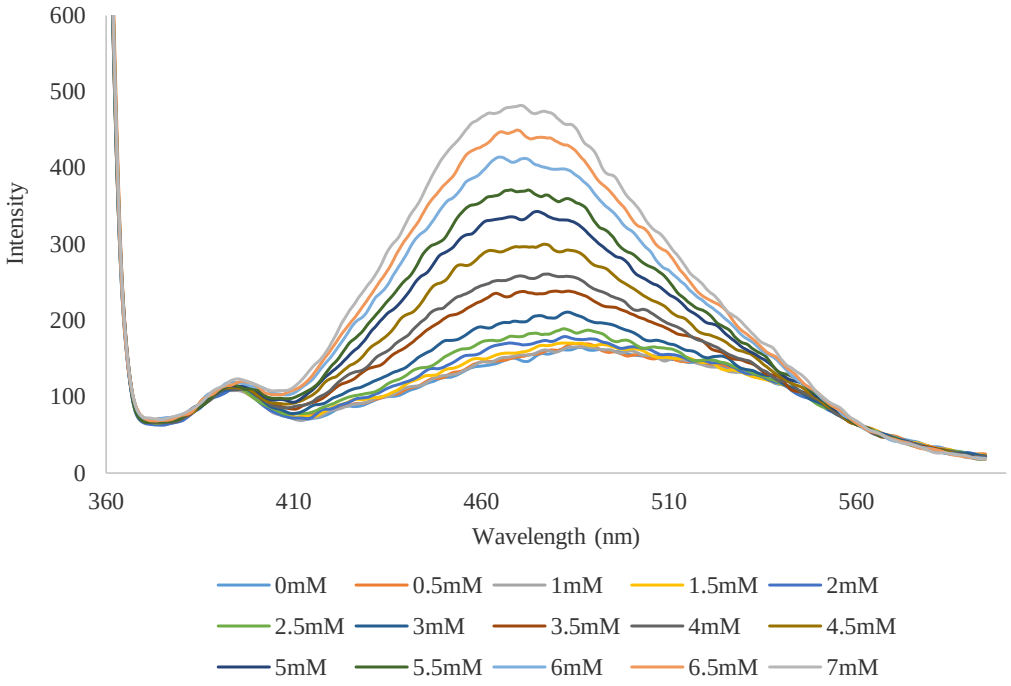

Figure 82. Fluorescent spectra showing changes in emission intensity as H_2O_2 concentration is increased. Probe **77** (30 nM) and H_2O_2 (0 mM – 7 mM) in pH 7.25 PBS buffer, analysed 10 minutes after additional H_2O_2 was introduced. Excitation wavelength 350 nm.

The improved method was applied to produce a titration curve (Figure 83) showing an increase in intensity with increasing H_2O_2 concentrations. Higher concentrations of H_2O_2 are needed to determine the upper limit of detection, where probe **77** has reacted completely.

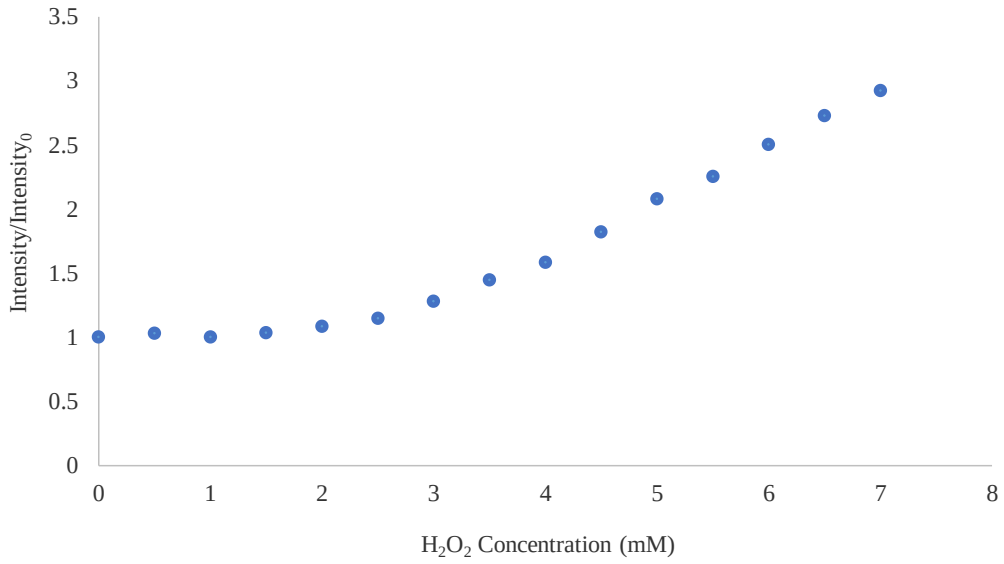

Figure 83. Plot of relative intensity against H_2O_2 concentration (0 mM – 7 mM). Probe **77** (30 nM). Relative intensity = Intensity (max. emission intensity in the presence of H_2O_2)/ $Intensity_0$ (max. emission intensity in the absence of H_2O_2).

Figure 83 shows a constant increase in emission intensity with increasing concentrations of H_2O_2, but shows no evidence of reaching a plateau. Increasing H_2O_2 concentration in greater increments will increase the speed at which probe **77** reaches a plateau. The experiment was repeated adding larger quantities of H_2O_2 (Figure 84).

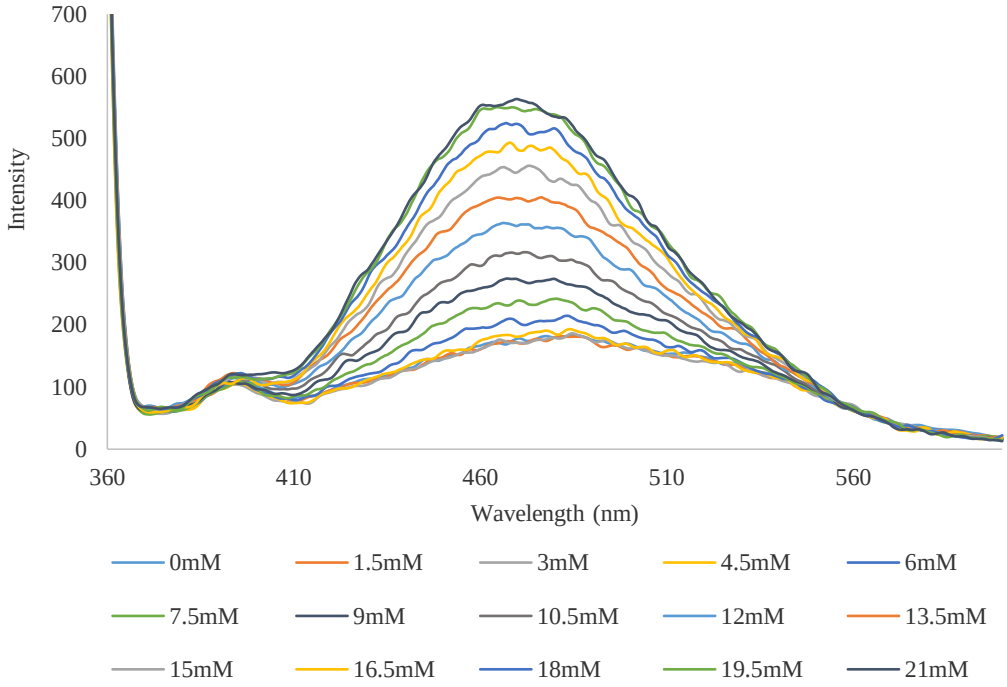

Figure 84. Fluorescent spectra showing changes in emission intensity as H_2O_2 concentration is increased. Probe **77** (30 nM) and H_2O_2 (0 mM – 21 mM) in pH 7.25 PBS buffer, analysed 10 minutes after additional H_2O_2 was introduced. Excitation wavelength 350 nm.

A repeat of the titration curve was carried out to ensure results were consistent (Appendix 2). Both fluorescent spectra show probe **77** reaching complete conversion to the phenol where the intensity of emission no longer increases. The fluorescent spectra show that this plateau occurs after the addition of a total concentration of 19.5 mM of H_2O_2.

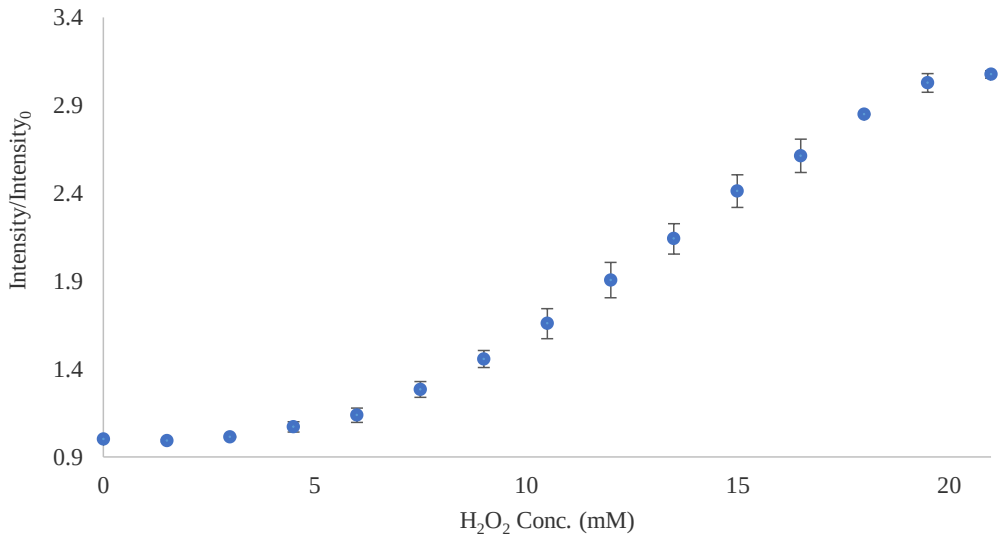

Figure 85. Plot of mean relative intensity against H_2O_2 concentration (0 mM – 21 mM). Probe **77** (30 nM). Relative intensity = Intensity (max. emission intensity in the presence of H_2O_2)/ $Intensity_0$ (max. emission intensity in the absence of H_2O_2). Error bars show the standard deviation.

The intensity plot (Figure 85) shows a clear increase in relative intensity of fluorescence emission at higher H_2O_2 concentrations. This plot shows that a 30 nM concentration of probe **77** is able to detect a range of H_2O_2 concentrations under neutral pH conditions, suggesting its suitability as an *in vivo* H_2O_2 fluorescent sensor.

4.2.3 Cell Imaging

After the dimethylamino oxazole probe **77** showed promising fluorescence in preliminary studies, it was sent away for testing *in vitro* (with thanks to Gyoungmi Kim and Juyoung Yoon from Ewha Womans University, South Korea for carrying out the cell imaging studies). The probe was examined within HeLa cells and RAW 264.7 cells.

Figure 86a shows probe **77** within HeLa cells at two different wavelengths. Figure 86b-e shows the probe with added amounts of different reactive oxygen species. The probe was able to enter the cells and act as a fluorescent stain. However, unfortunately, no change in fluorescence was observed upon addition of various reactive oxygen species within the cellular environment.

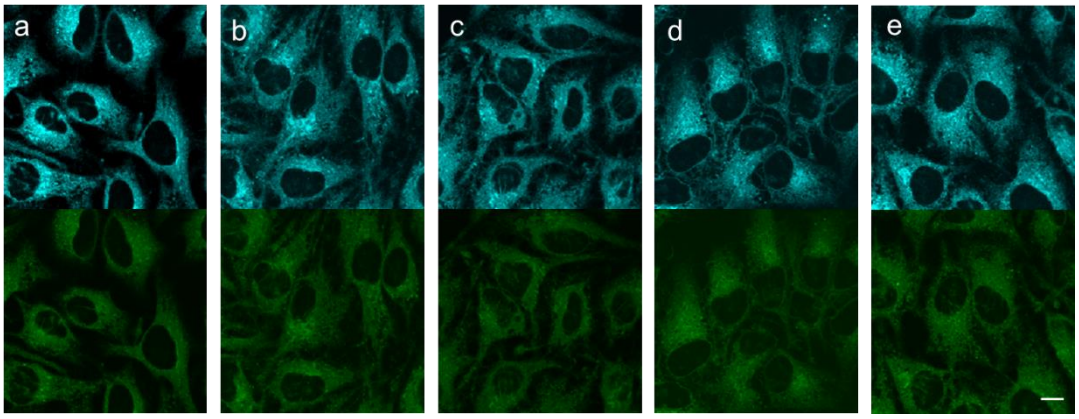

Figure 86. HeLa cells were incubated with 5 μM probe **77** for 15 min and washed with DPBS and treated with (a) no, (b) 300 μM H_2O_2, (c) 300 μM KO_2, (d) 300 μM NaOCl, (e) 300 μM $ONOO^-$ for 15 min and acquired fluorescence images by confocal microscopy. Cyan: ex. 405nm/em. 465-495nm, green: ex. 405nm/em. 490-590nm. Scale bar: 10 μm.

Figure 87a shows fluorescent probe **77** in RAW 264.7 cells at two different wavelengths. Again, the probe was able to enter the cells and act as a fluorescent stain. The cells in Figure 87b-g have all been stimulated to produce reactive oxygen species by addition of lipopolysaccharide (LPS) and interferon gamma (IFN-γ). Different scavenger species were then added that are specific for a certain reactive oxygen species. Unfortunately, no change in fluorescence was observed within the cells in the presence of hydrogen peroxide, peroxynitrite, hydroxyl radicals, singlet oxygen or superoxide.

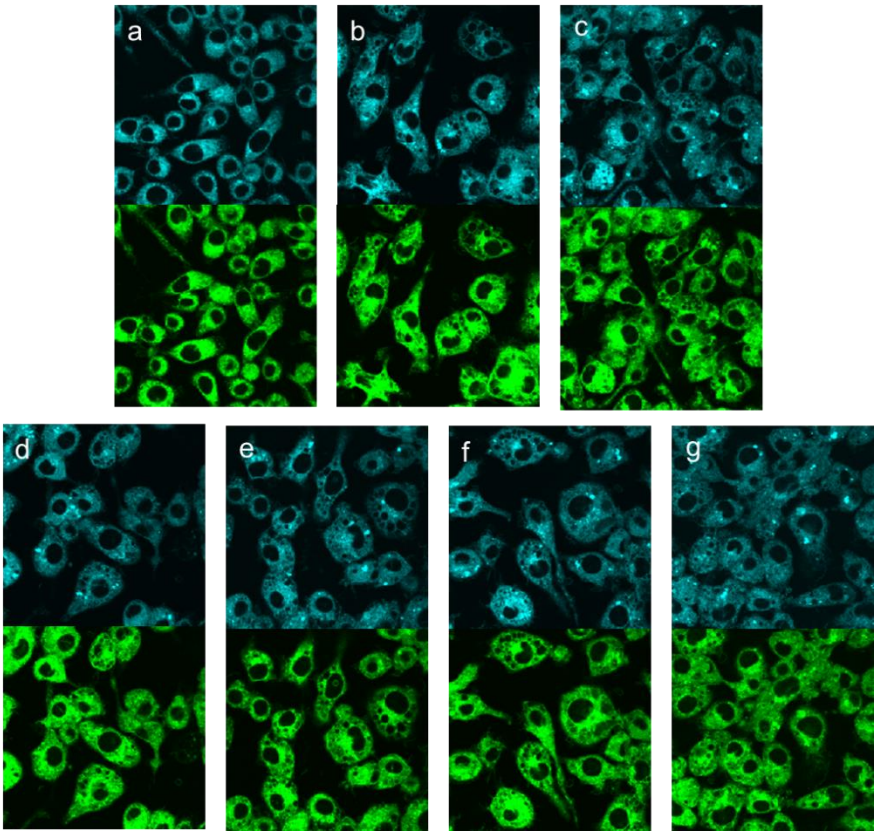

Figure 87. RAW 264.7 cells were incubated with 500 ng/ml LPS, 50 ng/ml IFN-γ for 4 hr and washed with DPBS and treated with (a) no, (b-g all) LPS, IFN-γ, (c) DMTU (H_2O_2 scavenger), (d) ebselen ($ONOO^-$ scavenger), (e) mannitol (·OH scavenger), (f) NaN_3 (singlet oxygen scavenger), (g) tiron (superoxide scavenger) and stained with 5 μM probe **77** for 15min. After washing with DPBS, the fluorescence images were acquired by confocal microscopy.

4.3 Conclusions

A series of boronic acid pinacol ester probes were synthesised and analysed for their ability to detect hydrogen peroxide. The dimethylamino stilbene probe **68** and methoxy stilbene probe **69** displayed an 'Off-On' fluorescence response upon reaction with hydrogen peroxide, accompanied by a blue shift of the fluorescence emission spectrum. The unsubstituted stilbene probe **70** displayed a decrease in fluorescence intensity upon reaction with H_2O_2 accompanied by a small blue shift of the fluorescence spectrum. The cyano stilbene probe **71** displayed a decrease in fluorescence intensity and a redshift of the fluorescence emission spectrum upon reaction with H_2O_2. The direction of the wavelength shift of the fluorescence emission spectrum can be explained by consideration of ICT states. When an electron-donating and electron-accepting group are present at opposite ends of the fluorophore, charge transfer is possible in the excited state, lowering the energy of the excited state by an ICT mechanism. Perturbation of this ICT state removes this charge transfer, and as a result the emission wavelength of the fluorophore is shifted to higher energy.

The dimethylamino stilbene probe **68** displayed the largest increase in fluorescence emission intensity and largest wavelength shift of all the stilbene probes upon reaction with H_2O_2. Therefore, this probe was chosen for further modification in an attempt to shift the fluorescence profiles to longer wavelengths. The dimethylamino naphthalene stilbene probe **76** was synthesised, and although the fluorescence profiles had shifted to longer wavelengths relative to the dimethylamino stilbene probe **68**, the probe now displayed a decrease in fluorescence intensity upon reaction with hydrogen peroxide.

The stilbene based probes all suffer from low photostability, due to *trans-cis* isomerisation of the central ethylene bridging unit. The dimethylamino oxazole probe **77** was then synthesised. As it contains no central ethylene unit, *cis-trans* isomerisation is not possible, leading to a probe with increased photostability.

The dimethylamino oxazole probe **77** showed a larger increase in fluorescence intensity upon reaction with H_2O_2 compared to the previously synthesised probes, accompanied by a small blue shift of the fluorescence emission profile. Further fluorescence experiments were carried out and it was found that a 30 nM concentration of probe **77** was able to detect a range of H_2O_2 concentrations under neutral pH conditions, suggesting its suitability as an *in vivo* H_2O_2 fluorescent sensor. Probe **77** was then sent

off for cell imaging studies. It was found that although the probe was able to enter the cells and act as a fluorescent stain, no change in fluorescence intensity was observed upon addition of various different reactive oxygen species within the cellular environment.

4.4 Future Work

Whilst the oxazole probe **77** did permeate the cell membrane, as can be seen from the cell images the probe did not enter the nucleus. By increasing the hydrophilicity of the probe, its solubility within the cellular environment may be improved. This could be done by modification of the probe, replacing the methyl groups on the nitrogen with polyethylene glycol (PEG) groups. Polyethylene glycol is a biologically inert, non-immunogenic chemical that confers greater water solubility to proteins, labelling tags and crosslinkers when it is incorporated as a constituent chemical group.[253] This modification, known as PEGylation has been known to alter the absorption and distribution patterns of therapeutic agents, and increase drug stability.

Alternatively, probes which display fluorescence profiles at even longer wavelengths could be synthesised. Lakowicz *et al.* have reported that the chalcone probe **81** shows fluorescence emission at longer wavelengths compared to the previously reported stilbene and diphenyloxazole probes (Figure 88).[254] Interestingly, in this probe the boronic acid group is not directly involved in the ICT. The ICT in this probe is between the electron-donating dimethylamino group and the electron-withdrawing carbonyl group. The boronic acid group is in resonance with the electron-withdrawing carbonyl group. Since the boronic acid group becomes an electron-donor in its anionic form, at high pH the electron-withdrawing character of the carbonyl should be decreased due to charge transfer from the boronate group to the carbonyl. The increase of electron density on the carbonyl group decreases the ICT from the dimethylamino group, resulting in spectral changes due to perturbation of the ICT nature of the excited state. It is expected that the corresponding Bpin-functionalised probe **82** could function as a probe for H_2O_2 based upon the conversion of the electron-withdrawing boronic ester to the electron-donating phenol, perturbing the ICT nature of the excited state, leading to changes in the fluorescence emission spectrum.

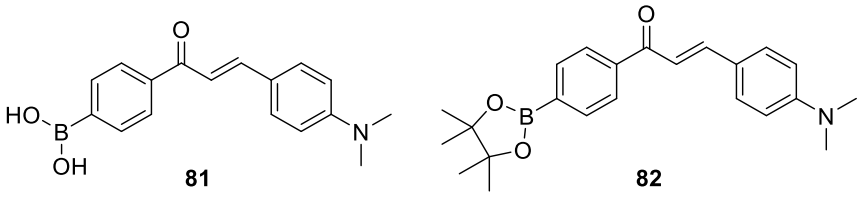

Figure 88. Structure of previously reported boronic acid chalcone probe **81**, and proposed boronic acid pinacol ester probe **82**.

5 Experimental Procedures

5.1 Materials and Reagents

All starting materials and reagents were purchased from Sigma Aldrich, Alfa Aesar, Fluorochem, Acros Organics or Apollo Scientific and used as received without any further purification. Unless otherwise stated all solvents used were reagent grade and were used without distillation. Dry solvents were obtained from an Innovative Technology Inc. PS-400-7 solvent purification system. All water used was distilled.

Thin layer chromatography was carried out on commercially available aluminium backed plates, pre-coated with a 0.20 mm layer of silica gel 60 with fluorescent indicator UV254. Plates were visualised using UV light (254 nm) or by staining the plates with ninhydrin or curcumin dip, followed by gentle heating. Flash chromatography was performed using chromatography grade silica, 60 Å particle size 35-70 microns obtained from Fisher Scientific UK.

5.2 Instrumentation

Nuclear Magnetic Resonance Spectroscopy (NMR)

Unless otherwise stated, all NMR spectra were obtained using a Bruker Advance 300 with all spectra recorded in chloroform-*d* or DMSO-d_6. ^{1}H NMR spectra were recorded at an operating frequency of 300 MHz, ^{11}B NMR spectra were recorded at an operating frequency of 96 MHz, and ^{13}C NMR spectra were recorded at an operating frequency of 75 MHz, with proton decoupling for all ^{13}C NMR spectra. All chemical shift values (δ) are reported in parts per million and a relative to the residual, non-deuterated solvent peak, for ^{1}H NMR spectra: chloroform-*d*, δ 7.26 ppm or DMSO-d_6, δ 2.50 ppm; for ^{13}C NMR spectra: chloroform-*d*, δ 77.16 ppm or DMSO-d_6, δ 39.52 ppm. Chemical shift is recorded in parts per million (ppm) and all coupling constants, *J*, are reported in hertz (Hz). The multiplicity of the signals is designated by the following abbreviations: s, singlet; d, doublet; dd, doublet of doublets; t, triplet; q, quartet; m, multiplet; br, broad.

Fourier Transform Infra-Red Spectroscopy (FT-IR)

Infra-red spectra were recorded on a PerkinElmer 100 FT-IR spectrometer, using a Universal ATR accessory for sampling. Spectra were recorded as thin films. Selected absorbances are reported as ν in cm^{-1}. The spectrometer was calibrated by running a background scan prior to the analysis of each sample.

Mass Spectrometry

High resolution mass spectra were recorded using an electrospray Time-Of-Flight MicroTOF^{TM} mass spectrometer with external calibration. Masses were recorded in either positive or negative mode. Samples were introduced either by syringe pump or flow injection using an autosampler in an Agilent 1100 LC system. Samples were diluted with HPLC grade methanol or acetonitrile. Data acquisition and automated processing were controlled *via* Compass Open Access 1.3 software. Masses are accurate to 5 ppm and data was processed using Data Analysis software available from Bruker Daltonics.

Melting points

All capillary melting points were measured using Stuart digital SMP10 melting point apparatus with 1 degree resolution.

UV-Vis Spectroscopy

UV-Vis absorption measurements were performed using a Perkin-Elmer UV-Vis spectrometer Lambda 20, with cuvettes of a 10 mm path length. Baseline corrections using phosphate buffer (pH 7.3) were carried out before any samples were analysed. The machine was operated using UV Winlab software.

Fluorescence Spectroscopy

Fluorescence measurements were performed on a Perkin-Elmer Luminescence Spectrophotometer LS 50B, utilising silica (quartz) cuvettes with 10 mm path length, four faces polished. Data was collected *via* the Perkin-Elmer FL Winlab software. All solvents used in fluorescence measurements were HPLC or fluorescence grade and the water was de-ionised.

pH Measurements

Hanna Instruments HI 9321 Microprocessor pH meter was used to measure the pH of buffers, and was routinely calibrated using Fisher chemicals standard buffer solutions (pH 4.0 – phthalate, pH 7.0 – phosphate, pH 10.0 – borate).

5.3 Preparation of buffers

pH 8.21 methanolic buffer was prepared following the literature method containing 52.1 wt.% methanol, KCl, 0.01000 mol/L, KH_2PO_4, 0.002752 mol/L and Na_2HPO_4, 0.002757 mol/L.[255]

pH 7.3 phosphate buffer was prepared by dissolving one Thermo Scientific™ Oxoid™ Phosphate Buffered Saline Tablet in 100 mL of distilled water to give a buffered saline solution containing NaCl 8.0 g/L, KCl 0.2 g/L, Na_2HPO_4 1.15 g/L and KH_2PO_4 0.2 g/L.

For gel swelling studies, the pH of the buffers was increased by addition of 0.1 M aqueous NaOH solution.

5.4 Experimental Data for Chapter 2

5.4.1 Synthesis of Compounds

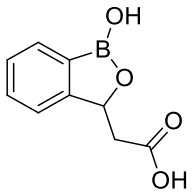

2-(1-hydroxy-1,3-dihydrobenzo[*c*][1,2]oxaborol-3-yl)acetic acid - 23

Pyridine (0.81 mL, 10.00 mmol) was added to a solution of 2-formylphenylboronic acid (1.00 g, 6.67 mmol) and malonic acid (1.04 g, 10.00 mmol) in anhydrous 1,4-dioxane (10 mL). The reaction mixture was heated to 100 °C and refluxed for 16 hours. The reaction mixture was allowed to cool, and the solvent was removed under reduced pressure to give a yellow tar. This compound was not successfully isolated and the following data was obtained from a mixture. ^{1}H NMR (300 MHz, MeOD-d_4): δ 8.74 (1H, OH, s(br)), 7.65 (1H, ArH, d J = 7.2 Hz), 7.34 – 7.41 (3H, ArH, m), 5.59 (1H, CH, dd, J_1 = 8.8, J_2 = 4.4 Hz), 2.92 (1H, CH_2, dd, J_1 = 15.7, J_2 = 4.4 Hz), 2.51 (1H, CH_2, dd, J_1 = 15.7, J_2 = 8.8 Hz); ^{13}C NMR (75 MHz, MeOD-d_4): δ 174.8, 132.5, 131.9, 129.6, 129.1, 122.7, 80.0, 43.3; ^{11}B NMR (96 MHz, MeOD-d_4): δ 34; HRMS (ES) *m/z* calculated for $C_9H_8O_4B_1$: $[M-H]^-$ 191.0516, found 191.0534

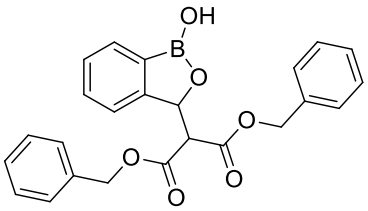

dibenzyl 2-(1-hydroxy-1,3-dihydrobenzo[*c*][1,2]oxaborol-3-yl)malonate - 24

To a stirred solution of dibenzyl malonate (3.00 mL, 12.00 mmol) in THF (20 mL), sodium methoxide (972 mg, 18.00 mmol) was added and stirred at room temperature for 30 minutes. 2-formylphenylboronic acid (2.70 g, 18.00 mmol) was added and the reaction mixture was left to stir at room temperature for 2 days. The reaction was quenched with NH_4Cl and the product was extracted 3 times into ethyl acetate. The organic layers were combined, dried over $MgSO_4$, filtered, and the solvent was removed

under reduced pressure to give a pale yellow oil. The crude product was purified using flash silica chromatography (2:1 to 1:1 pentane: EtOAc) to afford the desired product as a white powder in 71% yield. ^{1}H NMR (300 MHz, DMSO-*d*$_6$): δ 9.39 (1H, OH, s), 7.71 (1H, ArH, d, *J* = 5.7 Hz), 7.25-7.44 (11H, ArH, m), 7.10 (2H, ArH, m), 5.75 (1H, CH, d, *J* = 5.7 Hz), 5.21 (2H, CH_2, s), 4.99 (2H, CH_2, s), 4.28 (1H, CH, d, *J* = 5.7 Hz); ^{13}C NMR (75 MHz, DMSO-*d*$_6$): δ 167.0, 166.2, 153.4, 135.7, 135.7, 131.1, 130.8, 128.8, 128.7, 128.6, 128.3, 128.1, 127.9, 122.2, 78.1, 67.0, 66.5, 56.7; ^{11}B NMR (96 MHz, DMSO-*d*$_6$): δ 35; FTIR ν (cm^{-1}): 3396, 3037, 1751, 1727, 1290, 1277; HRMS (ES) *m/z* calculated for $C_{24}H_{20}O_6B_1$: $[M-H]^-$ 415.1353, found 415.1370; Mp: 106-108 °C

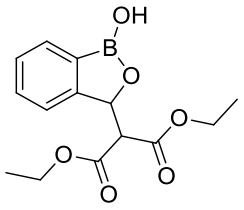

diethyl 2-(1-hydroxy-1,3-dihydrobenzo[*c*][1,2]oxaborol-3-yl)malonate - 26

Sodium methoxide (234 mg, 4.33 mmol) was added to a solution of 2-formylphenylboronic acid (500 mg, 3.33 mmol) and diethyl malonate (0.56 mL, 3.66 mmol) in THF (10 mL). The resulting solution was stirred for 48 hours at room temperature. The reaction was quenched with NH_4Cl and the product was extracted 3 times into ethyl acetate. The organic layers were combined, dried over $MgSO_4$, filtered, and the solvent was removed under reduced pressure to give a pale yellow oil. The crude product was purified using flash silica chromatography (2:1 pentane: EtOAc) to afford the desired product as a pale yellow oil in 62% yield. ^{1}H NMR (300 MHz, DMSO-*d*$_6$): δ 9.35 (1H, OH, s), 7.68 (1H, ArH, d, *J* = 7.2 Hz), 7.32-7.48 (3H, ArH, m), 5.68 (1H, CH, d, *J* = 5.5 Hz), 4.15 (2H, CH_2, q, *J* = 7.2 Hz), 4.04 (1H, CH, d, *J* = 5.5 Hz), 3.95 (2H, CH_2, q, *J* = 7.2 Hz), 1.16 (3H, CH_3, t, *J* = 7.2 Hz), 0.96 (3H, CH_3, t, *J* = 7.2 Hz); ^{13}C NMR (75 MHz, DMSO-*d*$_6$): δ 167.2, 166.4, 153.5, 131.0, 130.6, 128.0, 122.2, 78.0, 61.6, 60.9, 60.1, 56.8, 14.4; ^{11}B NMR (96 MHz, DMSO-*d*$_6$): δ 28; FTIR ν (cm^{-1}): 3398, 2984, 1728, 1290, 1030; HRMS (ES) *m/z* calculated for $C_{14}H_{18}O_6B_1$: $[M+H]^+$ 293.1196, found 293.1198

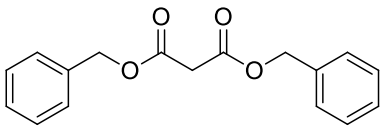

dibenzyl malonate

Malonic acid (5.00 g, 48.05 mmol), benzyl alcohol (9.94 mL, 96.10 mmol) and *para*-toluenesulfonic acid (27 mg, 0.14 mmol) were dissolved in toluene (20 mL) and heated under reflux in a round bottomed flask fitted with a Dean-Stark apparatus for 6 hours. The solvent was evaporated under reduced pressure to give a colourless oil. The crude product was purified using flash silica chromatography (2:1 pentane: EtOAc) to afford the desired product as a colourless oil in 84% yield. ^{1}H NMR (300 MHz, DMSO-d_6): δ 7.35 (10H, ArH, s), 5.16 (4H, CH_2, s), 3.66 (2H, CH_2, s); ^{13}C NMR (75 MHz, DMSO-d_6): δ 166.8, 136.0, 128.8, 128.5, 128.4, 66.7, 41.5; FTIR ν (cm^{-1}): 3035, 1730, 1142; HRMS (ES) *m/z* calculated for $C_{17}H_{17}O_4$: $[M+H]^+$ 285.1129, found 285.1118

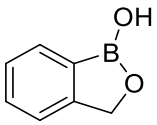

benzoxaborole - 8

2-formylphenylboronic acid (10.00 g, 66.69 mmol) was dissolved in methanol (100 mL). $NaBH_4$ (2.78 g, 73.36 mmol) was added in portions and the resulting solution was left to stir at room temperature for 1 hour. The reaction mixture was acidified with 3 M HCl and the aqueous phase was extracted into diethyl ether 3 times. The combined organic layers were dried over $MgSO_4$, filtered, and the solvent was removed under reduced pressure to give a white powdery solid in 99.8% yield. ^{1}H NMR (500 MHz, DMSO-d_6): δ 9.17 (1H, OH, s (br)) 7.74 (1H, ArH, d, J = 7.3 Hz), 7.47 (1H, ArH, m), 7.40 (1H, ArH, m), 7.34 (1H, ArH, m), 4.98 (2H, CH_2, s); ^{13}C NMR (75 MHz, DMSO-d_6): δ 154.2, 130.9, 130.8, 127.2, 121.7, 70.3 ^{11}B NMR (96 MHz, DMSO-d_6): δ 35; FTIR ν (cm^{-1}): 3291, 3212, 3052, 968; HRMS (ES) *m/z* calculated for $C_7H_6O_2B_1$: $[M-H]^-$ 133.0461, found 133.0476; Mp: 96-98 °C (lit. 96-99 °C)[256]

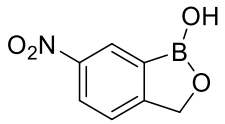

6-nitrobenzoxaborole - 27

To 40 mL fuming nitric acid maintained at -30 to -40 ℃, using dry ice and acetone, benzoxaborole **8** (8.00 g, 59.73 mmol) was added in portions with stirring. N_2 gas was flowed over the top of the reaction flask during addition to stop atmospheric air condensing inside. The reaction mixture was maintained at -30 to -40 ℃ and left to stir for 1 hour. The reaction mixture was poured onto ice water and left to stir until the ice had melted. The precipitated pale yellow compound was filtered, washed with water and dried under vacuum to give a pale yellow powdery solid. The crude reaction product was recrystallized from hot EtOH. The purified product was collected as a pale yellow powder in 66% yield. ^{1}H NMR (300 MHz, DMSO-d_6): δ 9.56 (1H, OH, s (br)), 8.58 (1H, ArH, d, J = 2.4 Hz), 8.33 (1H, ArH, dd, J_1 = 8.4, J_2 = 2.4 Hz), 7.69 (1H, ArH, d, J = 8.4 Hz), 5.13 (2H, CH_2, s); ^{13}C NMR (75 MHz, DMSO-d_6): δ 161.0, 147.5, 126.0, 125.8, 123.4, 70.4; ^{11}B NMR (96 MHz, DMSO-d_6): δ 34; FTIR ν (cm^{-1}): 3257, 3072, 1512, 1339, 979; HRMS (ES) *m/z* calculated for $C_7H_6N_1O_4B_1Na_1$: $[M+Na]^+$ 202.0289, found 202.0279; Mp: 176-179 ℃ (lit. 178-180 ℃)[257]

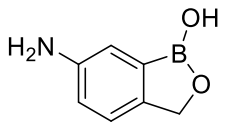

6-aminobenzoxaborole - 28

6-nitrobenzoxaborole **27** (2.00 g, 11.18 mmol) was dissolved in 10% acetic acid/THF (40 mL). Pd/C (1.19 g, 11.18 mmol) was added in portions, followed by stirring at room temperature for 24 hours with continuously bubbled H_2 under atmospheric pressure. The reaction mixture was purged with N_2 for a few minutes. After removing Pd/C by filtration through celite, the filtrate was evaporated to a brown oil under reduced pressure. The product was resolved in EtOAc (50 mL) and treated with 1 M aq. LiOH (100 mL) at room temperature for 30 minutes. The EtOAc layer was separated out and washed 3 times with 1 M LiOH. The alkaline layers were combined, acidified to pH 6-7 with 3 M aq. HCl and extracted 5 times into EtOAc. The organic extracts were

combined, dried over $MgSO_4$, filtered, and the solvent was removed under reduced pressure to give a brown solid in 78% yield. ^{1}H NMR (300 MHz, DMSO-d_6): δ 8.89 (1H, OH, s), 7.03 (1H, ArH, d, J = 8.2 Hz), 6.88 (1H, ArH, d, J = 2.2 Hz), 6.70 (1H, ArH, dd, J_1 = 8.2, J_2 = 2.2 Hz), 4.96 (2H, NH_2, s (br)), 4.81 (2H, CH_2, s); ^{13}C NMR (75 MHz, DMSO-d_6): δ 147.93, 141.7, 121.8, 117.9, 114.9, 70.0; ^{11}B NMR (96 MHz, DMSO-d_6): δ 36; FTIR ν (cm^{-1}): 3352, 2926, 2874, 1621, 981; HRMS (ES) *m/z* calculated for $C_7H_9N_1O_2B_1$: $[M+H]^+$ 150.0726, found 150.0739; Mp: 142-144 °C (lit. 145-148 °C)[258]

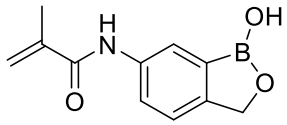

6-methacrylamidebenzoxaborole - 29

6-aminobenzoxaborole **28** (1.00 g, 6.71 mmol) and sodium hydrogen carbonate (2.26 g, 26.84 mmol) were dissolved in a 1:1 mixture of THF (20 mL) and water (20 mL). The resulting solution was cooled down to 0 °C and methacryloyl chloride (1.32 mL, 13.42 mmol) was added dropwise. The reaction was kept at 0 °C for 2 hours and was then allowed to warm to room temperature and stirred overnight. A solid crude product was obtained after THF was evaporated under reduced pressure, and extracted into EtOAc for 2 hours. The EtOAc layer was washed continuously with water, saturated sodium bicarbonate solution, water, and brine. The organic layer was dried over $MgSO_4$, filtered and the solvent was removed under reduced pressure to give a pale brown solid in 82% yield. ^{1}H NMR (300 MHz, DMSO-d_6): δ 9.81 (1H, NH, s), 9.19 (1H, OH, s), 8.07 (1H, ArH, d, J = 1.8 Hz), 7.68 (1H, ArH, dd, , J_1 = 8.2, J_2 = 1.8 Hz), 7.35 (1H, ArH, d, J = 8.2 Hz), 5.82 (1H, CH, s), 5.51 (1H, CH, s), 4.95 (2H, CH_2, s), 1.97 (3H, CH_3, s); ^{13}C NMR (75 MHz, DMSO-d_6): δ 167.1, 149.3, 140.8, 138.1, 123.9, 122.6, 121.7, 120.2, 70.1, 18.5; ^{11}B NMR (96 MHz, DMSO-d_6): δ 24; FTIR ν (cm^{-1}): 3276, 3086, 2973, 1655, 1214, 979; HRMS (ES) *m/z* calculated for $C_{11}H_{13}N_1O_3B_1$: $[M+H]^+$ 218.0988, found 218.0993; Mp: 167-170 °C (lit. 171-174 °C)[259]

5.5 Experimental Data for Chapter 3

5.5.1 Synthesis of Compounds

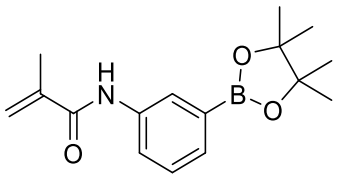

3-methacryloylamino phenylboronic acid pinacol ester – 55b

3-Aminophenylboronic acid pinacol ester (0.50 g, 2.28 mmol) and sodium hydrogen carbonate (0.77 g, 9.13 mmol) were dissolved in a 1:1 mixture of THF (10 mL) and water (10 mL). The resulting solution was cooled down to 0 ℃ and methacryloyl chloride (0.45 mL, 4.56 mmol) was added dropwise. The reaction was kept at 0 ℃ for 2 hours and was then allowed to warm to room temperature and stirred overnight. A solid crude product was obtained after THF was evaporated under reduced pressure, and extracted into EtOAc for 2 hours. The EtOAc layer was washed continuously with water, saturated sodium bicarbonate solution, water, and brine. The organic layer was dried over $MgSO_4$, filtered and the solvent was removed under reduced pressure to give a white solid. The crude product was purified by recrystallization in DCM/hexane to give a white powdery solid in 57% yield. ^{1}H NMR (300 MHz, $CDCl_3$): δ 8.01 (1H, ArH, ddd, J_1 = 8.1, J_2 = 2.5, J_3 = 1.2 Hz), 7.65 (1H, ArH, dd, J_1 = 2.5, J_2 = 1.2 Hz), 7.56 (1H, ArH, app. dt, J_1 = 7.4, J_2 = 1.2 Hz), 7.51 (1H, NH, br s), 7.37 (1H, ArH, app. t, J = 7.7 Hz), 5.79 (1H, methacryloyl CH, dd, J_1 = 0.9, J_2 = 0.6 Hz), 5.45 (1H, methacryloyl CH, dd, J_1 = 1.4, J_2 = 0.6 Hz), 2.06 (3H, methacryloyl CH_3, dd, J_1 = 1.4, J_2 = 0.9 Hz), 1.34 (12H, pin CH_3, s); ^{13}C NMR (75 MHz, DMSO-d_6): δ 167.1, 140.6, 139.1, 129.8, 128.6, 126.7, 123.6, 120.5, 84.1, 25.2, 19.2; ^{11}B NMR (96 MHz, DMSO-d_6): δ 30; FTIR ν (cm^{-1}): 3355, 2976, 1662, 1622, 1534, 1421, 1356, 1141, 704; HRMS (ES) *m/z* calculated for $C_{16}H_{22}N_1O_3B_1$: $[M-H]^-$ 286.1623, found 286.1625; Mp: 138-142 ℃

5.5.2 Preparation of Hydrogels

5.5.2.1 General Procedure for Preparation of Hydrogels

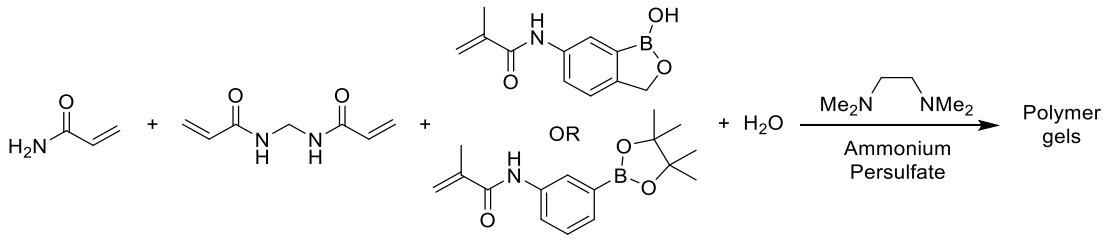

Hydrogels were formed by copolymerisation of acrylamide with methylene bisacrylamide in the presence of water. Polymerisation was initiated by ammonium persulfate and TMEDA (tetramethylethylenediamine). Hydrogels were prepared as follows:

1. An aqueous ammonium persulfate (APS) stock solution (10% wt./vol) was prepared and kept cool until required (< 4 °C).
2. Acrylamide (3.9 g) and methylene bisacrylamide (0.1 g) were dissolved in distilled water (10 mL).
3. A 2 mL aliquot of this mixture was diluted with a further 2 mL of distilled water.
4. To this diluted aliquot was added tetramethylethylenediamine (10 µL) along with the freshly prepared ammonium persulfate solution (30 µL).
5. The mixture was then poured into the chosen mould and allowed to set.
6. After the mixture was set (approximately 60 minutes, judged by visual inspection) the gels were removed from the moulds, and their weights recorded.
7. Hydrogels were stored in phosphate buffer (pH 7.3) in order to prevent drying.

5.5.2.2 Modifications to General Procedure for Preparation of Benzoxaborole-Functionalised Hydrogels

6-methacrylamidebenzoxaborole **29** (0.1 g) was added in place of the same mass of acrylamide. A small amount of ethanol (0.5 mL) was added in place of the same volume of distilled water in order to aid dissolution. Extended times of approximately 8 hours were required for the gels to set, judged by visual inspection.

5.5.2.3 Modifications to General Procedure for Preparation of Phenylboronic Acid Pinacol Ester-Functionalized Hydrogels

3-methacrylamide phenylboronic acid pinacol ester **55b** (0.1 g) was added in place of the same mass of acrylamide. In order to aid dissolution, the 3-methacrylamide phenylboronic acid pinacol ester was added to distilled water (10 mL) and heated for extended periods of time until all of the 3-methacrylamide phenylboronic acid pinacol ester had dissolved. After the solution had cooled to room temperature, acrylamide and methylene bisacrylamide were added. Shortened times of approximately 30 minutes were required for the gels to set, judged by visual inspection.

5.5.2.4 Syringe Method for Polymerisation

Hydrogels were prepared using plastic disposable syringes as moulds, as described below. The syringe method allows for the size of hydrogels produced to be easily changed simply by using a different size of syringe.

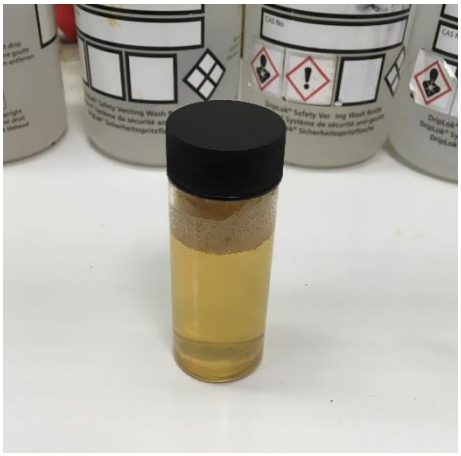

1. Dissolve acrylamide, methylene bisacrylamide (and benzoxaborole or phenylboronic acid pinacol ester monomer) in distilled water.

2. Add TMEDA and ammonium persulfate. Shake gently to mix.

3. Using the volume increments on the side of the syringe carefully draw up the required amount of polymer solution.

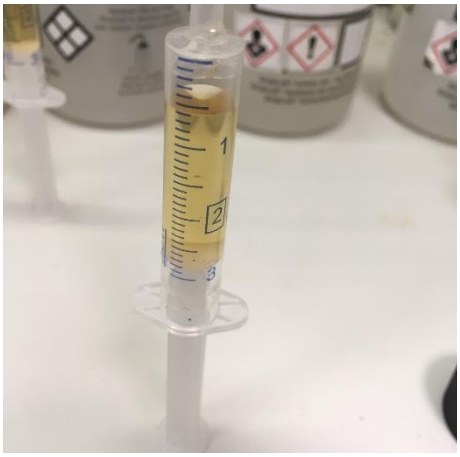

4. Carefully invert the syringes and leave to set.

5.5.3 Gel Swelling Studies

The weights of a series of blank, benzoxaborole-functionalised and phenylboronic acid pinacol ester-functionalised hydrogels were recorded as the gels were removed from their moulds. Each type of hydrogel was then immersed in pure water, pH 7.3 phosphate buffer, pH 8.5 phosphate buffer, pH 10 phosphate buffer, pH 8.21 phosphate buffer (containing 52.1 wt. % MeOH) or pH 10 phosphate buffer (containing 52.1 wt. % MeOH). The pH of the buffers was adjusted by addition of 0.1 M aqueous NaOH solution. The gels were then left to stand in the buffer solutions at room temperature for 16 hours. After 16 hours, the hydrogels were removed from the buffer solutions and their weights were once again recorded.

5.5.4 General Procedures for Dye Uptake and Release Experiments

5.5.4.1 Alizarin Red S Uptake

Individual hydrogels were placed in phosphate buffered ARS solution (3 mL, 2.0×10^{-4} M, pH 7.3) and stirred gently at 100 rpm. The absorbance of the solution was recorded at defined time intervals. A meaningful comparison between the hydrogels can be made by plotting the absorbance of the solution per unit mass of gel (Abs/g) versus time for dye uptake. The decrease in absorbance of the ARS solution corresponds to the amount of dye uptake.

5.5.4.2 Removal of Non-Specifically Bound ARS

After the dye uptake procedure described above, the hydrogels were removed from the buffered ARS solution, gently dried on tissue paper, then placed into fresh phosphate buffer solution (3 mL, pH 7.3) and stirred gently at 100 rpm. The absorbance of the solution was recorded at defined time intervals. A meaningful comparison between the hydrogels can be made by plotting the absorbance of the solution per unit mass of gel (Abs/g) versus time for dye release. The increase in absorbance is due to the release of ARS dye which is non-specifically bound within the pores of the gel after the dye uptake experiments.

5.5.4.3 Dye Displacement Assays with Monosaccharides

After the dye uptake and release experiments, the hydrogels were gently dried on tissue paper, then placed into fresh phosphate buffer solution (3 mL, pH 7.3) and stirred gently at 100 rpm. Portions of solid monosaccharide sugar were added, and the solution's absorbance was recorded 30 minutes after each sugar addition. Sugar concentrations of 0.01 M, 0.025 M, 0.05 M. 0.075 M, 0.1 M, 0.25 M, 0.5 M and 1 M were investigated. A meaningful comparison between the hydrogels can be made by plotting the absorbance of the solution per unit mass of gel (Abs/g) versus sugar concentration. The increase in absorbance corresponds to ARS dye that is competitively displaced from boron by the sugar.

Data points are an average of at least two experiments. Error bars showing the standard error were used, calculated by the following equation:

$$SE_{\bar{x}} = \frac{\sigma}{\sqrt{n}}$$

Where

$SE_{\bar{x}}$ = standard error of the mean

σ = standard deviation of the sample

n = sample size (number of observations)

5.6 Experimental Data for Chapter 4

5.6.1 General Synthetic Procedures

5.6.1.1 General Procedure 1 – Horner-Wadsworth-Emmons Reaction for Synthesis of Bromo-Substituted Intermediates

4-bromobenzyl bromide (1.0 equiv.) and triethyl phosphite (1.2 equiv.) were heated to 150 °C with stirring for 3 hours under N_2. Reaction completion was confirmed by the disappearance of the P-OEt peak at δ 139.69 ppm and the appearance of the P=O peak at ~ δ 26.3 ppm in the ^{31}P NMR spectrum. The reaction mixture was cooled to room temperature, and anhydrous DMF (15 mL) was added. The resulting solution was cooled in an ice bath and sodium hydride (1.5 equiv.) was added. After stirring at 0 °C for 20 minutes, a solution of the corresponding aldehyde (1.0 equiv.) in anhydrous DMF (5 mL) was slowly added. The resulting slurry was allowed to warm to room temperature and left to stir overnight. The reaction mixture was poured into ice water and left to stir until the ice had melted. The precipitated product was collected by filtration, washed with water and dried under vacuum.

5.6.1.2 General Procedure 2 – Suzuki Reaction for Synthesis of Boronic Acid Pinacol Ester Probes

The corresponding bromo-substituted styrene intermediate (1.0 equiv.), bis(pinacolato)diboron (1.07 equiv.) and potassium acetate (2.91 equiv.) were partially dissolved in DMSO/dioxane (6 mL/2 mL). $PdCl_2(dppf).CH_2Cl_2$ (0.04 equiv.) was partially dissolved in DMSO/dioxane (3 mL/1 mL) and was added drop-wise to the reaction mixture. The reaction was heated to 80 °C and stirred under N_2 for 4 hours. The reaction mixture was cooled to room temperature and quenched with saturated NH_4Cl. The crude product was extracted 3 times into ethyl acetate. The combined organic layers were dried over $MgSO_4$, filtered, and the solvent was removed under reduced pressure to give the crude reaction product.

5.6.2 Isolated Compounds

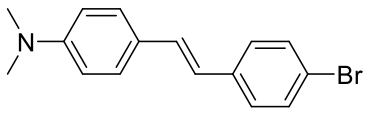

(*E*)-4-(4-bromostyryl)-*N*,*N*-dimethylaniline - 72

The title compound was prepared according to General Procedure 1 using 4-bromobenzyl bromide (1.68 g, 6.71 mmol), triethyl phosphite (1.40 mL, 8.05 mmol), sodium hydride (0.40 g, 10.07 mmol) and 4-(dimethylamino)benzaldehyde (1.00 g, 6.71 mmol). The crude reaction product was recrystallized in DCM/hexane. The purified product was collected as a pale yellow crystalline solid in 73% yield. ^{1}H NMR (300 MHz, $CDCl_3$): δ 7.49 - 7.29 (6H, ArH, m), 7.03 (1H, alkene CH, d, *J* = 16.3 Hz), 6.83 (1H, alkene CH, d, *J* = 16.3 Hz), 6.71 (2H, ArH, d, *J* = 8.7 Hz), 2.99 (6H, CH_3, s); ^{13}C NMR (75 MHz, $CDCl_3$): δ 150.3, 137.2, 131.6, 129.5, 127.7, 127.5, 125.3, 123.0, 120.1, 112.4, 40.5; FTIR ν (cm^{-1}): 2796, 1065, 967, 819; HRMS (ES) *m/z* calculated for $C_{16}H_{17}N_1Br_1$: $[M+H]^+$ 302.0544, found 302.0526; Mp: 207-209 °C (lit. 205-207 °C)[260]

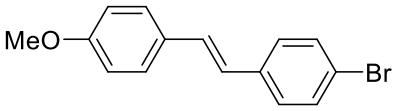

(*E*)-1-bromo-4-(4-methoxystyryl)benzene - 73

The title compound was prepared according to General Procedure 1 using 4-bromobenzyl bromide (1.68 g, 6.71 mmol), triethyl phosphite (1.40 mL, 8.05 mmol), sodium hydride (0.40 g, 10.07 mmol) and 4-methoxybenzaldehyde (0.81 mL, 6.71 mmol). The crude reaction product was recrystallized in DCM/hexane. The purified product was collected as a white crystalline solid in 60% yield. ^{1}H NMR (300 MHz, $CDCl_3$): δ 7.50 – 7.40 (4H, ArH, m), 7.39 – 7.31 (2H, ArH, m), 7.05 (1H, alkene CH, d, *J* = 16.3 Hz), 6.90 (1H, alkene CH, d, *J* = 16.3 Hz), 6.93 – 6.86 (2H, ArH, m), 3.83 (3H, OCH_3, s); ^{13}C NMR (75 MHz, $CDCl_3$): δ 159.5, 136.6, 131.7, 129.8, 129.0, 127.8, 127.7, 125.3, 120.8, 114.2, 55.4; FTIR ν (cm^{-1}): 3010, 1600, 1511, 968, 825; Mp: 201-204 °C (lit. 202-204 °C)[260]

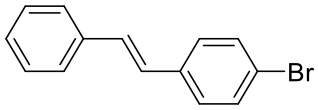

(*E*)-1-bromo-4-styrylbenzene - 74

The title compound was prepared according to General Procedure 1 using 4-bromobenzyl bromide (1.68 g, 6.71 mmol), triethyl phosphite (1.40 mL, 8.05 mmol), sodium hydride (0.40 g, 10.07 mmol) and benzaldehyde (0.68 mL, 6.71 mmol). The crude reaction product was recrystallized in DCM/hexane. The purified product was collected as a white crystalline solid in 47% yield. ^{1}H NMR (300 MHz, $CDCl_3$): δ 7.55-7.44 (4H, ArH, m), 7.42-7.33 (4H, ArH, m), 7.32-7.24 (1H, ArH, m), 7.11 (1H, alkene CH, d, *J* = 16.3 Hz), 7.03 (1H, alkene CH, d, *J* = 16.3 Hz); ^{13}C NMR (75 MHz, $CDCl_3$): δ 137.0, 136.3, 131.8, 129.5, 128.8, 128.0, 127.9, 127.4, 126.6, 121.3; FTIR ν (cm^{-1}): 2925, 1484, 1003, 811; Mp: 134-136 °C (lit. 132-135 °C)[260]

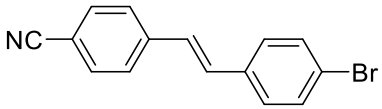

(*E*)-4-(4-bromostyryl)benzonitrile - 75

The title compound was prepared according to General Procedure 1 using 4-bromobenzyl bromide (1.68 g, 6.71 mmol), triethyl phosphite (1.40 mL, 8.05 mmol), sodium hydride (0.40 g, 10.07 mmol) and 4-cyanobenzaldehyde (0.88 g, 6.71 mmol). The crude reaction product was recrystallized in DCM/hexane. The purified product was collected as a yellow crystalline solid in 29% yield. ^{1}H NMR (300 MHz, $CDCl_3$): δ 7.67-7.54 (4H, ArH, m), 7.54-7.47 (2H, ArH, m), 7.14 (2H, ArH, m), 7.14 (1H, alkene CH, d, *J* = 16.3 Hz), 7.06 (1H, alkene CH, d, *J* = 16.3 Hz); ^{13}C NMR (75 MHz, $CDCl_3$): δ 141.4, 135.2, 132.6, 132.0, 131.1, 128.4, 127.4, 127.0, 122.6, 119.0, 110.9; FTIR ν (cm^{-1}): 2975, 2219, 1599, 961, 825; HRMS (ES) *m/z* calculated for $C_{15}H_{10}N_1Br_1Na_1$: $[M+Na]^+$ 305.9894, found 305.9877; Mp: 190-192 °C (lit. 192-194 °C)[261]

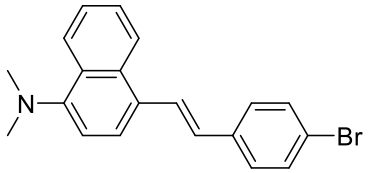

(*E*)-4-(4-bromostyryl)-*N*,*N*-dimethylnaphthalen-1-amine - 83

The title compound was prepared according to General Procedure 1 using 4-bromobenzyl bromide (0.84 g, 3.36 mmol), triethyl phosphite (0.70 mL, 4.03 mmol), sodium hydride (0.20 g, 5.04 mmol) and 4-dimethylamino-1-naphthaldehyde (0.67 g, 3.36 mmol). The precipitated product was collected by filtration, washed with water and dried under vacuum to give a yellow solid in 93% yield. ^{1}H NMR (250 MHz, $CDCl_3$): δ 8.35-8.24 (1H, ArH, m), 8.22-8.12 (1H, ArH, m), 7.83 (1H, alkene CH, d, *J* = 16.0 Hz), 7.67 (1H, ArH, d, *J* = 7.9 Hz), 7.59-7.38 (6H, ArH, m), 7.09 (1H, ArH, d, *J* = 7.9 Hz), 7.00 (1H, alkene CH, d, *J* = 16.0 Hz), 2.93 (6H, CH_3, s); ^{13}C NMR (75 MHz, $CDCl_3$): δ 151.2, 136.9, 132.5, 131.8, 129.3, 128.7, 128.7, 128.0, 126.7, 126.1, 125.2, 124.8, 124.1, 123.9, 121.1, 113.9, 45.2; FTIR ν (cm^{-1}): 2925, 2785, 961, 825; HRMS (ES) *m/z* calculated for $C_{20}H_{19}N_1Br_1$: $[M+H]^+$ 352.0701, found 352.0675; Mp: 92-97 °C

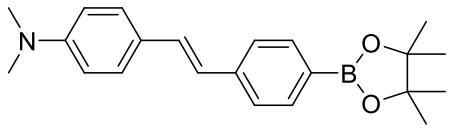

(*E*)-*N*,*N*-dimethyl-4-(4-(4,4,5,5-tetramethyl-1,3,2-dioxaborolan-2-yl)styryl)aniline - 68

The title compound was prepared according to General Procedure 2 using (*E*)-4-(4-bromostyryl)-*N*,*N*-dimethylaniline **72** (0.50 g, 1.66 mmol), bis(pinacolato)diboron (0.45 g, 1.78 mmol), potassium acetate (0.47 g, 4.83 mmol) and $PdCl_2$(dppf).CH_2Cl_2 (50 mg, 0.06 mmol). The crude reaction product was recrystallized in DCM/hexane. The purified product was collected as a yellow fibrous solid in 52% yield. ^{1}H NMR (300 MHz, $CDCl_3$): δ 7.77 (2H, ArH, d, *J* = 8.2 Hz), 7.50 – 7.37 (4H, ArH, m), 7.12 (1H, alkene CH, d, *J* = 16.3 Hz), 6.91 (1H, alkene CH, d, *J* = 16.3 Hz), 6.71 (2H, ArH, d, *J* = 8.9 Hz), 2.99 (6H, CH_3, s), 1.35 (12H, pin CH_3, s); ^{13}C NMR (75 MHz $CDCl_3$): δ 150.2, 141.0, 135.1, 129.8, 127.8, 125.5, 125.3, 124.2, 112.4, 83.7, 40.5, 24.9; ^{11}B NMR (96 MHz, $CDCl_3$): δ 33; FTIR ν (cm^{-1}): 2796, 1596, 1354, 966; HRMS (ES)

m/z calculated for $C_{22}H_{28}N_1O_2B_1Na_1$: $[M+Na]^+$ 372.2111, found 372.2127; Mp: 184-187 °C (lit. 181-183 °C)[248]

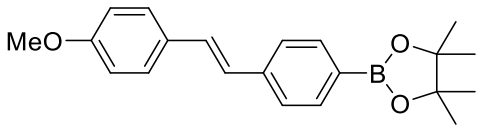

(*E*)-2-(4-(4-methoxystyryl)phenyl)-4,4,5,5-tetramethyl-1,3,2-dioxaborolane - 69

The title compound was prepared according to General Procedure 2 using (*E*)-1-bromo-4-(4-methoxystyryl)benzene **73** (0.48 g, 1.66 mmol), bis(pinacolato)diboron (0.45 g, 1.78 mmol), potassium acetate (0.47 g, 4.83 mmol) and $PdCl_2(dppf).CH_2Cl_2$ (50 mg, 0.06 mmol). The crude reaction product was recrystallized in DCM/hexane. The purified product was collected as a pale brown solid in 36% yield. ^{1}H NMR (300 MHz, $CDCl_3$): δ 7.79 (2H, ArH, d, *J* = 8.1 Hz), 7.54-7.43 (4H, ArH, m), 7.14 (1H, alkene CH, d, *J* = 16.3 Hz), 6.98 (1H, alkene CH, d, *J* = 16.3 Hz), 6.90, (2H, ArH, d, *J* = 8.8 Hz), 3.83 (3H, OCH_3, s), 1.35 (12H, pin CH_3, s); ^{13}C NMR (75 MHz, $CDCl_3$): δ 159.5, 140.4, 135.2, 130.0, 129.2, 127.9, 126.5, 125.6, 114.2, 83.8, 55.3, 24.9; ^{11}B NMR (96 MHz, $CDCl_3$): δ 33; FTIR ν (cm^{-1}): 2974, 1599, 1357, 963, 830; HRMS (ES) *m/z* calculated for $C_{21}H_{25}O_3B_1Na_1$: $[M+Na]^+$ 359.1794, found 359.1775; Mp: 171-173 °C (lit. 165-169 °C)[248]

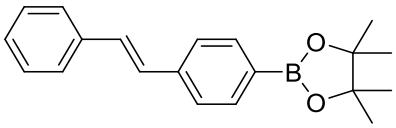

(*E*)-4,4,5,5-tetramethyl-2-(4-styrylphenyl)-1,3,2-dioxaborolane - 70

The title compound was prepared according to General Procedure 2 using (*E*)-1-bromo-4-styrylbenzene **74** (0.43 g, 1.66 mmol), bis(pinacolato)diboron (0.45 g, 1.78 mmol), potassium acetate (0.47 g, 4.83 mmol) and $PdCl_2(dppf).CH_2Cl_2$ (50 mg, 0.06 mmol). The crude reaction product was recrystallized in hot MeOH. The purified product was collected as a pale brown solid in 47% yield. ^{1}H NMR (250 MHz, $CDCl_3$): δ 7.84 (2H, ArH, d, *J* = 7.7 Hz), 7.56 (4H, ArH, d, *J* = 7.7 Hz), 7.40 (2H, ArH, m), 7.35-7.29 (1H, ArH, m), 7.23 (1H, alkene CH, d, *J* = 16.3 Hz), 7.14 (1H, alkene CH, d, *J* = 16.3 Hz),

1.39 (12H, pin CH_3, s); ^{13}C NMR (75 MHz, $CDCl_3$): δ 140.0, 137.2, 135.2, 129.7, 128.7, 128.6, 127.8, 126.6, 125.8, 83.8, 24.9; ^{11}B NMR (96 MHz, $CDCl_3$): δ 33; FTIR ν (cm^{-1}): 2979, 1604, 1357, 1140, 963; Mp: 125-127 °C (lit. 123-125 °C)[262]

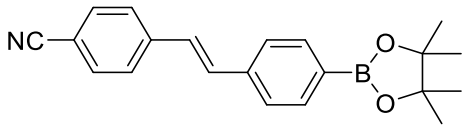

(*E*)-4-(4-(4,4,5,5-tetramethyl-1,3,2-dioxaborolan-2-yl)styryl)benzonitrile - 71

The title compound was prepared according to General Procedure 2 using (*E*)-4-(4-bromostyryl)benzonitrile **75** (0.47 g, 1.66 mmol), bis(pinacolato)diboron (0.45 g, 1.78 mmol), potassium acetate (0.47 g, 4.83 mmol) and $PdCl_2$(dppf).CH_2Cl_2 (50 mg, 0.06 mmol). The crude reaction product was recrystallized in DCM/hexane. The purified product was collected as a pale brown solid in 60% yield. ^{1}H NMR (300 MHz, $CDCl_3$): δ 7.82 (2H, ArH, d, *J* = 8.1 Hz), 7.61 (4H, ArH, q, *J* = 8.6 Hz), 7.53 (2H, ArH, d, *J* = 8.1 Hz), 7.23 (1H, alkene CH, d, *J* = 16.3 Hz), 7.14 (1H, alkene CH, d, *J* = 16.3 Hz), 1.36 (12H, pin CH_3, s); ^{13}C NMR (75 MHz, $CDCl_3$): δ 141.7, 138.9, 135.3, 132.5, 132.3, 127.6, 127.0, 126.2, 119.0, 110.8, 83.9, 24.9; ^{11}B NMR (96 MHz, $CDCl_3$): δ 35; FTIR ν (cm^{-1}): 2977, 2221, 1354, 959, 653; HRMS (ES) *m/z* calculated for $C_{21}H_{22}N_1B_1O_2Na_1$: $[M+Na]^+$ 354.1641, found 354.1617; Mp: 192-194 °C

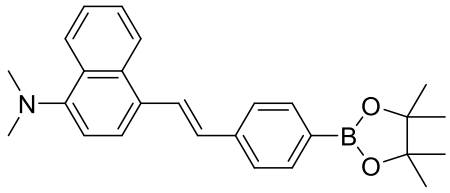

(*E*)-*N*,*N*-dimethyl-4-(4-(4,4,5,5-tetramethyl-1,3,2-dioxaborolan-2-yl)styryl)naphthalen-1-amine - 76

The title compound was prepared according to General Procedure 2 using (*E*)-4-(4-bromostyryl)-*N*,*N*-dimethylnaphthalen-1-amine **83** (0.58 g, 1.66 mmol), bis(pinacolato)diboron (0.45 g, 1.78 mmol), potassium acetate (0.47 g, 4.83 mmol) and $PdCl_2$(dppf).CH_2Cl_2 (50 mg, 0.06 mmol). The reaction was heated to 80 °C and stirred under N_2 for an extended reaction time of 18 hours. The crude reaction product was

recrystallized in hot MeOH. The purified product was collected as a dark green solid in 33% yield. ^{1}H NMR (300 MHz, $CDCl_3$): δ 8.31-8.25 (1H, ArH, m), 8.24-8.18 (1H, ArH, m), 7.91 (1H, alkene CH, d, *J* = 16.0 Hz), 7.83 (2H, ArH, d, *J* = 8.0 Hz), 7.69 (1H, ArH, d, *J* = 7.9 Hz), 7.59 (2H, ArH, d, *J* = 8.0 Hz), 7.56-7.48 (2H, ArH, m), 7.11 (1H, ArH, d, *J* = 7.9 Hz), 7.07 (1H, alkene CH, d, *J* = 16.0 Hz), 2.92 (6H, CH_3, s), 1.37 (12H, pin CH_3, s); ^{13}C NMR (75 MHz, $CDCl_3$): δ 151.1, 140.6, 135.2, 132.6, 130.1, 129.5, 128.7, 126.9, 126.0, 125.8, 125.1, 124.8, 124.2, 123.9, 113.9, 83.8, 45.2, 24.9; ^{11}B NMR (96 MHz, $CDCl_3$): δ 36; FTIR ν (cm^{-1}): 2979, 2829, 1604, 1357, 1140, 760; HRMS (ES) *m/z* calculated for $C_{26}H_{31}N_1B_1O_2$: $[M+H]^+$ 400.2448, found 400.2427; Mp: 159-164 °C

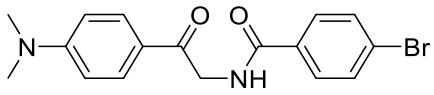

4-bromo-*N*-(2-(4-(dimethylamino)phenyl)-2-oxoethyl)benzamide - 79

2-amino-4-dimethylaminoacetophenone hydrochloride (100 mg, 0.47 mmol) and 4-bromobenzoyl chloride (204 mg, 0.94 mmol) were suspended in anhydrous DCM (40 mL) and the resulting mixture was cooled down to 0 °C. Anhydrous pyridine (188 µL) was added drop-wise to the reaction mixture with stirring. The resulting mixture was allowed to warm to room temperature and left to stir overnight. The reaction mixture was diluted with chloroform, and the resulting solution was washed twice with water. The organic layer was dried over $MgSO_4$, filtered, and the solvent was removed under reduced pressure to give a peachy-brown coloured powder in 113% yield (crude). ^{1}H NMR (300 MHz, $CDCl_3$): δ 7.93 (2H, ArH, d, *J* = 9.2 Hz), 7.77 (2H, ArH, d, *J* = 8.7 Hz), 7.61 (2H, ArH, d, *J* = 8.7 Hz),7.43 (1H, NH, s (br)), 6.70 (2H, ArH, d, *J* = 9.2 Hz), 4.84 (2H, CH_2, s), 3.11 (6H, CH_3, s); ^{13}C NMR (75 MHz, $CDCl_3$): δ 191.3, 161.5, 132.4, 132.0, 131.9, 131.9, 130.3, 128.8, 127.5, 110.8, 46.0, 40.0; FTIR ν (cm^{-1}): 3402, 3093, 1676, 1642; HRMS (ES) *m/z* calculated for $C_{17}H_{18}N_2O_2Br_1$: $[M+H]^+$ 361.0552, found 361.0538

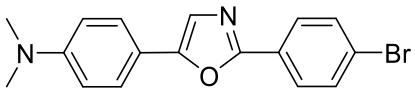

4-(2-(4-bromophenyl)oxazol-5-yl)-*N*,*N*-dimethylaniline - 80

4-bromo-*N*-(2-(4-(dimethylamino)phenyl)-2-oxoethyl)benzamide **79** (200 mg, 0.55 mmol) was suspended in concentrated H_2SO_4 (1 mL) and stirred for 24 hours at room temperature. The resulting solution was poured onto ice, stirred until the ice had melted and left to stand in an ice bath for a further 2 hours to allow for more product to crash out. The precipitated product was collected by filtration, washed with water and dried under vacuum. The crude product was dissolved in DCM and washed twice with 1 M NaOH to remove any unreacted 4-bromobenzoyl chloride leftover from the previous reaction. The organic layer was dried over $MgSO_4$, filtered, and the solvent was removed under reduced pressure to give a pale yellow powdery solid in 34% yield. ^{1}H NMR (300 MHz, DMSO-d_6): δ 7.97 (2H, ArH, d, J = 8.4 Hz), 7.74 (2H, ArH, d, J = 8.4 Hz), 7.64 (2H, ArH, d, J = 8.9 Hz), 7.57 (1H, oxazole H, s), 6.80 (2H, ArH, d, J = 8.9 Hz), 2.96 (6H, CH_3, s); ^{13}C NMR (75 MHz, DMSO-d_6): δ 158.3, 152.5, 150.8, 132.5, 127.8, 126.6, 125.7, 123.8, 121.4, 115.2, 112.5, 40.2; FTIR ν (cm^{-1}): 2920, 2852, 1228, 1068; HRMS (ES) *m/z* calculated for $C_{17}H_{16}N_2O_1Br_1$: $[M+H]^+$ 343.0446, found 343.0430

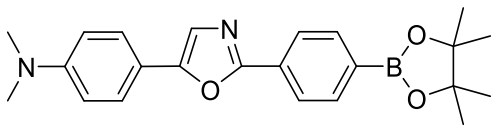

***N*,*N*-dimethyl-4-(2-(4-(4,4,5,5-tetramethyl-1,3,2-dioxaborolan-2-yl)phenyl)oxazol-5-yl)aniline - 77**

4-(2-(4-bromophenyl)oxazol-5-yl)-*N*,*N*-dimethylaniline **80** (47 mg, 0.14 mmol), bis(pinacolato)diboron (38 mg, 0.15 mmol) and potassium acetate (40 mg, 0.41 mmol) were partially dissolved in 3:1 DMSO/dioxane (2 mL). $PdCl_2$(dppf).CH_2Cl_2 (4.6 mg, 0.006 mmol) was partially dissolved in 3:1 DMSO/dioxane (0.75 mL) and was added drop-wise to the reaction mixture. The reaction was heated to 80 °C and stirred under N_2 for 16 hours. The reaction mixture was cooled to room temperature and quenched with saturated NH_4Cl. The crude product was extracted 3 times into ethyl acetate. The

combined organic layers were dried over $MgSO_4$, filtered, and the solvent was removed under reduced pressure to give a yellowy green solid. The crude reaction product was recrystallized in DCM/hexane. The product was collected as a bright yellow solid in 44% yield. ^{1}H NMR (300 MHz, DMSO-d_6): δ 8.05 (2H, ArH, d, J = 8.3 Hz), 7.82 (2H, ArH, d, J = 8.3 Hz), 7.65 (2H, ArH, d, J = 8.9 Hz), 7.59 (1H, oxazole H, s), 6.81 (2H, ArH, d, J = 8.9 Hz), 2.97 (6H, CH_3, s), 1.32 (12H, CH_3, s); ^{13}C NMR (75 MHz, DMSO-d_6): δ 158.9, 152.5, 150.8, 135.4, 129.8, 125.7, 125.2, 121.5, 115.2, 112.5, 84.3, 40.2, 25.1; ^{11}B NMR (96 MHz, DMSO-d_6): δ 33; FTIR ν (cm^{-1}): 2976, 1610, 1356, 1325; HRMS (ES) *m/z* calculated for $C_{23}H_{28}N_2O_3B_1$: $[M+H]^+$ 391.2193, found 391.2185

5.6.3 Preparation of H_2O_2 Solutions

Hydrogen peroxide solution (30% w/w in H_2O) was diluted 50 or 100 times to give concentrations of approximately 200 mM or 100 mM. The exact concentrations were determined by UV-Vis analysis using the Beer-Lambert law. The concentration of H_2O_2 was determined from the absorption at 240 nm ($\varepsilon = 43.6\ M^{-1}\ cm^{-1}$).

5.6.4 General UV-Vis Analysis Procedure

A detection solution of each probe was made up by diluting a stock solution of the probe down to a concentration of 10 µM for UV-Vis analysis. All detection solutions were made up in pH 8.21 phosphate buffer (52.1 wt. % MeOH). Blank scans were run with the phosphate buffer before any measurements were carried out. The wavelength of maximum absorbance (λ_{max}) of the probe was then determined. A 13.1 mM solution of H_2O_2 was made up in each of the probe solutions, by addition of the corresponding amount of the ~200 mM H_2O_2 solution. The probes were left to react with the H_2O_2 for 15 minutes, then the wavelength of maximum absorbance of each probe in the presence of H_2O_2 was determined.

5.6.5 General Fluorescence Analysis Procedure

A detection solution of each probe was made up by diluting a stock solution of the probe down to a concentration of either 1 µM or 5 µM for fluorescence analysis. All detection solutions were made up in pH 8.21 phosphate buffer (52.1 wt. % MeOH). Blank scans were run with the phosphate buffer before any measurements were carried out. The wavelength of maximum fluorescence emission, λ_{max}, of the probe was then determined.

A 2 mM solution of H_2O_2 was made up in each of the probe solutions, by addition of the corresponding amount of the ~100 mM H_2O_2 solution. The probes were left to react with the H_2O_2 for 30 minutes, then the wavelength of maximum fluorescence emission of each probe in the presence of H_2O_2 was determined.

5.6.5.1 Fluorescence Parameters for Analysis of Dimethylamino Stilbene Boronic Acid Pinacol Ester Probe 68

The general fluorescence analysis procedure was followed using a 5 µM concentration of probe **68**. An excitation wavelength of 350 nm was used, slit widths were 10 nm for excitation and 3 nm for emission.

5.6.5.2 Fluorescence Parameters for Analysis of Methoxy Stilbene Boronic Acid Pinacol Ester Probe 69

The general fluorescence analysis procedure was followed using a 5 µM concentration of probe **69**. An excitation wavelength of 330 nm was used, slit widths were 10 nm for excitation and 3 nm for emission.

5.6.5.3 Fluorescence Parameters for Analysis of Unsubstituted Stilbene Boronic Acid Pinacol Ester Probe 70

The general fluorescence analysis procedure was followed using a 5 µM concentration of probe **70**. An excitation wavelength of 315 nm was used, slit widths were 10 nm for excitation and 3 nm for emission.

5.6.5.4 Fluorescence Parameters for Analysis of Cyano Stilbene Boronic Acid Pinacol Ester Probe 71

The general fluorescence analysis procedure was followed using a 5 µM concentration of probe **71**. An excitation wavelength of 330 nm was used, slit widths were 10 nm for excitation and 3 nm for emission.

5.6.5.5 Fluorescence Parameters for Analysis of Dimethylamino Naphthalene Boronic Acid Pinacol Ester Probe 76

The general fluorescence analysis procedure was followed using a 5 µM concentration of probe **76**. An excitation wavelength of 350 nm was used, slit widths were 10 nm for excitation and 3 nm for emission.

5.6.5.6 Fluorescence Parameters for Analysis of Dimethylamino Oxazole Boronic Acid Pinacol Ester Probe 77

The general fluorescence analysis procedure was followed using a 1 μM concentration of probe **77** after initial scans showed the probe was too fluorescent at a concentration of 5 μM. An excitation wavelength of 350 nm was used, slit widths were 10 nm for excitation and 3 nm for emission.

6 References

(1) Gellman, S. H. *Chem. Rev.* **1997**, *97*, 1231.
(2) Sun, X. L.; James, T. D. *Chem. Rev.* **2015**, *115*, 8001.
(3) Galbraith, E.; James, T. D. *Chem. Soc. Rev.* **2010**, *39*, 3831.
(4) Hulanicki, A.; Glab, S.; Ingman, F. *Pure Appl. Chem.* **1991**, *63*, 1247.
(5) James, T. D. In *Creative Chemical Sensor Systems*; Schrader, T., Ed. 2007; Vol. 277, p 107.
(6) McLachlan, B. G.; Bell, J. H. *Experimental Thermal and Fluid Science* **1995**, *10*, 470.
(7) Banica, G. G. *Chemical Sensors and Biosensors: Fundamentals and Applications*; John Wiley & Sons Ltd: Chichester, 2012.
(8) Lieberzeit, P. A.; Dickert, F. L. *Anal. Bioanal. Chem.* **2007**, *387*, 237.
(9) Badihi-Mossberg, M.; Buchner, V.; Rishpon, J. *Electroanalysis* **2007**, *19*, 2015.
(10) D'Orazio, P. *Clin. Chim. Acta* **2011**, *412*, 1749.
(11) Wang, J. *Electroanalysis* **2001**, *13*, 983.
(12) Nayak, M.; Kotian, A.; Marathe, S.; Chakravortty, D. *Biosens. Bioelectron.* **2009**, *25*, 661.
(13) Mascini, M.; Tombelli, S. *Biomarkers* **2008**, *13*, 637.
(14) Leonard, P.; Hearty, S.; Brennan, J.; Dunne, L.; Quinn, J.; Chakraborty, T.; O'Kennedy, R. *Enzyme Microb. Tech.* **2003**, *32*, 3.
(15) Kim, H.-J.; Sudduth, K. A.; Hummel, J. W. *J. Environ. Monitor.* **2009**, *11*, 1810.
(16) Mulchandani, A.; Bassi, A. S. *Crit. Rev. Biotechnol.* **1995**, *15*, 105.
(17) Smith, R. G.; D'Souza, N.; Nicklin, S. *Analyst* **2008**, *133*, 571.
(18) Gooding, J. J. *Anal. Chim. Acta* **2006**, *559*, 137.
(19) *Boron: Sensing, Synthesis and Supramolecular Self-Assembly*; Li, M.; Fossey, J. S.; James, T. D., Eds.; The Royal Society of Chemistry: Cambridge, 2016.
(20) Greenwood, N. N.; Earnshaw, A. *Chemistry of the Elements*; Second Edition ed.; Burlington: Elsevier Science, 1997.
(21) Hall, D. G. *Boronic Acids: Preparation, Applications in Organic Synthesis and Medicine*; Wiley-VCH: Weinheim, 2005.
(22) Lorand, J. P.; Edwards, J. O. *J. Org. Chem.* **1959**, *24*, 769.
(23) Brooks, W. L. A.; Sumerlin, B. S. *Chem. Rev.* **2016**, *116*, 1375.
(24) Lacina, K.; Skladal, P.; James, T. D. *Chem. Cent. J.* **2014**, *8*.
(25) Guan, Y.; Zhang, Y. *Chem. Soc. Rev.* **2013**, *42*, 8106.
(26) Frankland, E.; Duppa, B. F. *Liebigs Ann. Chem.* **1860**, *115*, 319.
(27) James, T. D.; Phillips, M. D.; Shinkai, S. *Boronic Acids in Saccharide Recognition*; The Royal Society of Chemistry: Cambridge, 2006.
(28) Nishiyabu, R.; Kubo, Y.; James, T. D.; Fossey, J. S. *Chem. Comm.* **2011**, *47*, 1106.
(29) Fujita, N.; Shinkai, S.; James, T. D. *Chem-Asian J.* **2008**, *3*, 1076.
(30) Frankland, E. *Liebigs Ann. Chem.* **1862**, *124*, 129.
(31) Bosch, L. I.; Fyles, T. M.; James, T. D. *Tetrahedron* **2004**, *60*, 11175.
(32) Wulff, G. *Pure Appl. Chem.* **1982**, *54*, 2093.
(33) Wiskur, S. L.; Lavigne, J. J.; Ait-Haddou, H.; Lynch, V.; Chiu, Y. H.; Canary, J. W.; Anslyn, E. V. *Org. Lett.* **2001**, *3*, 1311.

(34) Zhu, L.; Shabbir, S. H.; Gray, M.; Lynch, V. M.; Sorey, S.; Anslyn, E. V. *J. Am. Chem. Soc.* **2006**, *128*, 1222.
(35) Shriver, D. F.; Biallas, M. J. *J. Am. Chem. Soc.* **1967**, *89*, 1078.
(36) Zhou, Y.; Zhang, J. F.; Yoon, J. *Chem. Rev.* **2014**, *114*, 5511.
(37) Wade, C. R.; Broomsgrove, A. E. J.; Aldridge, S.; Gabbai, F. P. *Chem. Rev.* **2010**, *110*, 3958.
(38) Torssell, K. *Ark. Kemi* **1957**, *10*, 507.
(39) Haynes, R. R.; Snyder, H. R. *J. Org. Chem.* **1964**, *29*, 3229.
(40) Berube, M.; Dowlut, M.; Hall, D. G. *J. Org. Chem.* **2008**, *73*, 6471.
(41) Dowlut, M.; Hall, D. G. *J. Am. Chem. Soc.* **2006**, *128*, 4226.
(42) Markham, A. *Drugs* **2014**, *74*, 1555.
(43) Adamczyk-Wozniak, A.; Borys, K. M.; Sporzynski, A. *Chem. Rev.* **2015**, *115*, 5224.
(44) Liu, C. T.; Tomsho, J. W.; Benkovic, S. J. *Bioorgan. Med. Chem.* **2014**, *22*, 4462.
(45) Baker, S. J.; Tomsho, J. W.; Benkovic, S. J. *Chem. Soc. Rev.* **2011**, *40*, 4279.
(46) Li, X.; Plattner, J. J.; Hernandez, V.; Ding, C. Z.; Wu, W.; Yang, Y.; Xu, M. *Tetrahedron Lett.* **2011**, *52*, 4924.
(47) Xia, Y.; Cao, K.; Zhou, Y. S. E.; Alley, M. R. K.; Rock, F.; Mohan, M.; Meewan, M.; Baker, S. J.; Lux, S.; Ding, C. Z.; Jia, G. F.; Kully, M.; Plattner, J. J. *Bioorgan. Med. Chem. Lett.* **2011**, *21*, 2533.
(48) Tomsho, J. W.; Pal, A.; Hall, D. G.; Benkovic, S. J. *ACS Med. Chem. Lett.* **2012**, *3*, 48.
(49) Cummings, W. M.; Cox, C. H.; Snyder, H. R. *J. Org. Chem.* **1969**, *34*, 1669.
(50) Adamczyk-Wozniak, A.; Cyranski, M. K.; Zubrowska, A.; Sporzynski, A. *J. Organomet. Chem.* **2009**, *694*, 3533.
(51) Ding, C. Z.; Zhang, Y.-K.; Li, X.; Liu, Y.; Zhang, S.; Zhou, Y.; Plattner, J. J.; Baker, S. J.; Liu, L.; Duan, M.; Jarvest, R. L.; Ji, J.; Kazmierski, W. M.; Tallant, M. D.; Wright, L. L.; Smith, G. K.; Crosby, R. M.; Wang, A. A.; Ni, Z.-J.; Zou, W.; Wright, J. *Bioorgan. Med. Chem. Lett.* **2010**, *20*, 7317.
(52) Akama, T.; Baker, S. J.; Zhang, Y. K.; Hernandez, V.; Zhou, H. C.; Sanders, V.; Freund, Y.; Kimura, R.; Maples, K. R.; Plattner, J. J. *Bioorgan. Med. Chem. Lett.* **2009**, *19*, 2129.
(53) Snyder, H. R.; Reedy, A. J.; Lennarz, W. J. *J. Am. Chem. Soc.* **1958**, *80*, 835.
(54) Lulinski, S.; Madura, I.; Serwatowski, J.; Szatylowicz, H.; Zachara, J. *New J. Chem.* **2007**, *31*, 144.
(55) Lennarz, W. J.; Snyder, H. R. *J. Am. Chem. Soc.* **1960**, *82*, 2172.
(56) Zhdankin, V. V.; Persichini, P. J.; Zhang, L.; Fix, S.; Kiprof, P. *Tetrahedron Lett.* **1999**, *40*, 6705.
(57) Grassberger, M. A. *Liebigs Ann. Chem.* **1985**, 683.
(58) Yamamoto, Y.; Ishii, J.; Nishiyama, H.; Itoh, K. *J. Am. Chem. Soc.* **2005**, *127*, 9625.
(59) Gunasekera, D. S.; Gerold, D. J.; Aalderks, N. S.; Chandra, J. S.; Maanu, C. A.; Kiprof, P.; Zhdankin, V. V.; Reddy, M. V. R. *Tetrahedron* **2007**, *63*, 9401.
(60) Cyranski, M. K.; Jezierska, A.; Klimentowska, P.; Panek, J. J.; Sporzynski, A. *J.Phys. Org. Chem.* **2008**, *21*, 472.
(61) Lulinski, S.; Serwatowski, J. *J. Organomet. Chem.* **2007**, *692*, 2924.
(62) Dabrowski, M.; Kurach, P.; Lulinski, S.; Serwatowski, J. *Appl. Organomet. Chem.* **2007**, *21*, 234.
(63) Wu, P. H.; Meng, Q. Q.; Zhou, H. C. *Chinese Chem. Lett.* **2011**, *22*, 1411.

(64) Zhu, J.; Wei, Y.; Lin, D.; Ou, C.; Xie, L.; Zhao, Y.; Huang, W. *Org. Biomol. Chem.* **2015**, *13*, 11362.
(65) Ma, W. M. J.; Morais, M. P. P.; D'Hooge, F.; van den Elsen, J. M. H.; Cox, J. P. L.; James, T. D.; Fossey, J. S. *Chem. Comm.* **2009**, 532.
(66) Hawkins, R. T.; Lennarz, W. J.; Snyder, H. R. *J. Am. Chem. Soc.* **1960**, *82*, 3053.
(67) Tschampel, P.; Snyder, H. R. *J. Org. Chem.* **1964**, *29*, 2168.
(68) Sporzynski, A.; Lewandowski, M.; Rogowska, P.; Cyranski, M. K. *Appl. Organomet. Chem.* **2005**, *19*, 1202.
(69) Kumar, J. S.; Alam, M. A.; Gurrapu, S.; Nelson, G.; Williams, M.; Corsello, M. A.; Johnson, J. L.; Jonnalagadda, S. C.; Mereddy, V. R. *J. Heterocyclic Chem.* **2013**, *50*, 814.
(70) Tan, Y. L.; White, A. J. P.; Widdowson, D. A.; Wilhelm, R.; Williams, D. J. *J. Chem. Soc. Perk. T. 1* **2001**, 3269.
(71) Nicolaou, K. C.; Ramanjulu, J. M.; Natarajan, S.; Brase, S.; Li, H.; Boddy, C. N. C.; Rubsam, F. *Chem. Comm.* **1997**, 1899.
(72) Ishiyama, T.; Murata, M.; Miyaura, N. *J. Org. Chem.* **1995**, *60*, 7508.
(73) VanVeller, B.; Aronoff, M. R.; Raines, R. T. *RSC Adv.* **2013**, *3*, 21331.
(74) Li, X. F.; Zhang, S. M.; Zhang, Y. K.; Liu, Y.; Ding, C. Z.; Zhou, Y.; Plattner, J. J.; Baker, S. J.; Bu, W.; Liu, L. A.; Kazmierski, W. M.; Duan, M. S.; Grimes, R. M.; Wright, L. L.; Smith, G. K.; Jarvest, R. L.; Ji, J. J.; Cooper, J. P.; Tallant, M. D.; Crosby, R. M.; Creech, K.; Ni, Z. J.; Zou, W. X.; Wright, J. *Bioorgan. Med. Chem. Lett.* **2011**, *21*, 2048.
(75) Qiao, Z. T.; Wang, Q.; Zhang, F. L.; Wang, Z. L.; Bowling, T.; Nare, B.; Jacobs, R. T.; Zhang, J.; Ding, D. Z.; Liu, Y. G.; Zhou, H. C. *J. Med. Chem.* **2012**, *55*, 3553.
(76) Zhang, J.; Zhu, M. Y.; Lin, Y. N.; Zhou, H. C. *Sci. China Chem.* **2013**, *56*, 1372.
(77) Baker, S. J.; Zhang, Y. K.; Akama, T.; Lau, A.; Zhou, H.; Hernandez, V.; Mao, W. M.; Alley, M. R. K.; Sanders, V.; Plattner, J. J. *J. Med. Chem.* **2006**, *49*, 4447.
(78) Pal, A.; Berube, M.; Hall, D. G. *Angew. Chem. Int. Edit.* **2010**, *49*, 1492.
(79) Li, H. Y.; Wang, H. Y.; Liu, Y. C.; Liu, Z. *Chem. Comm.* **2012**, *48*, 4115.
(80) Li, H. Y.; Liu, Z. *Trac-Trend. Anal. Chem.* **2012**, *37*, 148.
(81) Zhang, Y. T.; Ma, W. F.; Li, D.; Yu, M.; Guo, J.; Wang, C. C. *Small* **2014**, *10*, 1379.
(82) Kim, H.; Kang, Y. J.; Kang, S.; Kim, K. T. *J. Am. Chem. Soc.* **2012**, *134*, 4030.
(83) Patterson, D.; Davey, C.; Rohani, R. In *Chemical Processes for a Sustainable Future*; Letcher, T., Scott, J., Patterson, D. A., Eds.; Royal Society of Chemistry: Cambridge, 2014, p 467.
(84) Rohani, R.; Hyland, M.; Patterson, D. *J. Membrane Sci.* **2011**, *382*, 278.
(85) Allcock, H. R. *Introduction to Materials Chemistry*; John Wiley & Sons: Hoboken, 2011.
(86) Kaiser, A.; Stark, W. J.; Grass, R. N. *J. Chem. Educ.* **2017**, *94*, 483.
87) Greenlee, L. F.; Lawler, D. F.; Freeman, B. D.; Marrot, B.; Moulin, P. *Water Res.* **2009**, *43*, 2317.
(88) Chollangi, A.; Hossain, M. M. *Chem. Eng. Process.* **2007**, *46*, 398.
(89) Cheryan, M.; Rajagopalan, N. *J. Membrane Sci.* **1998**, *151*, 13.

(90) Yoon, Y.; Westerhoff, P.; Snyder, S. A.; Wert, E. C.; Yoon, J. *Desalination* **2007**, *202*, 16.
(91) Ayoob, S.; Gupta, A. K. *Crit. Rev. Env. Sci. Tech.* **2006**, *36*, 433.
(92) Lantz, O.; Jouvin, M. H.; Devernejoul, M. C.; Druet, P. *Am. J. Kidney Dis.* **1987**, *10*, 136.
(93) Heard, K.; Hill, R. E.; Cairns, C. B.; Dart, R. C. *J. Toxicol.-Clin. Toxic.y* **2001**, *39*, 349.
(94) Marya, C. M. *A Textbook of Public Health Dentistry*; Jaypee Brothers Medical Publishers Ltd: New Delhi, 2011.
(95) *Guidelines for Drinking-water Quality*; 4th ed.; World Health Organization Geneva, 2011.
(96) Karpe, A. V.; Beale, D. J.; Harding, I. H.; Palombo, E. A. *J. Chem.Technol. Biot.* **2015**, *90*, 1793.
(97) Yu, J. M.; Ahmedna, M. *Int. J. Food Sci. Tech.* **2013**, *48*, 221.
(98) Corbin, K. R.; Hsieh, Y. S. Y.; Betts, N. S.; Byrt, C. S.; Henderson, M.; Stork, J.; DeBolt, S.; Fincher, G. B.; Burton, R. A. *Bioresource Technol.* **2015**, *193*, 76.
(99) Xia, E. Q.; Deng, G. F.; Guo, Y. J.; Li, H. B. *Int J. Mol. Sci.* **2010**, *11*, 622.
(100) Bagchi, D.; Bagchi, M.; Stohs, S. J.; Das, D. K.; Ray, S. D.; Kuszynski, C. A.; Joshi, S. S.; Pruess, H. G. *Toxicology* **2000**, *148*, 187.
(101) Sartor, L.; Pezzato, E.; Dell'Aica, I.; Caniato, R.; Biggin, S.; Garbisa, S. *Biochem. Pharmacol.* **2002**, *64*, 229.
(102) Bagchi, D. B.; Sen, C. K.; Ray, S. D.; Das, D. K.; Bagchi, M.; Preuss, H. G.; Vinson, J. A. *Mutat. Res.-Fund. Mol. M.* **2003**, *523*, 87.
(103) Valenzano, D. R.; Terzibasi, E.; Genade, T.; Cattaneo, A.; Domenici, L.; Cellerino, A. *Curr. Biol.* **2006**, *16*, 296.
(104) Daglia, M.; Papetti, A.; Grisoli, P.; Aceti, C.; Dacarro, C.; Gazzani, G. *J. Agr. Food Chem.* **2007**, *55*, 5038.
(105) Papadopoulou, C.; Soulti, K.; Roussis, I. G. *Food Technol. Biotech.* **2005**, *43*, 41.
(106) Tomsho, J. W.; Benkovic, S. J. *J. Org. Chem.* **2012**, *77*, 11200.
(107) Pearlman, W. M. *Tetrahedron Lett.* **1967**, 1663.
(108) Albers, P. W.; Moebus, K.; Wieland, S. D.; Parker, S. F. *Phys. Chem. Chem. Phys.* **2015**, *17*, 5274.
(109) Bowers, G. D.; Tenero, D.; Patel, P.; Phuong, H.; Sigafoos, J.; O'Mara, K.; Young, G. C.; Dumont, E.; Cunningham, E.; Kurtinecz, M.; Stump, P.; Conde, J. J.; Chism, J. P.; Reese, M. J.; Yueh, Y. L.; Tomayko, J. F. *Drug Metab. Dispos.* **2013**, *41*, 1070.
(110) Fu, Z.; He, J.; Tong, A.; Xie, Y.; Wei, Y. *Synthesis-Stuttgart* **2013**, *45*, 2843.
(111) Hoggett, J. G.; Moodie, R. B.; Penton, J. R.; Schofield, K. *Nitration and Aromatic Reactivity*; Cambridge University Press: London, 1971.
(112) Lin, M.; Chen, G.; Jiang, M. *Polym. Chem.* **2014**, *5*, 234.
(113) Suman, P.; Patel, B. P.; Kasibotla, A. V.; Solano, L. N.; Jonnalagadda, S. C. *J. Organomet. Chem.* **2015**, *798*, 125.
(114) Dobrovolna, Z.; Cerveny, L. *Res. Chem. Intermediat.* **2000**, *26*, 489.
(115) Paryzek, Z.; Koenig, H.; Tabaczka, B. *Synthesis-Stuttgart* **2003**, 2023.
(116) Schumacher, S.; Grueneberger, F.; Katterle, M.; Hettrich, C.; Hall, D. G.; Scheller, F. W.; Gajovic-Eichelmann, N. *Polymer* **2011**, *52*, 2485.
(117) D'Hooge, F.; Rogalle, D.; Thatcher, M. J.; Perera, S. P.; van den Elsen, J. M. H.; Jenkins, A. T. A.; James, T. D.; Fossey, J. S. *Polymer* **2008**, *49*, 3362.

(118) Kotsuchibashi, Y.; Agustin, R. V. C.; Lu, J.-Y.; Hall, D. G.; Narain, R. *ACS Macro Lett.* **2013**, *2*, 260.
(119) Jenkins, D. J. A.; Jenkins, A. L.; Wolever, T. M. S.; Thompson, L. H.; Rao, A. V. *Nutr. Rev.* **1986**, *44*, 44.
(120) Dwek, R. A.; Butters, T. D. *Chem. Rev.* **2002**, *102*, 283.
(121) Yamamoto, T.; Seino, Y.; Fukumoto, H.; Koh, G.; Yano, H.; Inagaki, N.; Yamada, Y.; Inoue, K.; Manabe, T.; Imura, H. *Biochem. Bioph. Res. Co.* **1990**, *170*, 223.
(122) Baxter, P.; Goldhill, J.; Hardcastle, J.; Hardcastle, P. T.; Taylor, C. J. *Gut* **1990**, *31*, 817.
(123) Elsas, L. J.; Rosenberg, L. E. *J. Clin. Invest.* **1969**, *48*, 1845.
(124) Wild, S.; Roglic, G.; Green, A.; Sicree, R.; King, H. *Diabetes Care* **2004**, *27*, 1047.
(125) Angyal, S. J. *Adv. Carbohyd. Chem. Bi.* **1991**, *49*, 19.
(126) Hartley, J. H.; Phillips, M. D.; James, T. D. *New J. Chem.* **2002**, *26*, 1228.
(127) Springsteen, G.; Wang, B. H. *Tetrahedron* **2002**, *58*, 5291.
(128) Friedman, S.; Pace, B.; Pizer, R. *J. Am. Chem. Soc.* **1974**, *96*, 5381.
(129) Edwards, J. O.; Sederstr.Rj *J. Phys. Chem.* **1961**, *65*, 862.
(130) Pizer, R.; Tihal, C. *Inorganic Chemistry* **1992**, *31*, 3243.
(131) Angyal, S. J. *Adv. Carbohyd. Chem. Bi.* **1984**, *42*, 15.
(132) Luppi, P.; Cifarelli, V.; Wahren, J. *Pediatric Diabetes* **2011**, *12*, 276.
(133) Skyler, J. S. *J. Med. Chem.* **2004**, *47*, 4113.
(134) Wang, G. F.; He, X. P.; Wang, L. L.; Gu, A. X.; Huang, Y.; Fang, B.; Geng, B. Y.; Zhang, X. J. *Microchim. Acta* **2013**, *180*, 161.
(135) Kitabchi, A. E.; Umpierrez, G. E.; Miles, J. M.; Fisher, J. N. *Diabetes Care* **2009**, *32*, 1335.
(136) Brown, T. M.; Tanner, R. M.; Carson, A. P.; Yun, H. F.; Rosenson, R. S.; Farkouh, M. E.; Woolley, J. M.; Thacker, E. L.; Glasser, S. P.; Safford, M. M.; Muntner, P. *Diabetes Care* **2013**, *36*, 2734.
(137) Harris, D. C. *Quantitative Chemical Analysis*; 7th ed.; W. H. Freeman and Company: New York, 2007.
(138) Steiner, M. S.; Duerkop, A.; Wolfbeis, O. S. *Chem. Soc. Rev.* **2011**, *40*, 4805.
(139) Davis, A. P.; Wareham, R. S. *Angew. Chem. Int. Ed.* **1999**, *38*, 2978.
(140) Aoyama, Y.; Tanaka, Y.; Toi, H.; Ogoshi, H. *J. Am. Chem. Soc.* **1988**, *110*, 634.
(141) Evan-Salem, T.; Baruch, I.; Avram, L.; Cohen, Y.; Palmer, L. C.; Rebek, J. *P. Natl. Acad. Sci. USA* **2006**, *103*, 12296.
(142) Davis, A. P.; Wareham, R. S. *Angew. Chem. Int. Ed.* **1998**, *37*, 2270.
(143) Klein, E.; Crump, M. P.; Davis, A. P. *Angew. Chem. Int. Ed.* **2005**, *44*, 298.
(144) Anderson, S.; Neidlein, U.; Gramlich, V.; Diederich, F. *Angew. Chem. Int. Ed.* **1995**, *34*, 1596.
(145) Neidlein, U.; Diederich, F. *Chem. Comm.* **1996**, 1493.
(146) Droz, A. S.; Neidlein, U.; Anderson, S.; Seiler, P.; Diederich, F. *Helv. Chim. Acta* **2001**, *84*, 2243.
(147) Yoon, J.; Czarnik, A. W. *J. Am. Chem. Soc.* **1992**, *114*, 5874.
(148) James, T. D.; Sandanayake, K.; Shinkai, S. *J. Chem. Soc. Chem. Comm.* **1994**, 477.
(149) James, T. D.; Sandanayake, K.; Shinkai, S. *Angew. Chem. Int. Ed.* **1994**, *33*, 2207.

(150) Arimori, S.; Bell, M. L.; Oh, C. S.; Frimat, K. A.; James, T. D. *J. Chem. Soc. Perk. T. 1* **2002**, 803.
(151) Mizusawa, E.; Dahlman, H. L.; Bennett, S. J.; Goldenberg, D. M.; Hawthorne, M. F. *Proc. Natl. Acad. Sci. USA* **1982**, *79*, 3011.
(152) Nagasaki, T.; Shinmori, H.; Shinkai, S. *Tetrahedron Lett.* **1994**, *35*, 2201.
(153) Chapin, B. M.; Metola, P.; Vankayala, S. L.; Woodcock, H. L.; Mooibroek, T. J.; Lynch, V. M.; Larkin, J. D.; Anslyn, E. V. *J. Am. Chem. Soc.* **2017**, *139*, 5568.
(154) Sandanayake, K.; Shinkai, S. *J. Chem. Soc. Chem. Comm.* **1994**, 1083.
(155) Ward, C. J.; Patel, P.; Ashton, P. R.; James, T. D. *Chem. Comm.* **2000**, 229.
(156) Nguyen, B. T.; Anslyn, E. V. *Coordin. Chem. Rev.* **2006**, *250*, 3118.
(157) Buryak, A.; Severin, K. *Angew. Chem. Int. Ed.* **2004**, *43*, 4771.
(158) Vilozny, B.; Schiller, A.; Wessling, R. A.; Singaram, B. *Anal. Chim. Acta* **2009**, *649*, 246.
(159) Wiskur, S. L.; Ait-Haddou, H.; Lavigne, J. J.; Anslyn, E. V. *Acc. Chem. Res.* **2001**, *34*, 963.
(160) Cabell, L. A.; Monahan, M. K.; Anslyn, E. V. *Tetrahedron Lett.* **1999**, *40*, 7753.
(161) Lavigne, J. J.; Anslyn, E. V. *Angew. Chem. Int. Ed.* **1999**, *38*, 3666.
(162) Piatek, A. M.; Bomble, Y. J.; Wiskur, S. L.; Anslyn, E. V. *J. Am. Chem. Soc.* **2004**, *126*, 6072.
(163) Zhang, T. Z.; Anslyn, E. V. *Org. Lett.* **2007**, *9*, 1627.
(164) Springsteen, G.; Wang, B. H. *Chem. Comm.* **2001**, 1608.
(165) Yan, J.; Springsteen, G.; Deeter, S.; Wang, B. H. *Tetrahedron* **2004**, *60*, 11205.
(166) Arimori, S.; Ward, C. J.; James, T. D. *Tetrahedron Lett.* **2002**, *43*, 303.
(167) Peppas, N. A.; Bures, P.; Leobandung, W.; Ichikawa, H. *Eur. J. Pharm. Biopharm.* **2000**, *50*, 27.
(168) He, L.; Fullenkamp, D. E.; Rivera, J. G.; Messersmith, P. B. *Chem. Comm.* **2011**, *47*, 7497.
(169) Deligkaris, K.; Tadele, T. S.; Olthuis, W.; van den Berg, A. *Sensor. Actuat. B-Chem.* **2010**, *147*, 765.
(170) Ahmed, E. M. *J. Adv. Res.* **2015**, *6*, 105.
(171) Iddon, P. D.; Armes, S. P. *Eur. Polym. J.* **2007**, *43*, 1234.
(172) Kotsuchibashi, Y.; Ebara, M.; Sato, T.; Wang, Y.; Rajender, R.; Hall, D. G.; Narain, R.; Aoyagi, T. *J. Phys. Chem. B* **2015**, *119*, 2323.
(173) Alexeev, V. L.; Sharma, A. C.; Goponenko, A. V.; Das, S.; Lednev, I. K.; Wilcox, C. S.; Finegold, D. N.; Asher, S. A. *Anal. Chem.* **2003**, *75*, 2316.
(174) Kikuchi, A.; Suzuki, K.; Okabayashi, O.; Hoshino, H.; Kataoka, K.; Sakurai, Y.; Okano, T. *Anal. Chem.* **1996**, *68*, 823.
(175) Cash, J. J.; Kubo, T.; Bapat, A. P.; Sumerlin, B. S. *Macromolecules* **2015**, *48*, 2098.
(176) Kataoka, K.; Miyazaki, H.; Bunya, M.; Okano, T.; Sakurai, Y. *J. Am. Chem. Soc.* **1998**, *120*, 12694.
(177) Lei, M.; Baldi, A.; Nuxoll, E.; Siegel, R. A.; Ziaie, B. *Diabetes Technol. The.* **2006**, *8*, 112.
(178) Meng, F. H.; Zhong, Z. Y.; Feijen, J. *Biomacromolecules* **2009**, *10*, 197.
(179) Kim, K. T.; Meeuwissen, S. A.; Nolte, R. J. M.; van Hest, J. C. M. *Nanoscale* **2010**, *2*, 844.
(180) Johnson, E. K.; Adams, D. J.; Cameron, P. J. *J. Mater. Chem.* **2011**, *21*, 2024.

(181) Jayawarna, V.; Ali, M.; Jowitt, T. A.; Miller, A. E.; Saiani, A.; Gough, J. E.; Ulijn, R. V. *Adv. Mater.* **2006**, *18*, 611.
(182) Wang, Q. G.; Yang, Z. M.; Ma, M. L.; Chang, C. K.; Xu, B. *Chem. Eur. J.* **2008**, *14*, 5073.
(183) Adams, D. J.; Topham, P. D. *Soft Matter* **2010**, *6*, 3707.
(184) Grigoriou, S.; Johnson, E. K.; Chen, L.; Adams, D. J.; James, T. D.; Cameron, P. J. *Soft Matter* **2012**, *8*, 6788.
(185) James, T. D.; Sandanayake, K.; Shinkai, S. *Angew. Chem. Int. Ed.* **1996**, *35*, 1910.
(186) Ferrand, Y.; Crump, M. P.; Davis, A. P. *Science* **2007**, *318*, 619.
(187) Bielecki, M.; Eggert, H.; Norrild, J. C. *J. Chem. Soc. Perk. T 2* **1999**, 449.
(188) Kuivila, H. G.; Keough, A. H.; Soboczenski, E. J. *J. Org. Chem.* **1954**, *19*, 780.
(189) Bull, S. D.; Davidson, M. G.; Van den Elsen, J. M. H.; Fossey, J. S.; Jenkins, A. T. A.; Jiang, Y. B.; Kubo, Y.; Marken, F.; Sakurai, K.; Zhao, J. Z.; James, T. D. *Acc. Chem. Res.* **2013**, *46*, 312.
(190) Kim, A.; Mujumdar, S.; Siegel, R. *Chemosensors* **2014**, *2*, 1.
(191) Tomsho, J. W.; Benkovic, S. J. *J. Org. Chem.* **2012**, *77*, 2098.
(192) Sun, X.; Lacina, K.; Ramsamy, E. C.; Flower, S. E.; Fossey, J. S.; Qian, X.; Anslyn, E. V.; Bull, S. D.; James, T. D. *Chem. Sci.* **2015**, *6*, 2963.
(193) Lakowicz, J. R. *Principles of Fluorescence Spectroscopy*; Third edition ed.; Springer: New York, 2006.
(194) Jabłoński, A. *Z. Phys.* **1935**, *94*, 38.
(195) Kasha, M. *Discuss. Faraday Soc.* **1950**, 14.
(196) Demchenko, A. P. *Introduction to Fluorescence Sensing*; 2 ed.; Springer: Switzerland, 2015.
(197) Piston, D. W.; Kremers, G. J. *Trends Biochem. Sci.* **2007**, *32*, 407.
(198) de Silva, A. P.; Moody, T. S.; Wright, G. D. *Analyst* **2009**, *134*, 2385.
(199) de Silva, A. P.; Fox, D. B.; Moody, T. S.; Weir, S. M. *Trends Biotechnol.* **2001**, *19*, 29.
(200) Daly, B.; Ling, J.; de Silva, A. P. *Chem. Soc. Rev.* **2015**, *44*, 4203.
(201) de Silva, A. P.; Gunaratne, H. Q. N.; Gunnlaugsson, T.; Huxley, A. J. M.; McCoy, C. P.; Rademacher, J. T.; Rice, T. E. *Chem. Rev.* **1997**, *97*, 1515.
(202) Grabowski, Z. R.; Rotkiewicz, K.; Rettig, W. *Chem. Rev.* **2003**, *103*, 3899.
(203) Li, L. H.; Li, Z.; Shi, W.; Li, X. H.; Ma, H. M. *Anal. Chem.* **2014**, *86*, 6115.
(204) Tian, Z.; Liu, Y.; Tian, B.; Zhang, J. *Res. Chem. Intermed.* **2015**, *41*, 525.
(205) Kuivila, H. G.; Armour, A. G. *J. Am. Chem. Soc.* **1957**, *79*, 5659.
(206) Sun, X.; Xu, S.-Y.; Flower, S. E.; Fossey, J. S.; Qian, X.; James, T. D. *Chem. Comm.* **2013**, *49*, 8311.
(207) Sun, X.; Xu, Q.; Kim, G.; Flower, S. E.; Lowe, J. P.; Yoon, J.; Fossey, J. S.; Qian, X.; Bull, S. D.; James, T. D. *Chem. Sci.* **2014**, *5*, 3368.
(208) Dickinson, B. C.; Chang, C. J. *Nat. Chem. Biol.* **2011**, *7*, 504.
(209) Dickinson, B. C.; Tang, Y.; Chang, Z. Y.; Chang, C. J. *Chem. Biol.* **2011**, *18*, 943.
(210) Dickinson, B. C.; Huynh, C.; Chang, C. J. *J. Am. Chem. Soc.* **2010**, *132*, 5906.
(211) Chen, X.; Chen, H.; Deng, R.; Shen, J. *Biomed. J* **2014**, *37*, 120.
(212) Ray, P. D.; Huang, B.-W.; Tsuji, Y. *Cell. Signal.* **2012**, *24*, 981.
(213) Bansal, M.; Kaushal, N. *Oxidative Stress Mechanisms and their Modulation* Springer: New Delhi, 2014.
(214) Lenaz, G. *Iubmb Life* **2001**, *52*, 159.

(215) Boveris, A. *Method Enzymol.* **1984**, *105*, 429.
(216) Mehta, J. L.; Rasouli, N.; Sinha, A. K.; Molavi, B. *Int. J. Biochem. Cell B.* **2006**, *38*, 794.
(217) Saran, M.; Bors, W. *Free Radical Res. Comm.* **1989**, *7*, 213.
(218) Demple, B.; Amabilecuevas, C. F. *Cell* **1991**, *67*, 837.
(219) Joseph, J. A.; Cutler, R. C.; *Ann. NY Acad. Sci.* **1994**, 738, 37.
(220) Cencioni, C.; Spallotta, F.; Martelli, F.; Valente, S.; Mai, A.; Zeiher, A. M.; Gaetano, C. *Int. J. Mol. Sci.* **2013**, *14*, 17643.
(221) Shukla, V.; Mishra, S. K.; Pant, H. C. *Adv. Phar. Sci.* **2011**, *2011*, 572634.
(222) Paravicini, T. M.; Touyz, R. M. *Cardiovasc. Res.* **2006**, *71*, 247.
(223) Trachootham, D.; Alexandre, J.; Huang, P. *Nat. Rev. Drug Discov.* **2009**, *8*, 579.
(224) Haigis, M. C.; Yankner, B. A. *Mol. Cell* **2010**, *40*, 333.
(225) Sohal, R. S.; Weindruch, R. *Science* **1996**, *273*, 59.
(226) Finkel, T.; Holbrook, N. J. *Nature* **2000**, *408*, 239.
(227) Halliwell, B. *Nutr. Rev.* **2012**, *70*, 257.
(228) Dikalov, S. I.; Dikalova, A. E.; Mason, R. P. *Arch. Biochem. Biophys.* **2002**, *402*, 218.
(229) Devaraj, N. K.; Hilderbrand, S.; Upadhyay, R.; Mazitschek, R.; Weissleder, R. *Angew. Chem. Int. Ed.* **2010**, *49*, 2869.
(230) Chen, X.; Zhong, Z.; Xu, Z.; Chen, L.; Wang, Y. *Free Radical Res.* **2010**, *44*, 587.
(231) Tarpey, M. M.; Fridovich, I. *Circ. Res.* **2001**, *89*, 224.
(232) Wardman, P. *Free Radical Bio. Med.* **2007**, *43*, 995.
(233) Mattson, M. P. *Nature* **2004**, *430*, 631.
(234) Ohshima, H.; Tatemichi, M.; Sawa, T. *Arch. Biochem. Biophys.* **2003**, *417*, 3.
(235) Miller, E. W.; Albers, A. E.; Pralle, A.; Isacoff, E. Y.; Chang, C. J. *J. Am. Chem. Soc.* **2005**, *127*, 16652.
(236) Chan, J.; Dodani, S. C.; Chang, C. J. *Nature Chemistry* **2012**, *4*, 973.
(237) Chang, M. C. Y.; Pralle, A.; Isacoff, E. Y.; Chang, C. J. *J. Am. Chem. Soc.* **2004**, *126*, 15392.
(238) Albers, A. E.; Okreglak, V. S.; Chang, C. J. *J. Am. Chem. Soc.* **2006**, *128*, 9640.
(239) Miller, E. W.; Tulyanthan, O.; Isacoff, E. Y.; Chang, C. J. *Nat. Chem. Biol.* **2007**, *3*, 263.
(240) Srikun, D.; Miller, E. W.; Dornaille, D. W.; Chang, C. J. *J J. Am. Chem. Soc.* **2008**, *130*, 4596.
(241) DiCesare, N.; Lakowicz, J. R. *J. Phys. Chem. A* **2001**, *105*, 6834.
(242) Miyaura, N.; Suzuki, A. *Chem. Rev.* **1995**, *95*, 2457.
(243) Taylor, D. L.; Salmon, E. D. *Method Cell Biol.* **1989**, *29*, 207.
(244) Silva, F.; Figueiras, A.; Gallardo, E.; Nerin, C.; Domingues, F. C. *Food Chem.* **2014**, *145*, 115.
(245) DiCesare, N.; Lakowicz, J. R. *Chem. Comm.* **2001**, 2022.
(246) Diwu, Z.; Lu, Y. X.; Zhang, C. L.; Klaubert, D. H.; Haugland, R. P. *Photoch. Photobiol.* **1997**, *66*, 424.
(247) Wasserman, H. H.; Vinick, F. J. *J. Org. Chem.* **1973**, *38*, 2407.
(248) Kulhanek, J.; Bures, F.; Ludwig, M. *Beilstein J. Org. Chem.* **2009**, *5*.
(249) Lee, S. W.; Rhee, H.-W.; Chang, Y.-T.; Hong, J.-I. *Chem. Eur. J.* **2013**, *19*, 14791.
(250) Di Cesare, N.; Lakowicz, J. R. *J. Photoch. Photobio. A* **2001**, *143*, 39.

(251) Dugave, C.; Demange, L. *Chem. Rev.* **2003**, *103*, 2475.
(252) Dou, Y. S.; Allen, R. E. *J. Chem. Phys.* **2003**, *119*, 10658.
(253) Veronese, F. M.; Mero, A. *Biodrugs* **2008**, *22*, 315.
(254) DiCesare, N.; Lakowicz, J. R. *Tetrahedron Lett.* **2002**, *43*, 2615.
(255) Perrin, D. D.; Dempsey, B. *Buffers for pH and Metal Ion Control*; Chapman and Hall Ltd: London, 1974.
(256) Adamczyk-Wozniak, A.; Madura, I.; Pawelko, A.; Sporzynski, A.; Zubrowska, A.; Zyla, J. *Cent. Eur. J. Chem.* **2011**, *9*, 199.
(257) Alterio, V.; Cadoni, R.; Esposito, D.; Vullo, D.; Di Fiore, A.; Monti, S. M.; Caporale, A.; Ruvo, M.; Sechi, M.; Dumy, P.; Supuran, C. T.; De Simone, G.; Winum, J.-Y. *Chem. Comm.* **2016**, *52*, 11983.
(258) Baker, S. J.; Sanders, V.; Akama, T.; Bellinger-Kawahara, C.; Freund, Y.; Maples, K. R.; Plattner, J. J.; Zhang, Y. K.; Zhou, H.; Hernandez, V. S. In *United States Patent Application*; Anacor Pharmaceuticals Inc.: 2007; Vol. US2007/293457.
(259) Alexander, C.; Smith, C. R.; Whitcombe, M. J.; Vulfson, E. N. *J. Am. Chem. Soc.* **1999**, *121*, 6640.
(260) Gigante, B.; Esteves, M. A.; Pires, N.; Davies, M. L.; Douglas, P.; Fonseca, S. M.; Burrows, H. D.; Castro, R. A. E.; Pina, J.; de Melo, J. S. *New J. Chem.* **2009**, *33*, 877.
(261) Skhiri, A.; Ben Salem, R.; Soule, J.-F.; Doucet, H. *Synthesis-Stuttgart* **2016**, *48*, 3097.
(262) Oehlke, A.; Auer, A. A.; Jahre, I.; Walfort, B.; Rueffer, T.; Zoufala, P.; Lang, H.; Spange, S. *J. Org. Chem.* **2007**, *72*, 4328.

7 Appendices

Appendix 1

Table A-1. Full tables for percentage weight changes for blank hydrogels after immobilisation in various buffers

	Repeat 1			Repeat 2			Repeat 3			
Buffer	Weight before / g	Weight after / g	% change	Weight before / g	Weight after / g	% change	Weight before / g	Weight after / g	% change	Average % change
Pure water	2.0320	2.7644	36.04	2.0679	2.8537	38.00	2.0607	2.8006	35.91	36.65
pH 7.3 phosphate	2.0665	2.8648	38.63	2.0782	2.9408	41.51	2.0157	2.7853	38.18	39.44
pH 8.5 phosphate	2.0564	2.8414	38.17	2.0619	2.9298	42.09	2.0629	2.8586	38.57	39.61
pH 10 phosphate	2.0660	2.8651	38.68	2.0744	2.9303	41.26	2.0154	2.7920	38.53	39.49
pH 8.21 phosphate (with MeOH)	2.0544	1.2873	-37.34	2.0640	1.2876	-37.62	2.0615	1.3078	-36.56	-37.17
pH 10 phosphate (with MeOH)	2.0520	1.2822	-37.51	2.0611	1.3092	-36.48	2.0780	1.3187	-36.54	-36.85

Table A-2. Full tables for percentage weight changes for benzoxaborole-functionalised hydrogels after immobilisation in various buffers

	Repeat 1			Repeat 2			Repeat 3			
Buffer	Weight before / g	Weight after / g	% change	Weight before / g	Weight after / g	% change	Weight before / g	Weight after / g	% change	Average % change
Pure water	2.0155	2.9542	46.57	2.0444	2.9747	45.50	2.0565	2.9825	45.03	45.70
pH 7.3 phosphate	2.0233	2.9118	43.91	2.0342	2.9892	46.95	2.0619	2.9787	44.46	45.11
pH 8.5 phosphate	2.0152	2.8905	43.43	2.0748	3.0047	44.82	2.0742	2.9798	43.66	43.97
pH 10 phosphate	2.0122	2.8992	44.08	2.0481	2.9864	45.81	2.0409	2.9789	45.96	45.28
pH 8.21 phosphate (with MeOH)	2.0376	1.2705	-37.65	2.0322	1.2022	-40.84	2.0216	1.2464	-38.35	-38.95
pH 10 phosphate (with MeOH)	1.9780	1.2441	-37.10	2.0669	1.2416	-39.93	2.0385	1.2536	-38.50	-38.51

Table A-3. Full tables for percentage weight changes for phenylboronic acid pinacol ester-functionalised hydrogels after immobilisation in various buffers

	Repeat 1			Repeat 2			Repeat 3			
Buffer	Weight before / g	Weight after / g	% change	Weight before / g	Weight after / g	% change	Weight before / g	Weight after / g	% change	Average % change
Pure water	2.0464	2.9030	41.86	2.0829	2.9691	42.55	2.0871	2.9522	41.45	41.95
pH 7.3 phosphate	2.0294	2.7896	37.46	2.0812	2.9226	40.43	2.0345	2.8434	39.76	39.22
pH 8.5 phosphate	1.9950	2.7752	39.11	2.0343	2.8987	42.49	2.0543	2.8588	39.16	40.25
pH 10 phosphate	2.0027	2.7898	39.30	2.0318	2.8864	42.06	2.0362	2.8241	38.69	40.02
pH 8.21 phosphate (with MeOH)	2.0084	1.2920	-35.67	2.0157	1.2567	-37.65	2.0720	1.3062	-36.96	-36.76
pH 10 phosphate (with MeOH)	2.0292	1.2970	-36.08	2.0790	1.3400	-35.55	2.0415	1.2899	-36.82	-36.15

Appendix 2

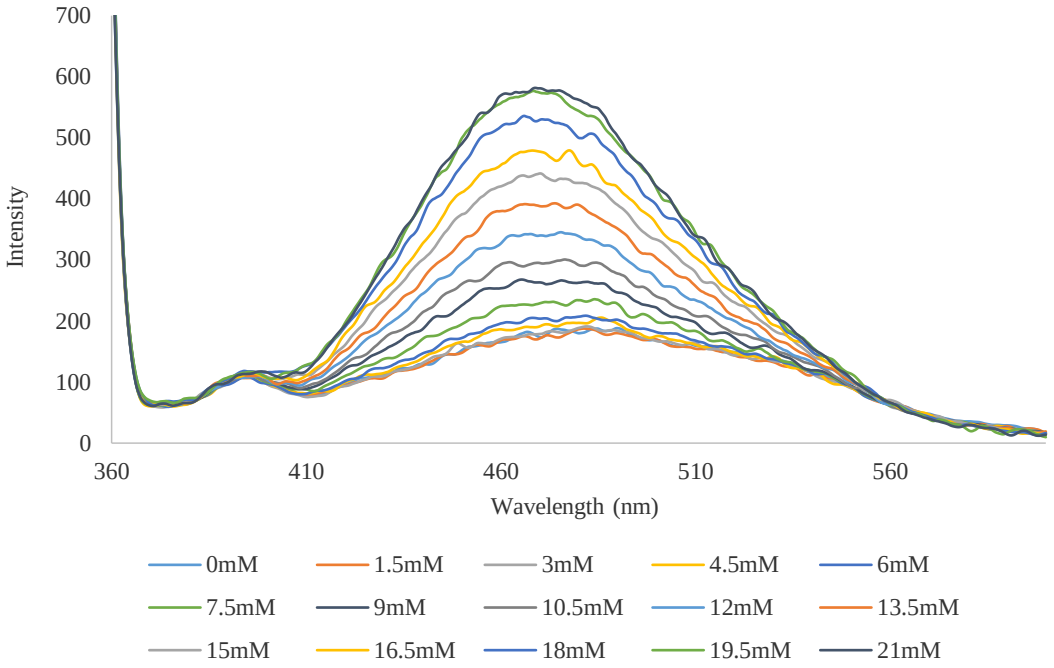

Graph A-1. Repeat of fluorescent spectra showing changes in emission intensity as H_2O_2 concentration is increased. Probe **77** (30 nM) and H_2O_2 (0 mM – 21 mM) in pH 7.25 PBS buffer, analysed 10 minutes after additional H_2O_2 was introduced. Excitation wavelength 350 nm.